NATIONAL UNIVERSITY OF IRELAND, GALWAY

PREDICTING THE LONG-TERM PERFORMANCE OF LOW-COST PHOSPHORUS-SORBING MATERIALS USING SMALL-SCALE ADSORPTION COLUMN EXPERIMENTS

Oisín Callery

Research Supervisor:

Dr. Mark G. Healy, Civil Engineering, NUI Galway

Thesis submitted to the College of Engineering and Informatics, National University of Ireland, Galway, in fulfilment of the requirements for the Degree of Doctor of Philosophy.

July 2017

The National University of Ireland, Galway requires the signatures of all persons using or photocopying this thesis. Please sign below, and give the address and date.

Abstract

Anthropogenic phosphorus (P) and nitrogen (N) inputs to aquatic environments have rapidly increased in magnitude since the middle of the twentieth century, and nutrient pollution has become the primary threat to global surface water quality. Because P is most often the nutrient limiting primary production in freshwater ecosystems, the control of P losses from anthropogenic sources is of paramount importance to the prevention of cultural eutrophication, i.e. the nutrient enrichment of water bodies as a result of human activities. Left unchecked, eutrophication causes optimal conditions for sudden, dramatic increases in populations of algae and many species of noxious aquatic weeds. The long-term effects of this are marked reductions of aquatic biodiversity, disruption of natural biogeochemical balances, and an accelerated ageing of water bodies resulting in their premature succession from clear water, to swamp/marsh, and finally to dry land. More obvious short-term effects are increased incidences of harmful algal blooms and associated fish kills resulting from low dissolved oxygen levels, i.e. hypoxic conditions, caused by the microbial decay of organic matter originating from the overgrowth of plants and algae.

Sources of P losses can be broadly divided into two main categories: point sources and nonpoint sources. The former represents easily identifiable, discreet sources of P such as outlets from municipal wastewater treatment plants, while the latter represents diffuse sources of P which are spatially and temporally heterogeneous. Advances in wastewater treatment technologies, coupled with increasingly strict legislative controls in recent decades, have lessened the threat posed by point source P losses, and nonpoint source P losses have become the dominant contributor to nutrient pollution in many regions, including Ireland, where nonpoint sources account for approximately 57% of P inputs to surface waters. Mitigation of nonpoint P losses is currently achieved through the implementation of source reduction strategies, such as matching fertilizer additions with crop deficiencies, and source interception strategies, such as trapping and retaining P-laden particles in runoff with the use of buffer zones. These best management practices (BMPs) can often fail to produce desired results, and sometimes their implementation is not practicable as a result of unfavourable onsite conditions. An example of such a case is the loss of dissolved P from clearfelling on blanket peat forestry plantations. These P losses are unamenable to mitigation with standard BMPs such as the use of buffer zones, and source control is not feasible either, as these P losses primarily originate from harvesting residues utilised to form brash mats. These mats

provide support to heavy harvesting machinery, and their use is therefore an integral part of the process of clearfelling on peat soils.

One solution in cases such as these may be to use low-cost P sorbing materials, and there has been much research in recent years attempting to identify and characterize novel sorbents for use in the treatment of various wastewaters. Such investigations more often than not use batch adsorption tests as a means of assessing the potential of such media, and, although these are an essential first step, there has been an overreliance on such methods which, when performed alone, provide insufficient information to predict media longevity. The purpose of this study was to develop a simple, economical, and rapid method by which to assess the potential in-field longevity of low-cost P sorbing materials, and then apply this method to identify media which might be suitable for use in pilot-scale in-filed filters to prevent P losses associated with peatland forestry harvesting.

After an initial screening process, using batch adsorption methods to identify potentially suitable materials, small-scale column adsorption tests were carried out using four media: aluminium water treatment residual (Al-WTR), ferric water treatment residual (Fe-WTR), and two grades of crushed concrete. Long-term, large-scale adsorption column studies were also performed using these media (excluding Fe-WTR, which performed poorly in the small-scale tests), and it was demonstrated that the behaviour of these large-scale filters could be predicted accurately based on the performances of small-scale columns subjected to equivalent loadings. A mathematical modelling approach was then developed which would enable researchers to use the results of the small-scale column tests to predict the propagation of saturation and pore concentration fronts within large-scale filters. With these modelling techniques, the performance of large-scale filters (of any size) subjected to any loading could be predicted using results from a number of small-scale column tests to determine the necessary model coefficients. This significantly improved the utility of small-scale tests, as it enabled performance predictions to be made for any possible large-scale filter configuration using results from small-scale column tests.

The experimental and modelling methodologies developed over the course of this study were applied to assess the suitability of crushed concrete and Al-WTR for the treatment of peatland forestry runoff. The results of these investigations suggest that Al-WTR could successfully be used to remove P from this runoff, and there were no issues which would preclude its usage in a peatland forestry environment; the media showed no significant release of metals (total

cumulative releases of nickel, copper, and aluminium were 0.16, 5.5, and 13.63 µg g^{-1} filter media, respectively**)** and the pH of effluent from Al-WTR filters was well within the EPA recommended environmental quality standard (EQS) of 6 to 9 (average effluent pH was 7.31±0.36). Crushed concrete was even more effective than Al-WTR at removing P from forestry runoff, due to a higher P adsorption affinity at low concentrations. However, the high pH of effluent from filters containing this media indicated that significant pre-washing (≥ 240 bed volumes) of the filter media would be required to bring the filter effluent below the recommended EQS of 9, were it to be used in a forestry context. Crushed concrete also released much greater quantities of Cu and Al (31.90 and 96.17 µg g^{-1} filter media, respectively), further highlighting the need for washing of the filter media prior to use. For these reasons, it was decided that Al-WTR shows greater promise, and it was concluded that its use for the treatment of peatland forestry runoff should be studied further in pilot-scale in-field filters. Al-WTR was also found to be effective in removing P from dairy soiled water, a wastewater which had a P concentration that was approximately 30 times that of forestry runoff; this suggests that Al-WTR holds great promise for the removal of P from point sources as well as nonpoint sources, and further research should be carried out on this topic.

Declaration

This dissertation is the result of my own work, except where explicit reference is made to the work of others, and has not been submitted for another qualification to this or any other university.

Oisín Callery

Acknowledgements

First and foremost, I'd like to sincerely thank my supervisor Dr. Mark Healy for his unwavering support, not just during my PhD, but also throughout my time as an undergraduate and working in industry. I know I can never repay the kindness he has shown me over these many years. Dr. Healy's knowledge and experience have been invaluable assets to me over the course of my PhD, and I am immensely fortunate that he was always so willing to selflessly offer his time and energy. I am even more thankful that he has become a highly valued friend. I'd also like to thank Dr. Raymond Brennan for his advice and support, particularly in the early stages of my research, when I was still finding my feet.

I am very grateful to the Irish Research Council for funding this study, to Dr. Eoghan Clifford and Prof. Padraic O'Donoghue, for providing valuable guidance and advice, and to the anonymous reviewers who provided feedback on my papers - their input no doubt greatly strengthened them, and addressing their comments certainly deepened my understanding of my research.

I've had the good fortune to work with many excellent undergraduate and postgraduate students over the course of my research - Florian, Ishan, Loïc, Greg, and Thomas, to name a few - and I am very grateful for their help in the laboratory. I'm also thankful to the other PhD and postdoctoral researchers with whom I've worked - John, Maebh, Collette, Tom, José, Patricia, Edelle, Kelly, Emma, Conor, Yan, Alan, Conan, and Ashish - the journey hasn't always been easy, but it's been a pleasure to share it with such genuinely nice people.

I'm eternally grateful to my parents - without their support I would never have started, let alone finished, this journey, and it's only in retrospect that I begin to fully appreciate the sacrifices that they have made to afford my siblings and me every opportunity in life. I was lucky enough to live with my brother Naoise for the past year; without his support I would have felt very much alone at times, and I can never thank him enough for his kindness and understanding. Also, I couldn't neglect to mention my sister Sineán, whom is in no small way responsible for my undertaking this PhD - seeing her outdo my every academic achievement, I knew I had to up my game!

I would especially like to thank Tara for her support and patience, not just for the duration of my research, but over the past 11 years. She has stood by me when I've been at my lowest, and I can only hope that I can be as supportive of her as she has been of me.

I'd like to thank Louis - the simple act of taking a break to go fishing with a friend often helped keep me sane when the task at hand sometimes seemed insurmountable. Also, I'm quite certain that there's no better way to remind oneself of the importance of environmental research than hooking a fresh Atlantic salmon!

Finally, I'd like to thank my coaches and training partners at Point Blank Gym. Brazilian Jiu-Jitsu has had an immensely positive influence on my life, and I feel privileged to be part of such a vibrant community. Nothing takes your mind off the stress of research quite like having a friend try to throttle you!

Table of Contents

List of Figures

List of Tables

Abbreviations

Al	Aluminium
Al-WTR	Aluminium Drinking Water Treatment Residual
As	Arsenic
BDST	Bed Depth Service Time
BTC	Breakthrough Curve
C	Carbon
Ca	Calcium
CC	Crushed Concrete
Cr	Chromium
Cu	Copper
DO	Dissolved Oxygen
DSW	Dairy Soiled Water
EBCT	Empty Bed Contact Time
EQS	Environmental Quality Standard
EU	European Union
Fe	Iron
Fe-WTR	Ferric Drinking Water Treatment Residual
GAC	Granular Activated Carbon
$H_2PO_4^-$	Dihydrogen Phosphate
HDPE	High Density Polyethylene
HLR	Hydraulic Loading Rate
HPO_4^{2-}	Hydrogen Phosphate
HRT	Hydraulic Retention Time
K_2HPO_4	Dipotassium Hydrogen Phosphate
LDPE	Low Density Polyethylene
$Mg(OH)_2$	Magnesium Hydroxide
MgO	Magnesium Oxide
Mn	Manganese
MPE	Mean Percentage Error
N	Nitrogen
Ni	Nickel
NO_3	Nitrate
P	Phosphorus
Pb	Lead
PO_4	Phosphate
PP	Particulate Phosphorus > 0.45µm
RSSCT	Rapid Small-Scale Column Test
SP	Soluble Phosphorus < 0.45µm
SRP	Soluble Reactive Phosphorus
SUP	Soluble Unreactive Phosphorus
TP	Total Phosphorus
Zn	Zinc

Chapter 1 - Literature Review

1.1 Background

As a result of terrestrial human activities, aquatic ecosystems worldwide are receiving excessive inputs of nitrogen (N) and phosphorus (P). Aquatic nutrient influxes have rapidly increased in magnitude since the middle of the twentieth century, and nutrient pollution has become the primary threat to global surface water quality (Zaimes and Schultz, 2002; Smith and Schindler, 2009).

The critical importance of P and N lie in their role as limiting nutrients. In most waters there is an abundance of plant micronutrients available, and it is therefore a lack of P and/or N that limits primary production (Lewis et al., 2011; Moore et al., 2013) - the photosynthetic (or rarely chemosynthetic) creation of organic matter through carbon fixation by plants and algae (Lieth and Whittaker, 2012). Though some exceptions exist, in salt and brackish waters it is usually N which acts as the main limiting nutrient (Howarth and Marino, 2006). Conversely, in freshwaters, the general consensus of the scientific community is that P is the limiting nutrient (Correll, 1999; Blomqvist et al., 2004; Hilton et al., 2006; Schoumans et al., 2014).

There may be joint P-N limitation in certain freshwater ecosystems (Lewis and Wurtsbaugh, 2008; Sterner, 2008), and synergistic effects caused by simultaneous inputs of both P and N have been observed (Elser et al., 2007). However, regardless of whether or not there is joint limitation, there is strong evidence that limiting inputs of N alone simply favours a shift in algal community structures toward, arguably more objectionable, blue-green N fixing species (Schindler, 1977; Smith, 1983; Schindler et al., 2008). For this reason, and because it is essentially impossible to control the exchange of atmospheric N by N-fixing algae (Sharpley et al., 2000), to prevent eutrophication, it is vital to control P inputs into freshwater bodies (Sharpley et al., 2003; Schindler et al., 2016).

1.2 Anthropogenic disruption of the natural phosphorus cycle

Before the dawn of the 20th century, P surpluses were generally small (Bouwman et al., 2013). Phosphorus makes up only a minute amount of the earth's crust (0.09% wt%), and is largely present in mineral forms such as fluorapatite and carbonate-fluorapatite (Filippelli, 2008). In natural ecosystems, i.e. those not subject to human interference, inputs of P into aquatic environments originate mainly from the gradual weathering of these mineral sources and the seasonal decay of organic material (Manzoni et al., 2010). Unlike other essential nutrients such as N and carbon (C), P has no atmospherically stable gaseous phases (ignoring the comparatively minute amount carried on aerosolized dust particles (Ruttenberg, 2003)). Phosphorus therefore relies more-or-less solely on water to carry it through its natural cycle (Filippelli, 2008). Upon being incorporated into runoff, in either dissolved or particulate form, P is quickly washed downstream until it reaches lakes and oceans, where it is ultimately deposited and sequestered by the sedimentation of organic and mineral matter; at this point, it is removed from the P-cycle until such time that this sediment is exposed again by natural tectonic uplift and subsequent weathering (Ruttenberg, 2003).

The introduction of chemical fertilizers (sourced from mined rock phosphate) in the mid 19th century (Grigg, 1987), and their widespread adoption in the early to mid 20th century, marked the beginning of a significant change to the natural P cycle (Cordell et al., 2009). Since this time, terrestrial exports of P have at least doubled (Compton et al., 2000), perhaps even tripled (Smil, 2000; Carpenter and Bennett, 2011). As a result, the primary inputs of P to aquatic environments are now anthropogenic, coming primarily from sources such as agriculture, industry, and municipal wastewater (Ruttenberg, 2003). The effect of this human destabilization of the natural P cycle is already having a profoundly deleterious effect on Earth's biosphere, and it is quite likely that we have already crossed the upper tolerable limit, the 'planetary boundary,' for freshwater eutrophication (Carpenter and Bennett, 2011).

Moving forward, there are even more pressing issues than this immediate environmental cost: global food production relies on there being sufficient P to meet the demands of crops and livestock, and serious concerns have been raised over the security of future P supply (Beardsley, 2011; Cordell and White, 2011; Neset and Cordell, 2012). There was a massive intensification of agriculture post-World War II - the 'green revolution' - and this was largely fueled by the advent of fertilization with P sourced from mined rock phosphate (Ashley et al., 2011). Historically, agricultural needs were met by P in the soil and the return of P in the

form of manure (and human excreta in some parts of Asia) and crop residues formed an almost closed cycle, with minor loses and inputs associated with runoff and mineral weathering, respectively (Cordell et al., 2009). Feeding the ever increasing world population is now almost entirely dependent on P inputs from finite mined sources, and it is patently obvious that a major global reformation of humanity's approach to P use and recovery is needed if we are to ensure future food security and avoid further environmental degradation (Cordell and White, 2011). Figure 1.1 shows the increase in agricultural reliance on fertilizer sourced from mined rock phosphate over the past 50-60 years.

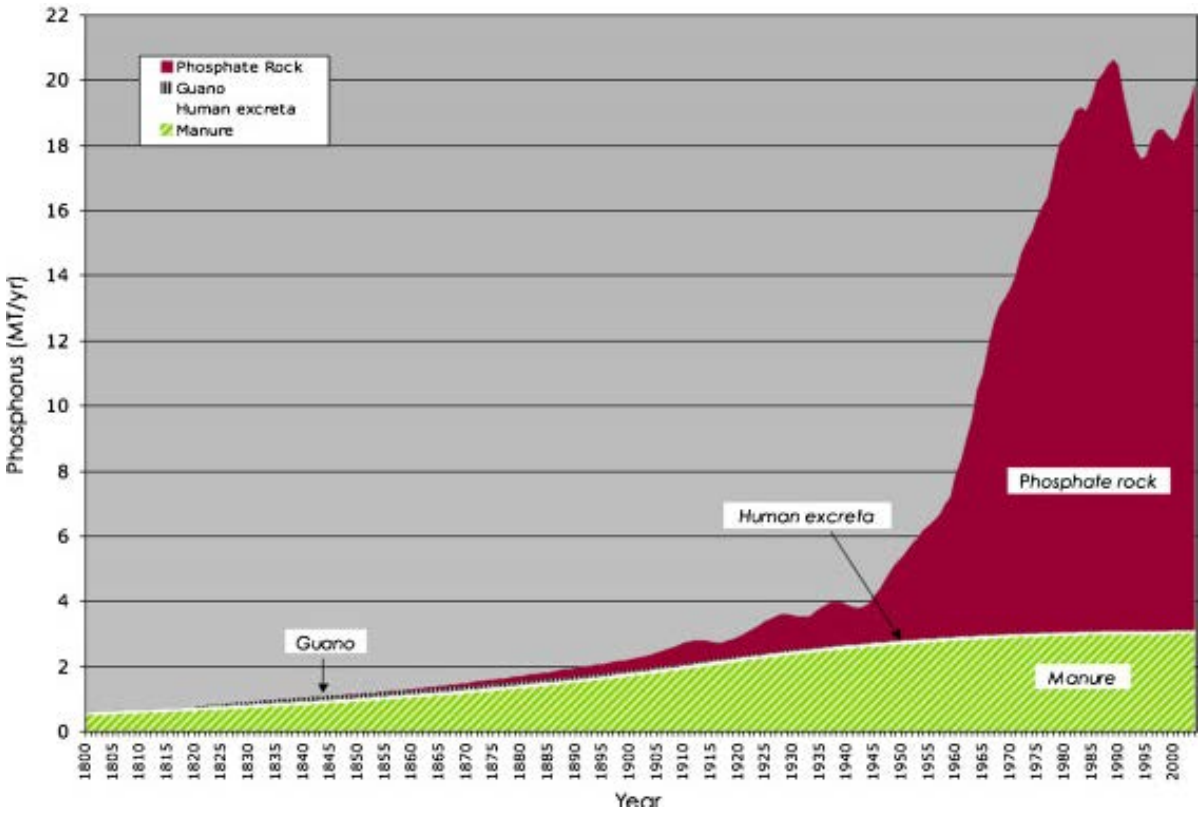

Figure 1.1 Historical global sources of phosphorus fertilizers (Cordell et al., 2009)

1.3 Eutrophication

Based on nutrient availability, water bodies may be classed as oligotrophic (low nutrient availability), mesotrophic (intermediate nutrient availability), eutrophic (high nutrient availability), or hypereutrophic (very high nutrient availability), with each ecosystem supporting unique assemblages of aquatic plant and animal life (Jeppesen et al., 2000; Reynolds, 1998). Of particular value are the nutrient-poor oligotrophic waters, as these typically have high levels of dissolved oxygen (DO), and provide unique habitat for many protected species of fish and other wildlife (Moorkens, 1999). They are also of great societal value, providing clear waters ideal for drinking water abstractions, crop irrigation, and amenity use (Wilson and Carpenter, 1999; Cooke and Kennedy, 2001; Pretty et al., 2003; Gössling et al., 2012).

Barring some external influence, oligotrophic conditions are usually quite stable, and are very slow to change over time, as the low P content of sediments in these waters allows for little recycling of settled P between solid and aqueous phases (Carpenter, 2005). However, due to their low nutrient contents, these waters are also uniquely sensitive to the effects of nutrient pollution (Figure 1.2), as even slight eutrophication, i.e. nutrient enrichment, can result in a change in such a water body's trophic state (Downing and McCauley, 1992; Carey and Migliaccio, 2009), with potentially serious knock-on implications for downstream systems (Dodds and Welch, 2000; Alexander et al., 2007). Similarly, once eutrophic conditions become established, it can be extremely challenging to effect recovery, as internal cycling of P between water and enriched sediments can potentially maintain high productivity levels long after external P inputs have been reduced (Havens et al., 1996).

Eutrophication is a natural aging process, and with continuous terrestrial influxes of nutrients and eroded particles, all initially oligotrophic inland water bodies naturally become eutrophic over a timeframe of many millennia (Khan and Ansari, 2005). These water bodies are ultimately inundated by mineral and organic sediments and plant life, which cumulates in a natural succession of lakes becoming ponds, then marshes and swamps, and finally, dry land (Greeson, 1969; Salameh and Harahsheh, 2010). It is therefore important to note that eutrophication itself is not necessarily a problem: it is inevitable, and it is, in fact, accelerated "cultural" eutrophication (i.e. eutrophication due to anthropogenic nutrient influxes) which poses a major concern, as it causes ecological changes which would naturally take place over millennia to occur in just decades (Havens et al., 1996).

Excessive anthropogenic inputs of nutrients to surface waters creates optimal conditions for the overgrowth of algae and many species of nuisance aquatic plants. In the long-term, the overabundance of these plants and algae seriously impairs the biodiversity of aquatic ecosystems, ageing the water body unnaturally. There are also much more immediate threats posed by the sudden unnatural accumulation of large amounts of biomass. Plants and algae die, and subsequent decay of the biological material in their cells removes massive amounts of DO from the water, creating hypoxic conditions which can result in fish kills and serious long-term disruption to prevailing biogeochemical conditions (Conley et al., 1993). Figure 1.2 shows the relationship between trophic status, water DO concentrations, and species richness.

Algae, in the form of free-floating phytoplankton and the more generally sessile periphyton communities, have long been recognized as being responsible for the bulk of primary production in aquatic ecosystems (Wetzel, 1964; Vadeboncoeur et al., 2003; Paerl et al., 2003), hence algal blooms have become one of the hallmarks of cultural eutrophication (Heisler et al., 2008). Though they can be a natural phenomenon, there has been an apparent increase in the incidence of algal blooms in recent decades, and their occurrence has often been linked to the effects of cultural eutrophication (Anderson et al., 2002). With soluble reactive phosphorus (SRP) concentrations as low as 2 μg L^{-1} sufficient to satisfy the P requirements of some algae (Grobbelaar and House, 1995), these blooms can easily cause serious environmental problems - either from their production of toxins, or simply from the effect of their accumulated biomass on aquatic biogeochemistry and food web dynamics (Anderson et al., 2002).

Algae are obviously an integral part of any aquatic ecosystem, as they form the basis of the aquatic foodweb; however, algal overgrowth can have a host of detrimental ecological effects. The most immediate of these is the depletion of water DO levels, sometimes through their own respiration, but more often due to their decomposition. There are also other concerns associated with algal blooms including potent algal toxins entering the food chain and reaching humans, and harm to fish and invertebrates caused though the clogging of their gills (Hallegraeff, 1993). Oligotrophic waters tend to support small algae communities with a rich diversity of species, whereas algae are present in much greater numbers in eutrophic waters, but with less varieties of species (Greeson, 1969).

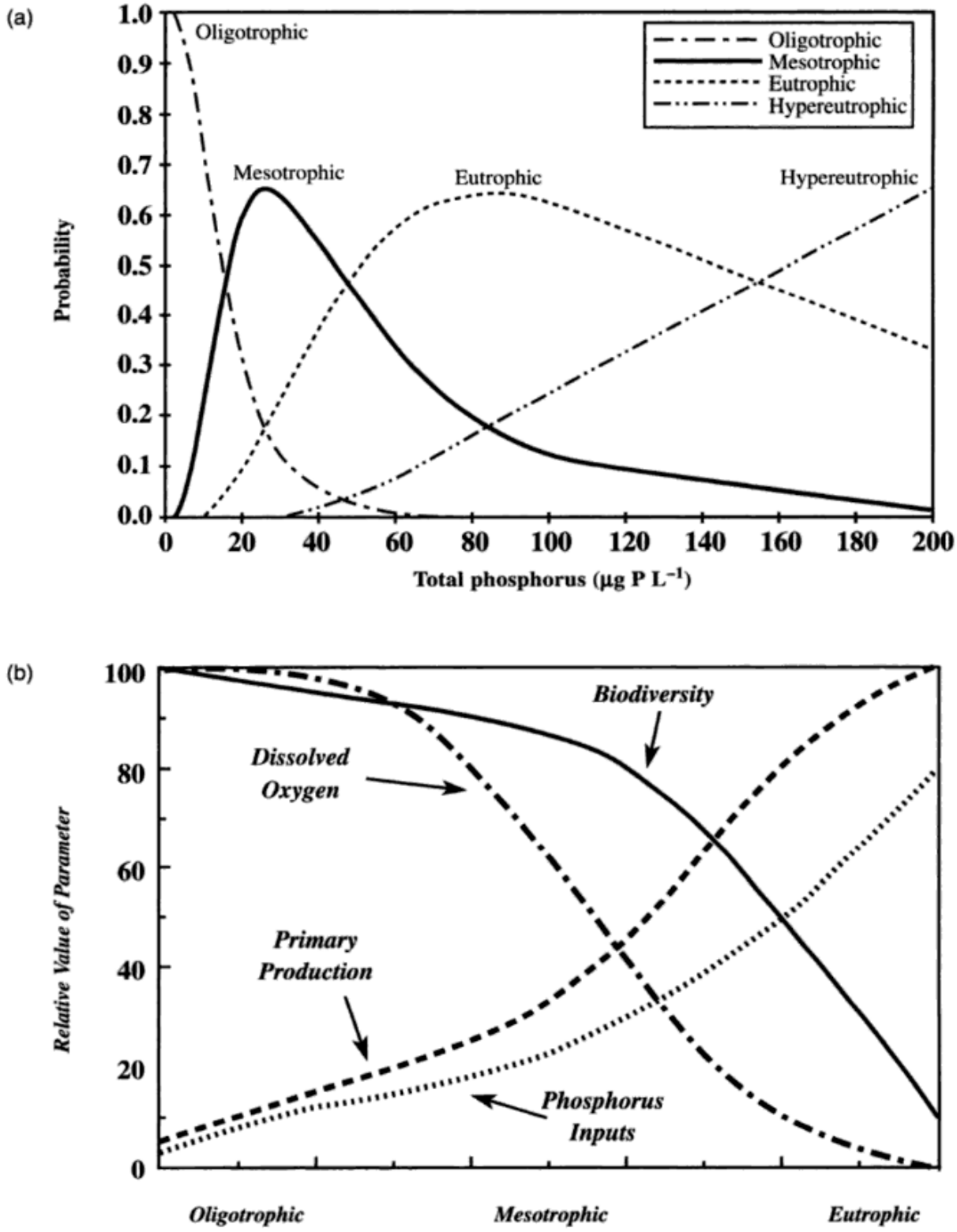

Figure 1.2 (a) The relationship between P concentrations and trophic status, highlighting the sensitivity of oligotrophic waters to eutrophication and (b) the relationship between P inputs, trophic status, primary production, DO concentrations, and biodiversity (Pierzynski et al., 2005)

1.4 Source apportionment of phosphorus losses

Sources of P pollution (and nutrient pollution in general) can be divided broadly into two categories: point sources and nonpoint sources. Easily identifiable discreet point sources such as, for example, outlets from municipal wastewater treatment plants and drains from livestock housing and farmyards, often represent high-concentration nutrient waste streams which are of comparatively low-volume compared to receiving waters (Bailey-Watts, 1997). In recent decades, these point sources have been subject to increasingly strict legislative controls (Carpenter, 2005), and consequently the threat posed by such sources, while still very relevant, has diminished slightly (Heathwaite et al., 2000). Nonpoint sources, such as runoff from pastures, arable lands, and forestry plantations, by comparison represent high-volume low-concentration nutrient pollution streams (Acreman, 2012). These diffuse sources of nutrient runoff are now recognized in many regions to be the largest contributor to the problem of nutrient pollution (Yang and Wang, 2010; Bouraoui and Grizzetti, 2014). Figure 1.3 summarizes sources of natural and anthropogenic P losses to aquatic environments.

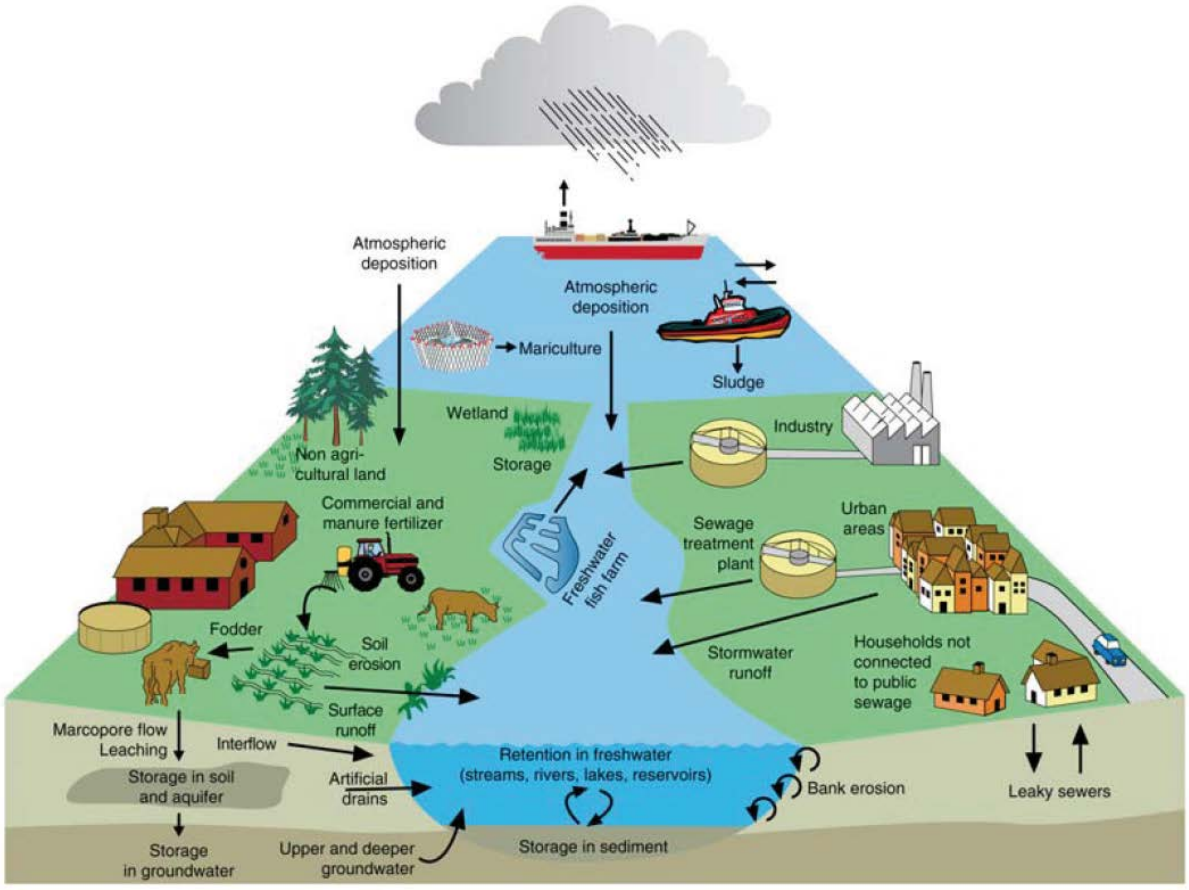

Figure 1.3 Sources of phosphorus pollution (Schoumans et al., 2011)

Nonpoint sources are particularly difficult to control for a number of reasons, though the primary challenge is simply that the pollution source is spread across such a large area that it is extremely challenging to implement effective runoff treatment strategies (Rao et al., 2009). Also, because many watersheds have been subjected to decades of over enrichment, there can be a significant temporal lag between the reduction of nutrient inputs and environmental recovery, as soils release stored nutrients (primarily P) long after surplus additions have ceased (Sharpley et al., 2013). Without intervention, anthropogenic nutrient losses will certainly continue to increase in magnitude, as global population growth and concomitant intensifications of agriculture and industry further exacerbate the problem.

Sources of nutrient pollution vary substantially from region to region, based on factors such as land use, land management, soil types, and climate. For this reason, source apportionment of P losses must be approached on a regional, or, ideally even a catchment basis. In Ireland, the primary P losses from come from diffuse sources (57%), with major contributions coming from agriculture, forestry and peat lands (Figure 1.4) (Mockler et al., 2017). Reduction of diffuse losses from these sources is therefore paramount to addressing the problem of P pollution in Ireland.

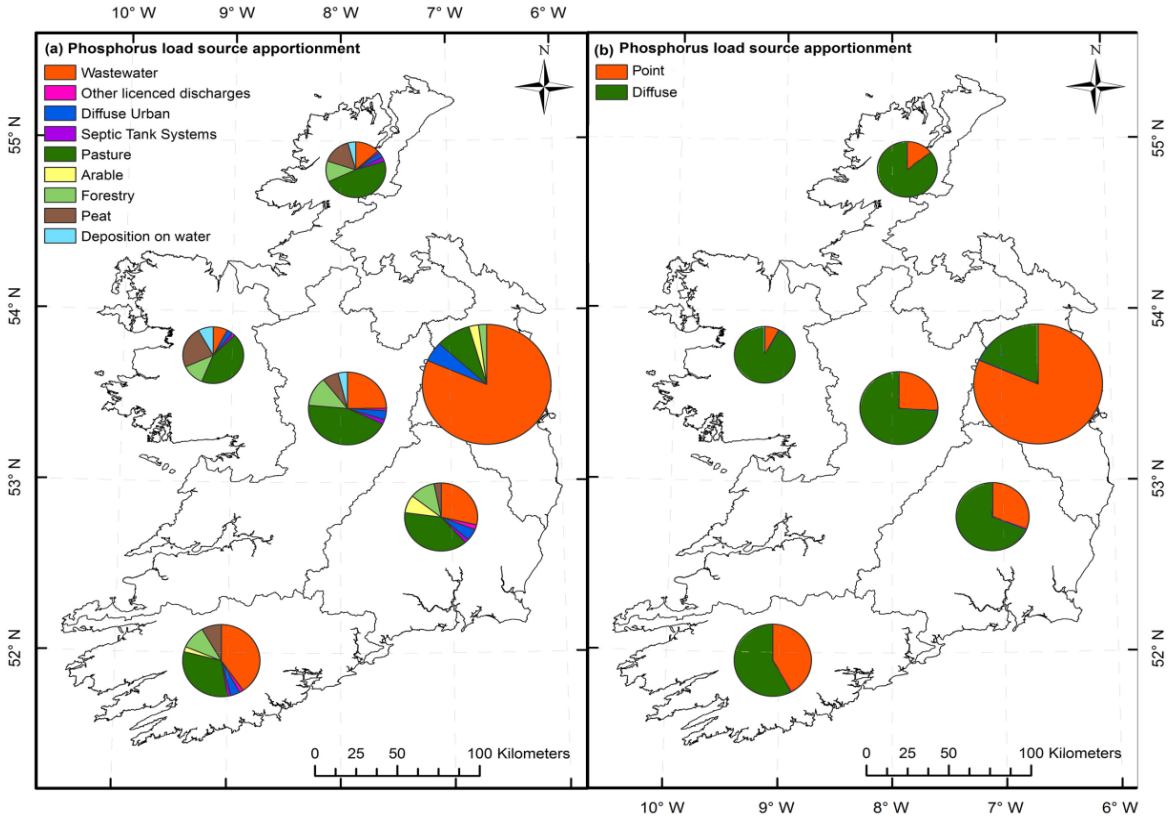

Figure 1.4 Source apportionment of Irish phosphorus loads, adapted from Mockler et al. (2017).

1.5 Phosphorus in the terrestrial environment

In soil, P is present in both organic and inorganic forms. Organic P normally comprises 30-65% of total P present in most soils (Condron et al., 2005), though it can make up as little as 5% or as much as 95% (Paul, 2014). This organic fraction comprises any P which is present in C-based molecules (C-P and C-O-P bonds (Baldwin, 1999)), and originates from plant residues, manure, and soil organic matter; it is comprised primarily of orthophosphate monoesters (largely inositol phosphates) and diesters (nucleic acids, phospholipids, teichoic acid), with a small proportion of phosphonates and certain polyphosphates (Condron et al., 2005). Inorganic P refers to P in all forms not involving carbon, including free, adsorbed, and complexed forms (Turner et al., 2005). Major sources of inorganic P include phosphate mineral species, of which there are about 300 (Nriagu and Moore, 2012), fertilisers, and the mineralisation of organic P by soil microbes.

Total soil P can be divided into three "pools": stable P, reactive P, and solution P (Hansen et al., 2002), with each having organic and inorganic fractions. The primary source of P for plants and microorganisms is the inorganic P present in the soil solution in the form of orthophosphate anions (Condron et al., 2005), generally either HPO_4^{2-} or $H_2PO_4^-$ at a normal soil pH range (Tan, 2000). Soil solution P concentrations are dependent on a host of soil properties including ionic strength, pH, and the concentrations of various anions and cations (Devau et al., 2009). Though the solution P represents only a tiny fraction of total soil P, *c.* 1% (Weil et al., 2016), all of the aforementioned P pools exist in a complex state of dynamic equilibrium with this dissolved fraction (Moody et al., 2013).

Internal cycling of P between these three major soil pools is controlled by a variety of biotic and abiotic processes. As P is continually lost from the soil solution to plant uptake, leaching, and surface runoff, it is constantly replaced by P from the reactive pool by the dissolution of easily soluble precipitates, and the desorption of P loosely bound to soil exchange sites (Frossard et al., 2000). Similarly, when P is added to the soil solution, for example in the form of fertilizer or through microbial mineralisation, it becomes bound in the reactive pool through adoption to available exchange sites and the formation of insoluble precipitates through reaction with minerals in the soil (predominantly Ca, Fe, and Al). The stable pool, which comprises occluded, insoluble, and tightly sorbed inorganic and organic P, in turn gradually replenishes the active pool through slow dissolution of phosphate minerals, though this process is extremely gradual compared to reactions between the reactive and solution

pools. Soil microbes also help to maintain equilibrium in the soil solution, converting organic P to soluble inorganic forms through the process of mineralisation, and also converting this plant-available P to non-available organic P in the process of immobilization (Richardson and Simpson, 2011). The internal cycling of soil P is illustrated in Figure 1.5.

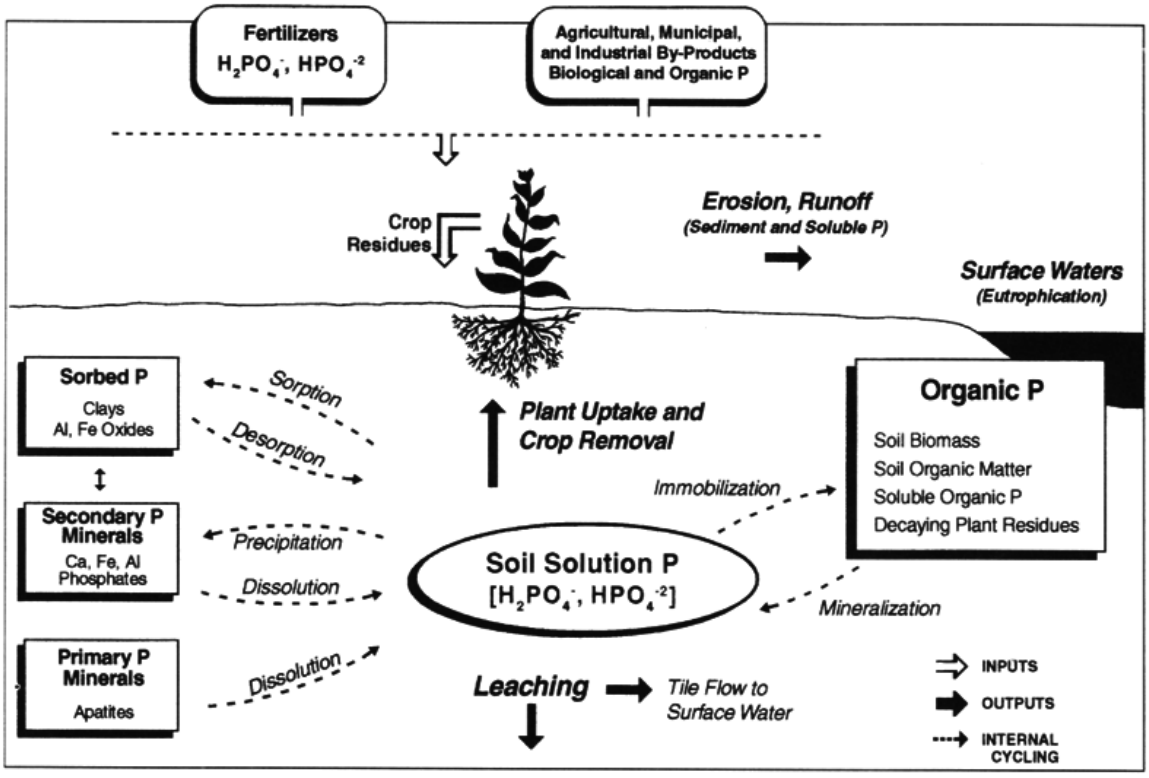

Figure 1.5 The soil phosphorus cycle (Pierzynski et al., 2005)

Regarding the protection of surface waters, two issues are of primary concern - the mobility of the P, which dictates whether or not losses will occur, and the bioavailability of the P, which dictates whether or not the P lost is likely to cause eutrophication of receiving waters. Again, as P relies on water for its transport through the environment, it is the dissolved P in the soil solution (HPO_4^{2-}/$H_2PO_4^-$, polyphosphates, and various organic phosphorus compounds) and particulate P (PP) susceptible to erosion (adsorbed, exchangeable P; organic P; precipitates such as fertilizer or reaction products with calcium (Ca), iron (Fe), aluminium (Al) or other cations; and crystalline minerals/amorphous P) that are potentially lost to receiving waters (Rigler, 1973). This loss occurs through hydrological pathways such as overland flow, subsurface flow (leaching and interflow), and groundwater discharge (base flow and springs) (Brogan et al., 2001). The actual distribution of these fractions in runoff water is largely dependent on local variances in climate, soil, hydrological conditions, and

land use/management (Ulén et al., 2007). Figure 1.6 shows the forms of P present in water.

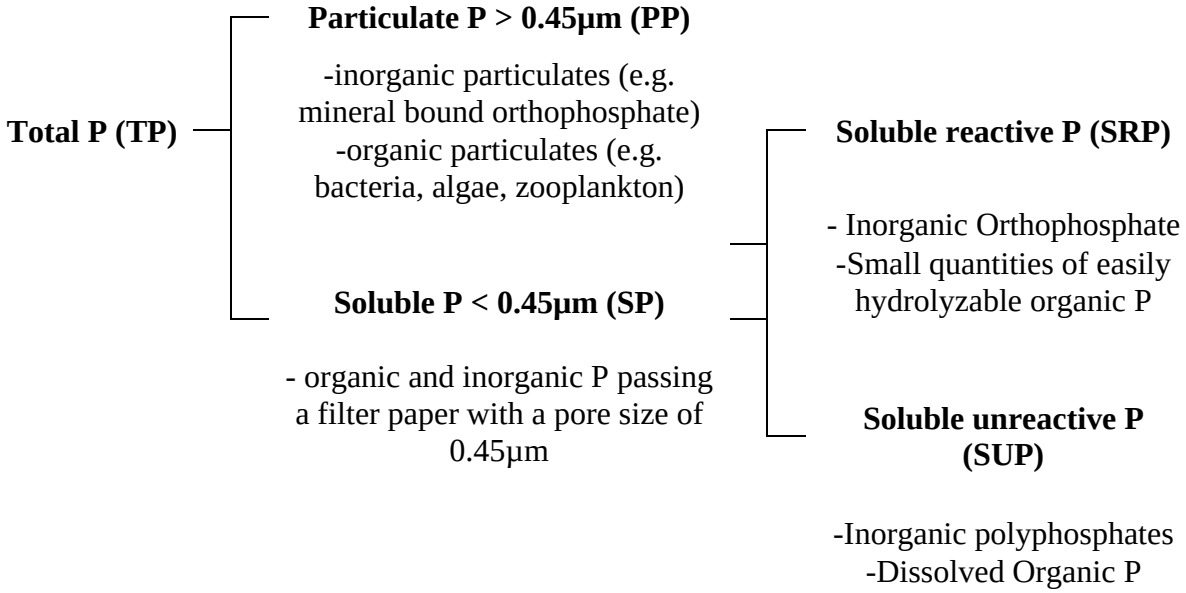

Figure 1.6 Forms and primary constituents of phosphorus in water (adapted from Rigler, 1973)

Regarding bioavailability, algal available P can be defined as "the amount of inorganic P a P-deficient algal population can utilize over a period of 24 h or longer" (Sonzogni et al., 1982). Total phosphorus (TP) has been shown to be a poor indicator of algal available P, as significant portions of particulate phosphorus lost to runoff can't be utilized by plants and algae (Sonzogni et al., 1982), though total soluble P (SP) correlates strongly (Bradford and Peters, 1987). The P forms most readily available to algae are the dissolved P and that fraction of the PP which is in equilibrium with this dissolved portion (Sharpley et al., 1996). Logically then, the protection of the aquatic environment should focus on reducing the inputs of these biologically available fractions of TP losses.

1.6 Mitigation of phosphorus pollution

A large variety of management practices and technologies have been developed to curtail P losses from point and nonpoint sources. Reduction of P losses from municipal wastewater is often achieved at wastewater treatment plants through chemical dosing, enhanced biological removal, or a combination of both (Yeoman et al., 1988; de-Bashan and Bashan, 2004). These techniques, however, are usually applied to wastewaters containing P concentrations which are orders of magnitude greater than those observed from nonpoint sources, and hence are often not applicable to nonpoint low-concentration wastewaters which, for example, may not contain sufficient nutrients to sustain a viable biomass to allow for biological treatment (Wang et al., 2010), or whose P concentrations are so low as to make chemical removal of P cost-prohibitive (Herath, 1996).

The primary strategies implemented to tackle nonpoint source P losses are source reduction and source interception (Ribaudo et al., 2001). Source reduction measures seek to reduce or eliminate P inputs into managed environments such as farmlands or forestry stands, while source interception seeks to interrupt the flow of P from critical source areas to receiving waters by trapping and retaining P present in runoff. The European Commission funded research between 2006 and 2011, COST Action 869 (COST Action, 2006), to evaluate the suitability and cost-effectiveness of various options to reduce P losses to receiving waters, and 83 mitigation methods were identified (Schoumans et al., 2014). Some critical examples of these mitigation measures include source reduction strategies such as matching fertilizer additions with crop deficiencies and balancing animal feed inputs with livestock nutritional requirements (fodder management), and source interception strategies such as utilizing buffer zones, cover vegetation, and wetlands to trap and retain P-laden particles in runoff, and to remove SRP through adsorption to soil and plant uptake. Some commonly implemented P loss control strategies are illustrated in Figure 1.7.

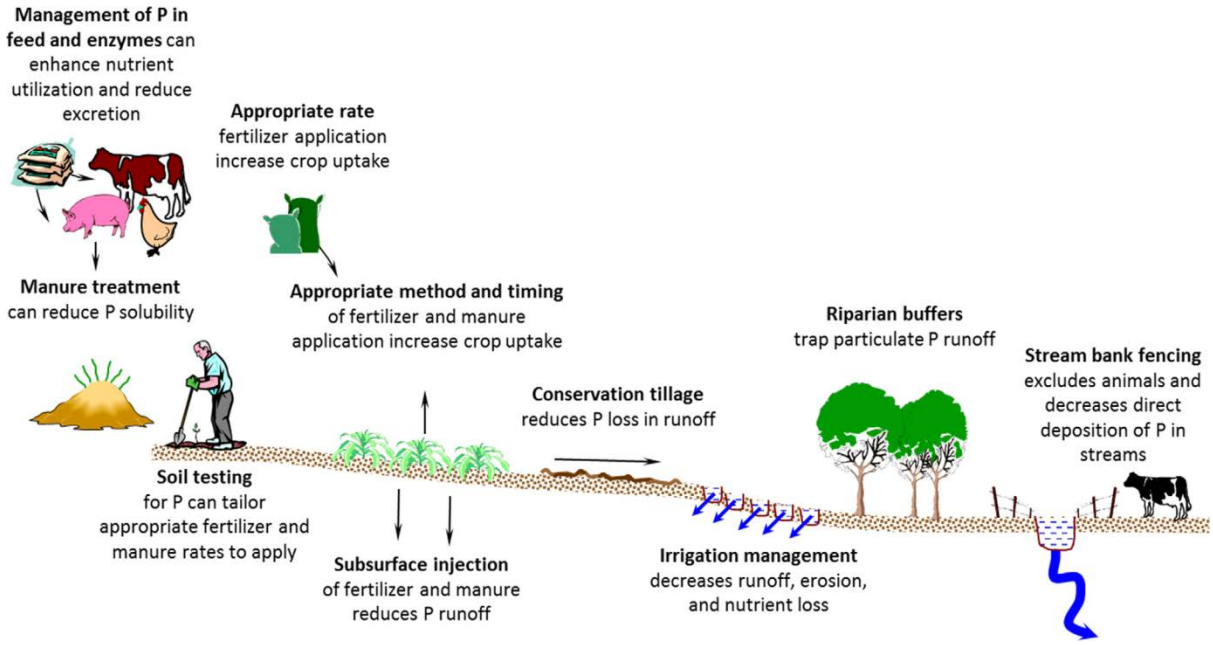

Figure 1.7 Phosphorus loss mitigation strategies (Dodd and Sharpley, 2015)

A large number of best management practices intended to reduce P losses take advantage of the fact that overland flow and transport of particulate P is of primary importance during large rainfall events (Gentry et al., 2007). One of the primary goals of utilizing riparian buffer zones, constructed wetlands, vegetated swales, and settlement ponds etc. is the reduction of suspended solid concentrations in runoff through straining and settling of runoff waters. These strategies are highly effective in situations where the majority of P in runoff is present in particulate form, for example from cultivated lands where 75-90% of P loss is in the form of PP (McDowell et al., 2001), though less so where SP is the dominant form of P in runoff (Kronvang et al., 2005; Uusi-Kämppä, 2005).

Even when implemented properly, these mitigation measures may still fail to produce desired results, and in many cases it may not be possible to implement such measures at all due to some site specific limitation or circumstance. An excellent example of onsite conditions precluding the effective implementation of standard P loss management strategies can be found in the case of forestry harvesting on blanket peat soils - an activity known to result in significant nonpoint P losses (Cummins and Farrell, 2003; Nieminen et al., 2004). Forestry guidelines specify riparian buffer zones as the recommended best management practice to prevent P losses associated with such forestry operations (DAFM, 2015), and while these may successfully retain mobilized sediments, they remain largely ineffective at preventing losses of SP because of the low P sorption capacity of the highly organic peat soil coupled

with insufficient P uptake by riparian vegetation (Rodgers et al., 2010). Given that the P released during harvesting operations largely originates from the harvesting residues (Asam et al., 2014; Finnegan et al., 2014), the reduction of P inputs to site is not a feasible option, as P stored by the trees in foliage essentially originates from fertilizer applications applied decades previously and long-term accumulation from the surrounding soil.

With source control impossible, as in the case of P release from forestry harvesting residues, and where traditionally applied management practices such as riparian buffer zones and constructed wetlands are ineffective, alternative strategies must be employed to prevent potential pollution. A solution may be found in the use of low-cost P sorbing materials, and there is an ever growing body of research emerging which has focused on the identification and characterization of novel sorbents which may be of use in the treatment of various wastewaters (Cucarella and Renman, 2009). Recently, there has also been great interest in the use of P sorbing materials for use in combating P losses from diffuse pollution sources (Buda et al., 2012), and these have been used in applications including substrates in constructed wetlands (Vohla et al., 2005), media in in-drain P removal structures (Penn et al., 2007; Postila et al., 2017) and permeable reactive barriers (Baker et al., 1997), and also the amendment of soils to improve their phosphorus retention capacity (Stout et al., 2000).

1.7 Assessment of potential phosphorus sorbing materials

Adsorption is a surface phenomenon involving the adhesion, via physical or chemical bonds, of molecules from one phase to the surface of another phase (the adsorbent) (Foo and Hameed, 2010); in the context of water and wastewater treatment, adsorption occurs at the interface between the water being treated and a solid adsorbent, though adsorption may also occur at other phase interfaces including liquid-gas, liquid-liquid, and solid-gas (Dąbrowski, 2001). The practical applications of adsorption are myriad, and the phenomenon is exploited across a diverse range of industries for the separation of mixtures and the removal of contaminants and impurities from liquids and gases. Examples of such applications include the removal of organic compounds during drinking water treatment (Crittenden et al., 2012), purification of natural gas (Yang, 2013), and the removal of heavy metals and dyes from industrial effluents (Kadirvelu et al., 2003).

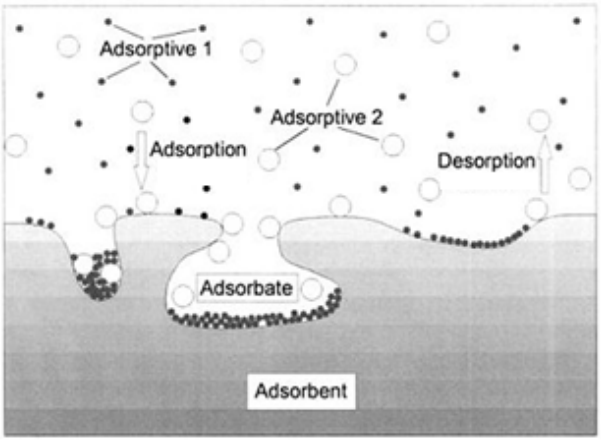

Figure 1.8 A hypothetical system involving the adsorption of two substances onto the surface of a solid adsorbent. (Keller and Staudt, 2005)

The hypothetical adsorption system shown in Figure 1.8 is in state of dynamic equilibrium, with molecules of Adsorptives 1 and 2 constantly moving from the liquid phase and attaching to the solid phase (adsorption), and detaching from the solid phase to enter the liquid phase (desorption). The quantity of adsorbate, i.e. adsorbed molecules, on the surface of the solid phase depends on the concentration of the liquid phase, and equilibrium is reached when rates of adsorption and desorption are equal to one another. This equilibrium relationship is described by a curve called an adsorption isotherm (Figure 1.9). Note also how molecules of Adsorptive 2 occlude adsorption sites that might otherwise be available for Adsorptive 1 in what is termed 'competitive adsorption'.

To prove effective as a filter media, a number of criteria must be met, but the media must first and foremost have a capacity to adsorb P under expected field conditions. In the majority of studies, this criterion is assessed using batch test methodologies (Ali and Gupta, 2007), whereby the reaction between a wastewater and a potential adsorbent is studied by simply placing the two in contact with each other in a container. A great deal of importance has been placed on using batch methods to obtain the adsorption isotherm of the system in question; this is usually achieved by obtaining results from a number of batch tests in which a given mass of adsorbent is allowed to reach equilibrium with solutions of varying initial concentration, though the isotherm may also be obtained by using various masses of adsorbent with the same initial solution concentration.

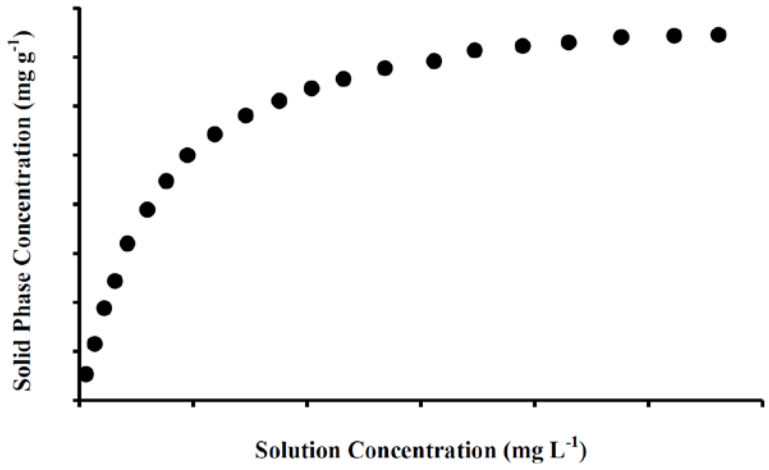

Figure 1.9 A representative adsorption isotherm

The shape of the adsorption isotherm is strongly affected by a multitude of factors including temperature (Aksu, 2001), solution pH (Martins et al., 2004), the presence of competing substances (Newcombe et al., 2002), the solid to liquid ratio (Limousin et al., 2007), the media particle size (Yean et al., 2005), and the agitation speed (Demirbaş et al., 2002). Furthermore, it is assumed that the isotherm describes the equilibrium state; however, some media are very slow to reach equilibrium and therefore, when using standard 24-48 hr batch adsorption techniques, there are many instances where sufficient time may not have been allowed for equilibrium to be achieved (Limousin et al., 2007). Considering the variability inherent in batch testing, their results are not considered to be suitably informative for the design of in-field filtration systems (Zeng, 2003; Rao et al., 2011), and instead, flow-through experiments are recommended for this purpose (Drizo et al., 2002).

Full-scale field testing is likely to be the only way to fully and confidently assess a media for a given purpose (Pratt and Shilton, 2009). However, it is obviously unjustifiable to perform such large-scale, costly investigations with an unproven material; it may have insufficient capacity or kinetic characteristics which render it ineffective, and there are other major considerations such as the possibility of metals or other polluting substances leaching from the media and causing environmental damage (Golder et al., 2006; Yilmaz et al., 2011; Velghe et al., 2012). For these reasons, laboratory-based flow-through experiments should form an integral part of any media assessment procedure (Ali and Gupta, 2007).

Rapid small-scale column tests (RSSCTs) have proven very popular as a flow-through testing methodology capable of producing quick results (Crittenden et al., 1991), and they are excellent for many applications. RSSCTs involve the use of equations to scale down media particle sizes and filter contact times in such a manner as to achieve exact similitude between large-scale and small-scale column tests. However, as a single RSSCT provides predictions for only one single large-scale filter in which exact similitude is maintained, thus individual RSSCTs are required for each possible permutation of full-scale filter design (in terms of loading rate, bed depth etc.); this is a major limitation of the RSSCT approach (Chowdhury, 2013). To obtain more versatile assessments of media performance, fixed-bed modelling approaches like the bed depth service time (BDST) technique proposed by Hutchins (1973) are often used.

Though flow-through experiments are most suitable for assessing the potential in-field performance of media, there has been an over-reliance on batch testing (Ali and Gupta, 2007), with this popularity largely attributable to their convenience and speed (Jang et al., 1998; Gupta et al., 2010). Large-scale flow-through experiments may, by comparison, take weeks (Razali et al., 2007), months (Heal et al., 2003; Bowden et al., 2009), or even years (Baker et al., 1998) to complete. When using RSSCT methodologies, the principles of similitude used to scale down full-scale filters may not always be applicable (Chowdhury, 2013), or even practicable when using adsorbents other than granular activated carbon (GAC) - the media with which the methodology was developed. For example, many low-cost P sorbing materials are of a highly heterogeneous composition compared to GAC, and different particle sizes may differ greatly in their physical, chemical, and therefore, their adsorptive properties, e.g. fly-ash (Erdoğdu and Türker, 1998; Kara et al., 2007), red mud (Gupta et al., 2001) and aluminium drinking water residual (Ippolito et al., 2011).

1.8 Mathematical modelling

The usefulness of batch and column experiments can be greatly expanded with the use of mathematical modelling. For example, in batch adsorption systems, the equilibrium solid-phase adsorbate concentration, q_e (mg g^{-1}), and the equilibrium liquid-phase adsorbate concentration, C_e (mg L^{-1}), may be related to one another thus:

$$qe = \frac{(C_o - C_e)V}{m} \qquad (1)$$

where C_o is the initial liquid-phase adsorbate concentration data (mg L^{-1}), V is the volume of solution (L), and m is the mass of adsorbent material (g). The equilibrium concentration data obtained from batch tests are often fit to an adsorption isotherm model to gain further insight into the adsorption system; the two most commonly used models are the Langmuir (Langmuir, 1918) and the Freundlich (Freundlich, 1906) equations.

The Langmuir equation is as follows:

$$q_e = q_m \frac{K_L C_e}{1 + K_L C_e} \qquad (2)$$

Where q_m is the theoretical maximum solid-phase concentration (i.e. the solid-phase concentration at media saturation) (mg g^{-1}), and K_L is a constant of the Langmuir equation.

As can be seen from the equation above, at high concentrations (i.e. at high values of C_e), the fractional term on the right-hand side of the equation will approach unity (as the 1 in the denominator of the fraction becomes negligible compared to the product of K_L and C_e) and q_e will therefore tend towards a value of q_m. Should the adsorption isotherm data obtained from batch tests fit the Langmuir model, the implication is that the adsorbent surface has a finite adsorption capacity; at high solution concentrations, a monolayer of adsorbate molecules forms on the surface of the adsorbent (once $q_e = q_m$), and after this point it is assumed that the medium has no further adsorption capacity.

The Freundlich adsorption model, in contrast, allows for multilayer adsorption; the Freundlich equation is as follows:

$$q_e = K_F C_e^{\frac{1}{n}} \qquad (3)$$

Where K_F and n are empirical constants of the Freundlich model.

In cases where batch adsorption data best fits the Freundlich model, it is indicative of there being no easily defined maximum adsorption capacity per se (as with the Langmuir equation), rather the Freundlich equation predicts multi-layer adsorption with an exponentially decreasing attraction as the adsorbent becomes increasingly saturated.
While the Langmuir and Freundlich equations are the most widely used isotherm models, there are a vast multitude of other adsorption models available. The Koble-Corrigan (Koble and Corrigan, 1952) equation is an example of a model which is essentially a hybrid of the Langmuir and Freundlich equations (Han et al., 2009), making it ideal for studying media with heterogeneous surfaces (Behnamfard and Salarirad, 2009). The Koble-Corrigan (K-C) equation is as follows:

$$q_e = \frac{A_{KC}C_e{}^P}{1+B_{KC}C_e{}^P} \qquad (4)$$

Where A_{KC}, B_{KC}, and p are constants of the K-C model.

As can be seen, the form of the K-C equation is very similar to that of the Langmuir equation, and indeed if we let p equal to 1, the equation reduces to the Langmuir equation (where B_{KC} is analogous to K_L, and A_{KC} is analogous to the product $q_m.K_L$). As with the Langmuir equation, at high concentrations the unity term in the denominator of the right-hand-side becomes negligible and q_e tends towards an upper limit (i.e. $q_e \approx A_{KC}/B_{KC}$); at low concentrations (where the product $B_{KC}C_e{}^p$ is very small and the denominator approaches a value of 1) however, the K-C model more closely resembles the Freundlich isotherm with A_{KC} being analogous to K_F and p being analogous to 1/n. Having 3 model parameters, the K-C model is particularly versatile for the description of adsorption on heterogeneous surfaces and can often describe a wider range of adsorptive behaviours than either the Freundlich or Langmuir models alone.

The utility of flow-through adsorption experiments is similarly improved with the application of mathematical modelling techniques. In the case of such experiments, modelling is often used as means of using the results from flow-through experiments to predict the breakthrough curves of flow-through filters subjected to loading rates and concentrations other than those used in the initial experiment. A highly popular example of the use of such modelling techniques can be seen in the bed depth service time (BDST) approach developed by Hutchins (1973). This was based on the Adams-Bohart model which is as follows:

$$\ln\left(\frac{C_O}{C_b}-1\right)=K_{BA}N_O\frac{z}{U}-k_{BA}C_Ot_b \qquad (5)$$

where C_b is the effluent breakthrough concentration at a corresponding breakthrough time (mg L^{-1}), t_b (min); K_{BA} is a kinetic constant associated with the B-A model, N_o is the adsorptive capacity of the medium per unit volume of the bed (mg L^{-1}), z is the depth of medium in the filter bed (m), and U is the linear flow velocity (m min^{-1}).

Rearranging this into a linear form gives Hutchins' BDST equation:

$$t_b=\frac{N_o}{C_oU}z-\frac{1}{K_{BA}C_o}\ln\left(\frac{C_o}{C_b}-1\right) \qquad (6)$$

Because this is in the form t_b=a.z-b the B-A model parameters N_o and K_{BA} may be easily calculated from a plot of t_b vs. z:

$$a=\text{slope}=\frac{N_o}{C_oU} \qquad (7)$$

$$b=\text{intercept}=\frac{1}{K_{BA}C_o}\ln\left(\frac{C_o}{C_b}-1\right) \qquad (8)$$

Suppose results are obtained from a number of flow-through adsorption experiments performed using a variety of bed depths; if a graph of t_b against bed depth, z, yields a linear plot, it may be assumed that the BDST model is appropriate for the description of the adsorbate-adsorbent system in question. Importantly, by interpolation and extrapolation using the linear BDST equation, predictions of breakthrough time can be made for filter beds which have depths greater than those initially studied. This allows for scaled down lab-based experiments to be used to design large scale in-field phosphorus removal structures and therefore significantly improves the usefulness of such flow-through investigations.

1.9 Knowledge gaps and project aims

Further research is urgently needed to identify methods of preventing P losses from sources where current best management practices are proving inefficient or ineffective. As outlined above, a prime example of such a case is losses of SRP associated with forestry harvesting on blanket peat soils. The primary goal of this study was to address this need, though it is hoped that the methods and models developed will ultimately also be of use to mitigation of P losses from sources other than peatland forestry. The knowledge gaps addressed by this research are outlined below:

1. It is well known that interactions between adsorbents and wastewaters are extremely complex, influenced by a multitude of factors including solution pH, ionic strength, and concentrations of competing anions and cations. There is a consequent need to investigate each adsorbent-wastewater system on an individual basis, and though low-cost adsorbents have shown great promise in reducing P losses from diffuse sources such as agriculture, their potential to reduce P losses associated with clearfelling of peatland forestry remains largely unexplored.

2. Large-scale column experiments are commonly used for the purpose of assessing a novel adsorbent, but these are labour- and cost-intensive, taking many weeks, months, or even years to complete. They also necessitate the use of very large volumes of wastewater, and this wastewater must be regularly sourced in order for it to be representative of onsite conditions. Limitations of current RSSCT methodologies can make them unsuitable for use with many low-cost adsorbents - particularly those which are highly variable in terms of physical and chemical makeup, and there is therefore a need for a rapid way to investigate media under flow-through conditions that will give comparable results to long-term column studies.

3. Another major limitation of current RSSCT methodologies is that individual RSSCTs are required to predict the performance of each possible large-scale filter. Mathematical models exist to address this concern, but these models are usually developed using well-structured 'ideal' adsorbents such as GAC, and hence often do not satisfactorily describe the performance of flow-through reactors utilising low-cost adsorbents of variable composition. There is therefore a need to develop a modelling strategy that will allow researchers to use experimental results from laboratory-based

tests with low-cost adsorbents to predict the potential performance of hypothetical large-scale filters with sufficient accuracy to warrant pilot-scale in-field trials.

4. With potential media identified, there is a need to perform column studies using real wastewater (in this case, forestry runoff and dairy-soiled water), both to address the shortcomings of batch tests, and to assess other practicalities such as potential pollution-swapping issues which might preclude a medium from in-field usage.

The primary aims of this study were:

1. To identify media which would be capable of removing dissolved P from solution in a solution matrix representative of peat forestry runoff. This is intended to address the first knowledge gap identified above.

2. To develop a RSSCT methodology that is applicable to low-cost adsorbents which have highly variable physical and chemical properties, and demonstrate that this methodology may be used to predict the performance of large scale columns. This is intended to address the second knowledge gap identified above.

3. To develop and demonstrate the validity of a modelling procedure which will allow the user to make predictions as to the potential efficacy of an in-field filter using results from the RSSCTs, whose methodology was developed previously. This is intended to address the third knowledge gap identified above.

4. To assess the in-field potential of the media which showed greatest promise in batch tests by applying the experimental and modelling approaches developed previously, while also addressing possible pollution swapping issues which might preclude their use in real world applications. This is intended to address the fourth knowledge gap identified above.

1.10 Structure of Dissertation

This thesis comprises four papers, the first three of which are published and the fourth of which is currently in review for publication.

Chapter 2 presents an overview of experimental methodologies and schematics of the experimental apparatuses used .

Chapter 3 comprises a published paper, "Use of amendments in a peat soil to reduce phosphorus losses from forestry operations" (Ecological Engineering 85: 193-200). This chapter reports on the results of batch tests performed with various P sorbing materials, and examines the influence of a peat soil environment on their ability to remove P from aqueous solution. This addresses the first aim of this study.

Chapter 4 comprises a published paper, "Evaluating the long-term performance of low-cost adsorbents using small-scale adsorption column experiments" (Water Research 101: 429-440). This chapter investigates the use of small-scale column experiments to predict the performances of large-scale adsorption and introduces a model, which can describe the convex breakthrough curves often observed in flow through experiments using low-cost adsorbents. This addresses the second aim of this study.

Chapter 5 comprises a published paper, "Predicting the propagation of concentration and saturation fronts in fixed-bed filters" (Water Research 123: 556-568). This chapter describes the development of a modelling strategy, which allows a user to predict the long-term performances of large-scale column experiments using results from multiple short-term small-scale column experiments. This addresses the third aim of this study.

Chapter 6 comprises a paper, currently under review, entitled, "A novel method to rapidly assess the suitability of low-cost adsorbents for the mitigation of point and nonpoint source phosphorus losses". This chapter reports on the results of small-scale column experiments using aluminium water treatment residual and crushed concrete to remove P from peatland forestry runoff and dairy-soiled water. The release of metals and the effect of each media on wastewater pH was also investigated. This addresses the fourth aim of this study.

Chapter 7 presents the conclusions and recommendations.

1.11 References

Acreman, M., 2012. The Hydrology of the UK: A Study of Change. Routledge.

Aksu, Z., 2001. Equilibrium and kinetic modelling of cadmium(II) biosorption by C. vulgaris in a batch system: effect of temperature. Sep. Purif. Technol. 21, 285–294. doi:10.1016/S1383-5866(00)00212-4

Alexander, R.B., Boyer, E.W., Smith, R.A., Schwarz, G.E., Moore, R.B., 2007. The Role of Headwater Streams in Downstream Water Quality1. JAWRA J. Am. Water Resour. Assoc. 43, 41–59. doi:10.1111/j.1752-1688.2007.00005.x

Ali, I., Gupta, V.K., 2007. Advances in water treatment by adsorption technology. Nat. Protoc. 1, 2661–2667. doi:10.1038/nprot.2006.370

Anderson, D.M., Glibert, P.M., Burkholder, J.M., 2002. Harmful algal blooms and eutrophication: Nutrient sources, composition, and consequences. Estuaries 25, 704–726. doi:10.1007/BF02804901

Ashley, K., Cordell, D., Mavinic, D., 2011. A brief history of phosphorus: From the philosopher's stone to nutrient recovery and reuse. Chemosphere, The Phosphorus Cycle 84, 737–746. doi:10.1016/j.chemosphere.2011.03.001

Bailey-Watts, A.E., 1997. Phytoplankton ecology of the larger Scottish lochs. Bot. J. Scotl. 49, 397–403. doi:10.1080/03746609708684884

Baker, M.J., Blowes, D.W., Placek, C.J., 1997. Phosphorous adsorption and precipitation in a permeable reactive wall: applications for wastewater disposal systems. USDOE, Washington, DC (United States).

Baker, M.J., Blowes, D.W., Ptacek, C.J., 1998. Laboratory Development of Permeable Reactive Mixtures for the Removal of Phosphorus from Onsite Wastewater Disposal Systems. Environ. Sci. Technol. 32, 2308–2316. doi:10.1021/es970934w

Baldwin, D.S., 1999. Nutrients in freshwater ecosystems. Best Pract. Land-Based Salmon. Farming Options Treat. Re-Use Dispos. Effl. Mar. Freshw. Resour. Inst. Alexandra 18–25.

Behnamfard, A., Salarirad, M.M., 2009. Equilibrium and kinetic studies on free cyanide adsorption from aqueous solution by activated carbon. J. Hazard. Mater. 170, 127–133. doi:10.1016/j.jhazmat.2009.04.124

Beardsley, T.M., 2011. Peak Phosphorus. BioScience 61, 91–91. doi:10.1525/bio.2011.61.2.1

Blomqvist, S., Gunnars, A., Elmgren, R., 2004. Why the limiting nutrient differs between temperate coastal seas and freshwater lakes: A matter of salt. Limnol. Oceanogr. 49, 2236–2241. doi:10.4319/lo.2004.49.6.2236

Bouraoui, F., Grizzetti, B., 2014. Modelling mitigation options to reduce diffuse nitrogen water pollution from agriculture. Sci. Total Environ. 468, 1267–1277. doi:10.1016/j.scitotenv.2013.07.066

Bouwman, L., Goldewijk, K.K., Hoek, K.W.V.D., Beusen, A.H.W., Vuuren, D.P.V., Willems, J., Rufino, M.C., Stehfest, E., 2013. Exploring global changes in nitrogen and phosphorus cycles in agriculture induced by livestock production over the 1900–2050 period. Proc. Natl. Acad. Sci. 110, 20882–20887. doi:10.1073/pnas.1012878108

Bowden, L.I., Jarvis, A.P., Younger, P.L., Johnson, K.L., 2009. Phosphorus Removal from Waste Waters Using Basic Oxygen Steel Slag. Environ. Sci. Technol. 43, 2476–2481. doi:10.1021/es801626d

Bradford, M.E., Peters, R.H., 1987. The relationship between chemically analyzed phosphorus fractions and bioavailable phosphorus1. Limnol. Oceanogr. 32, 1124–1137. doi:10.4319/lo.1987.32.5.1124

Brogan, J., Crowe, M., Carty, G., 2001. Developing a National Phosphorus Balance for Agriculture in Ireland: A Discussion Document. Environmental Protection Agency.

Buda, A.R., Koopmans, G.F., Bryant, R.B., Chardon, W.J., 2012. Emerging Technologies for Removing Nonpoint Phosphorus from Surface Water and Groundwater: Introduction. J. Environ. Qual. 41, 621–627. doi:10.2134/jeq2012.0080

Carey, R.O., Migliaccio, K.W., 2009. Contribution of Wastewater Treatment Plant Effluents to Nutrient Dynamics in Aquatic Systems: A Review. Environ. Manage. 44, 205–217. doi:10.1007/s00267-009-9309-5

Carpenter, S.R., 2005. Eutrophication of aquatic ecosystems: Bistability and soil phosphorus. Proc. Natl. Acad. Sci. U. S. A. 102, 10002–10005. doi:10.1073/pnas.0503959102

Carpenter, S.R., Bennett, E.M., 2011. Reconsideration of the planetary boundary for phosphorus. Environ. Res. Lett. 6, 014009. doi:10.1088/1748-9326/6/1/014009

Chowdhury, Z.K., 2013. Activated Carbon: Solutions for Improving Water Quality. American Water Works Association.

Compton, J., Mallinson, D., Glenn, C.R., Filippelli, G., Föllmi, K., Shields, G., Zanin, Y., 2000. Variations in the global phosphorus cycle.

Condron, L.M., Turner, B.L., Cade-Menun, B.J., 2005. Chemistry and Dynamics of Soil Organic Phosphorus. Phosphorus Agric. Environ. agronomymonogra, 87–121. doi:10.2134/agronmonogr46.c4

Conley, D.J., Schelske, C.L., Stoermer, E.F., 1993. Modification of the biogeochemical cycle of silica with eutrophication. Mar. Ecol. Prog. Ser. 101, 179–192.

Cooke, G.D., Kennedy, R.H., 2001. Managing drinking water supplies. Lake Reserv. Manag. 17, 157–174.

Cordell, D., Drangert, J.-O., White, S., 2009. The story of phosphorus: Global food security and food for thought. Glob. Environ. Change, Traditional Peoples and Climate Change 19, 292–305. doi:10.1016/j.gloenvcha.2008.10.009

Cordell, D., White, S., 2011. Peak Phosphorus: Clarifying the Key Issues of a Vigorous Debate about Long-Term Phosphorus Security. Sustainability 3, 2027–2049. doi:10.3390/su3102027

Correll, D.L., 1999. Phosphorus: a rate limiting nutrient in surface waters. Poult. Sci. 78, 674–682.

COST Action 869, 2006: Mitigation options for nutrient reduction in surface water and groundwaters, in: 164th CSO Meeting. pp. 29–30.

Crittenden, J.C., Howe, K.J., Hand, D.W., Tchobanoglous, G., Trussell, R.R., 2012. Principles of Water Treatment. John Wiley & Sons, Incorporated.

Crittenden, J.C., Reddy, P.S., Arora, H., Trynoski, J., Hand, D.W., Perram, D.L., Summers, R.S., 1991. Predicting GAC Performance With Rapid Small-Scale Column Tests. J. Am. Water Works Assoc. 83, 77–87.

Cucarella, V., Renman, G., 2009. Phosphorus Sorption Capacity of Filter Materials Used for On-site Wastewater Treatment Determined in Batch Experiments-A Comparative Study. J. Environ. Qual. 38, 381–392. doi:10.2134/jeq2008.0192

Cummins, T., Farrell, E.P., 2003. Biogeochemical impacts of clearfelling and reforestation on blanket peatland streams I. phosphorus. For. Ecol. Manag. 180, 545–555. doi:10.1016/S0378-1127(02)00648-5

Dąbrowski, A., 2001. Adsorption — from theory to practice. Adv. Colloid Interface Sci. 93, 135–224. doi:10.1016/S0001-8686(00)00082-8

Department of Agriculture, Food and the Marine (DAFM), 2015. Forestry Standards Manual.

de-Bashan, L.E., Bashan, Y., 2004. Recent advances in removing phosphorus from wastewater and its future use as fertilizer (1997–2003). Water Res. 38, 4222–4246. doi:10.1016/j.watres.2004.07.014

Demirbaş, E., Kobya, M., Öncel, S., Şencan, S., 2002. Removal of Ni(II) from aqueous solution by adsorption onto hazelnut shell activated carbon: equilibrium studies. Bioresour. Technol. 84, 291–293. doi:10.1016/S0960-8524(02)00052-4

Devau, N., Cadre, E.L., Hinsinger, P., Jaillard, B., Gérard, F., 2009. Soil pH controls the environmental availability of phosphorus: Experimental and mechanistic modelling approaches. Appl. Geochem. 24, 2163–2174. doi:10.1016/j.apgeochem.2009.09.020

Dodd, R.J., Sharpley, A.N., 2015. Recognizing the role of soil organic phosphorus in soil fertility and water quality. Resour. Conserv. Recycl., Losses and Efficiencies in Phosphorus Management 105, 282–293. doi:10.1016/j.resconrec.2015.10.001

Dodds, W.K.K., Welch, E.B., 2000. Establishing nutrient criteria in streams. J. North Am. Benthol. Soc. 19, 186–196. doi:10.2307/1468291

Downing, J.A., McCauley, E., 1992. The nitrogen: phosphorus relationship in lakes. Limnol. Oceanogr. 37, 936–945.

Drizo, A., Comeau, Y., Forget, C., Chapuis, R.P., 2002. Phosphorus saturation potential: A parameter for estimating the longevity of constructed wetland systems. Environ. Sci. Technol. 36, 4642–4648.

Elser, J.J., Bracken, M.E.S., Cleland, E.E., Gruner, D.S., Harpole, W.S., Hillebrand, H., Ngai, J.T., Seabloom, E.W., Shurin, J.B., Smith, J.E., 2007. Global analysis of nitrogen and phosphorus limitation of primary producers in freshwater, marine and terrestrial ecosystems. Ecol. Lett. 10, 1135–1142. doi:10.1111/j.1461-0248.2007.01113.x

Erdoğdu, K., Türker, P., 1998. Effects of fly ash particle size on strength of portland cement fly ash mortars. Cem. Concr. Res. 28, 1217–1222. doi:10.1016/S0008-8846(98)00116-1

Filippelli, G.M., 2008. The Global Phosphorus Cycle: Past, Present, and Future. Elements 4, 89–95. doi:10.2113/GSELEMENTS.4.2.89

Foo, K.Y., Hameed, B.H., 2010. Insights into the modeling of adsorption isotherm systems. Chem. Eng. J. 156, 2–10. doi:10.1016/j.cej.2009.09.013

Freundlich, 1906. Uber die adsorption in losungen. Z. Für Phys. Chem. 57, 384–470.

Frossard, E., Condron, L.M., Oberson, A., Sinaj, S., Fardeau, J.C., 2000. Processes Governing Phosphorus Availability in Temperate Soils. J. Environ. Qual. 29, 15–23. doi:10.2134/jeq2000.00472425002900010003x

Gentry, L.E., David, M.B., Royer, T.V., Mitchell, C.A., Starks, K.M., 2007. Phosphorus Transport Pathways to Streams in Tile-Drained Agricultural Watersheds. J. Environ. Qual. 36, 408–415. doi:10.2134/jeq2006.0098

Golder, A.K., Samanta, A.N., Ray, S., 2006. Removal of phosphate from aqueous solutions using calcined metal hydroxides sludge waste generated from electrocoagulation. Sep. Purif. Technol. 52, 102–109. doi:10.1016/j.seppur.2006.03.027

Gössling, S., Peeters, P., Hall, C.M., Ceron, J.-P., Dubois, G., Lehmann, L.V., Scott, D., 2012. Tourism and water use: Supply, demand, and security. An international review. Tour. Manag. 33, 1–15. doi:10.1016/j.tourman.2011.03.015

Greeson, P.E., 1969. Lake Eutrophication–a Natural Process1. JAWRA J. Am. Water Resour. Assoc. 5, 16–30. doi:10.1111/j.1752-1688.1969.tb04920.x

Grigg, D., 1987. industrial revolution and land transformation. Land Transform. Agric. Ed. MG Wolman FGA Fournier.

Grobbelaar, J.U., House, W.A., 1995. Phosphorus as a limiting resource in inland waters; interactions with nitrogen. SCOPE-Sci. Comm. Probl. Environ. Int. Counc. Sci. UNIONS 54, 255–274.

Gupta, V.K., Gupta, M., Sharma, S., 2001. Process development for the removal of lead and chromium from aqueous solutions using red mud—an aluminium industry waste. Water Res. 35, 1125–1134. doi:10.1016/S0043-1354(00)00389-4

Gupta, V.K., Rastogi, A., Nayak, A., 2010. Adsorption studies on the removal of hexavalent chromium from aqueous solution using a low cost fertilizer industry waste material. J. Colloid Interface Sci. 342, 135–141. doi:10.1016/j.jcis.2009.09.065

Hallegraeff, G.M., 1993. A review of harmful algal blooms and their apparent global increase. Phycologia 32, 79–99. doi:10.2216/i0031-8884-32-2-79.1

Han, R., Zhang, J., Han, P., Wang, Y., Zhao, Z., Tang, M., 2009. Study of equilibrium, kinetic and thermodynamic parameters about methylene blue adsorption onto natural zeolite. Chem. Eng. J. 145, 496–504. doi:10.1016/j.cej.2008.05.003

Hansen, N.C., Daniel, T.C., Sharpley, A.N., Lemunyon, J.L., 2002. The fate and transport of phosphorus in agricultural systems. J. Soil Water Conserv. 57, 408–417.

Havens, K.E., Aumen, N.G., James, R.T. (Okeechobee S.R.D., Smith, V.H., 1996. Rapid ecological changes in a large suptropical lake undergoing cultural eutrophication. Ambio Swed.

Heal, K., Younger, P.L., Smith, K., Glendinning, S., Quinn, P., Dobbie, K., 2003. Novel use of ochre from mine water treatment plants to reduce point and diffuse phosphorus pollution. Land Contam. Reclam. 11, 145–152. doi:10.2462/09670513.808

Heathwaite, L., Sharpley, A., Gburek, W., 2000. A Conceptual Approach for Integrating Phosphorus and Nitrogen Management at Watershed Scales. J. Environ. Qual. 29, 158–166. doi:10.2134/jeq2000.00472425002900010020x

Heisler, J., Glibert, P.M., Burkholder, J.M., Anderson, D.M., Cochlan, W., Dennison, W.C., Dortch, Q., Gobler, C.J., Heil, C.A., Humphries, E., Lewitus, A., Magnien, R., Marshall, H.G., Sellner, K., Stockwell, D.A., Stoecker, D.K., Suddleson, M., 2008. Eutrophication and harmful algal blooms: A scientific consensus. Harmful Algae, HABs and Eutrophication 8, 3–13. doi:10.1016/j.hal.2008.08.006

Herath, G., 1996. A Review of Costs of Removing Phosphorus to Control Algal Blooms Waterways. Aust.J.Environ.Manag.3, 189–201.doi:10.1080/14486563.1996.10648355

Hilton, J., O'Hare, M., Bowes, M.J., Jones, J.I., 2006. How green is my river? A new paradigm of eutrophication in rivers. Sci. Total Environ., Monitoring and modelling the impacts of global change on European freshwater ecosystems 365, 66–83. doi:10.1016/j.scitotenv.2006.02.055

Howarth, R.W., Marino, R., 2006. Nitrogen as the limiting nutrient for eutrophication in coastal marine ecosystems: Evolving views over three decades. Limnol. Oceanogr. 51, 364–376. doi:10.4319/lo.2006.51.1_part_2.0364

Hutchins, R., 1973. New method simplifies design of activated carbon systems, Water Bed Depth Service Time analysis. J Chem Eng Lond 81, 133–138.

Ippolito, J.A., Barbarick, K.A., Elliott, H.A., 2011. Drinking water treatment residuals: A review of recent uses. J. Environ. Qual. 40, 1–12.

Jang, A., Choi, Y.S., Kim, I.S., 1998. Batch and column tests for the development of an immobilization technology for toxic heavy metals in contaminated soils of closed mines. Water Sci. Technol. 37, 81–88.

Jeppesen, E., Peder Jensen, J., SØndergaard, M., Lauridsen, T., Landkildehus, F., 2000. Trophic structure, species richness and biodiversity in Danish lakes: changes along a phosphorus gradient. Freshw. Biol. 45, 201–218. doi:10.1046/j.1365-2427.2000.00675.x

Kadirvelu, K., Kavipriya, M., Karthika, C., Radhika, M., Vennilamani, N., Pattabhi, S., 2003. Utilization of various agricultural wastes for activated carbon preparation and application for the removal of dyes and metal ions from aqueous solutions. Bioresour. Technol. 87, 129–132. doi:10.1016/S0960-8524(02)00201-8

Kara, S., Aydiner, C., Demirbas, E., Kobya, M., Dizge, N., 2007. Modeling the effects of adsorbent dose and particle size on the adsorption of reactive textile dyes by fly ash. Desalination 212, 282–293. doi:10.1016/j.desal.2006.09.022

Keller, J.U., Staudt, R., 2005. Gas Adsorption Equilibria: Experimental Methods and Adsorptive Isotherms. Springer Science & Business Media.

Khan, F.A., Ansari, A.A., 2005. Eutrophication: An Ecological Vision. Bot. Rev. 71, 449–482. doi:10.1663/0006-8101(2005)071[0449:EAEV]2.0.CO;2

Koble, R.A., Corrigan, T.E., 1952. Adsorption Isotherms for Pure Hydrocarbons. Ind. Eng. Chem. 44, 383–387. doi:10.1021/ie50506a049

Kronvang, B., Laubel, A., Larsen, S.E., Andersen, H.E., Djurhuus, J., 2005. Buffer zones as a sink for sediment and phosphorus between the field and stream: Danish field experiences. Water Sci. Technol. 51, 55–62.

Langmuir, I., 1918. The adsorption of gases on plane surfaces of glass, mica and platinum. J. Am. Chem. Soc. 40, 1361–1403.

Lewis, W.M., Wurtsbaugh, W.A., 2008. Control of Lacustrine Phytoplankton by Nutrients: Erosion of the Phosphorus Paradigm. Int. Rev. Hydrobiol. 93, 446–465. doi:10.1002/iroh.200811065

Lewis, W.M., Wurtsbaugh, W.A., Paerl, H.W., 2011. Rationale for Control of Anthropogenic Nitrogen and Phosphorus to Reduce Eutrophication of Inland Waters. Environ. Sci. Technol. 45, 10300–10305. doi:10.1021/es202401p

Lieth, H., Whittaker, R.H., 2012. Primary Productivity of the Biosphere. Springer Science & Business Media.

Limousin, G., Gaudet, J.-P., Charlet, L., Szenknect, S., Barthès, V., Krimissa, M., 2007. Sorption isotherms: A review on physical bases, modeling and measurement. Appl. Geochem. 22, 249–275. doi:10.1016/j.apgeochem.2006.09.010

Manzoni, S., Trofymow, J.A., Jackson, R.B., Porporato, A., 2010. Stoichiometric controls on carbon, nitrogen, and phosphorus dynamics in decomposing litter. Ecol. Monogr. 80, 89–106. doi:10.1890/09-0179.1

Martins, R.J.E., Pardo, R., Boaventura, R.A.R., 2004. Cadmium(II) and zinc(II) adsorption by the aquatic moss Fontinalis antipyretica: effect of temperature, pH and water hardness. Water Res. 38, 693–699. doi:10.1016/j.watres.2003.10.013

McDowell, R.W., Sharpley, A.N., Condron, L.M., Haygarth, P.M., Brookes, P.C., 2001. Processes controlling soil phosphorus release to runoff and implications for agricultural management. Nutr. Cycl. Agroecosystems 59, 269–284. doi:10.1023/A:1014419206761

Mockler, E.M., Deakin, J., Archbold, M., Gill, L., Daly, D., Bruen, M., 2017. Sources of nitrogen and phosphorus emissions to Irish rivers and coastal waters: Estimates from a nutrient load apportionment framework. Sci. Total Environ. 601, 326–339. doi:10.1016/j.scitotenv.2017.05.186

Moody, P.W., Speirs, S.D., Scott, B.J., Mason, S.D., 2013. Soil phosphorus tests I: What soil phosphorus pools and processes do they measure? Crop Pasture Sci. 64, 461–468. doi:10.1071/CP13112

Moore, C.M., Mills, M.M., Arrigo, K.R., Berman-Frank, I., Bopp, L., Boyd, P.W., Galbraith, E.D., Geider, R.J., Guieu, C., Jaccard, S.L., Jickells, T.D., La Roche, J., Lenton, T.M., Mahowald, N.M., Marañón, E., Marinov, I., Moore, J.K., Nakatsuka, T., Oschlies, A., Saito, M.A., Thingstad, T.F., Tsuda, A., Ulloa, O., 2013. Processes and patterns of oceanic nutrient limitation. Nat. Geosci. 6, 701–710. doi:10.1038/ngeo1765

Moorkens, E.A., 1999. Conservation management of the freshwater pearl mussel Margaritifera margaritifera. Part 1: Biology of the species and its present situation in Ireland. Ir. Wildl. Man. 8, 4–31.

Neset, T.-S.S., Cordell, D., 2012. Global phosphorus scarcity: identifying synergies for a sustainable future. J. Sci. Food Agric. 92, 2–6. doi:10.1002/jsfa.4650

Newcombe, G., Morrison, J., Hepplewhite, C., Knappe, D.R.U., 2002. Simultaneous adsorption of MIB and NOM onto activated carbon. Carbon 40, 2147–2156. doi:10.1016/S0008-6223(02)00098-2

Nieminen, M., others, 2004. Export of dissolved organic carbon, nitrogen and phosphorus following clear-cutting of three Norway spruce forests growing on drained peatlands in southern Finland.

Nriagu, J.O., Moore, P.H., 2012. Phosphate Minerals. Springer Science & Business Media.

Paerl, H.W., Valdes, L.M., Pinckney, J.L., Piehler, M.F., Dyble, J., Moisander, P.H., 2003. Phytoplankton Photopigments as Indicators of Estuarine and Coastal Eutrophication. BioScience 53, 953–964. doi:10.1641/0006-3568(2003)053[0953:PPAIOE]2.0.CO;2

Paul, E.A., 2014. Soil Microbiology, Ecology and Biochemistry. Academic Press.

Penn, C.J., Bryant, R.B., Kleinman, P.J.A., Allen, A.L., 2007. Removing dissolved phosphorus from drainage ditch water with phosphorus sorbing materials. J. Soil Water Conserv. 62, 269–276.

Pierzynski, G.M., Vance, G.F., Sims, J.T., 2005. Soils and Environmental Quality. CRC Press.

Postila, H., Karjalainen, S.M., Kløve, B., 2017. Can limestone, steel slag or man-made sorption materials be used to enhance phosphate-phosphorus retention in treatment wetland for peat extraction runoff with low phosphorous concentration? Ecol. Eng. 98, 403–409. doi:10.1016/j.ecoleng.2016.05.042

Pratt, C., Shilton, A., 2009. Suitability of adsorption isotherms for predicting the retention capacity of active slag filters removing phosphorus from wastewater. Water Sci. Technol. 59, 1673–1678. doi:10.2166/wst.2009.163

Pretty, J.N., Mason, C.F., Nedwell, D.B., Hine, R.E., Leaf, S., Dils, R., 2003. Environmental Costs of Freshwater Eutrophication in England and Wales. Environ. Sci. Technol. 37, 201–208. doi:10.1021/es020793k

Rao, K.S., Anand, S., Venkateswarlu, P., 2011. Modeling the kinetics of Cd(II) adsorption on Syzygium cumini L leaf powder in a fixed bed mini column. J. Ind. Eng. Chem. 17, 174–181. doi:10.1016/j.jiec.2011.02.003

Rao, N.S., Easton, Z.M., Schneiderman, E.M., Zion, M.S., Lee, D.R., Steenhuis, T.S., 2009. Modeling watershed-scale effectiveness of agricultural best management practices to reduce phosphorus loading. J. Environ. Manage. 90, 1385–1395. doi:10.1016/j.jenvman.2008.08.011

Razali, M., Zhao, Y.Q., Bruen, M., 2007. Effectiveness of a drinking-water treatment sludge in removing different phosphorus species from aqueous solution. Sep. Purif. Technol. 55, 300–306.

Reynolds, C.S., 1998. What factors influence the species composition of phytoplankton in lakes of different trophic status?, in: Phytoplankton and Trophic Gradients, Developments in Hydrobiology. Springer, Dordrecht, pp. 11–26. doi:10.1007/978-94-017-2668-9_2

Ribaudo, M.O., Heimlich, R., Claassen, R., Peters, M., 2001. Least-cost management of nonpoint source pollution: source reduction versus interception strategies for controlling nitrogen loss in the Mississippi Basin. Ecol. Econ. 37, 183–197. doi:10.1016/S0921-8009(00)00273-1

Richardson, A.E., Simpson, R.J., 2011. Soil Microorganisms Mediating Phosphorus Availability Update on Microbial Phosphorus. Plant Physiol. 156, 989–996. doi:10.1104/pp.111.175448

Rigler, F.H., 1973. A dynamic view of the phosphorus cycle in lakes. Environ. Phosphorus Handb. 539–572.

Rodgers, M., O'Connor, M., Healy, M.G., O'Driscoll, C., Asam, Z.-Z., Nieminen, M., Poole, R., Müller, M., Xiao, L., 2010. Phosphorus release from forest harvesting on an upland blanket peat catchment. For. Ecol. Manag. 260, 2241–2248.

Ruttenberg, K.C., 2003. The Global Phosphorus Cycle. Treatise Geochem. 8, 682. doi:10.1016/B0-08-043751-6/08153-6

Salameh, E., Harahsheh, S., 2010. Eutrophication processes in Arid climates, in: Eutrophication: Causes, Consequences and Control. Springer, pp. 69–90.

Schindler, D.W., 1977. Evolution of phosphorus limitation in lakes. Science 195, 260–262.

Schindler, D.W., Carpenter, S.R., Chapra, S.C., Hecky, R.E., Orihel, D.M., 2016. Reducing Phosphorus to Curb Lake Eutrophication is a Success. Environ. Sci. Technol. 50, 8923–8929. doi:10.1021/acs.est.6b02204

Schindler, D.W., Hecky, R.E., Findlay, D.L., Stainton, M.P., Parker, B.R., Paterson, M.J., Beaty, K.G., Lyng, M., Kasian, S.E.M., 2008. Eutrophication of lakes cannot be controlled by reducing nitrogen input: Results of a 37-year whole-ecosystem experiment. Proc. Natl. Acad. Sci. 105, 11254–11258. doi:10.1073/pnas.0805108105

Schoumans, O.F., Chardon, W.J., Bechmann, M.E., Gascuel-Odoux, C., Hofman, G., Kronvang, B., Rubæk, G.H., Ulén, B., Dorioz, J.-M., 2014. Mitigation options to reduce phosphorus losses from the agricultural sector and improve surface water quality: A review. Sci. Total Environ. 468, 1255–1266. doi:10.1016/j.scitotenv.2013.08.061

Sharpley, A., Daniel, T.C., Sims, J.T., Pote, D.H., 1996. Determining environmentally sound soil phosphorus levels. J. Soil Water Conserv. 51, 160–166.

Sharpley, A., Foy, B., Withers, P., 2000. Practical and Innovative Measures for the Control of Agricultural Phosphorus Losses to Water: An Overview. J. Environ. Qual. 29, 1–9. doi:10.2134/jeq2000.00472425002900010001x

Sharpley, A., Jarvie, H.P., Buda, A., May, L., Spears, B., Kleinman, P., 2013. Phosphorus legacy: overcoming the effects of past management practices to mitigate future water quality impairment. J. Environ. Qual. 42, 1308–1326. doi:10.2134/jeq2013.03.0098

Sharpley, A.N., Daniel, T., Sims, T., Lemunyon, J., Stevens, R., Parry, R., 2003. Agricultural phosphorus and eutrophication. US Dep. Agric. Agric. Res. Serv. ARS–149 44.

Smil, V., 2000. Phosphorus in the Environment: Natural Flows and Human Interferences. Annu. Rev. Energy Environ. 25, 53–88. doi:10.1146/annurev.energy.25.1.53

Smith, V.H., 1983. Low nitrogen to phosphorus ratios favor dominance by blue-green algae in lake phytoplankton. Science(Washington) 221, 669–671.

Smith, V.H., Schindler, D.W., 2009. Eutrophication science: where do we go from here? Trends Ecol. Evol. 24, 201–207. doi:10.1016/j.tree.2008.11.009

Sonzogni, W.C., Chapra, S.C., Armstrong, D.E., Logan, T.J., 1982. Bioavailability of Phosphorus Inputs to Lakes. J. Environ. Qual. 11, 555–563. doi:10.2134/jeq1982.00472425001100040001x

Sterner, R.W., 2008. On the Phosphorus Limitation Paradigm for Lakes. Int. Rev. Hydrobiol. 93, 433–445. doi:10.1002/iroh.200811068

Stout, W.L., Sharpley, A.N., Landa, J., 2000. Effectiveness of coal combustion by-products in controlling phosphorus export from soils. J. Environ. Qual. 29, 1239–1244.

Tan, K.H., 2000. Environmental Soil Science, Third Edition. CRC Press.

Turner, B.L., Frossard, E., Baldwin, D.S., others, 2005. Organic phosphorus in the environment. CABI Pub.

Ulén, B., Bechmann, M., Fölster, J., Jarvie, H.P., Tunney, H., 2007. Agriculture as a phosphorus source for eutrophication in the north-west European countries, Norway, Sweden, United Kingdom and Ireland: a review. Soil Use Manag. 23, 5–15. doi:10.1111/j.1475-2743.2007.00115.x

Uusi-Kämppä, J., 2005. Phosphorus purification in buffer zones in cold climates. Ecol. Eng., Riparian buffer zones in agricultural watersheds 24, 491–502. doi:10.1016/j.ecoleng.2005.01.013

Vadeboncoeur, Y., Jeppesen, E., Zanden, M., Schierup, H.-H., Christoffersen, K., Lodge, D.M., 2003. From Greenland to green lakes: cultural eutrophication and the loss of benthic pathways in lakes. Limnol. Oceanogr. 48, 1408–1418.

Velghe, I., Carleer, R., Yperman, J., Schreurs, S., D'Haen, J., 2012. Characterisation of adsorbents prepared by pyrolysis of sludge and sludge/disposal filter cake mix. Water Res. 46, 2783–2794. doi:10.1016/j.watres.2012.02.034

Vohla C., Põldvere E., Noorvee A., Kuusemets V/, Mander Ü., 2005. Alternative Filter Media for Phosphorous Removal in a Horizontal Subsurface Flow Constructed Wetland. J. Environ. Sci. Health Part A 40, 1251–1264. doi:10.1081/ESE-200055677

Wang, L.K., Shammas, N.K., Hung, Y.-T., 2010. Advanced Biological Treatment Processes. Springer Science & Business Media.

Weil, R.R., Brady, N.C., Weil, R.R., 2016. The nature and properties of soils. Pearson.

Wetzel, R.G., 1964. A Comparative Study of the Primary Production of Higher Aquatic Plants, Periphyton, and Phytoplankton in a Large, Shallow Lake. Int. Rev. Gesamten Hydrobiol. Hydrogr. 49, 1–61. doi:10.1002/iroh.19640490102

Wilson, M.A., Carpenter, S.R., 1999. Economic Valuation of Freshwater Ecosystem Services in the United States: 1971–1997. Ecol. Appl. 9, 772–783. doi:10.1890/1051-0761(1999)009[0772:EVOFES]2.0.CO;2

Yang, R.T., 2013. Gas Separation by Adsorption Processes. Butterworth-Heinemann.

Yang, Y.S., Wang, L., 2010. A Review of Modelling Tools for Implementation of the EU Water Framework Directive in Handling Diffuse Water Pollution. Water Resour. Manag. 24, 1819–1843. doi:10.1007/s11269-009-9526-y

Yean, S., Cong, L., Yavuz, C.T., Mayo, J.T., Yu, W.W., Kan, A.T., Colvin, V.L., Tomson, M.B., 2005. Effect of magnetite particle size on adsorption and desorption of arsenite and arsenate. J. Mater. Res. 20, 3255–3264. doi:10.1557/jmr.2005.0403

Yeoman, S., Stephenson, T., Lester, J.N., Perry, R., 1988. The removal of phosphorus during wastewater treatment: A review. Environ. Pollut. 49, 183–233. doi:10.1016/0269-7491(88)90209-6

Yilmaz, A.E., Boncukcuoğlu, R., Kocakerim, M., Karakaş, İ.H., 2011. Waste utilization: The removal of textile dye (Bomaplex Red CR-L) from aqueous solution on sludge waste from electrocoagulation as adsorbent. Desalination 277, 156–163. doi:10.1016/j.desal.2011.04.018

Zaimes, G.N., Schultz, R.C., 2002. Phosphorus in agricultural watersheds. Lit. Rev. 2, 34.

Zeng, L., 2003. A method for preparing silica-containing iron(III) oxide adsorbents for arsenic removal. Water Res. 37, 4351–4358. doi:10.1016/S0043-1354(03)00402-0

Chapter 2

2.1 Experimental Methodologies

This study aimed to identify and assess the potential of phosphorus sorbing media (PSM) capable of removing dissolved P from aqueous solution. A number of different experimental methodologies were implemented to achieve this aim and descriptions of these methodologies, as they were applied in this study, are provided in this chapter.

2.2 Batch tests

Batch adsorption experiments are a common first step in the characterisation of adsorptive media (Crini and Badot, 2008) and, as described in Chapter 1, such tests are routinely used to examine the equilibrium relationship between the solid phase concentration (the amount of adsorbate associated with the solid adsorbent) and the liquid phase concentration (the amount of adsorbate dissolved in the adsorbate solution) for a given adsorption system.

To perform a basic batch adsorption test, known masses of a solid adsorbent (in this case a potential PSM), m (g), are first placed into a number of acid-washed glass Erlenmeyer flasks. A known volume, V (L), of phosphorus-spiked solution (prepared by adding K_2HPO_4 to distilled water) is then added to each of the flasks, which are then sealed with Parafilm M® and agitated at 250RPM on a reciprocal shaker until the adsorbent-solution system reaches equilibrium; an experimental duration of 24 hours is commonly used (Ok et al., 2007). The solution concentration at equilibrium, C_e (mg/L), is measured, and with the starting solution concentration, C_o (mg/L), already known, the solid concentration at equilibrium, q_e (mg/g), may be calculated by:

$$q_e = \frac{(C_O - C_e)m}{V}$$

The results of batch tests using a range of starting solution concentrations may be used to construct an adsorption isotherm which may then be fit to a suitable isotherm model (as discussed in sectio 1.8 of Chapter 1). In this study, batch tests were performed, in the manner described above, using a number of different potential PSM, and further batch tests were performed using a slightly modified methodology whereby small masses of peat soil were also added to the Erlenmeyer flasks at the beginning of each test. A detailed description of the batch test methodologies applied in this study may be found in Section 3.2 of Chapter 3.

2.3 Large-scale column tests

Although batch tests provide a rapid and convenient means of determining whether or not a potential medium has the capacity to remove P from solution, the experimental conditions of such experiments differ greatly from in-field conditions, and consequently these tests offer limited insight into a medium's in-field potential. Crucially, batch tests offer no information regarding a medium's longevity under flow-through conditions like those that might be encountered in phosphorus removal structures of the kind described in Chapter 1. For this reason, the performance of the medium under flow-through conditions representative of in-field usage must be investigated. This is most commonly achieved with the use of large-scale, laboratory-based column experiments.

In this study, large-scale filter-columns were constructed using PVC pipe with an internal diameter of 0.104m. These filters were loaded (in down-flow mode) with a synthetic phosphorus-spiked wastewater which was prepared by adding a small quantity of K_2HPO_4 to water. The filter-beds were created by packing the PVC columns (in 5 cm layers to ensure uniform packing density throughout) with various potential PSM to create 40 cm deep beds. An overflow pipe exited from the top of the columns, and the invert level of this overflow was located so as to allow for 25 cm of freeboard above the top surface of the filter media. Thus, when loading the columns from above, a constant head (and therefore constant flow rate) could easily be achieved. Influent was supplied to the top of the filter columns using a centrifugal pump, and the overflow pipe returned excess influent to the feed tank located at the base of the column. The filter effluents were collected in tanks which were positioned directly beneath the filter columns, and syringe ports located at bed depths of 0.05, 0.1, 0.18, and 0.25m allowed for the collection of pore water samples from within the filter-beds. Figure 2.1 shows the experimental setup, and further details regarding the large-scale column methodologies applied in this study may be found in sections 4.3 of chapter 4, and 5.3 of chapter 5.

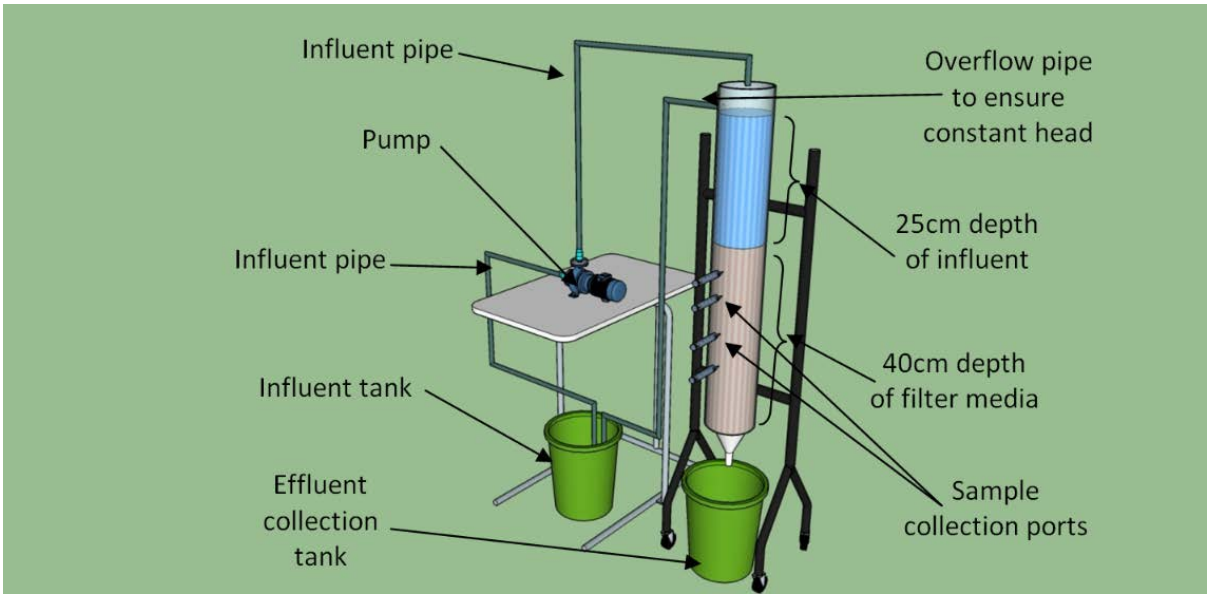

Figure 2.1 Schematic of large-scale filter column experiment

2.4 Small-scale column tests

Despite their usefulness, there are major drawbacks associated with large-scale column tests of the kind described above. As outlined in Chapter 1, operating multiple large filter-columns can be highly cost- and labour-intensive. Furthermore, large-scale filter studies often take months, if not years, to complete. For these reasons, small-scale column tests present a highly attractive alternative to large-scale tests, allowing the user to investigate a potential PSM under flow-through conditions representative of in-field conditions, while offering significant savings in time, labour, and expenditure.

In this study, small-scale filter columns (with lengths of 0.1, 0.15, 0.2, 0.3, and 0.4 m) were prepared by packing polycarbonate/HDPE tubing (internal diameter 0.094 m) with various PSM. The ends of each filter column were inserted into syringe barrels which were packed with small quantities of glass wool, and silicone influent/effluent lines were attached to the tips of the syringe barrels. The columns were attached to a retort stand to maintain a stable vertical orientation, and a peristaltic pump was used to supply wastewater to the base of each filter column. The effluent lines exiting the top of each filter column were routed to autosamplers, which divided the effluent from the columns into a number of acid-washed glass Erlenmeyer flasks. Figure 2.2 shows the experimental setup, and further details regarding the large-scale column methodologies applied in this study may be found in sections 4.3 of chapter 4, and 5.3 of chapter 5.

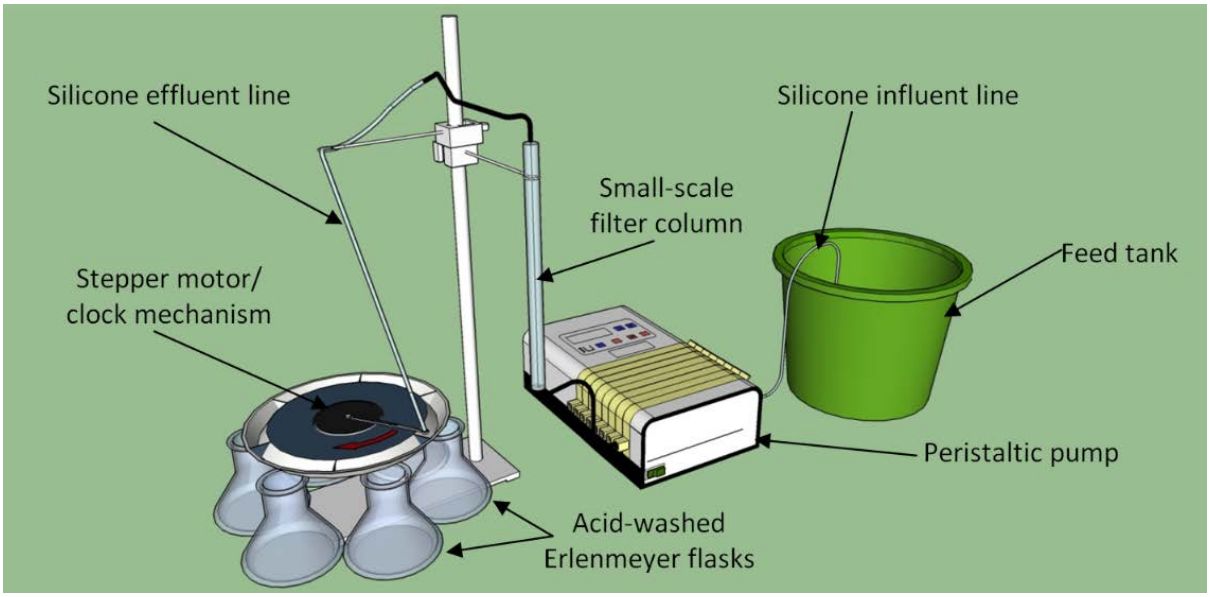

Figure 2.2 Schematic of small-scale filter column experiment

Sample collection was carried out using a simple autosampler as shown in Fig. 2.3. The autosampler consisted of a rotating arm (mounted on a central motor/clock mechanism), which guided the outlet of the silicone effluent line on a circular path around a v-shaped groove. This groove was divided into six sections, with a small outlet holes drilled in the centre of each section; the effluent was thus divided into six separate containers in sequence as the effluent line completed one revolution of the groove every 12 hours.

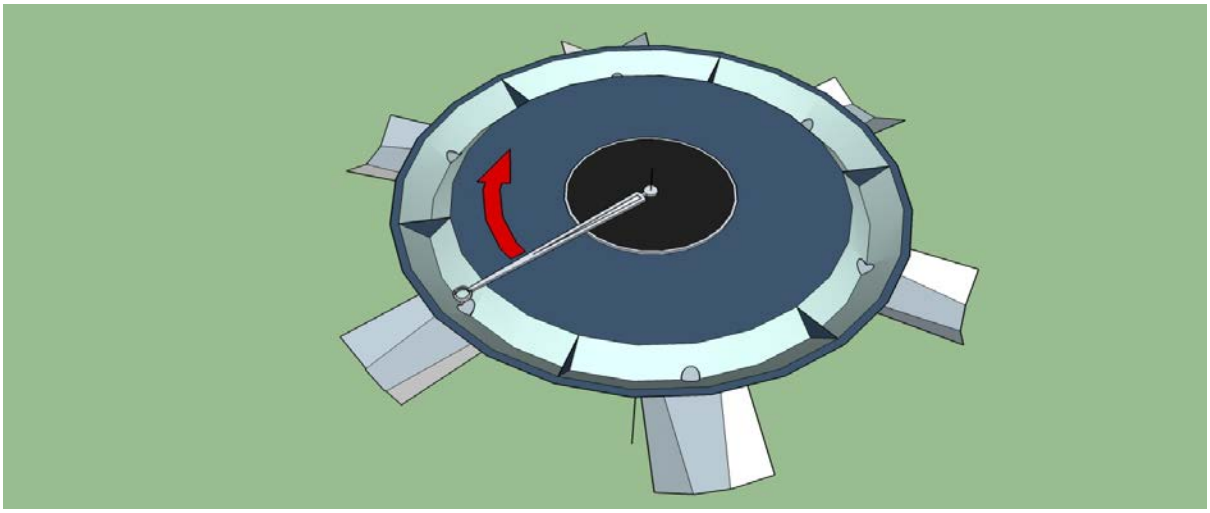

Figure 2.3 Schematic of autosampler

2.5 References

Crini, G., Badot, P.-M., 2008. Application of chitosan, a natural aminopolysaccharide, for dye removal from aqueous solutions by adsorption processes using batch studies: A review of recent literature. Prog. Polym. Sci. 33, 399–447. doi:10.1016/j.progpolymsci.2007.11.001

Ok, Y.S., Yang, J.E., Zhang, Y.-S., Kim, S.-J., Chung, D.-Y., 2007. Heavy metal adsorption by a formulated zeolite-Portland cement mixture. J. Hazard. Mater. 147, 91–96.

Chapter 3

Phosphorus (P) sorbing materials have shown great promise for the removal of P from a multitude of wastewaters, though their potential for treatment of peatland forestry runoff remains largely unexplored. The first aim this thesis was to address this knowledge gap. The study detailed in this chapter used batch adsorption tests to examine the ability of six materials, (1) aluminium water treatment residual (Al-WTR) (2) crushed concrete (3) gypsum, (4) magnesium hydroxide $Mg(OH)_2$ (5) magnesium oxide (MgO), and (6) steel wool, to remove P from aqueous solution in the presence of a forest peat soil.

The contents of this chapter have been published in Ecological Engineering [Ecol. Eng. 85, 193–200 (2015)]. Oisín Callery designed and set up the experiment, carried out all of the testing and analysis, and is the primary author of this publication. Dr. Mark G. Healy contributed to the experimental design and paper writing. Dr. Ray Brennan assisted with the data analysis. The published paper is included in Appendix A.

Use of amendments in a peat soil to reduce phosphorus losses from forestry operations

O. Callery, R.B. Brennan, M.G. Healy

Civil Engineering, National University of Ireland, Galway, Co. Galway, Rep. of Ireland.

Abstract

Forestry harvesting on peats is known to result in significant losses of soil phosphorus (P) to adjacent waters, and the issue is becoming an increasingly serious concern as peatland forest stocks mature and reach harvestable age. One potential solution could be the use of low-cost P recovery techniques based on the chemical precipitation and/or adsorption of the dissolved fraction of soil P, which would otherwise be lost. Such recovery techniques have shown promise in similar applications on mineral soils. However, the interaction of peat with P adsorbing materials can significantly alter their adsorptive characteristics, and it is consequentially not known what materials might be suitable for this application. This study compared the performance of six potential soil amendments (aluminum water treatment residual (Al-WTR), crushed concrete, gypsum, magnesium hydroxide, magnesium oxide, and steel wool) in removing P from aqueous solution in the presence of a typical forest peat soil. Comparison of adsorption isotherms plotted from these batch adsorption studies showed that the observed P adsorption maxima of Al-WTR and steel wool were increased by the presence of peat, from 10.6 mg g^{-1} and 20.4 mg g^{-1}, to 11.8 mg g^{-1} and 52.5 mg g^{-1}, respectively. In contrast, the observed P adsorption maxima of crushed concrete, gypsum, and magnesium oxide were reduced in the presence of peat, by 44%, 87%, and 37%, respectively. The maximum P adsorption achieved by magnesium hydroxide was increased from 29.8 mg g^{-1} to 59 mg g^{-1} at an amendment to peat-solid ratio of 1:4, but decreased from 73.9 mg g^{-1} to 23.6 mg g^{-1} at an amendment to peat-solid ratio of 1:10. It was concluded that Al-WTR, in particular, shows considerable promise for use as a soil amendment for P immobilization in a peat environment.

3.1 Introduction

Ireland's forestry stock of 731,000 ha covers about 10.5% of the country, of which 44% is planted on peats (National Forest Inventory, 2012). Peats, especially ombrotrophic upland blanket peats, are generally lacking in minerals like aluminum (Al) and iron (Fe), and consequently have extremely low soil phosphorus (P) sorption capacities (Renou et al., 2000). As a result, any P released by the forestry operations, such as clearfelling and afforestation, is liable to leach unimpeded into adjacent receiving waters, even with the application of current best management practices targeted at preventing such pollution (Finnegan et al., 2014).

Nutrient enrichment, or eutrophication, of inland waters is recognized as Ireland's most serious environmental pollution problem (Department of the Environment, 2002). As P has been identified as the primary nutrient limiting eutrophication in freshwaters (Carpenter et al., 1998; Boesch et al., 2001), preventing its migration from soil to aquatic environments is paramount. The oligotrophic nature of Ireland's upland catchments, and the unique flora and fauna present in these waters, make them particularly sensitive to eutrophication (Mainstone and Parr, 2002; Hutton et al., 2008). These forested peat catchments are headwaters for many of Ireland's river systems, a great number of which contain important salmonid populations (Giller and O'Halloran, 2004), as well as other species protected under European Union (EU) legislation (O'Driscoll et al., 2012; Reid et al., 2013). Consequentially, pollution from diffuse, low concentration sources of P, such as forestry, is capable of causing considerable environmental damage to an area much larger than that which is forested.

The sustained release of P following forestry harvesting has been highlighted as an issue of particular concern, as much of Ireland's current peatland forestry stock was planted between the 1950s and the 1990s (Renou and Farrell, 2005) and has now reached, or is reaching, harvestable age (Rodgers et al., 2010). Clearfelling is the harvesting technique most prevalent in Ireland, and accounted for 76.6% of timber felled between 2006 and 2012 (National Forest Inventory, 2012). Clearfelling involves the removal from site of the commercially-viable portions of the forestry crop (i.e. tree trunks), leaving large amounts of P to remain onsite, present both in the soil and in the non-commercial logging residues, or 'brash'. This brash accounts for a considerable percentage of the above ground nutrients contained in a typical coniferous tree (Moffat et al., 2006), and it has been shown to release these nutrients for many years following its deposition (Titus and Malcolm, 1999; Hyvönen et al., 2000). To compound the issue, the use of brash mats to form temporary driving surfaces for heavy

felling machinery is an essential management practice, as it prevents serious damage to the underlying soil (Moffat et al., 2006). Clearfelling completely disrupts natural P cycling in a forest ecosystem, with the deposition of brash mats resulting in increased P availability, while the concurrent removal of trees from site results in decreased P uptake and sequestration - a situation which greatly increases the threat of P leaching to aquatic ecosystems (Schaller et al., 2015).

While rates of afforestation on blanket peats have been in decline in recent years (National Forest Inventory, 2012), the harvesting of presently established forest is inevitable, as are the resulting water quality issues, if effective pollution mitigation measures are not implemented. Current best management practices advocate the use of riparian buffer strips between forestry and adjacent aquatic zones (Forest Service, 2000). Previous research has found the use of suitably large riparian buffer zones on peat soils to be largely successful in protecting surface waters from influxes of suspended sediments and associated particulate nutrients (Nieminen et al., 2005). However, with peat's low P adsorption capacity, the performance of these buffer zones in satisfactorily mitigating the flow of dissolved P off site varies greatly. Moreover, it has been found that these buffer zones' effect can be anywhere from positive, with total retention of released P (Vaananen et al., 2008), to negative, compounding the issue with additional P release (Vasander et al., 2003; Liljaniemi et al., 2003).

There has been increasing interest in the use of soil amendments to control P losses from diffuse sources, such as land spreading of manure from dairy cattle (Brennan et al., 2011a,b) and pigs (O' Flynn et al., 2012), land spreading of dairy waste water from washing of milking parlors (Serrenho et al., 2012), and construction of wetlands on sites previously used for agriculture (Ann et al., 1999). The use of chemical amendments has shown much promise in these instances, though there has been little to no investigation into the practice's potential in abating the loss of P from peatland forestry. The performance of chemical amendments in this context has the potential to be quite different, as the interaction of amendments with the complex chemistry of peat can significantly alter their P removal performance (James et al., 1992).

This study tested the hypothesis that chemical amendments could immobilize P in a forest peat soil. To address this hypothesis, the aim of this study was to identify and compare potential soil amendments which function well in a peat chemistry environment and, when mixed with peat onsite, could increase the adsorptive capacity of the amendment-soil mixture to the point where P losses from a forestry site would no longer pose a risk to receiving

surface waters. Specifically, the objectives of this study were to: (1) identify chemical amendments capable of removing P from an aqueous solution which mimics the chemistry of runoff/ground water on a forested peat site (2) compare the performance of each amendment and identify the amendment most ideally suited to application in a forested peat site (3) analyze the effect of peat on the performance of each amendment in terms of its adsorptive capacity.

3.2 Materials and Methods

3.2.1 Collection and characterization of peat samples

Samples of blanket peat were collected from a recently clearfelled riparian buffer zone, located near the town of Oughterard, County Galway, Ireland (approx. coordinates 53.375N, -9.419E). The peat was collected from a stratum of homogeneous composition, at a depth of 5-25cm from the surface (the surface layer of vegetation and semi-decayed sphagnum moss was discarded, along with any larger roots and plant fibers). The peat was moderately to strongly decomposed with only some recognizable plant structure visible and approximately one third to one half of the peat being extruded through the fingers on squeezing (corresponding to a Von Post (1922) classification of H6-H7) . Before testing, the samples were homogenized by repeatedly folding and kneading the peat until its texture and water content were entirely uniform. Once homogenized, peat samples were sealed in airtight Ziploc® bags and stored in a temperature-controlled room at 11°C until testing commenced. The water content of the homogenized peat was determined to be 872.12%±7.28% (calculated as a the mass of water divided by the mass of solids) by oven drying the peat for 24 h at 105°C (BSI, 1990).

3.2.2 Sourcing and characterization of amendments

The following amendments were used in this study (Table 3.1): dewatered aluminum sulphate water treatment residual (Al-WTR; oven dried for 24 h at 105°C and ground to pass a 0.5 mm sieve), crushed concrete cubes (pulverized with a mortar and pestle and ground to pass a 0.5 mm sieve), gypsum (sourced from recycled plasterboard, supplied as a powder, and passed through a 0.5 mm sieve to ensure uniformity), magnesium oxide (MgO; sourced from seawater, supplied as a powder, and passed through a 0.5 mm sieve to ensure uniformity), magnesium hydroxide ($Mg(OH)_2$; sourced from seawater, supplied as a paste, and passed through a 0.5 mm sieve to ensure uniformity) and steel wool (grade 00, fiber diameter approx. 0.04 mm).

Table 3.1 Peat and amendment characteristics

Material	Total exchange capacity (meq 100 g^{-1})	pH	Organic matter (%)	P† (mg kg^{-1})	Bray II P (mg kg^{-1})	Ca† (mg kg^{-1})	Mg† (mg kg^{-1})	Fe† (mg kg^{-1})	Al† (mg kg^{-1})
Peat	11.45	3.8	≈100	5	3	228	142	152	47
Al-WTR	16.78	7	21.62	2	< 1	2983	32	154	2159
Gypsum	64.3	8.8	1.85	6	14	11858	296	111	66
Crushed Concrete	145.15	11.7	0.82	< 1	< 1	27593	622	405	441
MgO	267.55	10	1.04	< 1	< 1	2734	29760	77	< 1
$Mg(OH)_2$	247.78	9.8	23.53	< 1	< 1	739	28660	57	< 1

†Mehlich -3 extractable

3.2.3 Batch test procedure

Samples were prepared comprising two grams (wet weight) of the homogenized peat, mixed with each of the six amendments, at amendment to peat-solid ratios of 1:10, 1:4 and 1:2. These masses provided a material to solution ratio that was small enough to ensure non-zero equilibrium concentrations, thus allowing the determination of the entire isotherm curve. The material to solution ratio used in the current study was comparable to ratios used in similar studies (Li et al., 2006; Chardon et al., 2012). The samples were placed in separate 50 ml conical flasks and overlain by 25 ml of deionized water, with ortho-phosphorus (PO_4-P) concentrations (prepared by adding various amounts of K_2HPO_4 to deionized water) of 0, 25, 50, 75, 100, and 150 mg P L^{-1}. This range of P concentrations was determined to be sufficiently wide to account for the variation in the amendments' adsorptive capacities, and the dependence of adsorption capacity on the initial concentration (Seo et al., 2005). The flasks were sealed with Parafilm and shaken in a reciprocal shaker (250 rpm) at room temperature (25°C) for 24 h. After 24 h had elapsed, the samples were centrifuged at 14,500 rpm for 5 min, and the supernatant water was passed through a 0.45 µm filter. Dissolved P concentrations of the supernatant water were determined using a nutrient analyzer (Konelab 20, Thermo Clinical Lab systems, Finland) after APHA (1998). Experiments were conducted at natural pH to ensure that all observed changes in pH could be attributed to the addition of peat to the solution. The same procedure was also carried out using identical masses of amendment but without the addition of peat.

3.2.4 Analysis of experimental data

The mass of P adsorbed per gram of adsorbent, q_e, at equilibrium was calculated by:

$$q_e = \frac{V(C_o - C_e)}{m} \quad (1)$$

where C_o and Ce are the initial and final PO_4-P concentrations of the solution (mg L^{-1}), V is the volume of solution (L), and m is the dry weight of adsorbent (g). For the purpose of these calculations, the PO_4-P adsorbency of the peat was measured and found to be negligible, and for solutions containing peat and amendment, only the dry weight of the amendment was considered in Eqn 1.

The C_e and q_e data obtained from the batch tests were fitted to the Koble-Corrigan equation, which was chosen for its ability to model adsorption over a wide range of data, as well as for its being more universally applicable than the commonly used Langmuir and Freundlich equations (Koble and Corrigan, 1952). The Koble-Corrigan equation is as follows:

$$q_e = \frac{A_{KC} C_e^p}{1 + B_{KC} C_e^p} \quad (2)$$

where A_{KC}, B_{KC} and p are the Koble-Corrigan isotherm constants determined by using an iterative approach to minimize the value returned by the hybrid fractional error function (HYBRID), an error function used to fit Eqn. 2 to the observed data (Porter et al., 1999):

$$\frac{100}{n-w} \sum_{i=1}^{n} \frac{(q_{e,i,meas} - q_{e,i,calc})^2}{q_{e,i,meas}} \quad (3)$$

where n is the number of experimental data points, w is the number of isotherm constants in the Koble-Corrigan equation (Eqn. 2), $q_{e,i,meas}$ is the value of q_e obtained from Eqn. (1), and $q_{e,i,calc}$ is the value of q_e obtained from Eqn. (2). By fitting the experimental data for each adsorbent to the Koble-Corrigan equation, it was possible to make predictions for values of C_e and q_e for any given C_o. Substituting Eqn. 1 into Eqn. 2 gives:

$$\frac{V(c_o - c_e)}{m} = \frac{A_{KC} C_e^p}{1 + B_{KC} C_e^p} \quad (4)$$

An iterative approach, using Microsoft Excel's Solver™, was then used to determine values of C_e for any given value of C_o. The impact of peat on the amendments' performance was evaluated using:

$$\phi = \frac{q_{e,a}^{calc}}{q_{e,b}^{calc}} \quad (5)$$

where $q_{e,a}^{calc}$ is the modelled mass of P adsorbed by the amendment in a solution containing peat, and $q_{e,b}^{calc}$ is the modelled mass of P adsorbed by the amendment in a solution containing no peat. Calculated values of $\Phi > 1$ indicate a synergistic effect was obtained by exposing an amendment to peat, i.e. the influence of peat chemistry was favorable for P adsorption, while values of $\Phi < 1$ suggest the opposite, i.e. that the effect was antagonistic. In this way, ϕ could be considered to be a coefficient of synergy.

3.3 Results and Discussion

All of the amendments were effective at removing P from aqueous solution, both with and without the presence of peat in solution. The addition of peat did, however, influence the behavior of all amendments, leading to either improved or diminished adsorptive performance.

3.3.1 Equilibrium adsorption isotherms

Figure 3.1 shows the adsorption isotherms obtained by fitting the Koble-Corrigan model to each of the peat amendment-mixtures (the adsorption isotherms obtained from tests using amendments only are omitted for clarity, but the model coefficients of these tests are provided in Table 3.2). The Koble-Corrigan fitting coefficients (A_{kc}, B_{kc}, and p) as well as slope, and R^2 values obtained from plots of $q_{e\ calc}$ (calculated using the Koble-Corrigan equation) vs $q_{e\ exp}$, are shown in Table 3.2. The Koble-Corrigan model fitted the experimental data well, and there was a very good correlation (average $R^2 = 0.94 \pm 0.1$) between predicted and experimental values. In general, higher values of q_e were observed when the ratio of adsorbent to solution was smaller. This is in agreement with a literature review conducted by Cucarella and Renman (2009), in which analyses of results from batch tests carried out using a wide range of materials demonstrated that smaller adsorbent-to-solution ratios may lead to higher concentrations of P sorbed to the adsorbent materials. Al-WTR, in particular, showed a much larger increase in P adsorption capacity (maximum observed $q_e = 11.8$ mg g^{-1}) when added to peat-containing solutions at an amendment to peat-solid ratio of 1:10, compared to amendment to peat-solid ratios of 1:4 and 1:2 (maximum observed $q_e = 3.3$ mg g^{-1} and 3.6 mg g^{-1}, respectively).

Maximum q_e values observed for concrete were 15 mg g^{-1}, 8.9 mg g^{-1}, and 6.8 mg g^{-1} at amendment to peat-solid ratios of 1:10, 1:4, and 1:2, which were similar to q_e values of 26.8 mg g^{-1}, 15.1 mg g^{-1}, and 6.6 mg g^{-1} observed for the same masses of concrete, but without the addition of peat. These values are all comparable to the q_e range of 5.1-19.6 mg g^{-1} observed by Egemose et al. (2012). With respect to gypsum, the presence of peat in solution resulted in greatly reduced maximum observed q_e values of 10.8 mg g^{-1}, 4.4 mg g^{-1}, and 3.6 mg g^{-1} at amendment to peat-solid ratios of 1:10, 1:4, and 1:2, compared to values of 84.8 mg g^{-1}, 58.4 mg g^{-1}, and 34 mg g^{-1} observed for the same masses without the addition of peat.

Magnesium oxide and $Mg(OH)_2$ displayed the highest P adsorption capacities, with MgO having the greatest of the two, with a maximum q_e of 102.7 mg g^{-1} observed at an amendment to peat-solid ratio of 1:10. Liu et al.(2011) found that removal of Arsenic (As(III)) from

aqueous solution by MgO was due to the *in situ* formation of $Mg(OH)_2$ by reaction of the MgO with water, followed by subsequent adsorption/reaction of the newly formed $Mg(OH)_2$ with the As anion. Liu et al.(2011) also reported that the adsorptive performance of $Mg(OH)_2$ formed *in situ* was greater than that of pre-formed $Mg(OH)_2$, at least partially as a result of

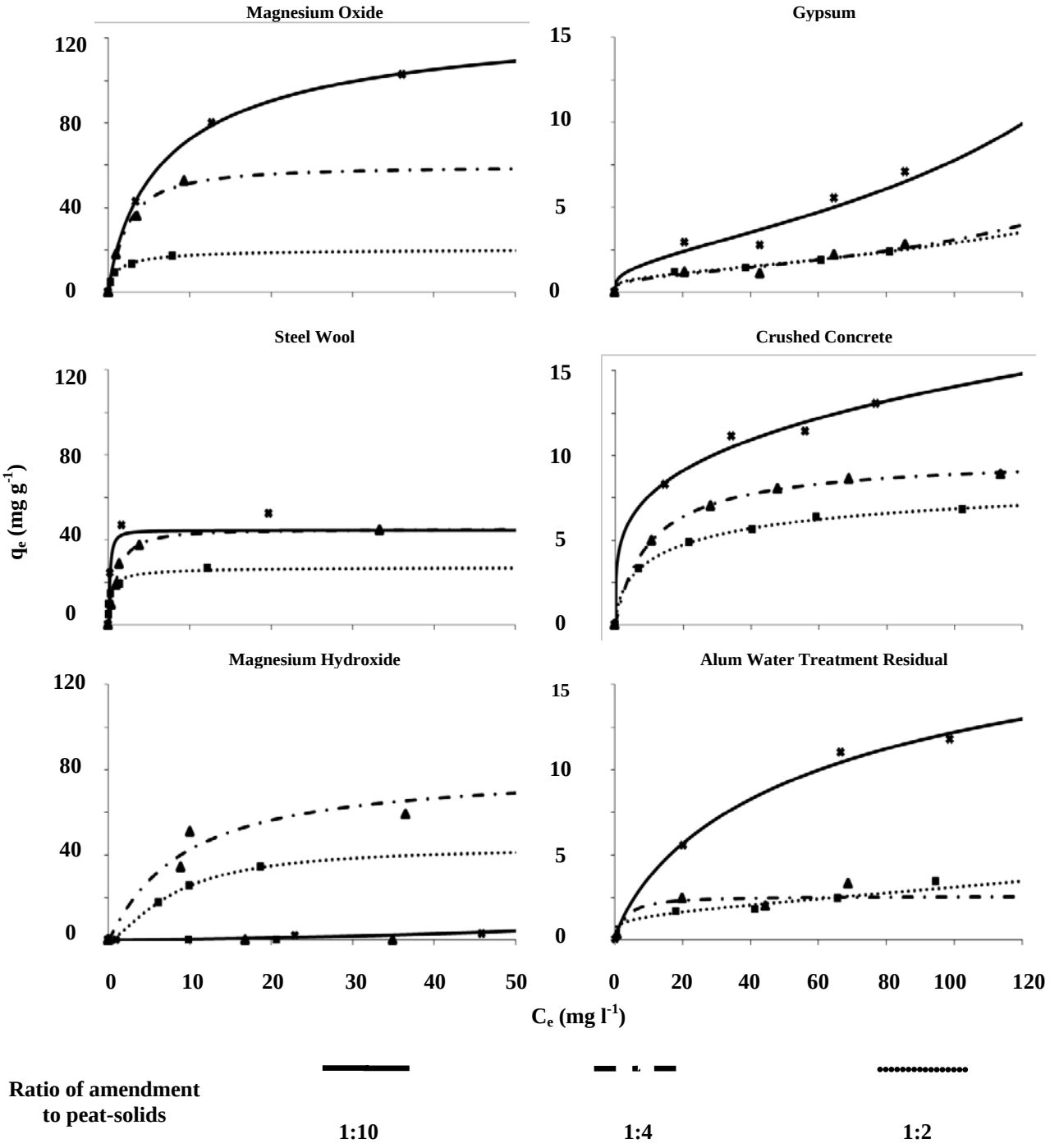

Figure 3.1 Best fit Koble-Corrigan adsorption isotherm models derived using non-linear regression methods for (a) magnesium oxide, (b) gypsum, (c) steel wool, (d) crushed concrete, (e) magnesium hydroxide, and (f) Al-WTR, at amendment to peat-solid ratios of 1:10, 1:4, and 1:2.

Table 3.2 Koble-Corrigan fitting coefficients, HYBRID errors, and values of slope and R^2 obtained from plots of $q_{e\ calc}$ vs $q_{e\ exp}$ for all amendments studied.

Amendment	Mass of amendment (g)	Mass of Peat (g)	Koble-Corrigan Parameters			Hybrid Error	$q_{e\ calc}$ vs $q_{e\ exp}$	
			A_{kc}	B_{kc}	p		R^2	Slope
Al-WTR	0.021	-	0.004	0.000	1.748	26.161	0.980	0.994
	0.051	-	0.002	0.001	1.844	21.142	0.870	1.016
	0.103	-	0.029	0.010	1.090	8.652	0.814	0.988
	0.021	2.000	0.710	0.032	0.795	4.725	0.995	1.001
	0.051	2.000	0.669	0.259	1.201	15.625	0.822	1.039
	0.103	2.000	0.001	-0.999	0.000	5.526	0.911	1.041
Crushed Concrete	0.021	-	1.031	-0.072	0.446	0.045	1.000	1.000
	0.051	-	0.510	0.020	0.873	33.659	0.881	1.016
	0.103	-	1.929	0.205	0.514	8.719	0.903	1.003
	0.021	2.000	3.964	-0.099	0.210	3.408	0.969	0.998
	0.051	2.000	1.087	0.109	0.935	0.187	0.997	1.000
	0.103	2.000	1.625	0.169	0.585	0.230	0.996	1.000
Gypsum	0.021	-	0.191	0.002	1.722	1.816	1.000	1.000
	0.051	-	0.004	0.000	2.841	8.108	0.998	0.999
	0.103	-	0.089	-0.950	0.016	72.056	0.963	1.007
	0.021	2.000	0.504	-0.381	0.176	23.740	0.963	0.981
	0.051	2.000	0.000	-0.999	0.000	10.299	0.962	1.011
	0.103	2.000	0.000	-0.999	0.000	0.826	0.994	0.998
Magnesium Oxide	0.021	-	1.686	0.012	2.406	742.198	0.895	1.036
	0.051	-	27.452	0.442	1.438	41.918	0.975	1.008
	0.103	-	17.694	0.252	0.520	17.290	0.986	1.000
	0.021	2.000	23.555	0.177	0.827	4.847	1.000	1.000
	0.051	2.000	24.286	0.407	1.197	34.473	0.994	1.000
	0.103	2.000	18.636	0.895	0.774	3.136	0.996	1.000
Magnesium Hydroxide	0.021	-	1.214	-0.159	0.379	287.793	0.933	0.999
	0.051	-	0.055	0.001	1.474	60.942	0.949	1.007
	0.103	-	0.152	-0.939	0.011	21.583	0.933	1.006
	0.021	2.000	0.047	-0.009	1.011	35.254	0.997	0.992
	0.051	2.000	7.849	0.098	1.065	408.260	0.937	0.932
	0.103	2.000	2.075	0.047	1.473	0.003	1.000	1.000
Steel wool	0.021	-	2.921	0.159	1.484	42.332	0.968	1.009
	0.051	-	4.128	0.411	0.996	0.870	0.999	1.001
	0.103	-	1.181	0.156	1.001	617.693	0.520	1.453
	0.021	2.000	434.832	9.756	1.352	137.919	0.715	1.003
	0.051	2.000	41.715	0.926	1.313	32.093	0.980	0.996
	0.103	2.000	68.370	2.490	0.728	62.409	0.959	0.975

the former's larger specific surface area, which was almost 5.5 times greater than that of the latter (58.4 m^2g^{-1} vs. 10.7 m^2g^{-1}, respectively). The results of our study indicate that $Mg(OH)_2$ formed *in situ* also had a greater adsorptive capacity for PO_4–P compared to that of pre-formed $Mg(OH)_2$. Stoichiometrically, MgO contains approximately 45% more Mg per unit weight than $Mg(OH)_2$; however, its P adsorption capacity was observed to be up to 120% greater than that of preformed $Mg(OH)_2$ in solutions where peat was absent (data not shown).

When steel wool was examined, P adsorption was observed to be inhibited at high initial PO_4-P concentrations (C_o), both with and without the addition of peat. This appeared to be the result of high PO_4-P concentrations inhibiting the formation of the iron oxides/hydroxides responsible for P removal, and it was observed that much less of the steel wool had rusted in these comparatively high concentration solutions. Similar observations were made by Pryor and Cohen (1953), who found that solutions of orthophosphate passivate iron; i.e. iron became less reactive due to presence of a micro-coating in the presence of dissolved air, and Harahuc et al. (2000), who found that phosphate at or above concentrations of 25 mmol inhibited the solubilization of iron.

3.3.2 pH effects

Figure 3.2 summarizes the effect that the addition of peat had on the pH of the solution at equilibrium (after 24 h). The peat displayed a strong buffering capacity, and its addition altered the final pH of the solution at equilibrium in all cases. In real-world applications, an amendment that has a strong effect on pH may not be desirable, as large fluctuations in pH may have a deleterious impact on the environment. For example, the addition of an amendment which increases the soil's pH may increase soil nitrate (NO_3) concentrations, and the risk of NO_3 leaching could be particularly great during the clearfelling of forestry (Wickström, 2002). After shaking for 24h, the pH of samples containing peat mixed with Al-WTR was found to be closest to those of a solution containing peat only; as can be seen in Figure 3.2, solutions containing peat only had an average pH of 6.04±0.64 and solutions containing Al-WTR mixed with peat had an average pH of 5.21±0.55. The performances of P adsorbent materials are known to be strongly affected by pH, and in acidic soils such as peats, Al and Fe are known to be responsible for the sorption of P (Sato et al., 2005), while binding by calcium (Ca) and magnesium (Mg) is responsible for P immobilization in alkaline soils (Faulkner and Richardson, 1989; Reddy et al., 1999).

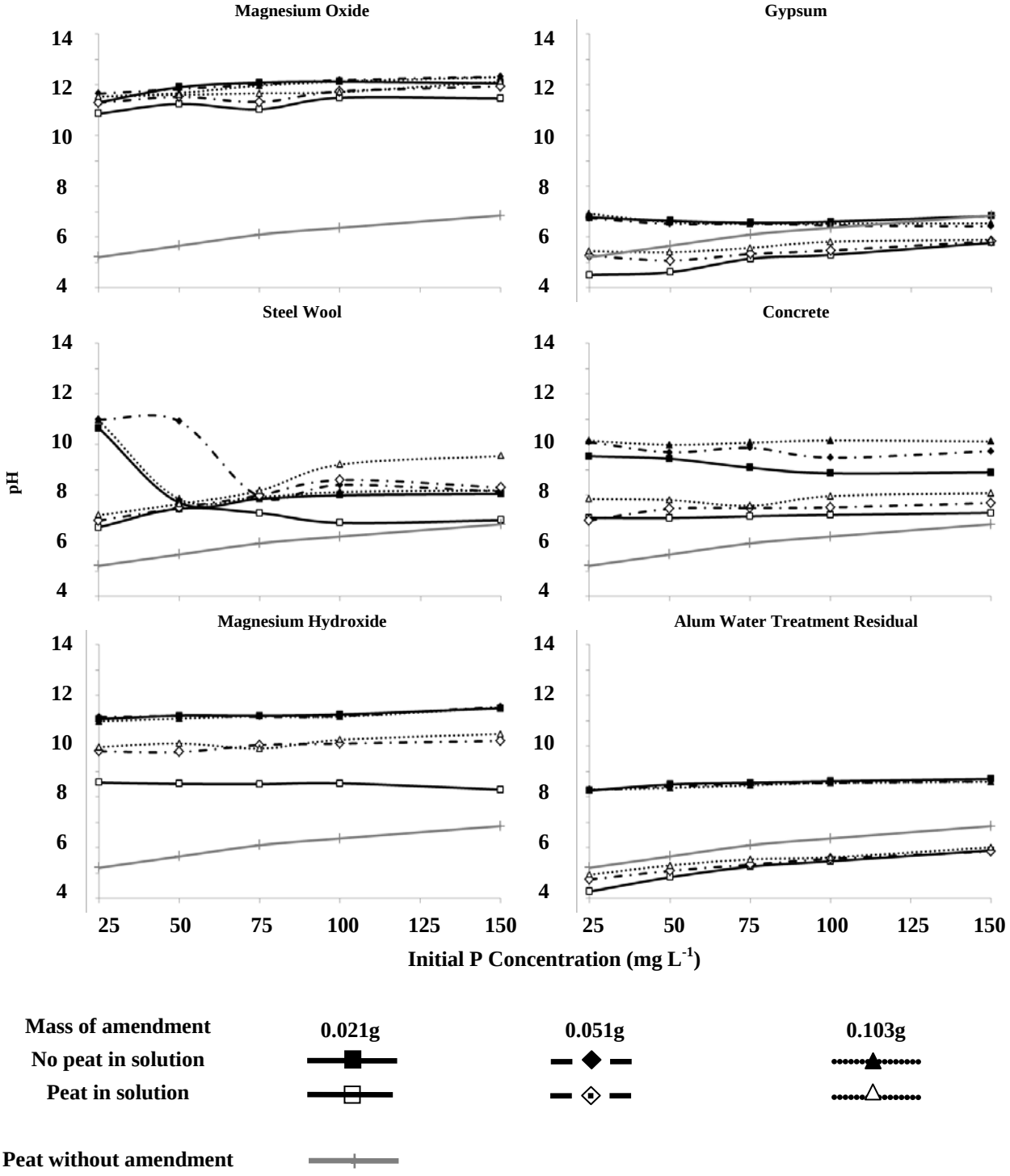

Figure 3.2 Effect of peat on pH at equilibrium

3.3.3 Synergistic Effects

The results indicate that, at certain initial PO_4–P concentrations, a degree of synergy exists between the peat and certain amendments; i.e. their adsorption performance was better in an environment whose chemistry was influenced by peat (Figure 3.3). Al-WTR and steel wool, in particular, showed improved performance across a large range of concentrations, while concrete, gypsum, and MgO showed largely diminished efficacy. The effect of peat on P adsorption by $Mg(OH)_2$ varied from beneficial to detrimental, depending on the ratio of peat to amendment in solution.

One mechanism by which an amendment's P sorption performance may improve when in a peat environment is as a result of the interaction of humic substances with soluble metal ions. Humic substances facilitate the removal of P through reactions with Al and Fe ions, which results in the formation of insoluble phosphate complexes (Bloom, 1981; Renou et al., 2000). Conversely, humic materials inhibit the removal of P by precipitation with Ca by competing with the phosphate anion for Ca, with this effect being more exaggerated at lower pH (Alvarez et al., 2004; Song et al., 2006; Cao et al., 2007). The formation of humic complexes may therefore contribute both to the observed improvement in Al-WTR and steel wool's adsorptive performance, as well as the diminished performance of concrete and gypsum. Phosphorus sorption by gypsum, for example, is directly related to its solubility, as its P removal is largely due to precipitation reactions (Penn et al., 2007) and thus the availability of Ca for the formation of calcium phosphates (Kordlaghari and Rowell, 2006).

The concrete used in this study had significantly higher levels of Al and Fe present than the gypsum (Table 3.1), which may explain why its P removal performance was not as adversely affected as gypsum's. Oğuz et al. (2003) found that P removal by concrete was by precipitation of metallic PO_4 salts, which were adsorbed onto the surface of the concrete, and $AlPO_4$ appeared to be the main product adsorbed onto the surface of the gas concrete examined in their study. This result suggests that the Al and Fe content of the concrete examined in this study, perhaps more so than its Ca content, plays a crucial role in P adsorption. Berg et al. (2005) reported that P removal by crushed gas concrete was not affected by the presence of organic matter in the form of dissolved organic carbon. However, as concrete's adsorption of P is strongly related to pH, and improves with increasing pH (Oğuz et al., 2003), it appears that the acidification of the solution by the peat is at least partially responsible for the observed reduction in performance.

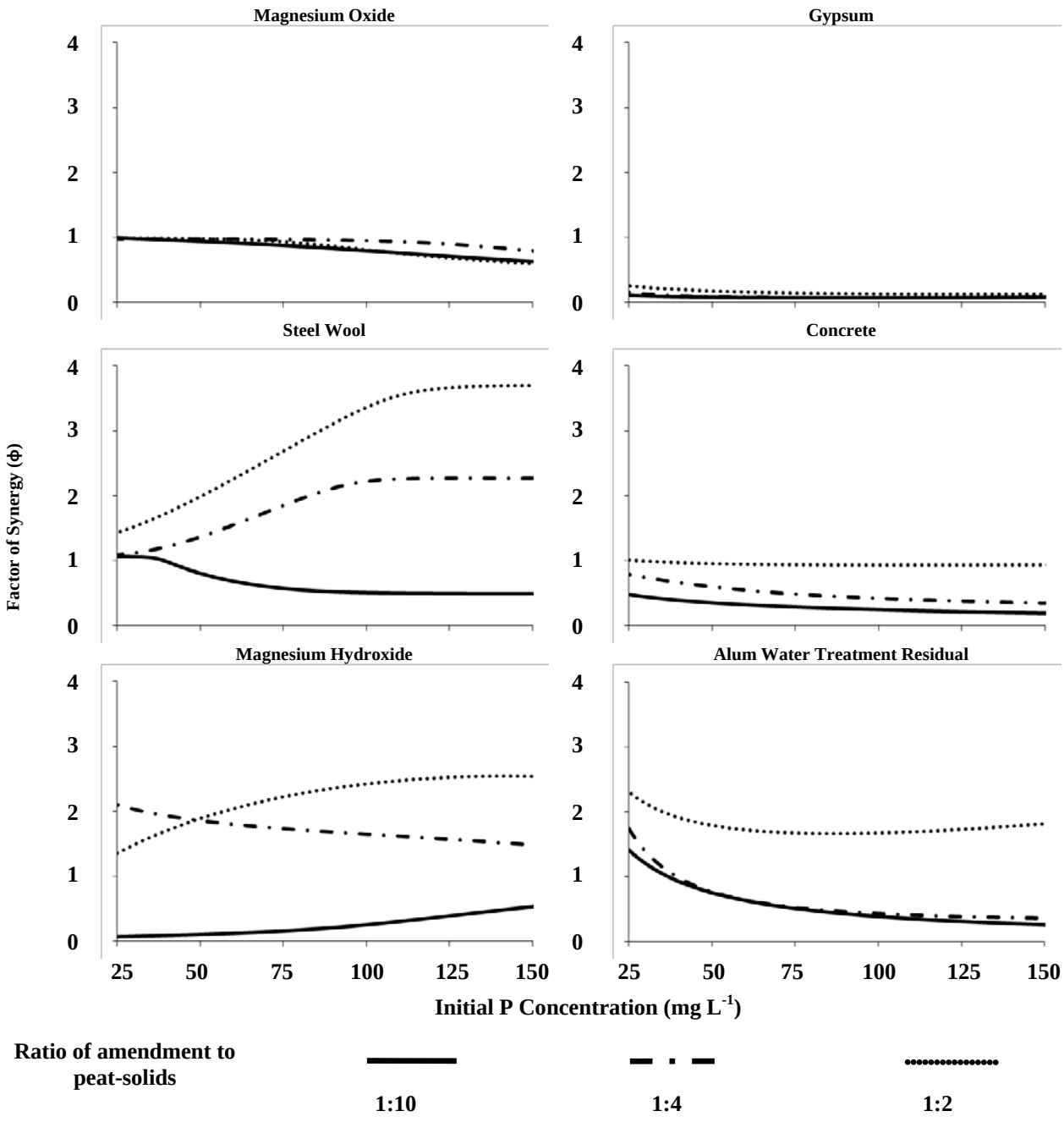

Figure 3.3 Synergistic effect of peat on P adsorption (Refer to Eqn. 5)

The pH buffering action of the peat is also likely to have contributed to the observed synergistic effects by lowering the solution pH, which can improve Al-WTR's P adsorption, as observed by Yang et al. (2006), and promote corrosion of the steel wool to form P adsorbing iron oxide/hydroxides. Consequently, the peat had a stronger effect on pH at this rate, with the final solution pH ranging from 8.3-8.6, compared to 9.8-10.2 and 9.9-10.5 at amendment to peat-solid ratios of 1:4 and 1:2, respectively. It was also observed that when $Mg(OH)_2$ was added at an amendment to peat-solid ratio of 1:10, recorded q_e values were

much lower than solutions containing $Mg(OH)_2$ at amendment to peat-solid ratios of 1:4 and 1:2. While the reason for this is not entirely clear, the marked difference in pH accompanied by the significant drop in P adsorption strongly suggests that the pH buffering effect of the peat may also be responsible for reducing the P adsorbency of $Mg(OH)_2$ at this lowest rate of amendment. Xie et al. (2013) reported that fulvic and humic acids had a slight negative effect on PO_4 adsorption by a magnesium oxide nanoflake-modified diatomite adsorbent, and attributed this observation to the effects of competitive adsorption. It is quite possible that at low $Mg(OH)_2$ to peat ratios this effect is more exaggerated.

3.4 Conclusions

This study found that the presence of peat in solution increased the P adsorption capacities of Al-WTR and steel wool, while the adsorptive capacities of crushed concrete, gypsum, and magnesium oxide were decreased. Magnesium hydroxide showed both increased and decreased adsorptive capacity, depending on the ratio of peat to amendment in solution. Throughout the study, peat displayed considerable ability to buffer the peat-amendment mixture pH. However, the equilibrium pH of solutions containing Al-WTR and gypsum were observed to be closest to the peat's natural pH, indicating that these amendments were best suited to the peat environment. Taking these factors into consideration, the results of this study indicate that Al-WTR, in particular, holds great promise for utilization in the mitigation of P runoff caused by forestry operations on blanket peat sites. Previous research into the use of Al-WTR has shown it to be effective in preventing P runoff when used as a soil amendment in an agricultural context, and this study's findings demonstrate that the chemistry of a peat forest environment is likely to interact with Al-WTR in such a manner as to improve its P removal performance at low P concentrations. As a waste material, an additional benefit lies in the fact that it does not have the production costs associated with other high performing amendments studied, i.e. steel wool and $Mg(OH)_2$.

3.5 Acknowledgements

The first author would like to acknowledge the Irish Research Council for funding.

3.6 References

Alvarez, R., L.A. Evans, P.J. Milham and M.A. Wilson. 2004. Effects of humic material on the precipitation of calcium phosphate. Geoderma 118: 245–260.

Ann, Y., K.R. Reddy, and J.J. Delfino. 1999. Influence of chemical amendments on phosphorus immobilization in soils from a constructed wetland. Ecol. Eng. 14: 157–167.

American Public Health Association. (APHA), American Water Works Association., and Water Environment Federation. 1998. Standard methods for the examination of water and wastewater. American Public Health Association, Washington, DC.

Berg, U., D. Donnert, A. Ehbrecht, W. Bumiller, I. Kusche, P.G. Weidler, and R. Nüesch. 2005. “Active filtration” for the elimination and recovery of phosphorus from waste water. Colloid. Surface. A 265: 141–148.

Bloom, P.R. 1981. Phosphorus Adsorption by an Aluminum-Peat Complex1. Soil Sci. Soc. Am. J. 45: 267.

Boesch, D.F., R.B. Brinsfield, and R.E. Magnien. 2001. Chesapeake Bay Eutrophication. J. Environ. Qual. 30: 303–320.

Brennan, R.B., O. Fenton, J. Grant, and M.G. Healy. 2011a. Impact of chemical amendment of dairy cattle slurry on phosphorus, suspended sediment and metal loss to runoff from a grassland soil. Sci. Tot. Environ. 409: 5111–5118.

Brennan, R.B., O. Fenton, M. Rodgers, and M.G. Healy. 2011b. Evaluation of chemical amendments to control phosphorus losses from dairy slurry. Soil Use Manage. 27: 238–246.

British Standards Institution (BSI). 1990. British Standard methods of test for soils for civil engineering purposes. British Standards Institution, Milton Keynes [England].

Cao, X., W.G. Harris, M.S. Josan, and V.D. Nair. 2007. Inhibition of calcium phosphate precipitation under environmentally-relevant conditions. Sci. Tot. Environ. 383: 205–215.

Carpenter, S.R., N.F. Caraco, D.L. Correll, R.W. Howarth, A.N. Sharpley, and V.H. Smith. 1998. Nonpoint Pollution of Surface Waters with Phosphorus and Nitrogen. Ecol. Appl. 8: 559–568.

Chardon, W.J., J.E. Groenenberg, E.J. Temminghoff, and G.F. Koopmans. 2012. Use of reactive materials to bind phosphorus. J. Environ. Qual. 41: 636–646.

Cucarella, V., and G. Renman. 2009. Phosphorus Sorption Capacity of Filter Materials Used for On-site Wastewater Treatment Determined in Batch Experiments-A Comparative Study. J. Environ. Qual. 38: 381–392.

Department of the Environment, C. and L.G. 2002 Making Ireland's Development Sustainable Review, Assessment and Future Action Available at http://www.environ.ie/en/Environment/SustainableDevelopment/PublicationsDocuments/FileDownLoad,1847,en.pdf (verified 9 Nov 2014).

Egemose, S., M.J. Sønderup, M.V. Beinthin, K. Reitzel, C.C. Hoffmann, and M.R. Flindt. 2012. Crushed concrete as a phosphate binding material: A potential new management tool. J. Environ. Qual. 41: 647–653.

Faulkner, S.P., and C.J. Richardson. 1989. Physical and chemical characteristics of freshwater wetland soils. p. 41 – 72. *In* D.A. Hammer (ed.) Constructed wetlands for wastewater treatment. CRC Press, Boca Raton, FL.

Finnegan, J., J.T. Regan, M. O'Connor, P. Wilson, and M.G. Healy. 2014. Implications of applied best management practice for peatland forest harvesting. Ecol. Eng. 63: 12–26.

Forest Service. 2000. Code of Best Forest Practice. Available at http://www.agriculture.gov.ie/forestservice/publications/codeofbestforestpractice/ (verified 10 Nov 2014).

Giller, P.S., and J. O'Halloran. 2004. Forestry and the aquatic environment: studies in an Irish context. Hydrol. Earth Syst. Sc. 8: 314–326.

Harahuc, L., H.M. Lizama, and I. Suzuki. 2000. Selective Inhibition of the Oxidation of Ferrous Iron or Sulfur in Thiobacillus ferrooxidans. Appl. Environ. Microbiol. 66: 1031–1037.

Hutton, S., S. Harrison, and J. O'Halloran. 2008. An evaluation of the role of forests and forest practices in the eutrophication and sedimentation of receiving waters. Available at http://www.wfdireland.net/docs/22_ForestAndWater/Forest%20and%20Water_UCC_Draft%20Final%20Report.pdf (verified 9 May 2014).

Hyvönen, R., B.A. Olsson, H. Lundkvist, and H. Staaf. 2000. Decomposition and nutrient release from Picea abies (L.) Karst. and Pinus sylvestris L. logging residues. For. Ecol. Manag. 126: 97–112.

James, B.R., M.C. Rabenhorst, and G.A. Frigon. 1992. Phosphorus Sorption by Peat and Sand Amended with Iron Oxides or Steel Wool. Wat. Environ. Res. 64: 699–705.

Koble, R.A., and T.E. Corrigan. 1952. Adsorption Isotherms for Pure Hydrocarbons. Ind. Eng. Chem. 44: 383–387.

Kordlaghari, M.P., and D.L. Rowell. 2006. The role of gypsum in the reactions of phosphate with soils. Geoderma 132: 105–115.

Li, Y., C. Liu, Z. Luan, X. Peng, C. Zhu, Z. Chen, Z. Zhang, J. Fan, and Z. Jia. 2006. Phosphate removal from aqueous solutions using raw and activated red mud and fly ash. J. Haz. Mat. 137: 374–383.

Liljaniemi, P., K.-M. Vuori, T. Tossavainen, J. Kotanen, M. Haapanen, A. Lepistö, and K. Kenttämies. 2003. Effectiveness of Constructed Overland Flow Areas in Decreasing Diffuse Pollution from Forest Drainages. Environ. Manage. 32: 602–613.

Liu, Y., Q. Li, S. Gao, and J.K. Shang. 2011. Exceptional As (III) sorption capacity by highly porous magnesium oxide nanoflakes made from hydrothermal synthesis. J. Am. Ceram. Soc. 94: 217–223.

Mainstone, C.P., and W. Parr. 2002. Phosphorus in rivers — ecology and management. Sci. Tot. Environ. 282–283: 25–47.

Moffat, A.J., B.M. Jones, W.L. Mason, and G. Britain. 2006. Managing brash on conifer clearfell sites. Forestry Commission. http://www.forestry.gov.uk/pdf/FCPN 013.pdf/$FILE/FCPN013.pdf (verified 26 Nov. 14)

National Forest Inventory. 2012. National Forest Inventory. Available at https://www.agriculture.gov.ie/nfi/nfisecondcycle2012/nationalforestinventorypublications2012/ (verified 9 May 2014).

Nieminen, M., E. Ahti, H. Nousiainen, S. Joensuu, and M. Vuollekoski. 2005. Capacity of riparian buffer zones to reduce sediment concentrations in discharge from peatlands drained for forestry. Silva Fennica 39: 331–339.

O'Driscoll, C., E. de Eyto, M. Rodgers, M. O'Connor, Z.-Z. Asam, and L. Xiao. 2012. Diatom assemblages and their associated environmental factors in upland peat forest rivers. Ecol. Indic. 18: 443–451.

O'Flynn, C.J., O. Fenton, and M.G. Healy. 2012. Evaluation of amendments to control phosphorus losses in runoff from pig slurry applications to land. CLEAN–Soil Air Water 40: 164–170.

Oğuz, E., A. Gürses, and N. Canpolat. 2003. Removal of phosphate from wastewaters. Cement Concrete Res. 33: 1109–1112.

Penn, C.J., R.B. Bryant, P.J.A. Kleinman, and A.L. Allen. 2007. Removing dissolved phosphorus from drainage ditch water with phosphorus sorbing materials. J. Soil Water Conserv. 62: 269–276.

Porter, J.F., G. McKay, and K.H. Choy. 1999. The prediction of sorption from a binary mixture of acidic dyes using single- and mixed-isotherm variants of the ideal adsorbed solute theory. Chem. Eng. Sci. 54: 5863–5885.

Pryor, M.J., and M. Cohen. 1953. The Inhibition of the Corrosion of Iron by Some Anodic Inhibitors. J. Electrochem. Soc. 100: 203–215.

Reddy, K.R., R.H. Kadlec, E. Flaig, and P.M. Gale. 1999. Phosphorus Retention in Streams and Wetlands: A Review. Crit. Rev. Env. Sci. Tec. 29: 83–146.

Reid, N., A. Keys, J.S. Preston, E. Moorkens, D. Roberts, and C.D. Wilson. 2013. Conservation status and reproduction of the critically endangered freshwater pearl mussel (Margaritifera margaritifera) in Northern Ireland. Aquatic Conserv: Mar. Freshw. Ecosyst. 23: 571–581.

Renou, F., and E.P. Farrell. 2005. Reclaiming peatlands for forestry: the Irish experience. Restoration of boreal and temperate forests. CRC Press, Boca Raton: 541–557.

Renou, F., S. Jones, and E.P. Farrell. 2000. Leaching of phosphorus fertilizer applied on cutaway peatland forests recently established in central Ireland. Sustaining our peatlands 2: 984–990.

Rodgers, M., M. O'Connor, M.G. Healy, C. O'Driscoll, Z.-Z. Asam, M. Nieminen, R. Poole, M. Müller, and L. Xiao. 2010. Phosphorus release from forest harvesting on an upland blanket peat catchment. Forest Ecology and Management 260(12): 2241–2248.

Sato, S., D. Solomon, C. Hyland, Q.M. Ketterings, and J. Lehmann. 2005. Phosphorus Speciation in Manure and Manure-Amended Soils Using XANES Spectroscopy. Environ. Sci. Technol. 39: 7485–7491.

Seo, D.C., Cho, J.S., Lee, H.J., Heo, J.S., 2005. Phosphorus retention capacity of filter media for estimating the longevity of constructed wetland. Water Res. 39, 2445–2457.

Serrenho, A., O. Fenton, P.N.C. Murphy, J. Grant, and M.G. Healy. 2012. Effect of chemical amendments to dairy soiled water and time between application and rainfall on phosphorus and sediment losses in runoff. Sci. Tot. Environ. 430: 1–7.

Schaller, J., Tischer, A., Struyf, E., Bremer, M., Belmonte, D.U., Potthast, K., 2015. Fire enhances phosphorus availability in topsoils depending on binding properties. Ecology 96, 1598–1606.

Song, Y., H.H. Hahn, E. Hoffmann, and P.G. Weidler. 2006. Effect of humic substances on the precipitation of calcium phosphate. J. Environ. Sci. 18: 852–857.

Titus, B.D., and D.C. Malcolm. 1999. The long-term decomposition of Sitka spruce needles in brash. Forestry 72(3): 207–221.

Vaananen, R., M. Nieminen, M. Vuollekoski, H. Nousiainen, T. Sallantaus, E. Tuittila, and H. Ilvesniemi. 2008. Retention of phosphorus in peatland buffer zones at six forested catchments in southern Finland. Silva Fennica 42(2): 211.

Vasander, H., E.-S. Tuittila, E. Lode, L. Lundin, M. Ilomets, T. Sallantaus, R. Heikkilä, M.-L. Pitkänen, and J. Laine. 2003. Status and restoration of peatlands in northern Europe. Wetland. Ecol. Manage.11: 51–63.

Wickström, H. 2002. Action plan to counteract soil acidification and to promote sustainable use of forestland. National Board of Forestry, Jönköping. Available at http://shop.skogsstyrelsen.se/shop/9098/art63/4645963-efc63c-1546.pdf (verified 26 Nov. 14)

Xie, F., F. Wu, G. Liu, Y. Mu, C. Feng, H. Wang, and J.P. Giesy. 2013. Removal of Phosphate from Eutrophic Lakes through Adsorption by in Situ Formation of Magnesium Hydroxide from Diatomite. Env. Sci. Tech. 48: 582–590.

Yang, Y., Y.Q. Zhao, A.O. Babatunde, L. Wang, Y.X. Ren, and Y. Han. 2006. Characteristics and mechanisms of phosphate adsorption on dewatered alum sludge. Sep. Purif. Technol. 51: 193–200.

Chapter 4

Chapter 3 detailed the results of batch adsorption tests performed to identify media suitable for use in the removal of phosphorus (P) from runoff originating from forestry plantations on blanket peat soils. The results of this study indicated that three materials - aluminum drinking water treatment residual (Al-WTR), crushed concrete, and steel wool - might be suitable for this use. Though batch tests are an important first step in the assessment of P sorbing materials, they don't provide sufficient information to predict the in-field performance of filter media. Large-scale column studies are often used for this purpose; however, these may take weeks, months, or even years to perform. Therefore, there is a need for a rapid way to investigate media under flow-through conditions that will give comparable results to long-term column studies. The second aim of this thesis was to address this knowledge gap.

This chapter details the development of a rapid small-scale flow-through testing methodology that is applicable to low-cost adsorbents which have highly variable physical and chemical properties, and demonstrates that this methodology produces comparable results to large-scale column studies, thus addressing the second aim of this thesis. Initial small-scale filter tests with steel wool indicated that accumulation of iron oxides and hydroxides in the filter-columns rapidly caused filter clogging and rendered it unusable as a filter media. Ferric drinking water treatment residual (Fe-WTR) was therefore substituted for steel wool as an iron-based adsorbent.

The contents of this chapter have been published in Water Research [Water Res. 101, 429–440 (2016)]. Oisín Callery designed and set up the experiment, carried out testing and analysis, developed the mathematical approach used to model experimental data, and is the primary author of this publication. Florian Rognard and Loïc Barthelemy assisted in data collection and analysis. Dr. Mark G. Healy contributed to the experimental design and paper writing. Dr. Ray Brennan assisted with the data analysis. The published paper is included in Appendix B.

Evaluating the long-term performance of low-cost adsorbents using small-scale adsorption column experiments

O. Callery [a], M.G. Healy [a], F. Rognard [b], L. Barthelemy [c], R.B. Brennan [a]

[a] Civil Engineering, National University of Ireland, Galway, Co. Galway, Rep. of Ireland.

[b] Université François Rabelais de Tours, Tours, France.

[c] École Nationale du Génie de l'Eau et de l'Environnement de Strasbourg, Strasbourg, France.

Abstract

This study investigated a novel method of predicting the long-term phosphorus removal performance of large-scale adsorption filters, using data derived from short-term, small-scale column experiments. The filter media investigated were low-cost adsorbents such as aluminum sulfate drinking water treatment residual, ferric sulfate drinking water treatment residual, and fine and coarse crushed concretes. Small-bore adsorption columns were loaded with synthetic wastewater, and treated column effluent volume was plotted against the mass of phosphorus adsorbed per unit mass of filter media. It was observed that the curve described by the data strongly resembled that of a standard adsorption isotherm created from batch adsorption data. Consequently, it was hypothesized that an equation following the form of the Freundlich isotherm would describe the relationship between filter loading and media saturation. Moreover, the relationship between filter loading and effluent concentration could also be derived from this equation. The proposed model was demonstrated to accurately predict the performance of large-scale adsorption filters over a period of up to three months with a very high degree of accuracy. Furthermore, the coefficients necessary to produce said model could be determined from just 24 hours of small-scale experimental data.

4.1 Introduction

Adsorption and surface precipitation are fast, cost-effective, and therefore highly attractive water treatment techniques that are applicable to the removal of a broad range of contaminants. In particular, there is considerable interest in low-cost adsorbents, which may be suitable for use in the treatment of water contaminated by pollutants such as heavy metals, industrial dyes, and nutrients (Demirbas, 2008; Vohla et al., 2011; Yagub et al., 2014). Natural materials, as well as industrial and agricultural wastes, are ideal in this regard, due to their low cost, local availability, and the added economic value associated with avoiding disposal routes such as landfill and incineration (Babel and Kurniawan, 2003; Crini, 2006).

When assessing the suitability of a potential filter medium, batch adsorption experiments are the most commonly utilized test, favored by researchers for their convenience and low cost (Crini and Badot, 2008). In fact, a large proportion of studies (arguably erroneously) rely solely on batch experiments to make inferences as to the behaviour of media in real-world filters (Ali and Gupta, 2007). The data from these batch adsorption tests are used in the construction of adsorption isotherms - curves that describe the removal of a contaminant from a mobile (liquid or gaseous) phase by its binding to a solid phase, across a range of contaminant concentrations. The determination of these isotherms is considered a critical step in the design and optimization of any adsorption process (Behnamfard and Salarirad, 2009; Hamdaoui and Naffrechoux, 2007), and there are a multitude of models describing these equilibrium curves.

Whilst important in the characterisation of potential adsorptive materials, it has been noted that batch adsorption tests have a number of potential shortcomings. Data obtained from batch studies are heavily influenced by factors such as initial solution concentration (Drizo et al., 2002), pH (Cucarella and Renman, 2009), and contact time (McKay, 1996), as well as by experimental conditions which are sometimes very different to real world applications - for example the use of unrealistic solid-to-solution ratios, and the agitation of batch samples (Ádám et al., 2007; Søvik and Kløve, 2005).

Adsorption isotherms may also be determined using flow-through experiments, and the utilization of such methodologies, while not offering an all-encompassing solution, may help to address many of the shortcomings associated with batch studies. Buergisser et al. (1993) note that the solid-to-liquid ratio used when determining sorption isotherms with flow-

through experiments is much closer to ratios that might be found in real-life systems where the adsorption of contaminants plays an important role in the treatment of contaminated waters (e.g. wastewater filtration units, constructed wetland substrates, and riparian buffer zones). Grolimund et al. (1995) also highlighted a number of other advantages of flow-through methodologies, such as the ease of prewashing the media under investigation, the reduced cost of the equipment necessary to perform the analysis, and the mitigation of experimental errors caused by the shaking motions used in batch experiments. A question still remains, however, regarding the applicability of the obtained isotherm to real-world situations. The isotherm alone provides no useful information regarding the longevity of a system (Seo et al., 2005), and when considering potential practical applications, predicting the lifespan of a given filter media is of paramount importance (Johansson, 1999).

Pratt et al. (2012) argue that the only reliable method of predicting the long-term performance of a filter media is full-scale field testing. While this may be true, it is obviously impractical to conduct such a study with an unproven material, and it is therefore desirable to perform short-term, laboratory-based experiments prior to undertaking any such large-scale study. Therefore, to address the question of adsorbent longevity, flow-through experiments in large-scale, laboratory-based columns are the most commonly utilised method, though Crittenden et al. (1991) demonstrated that rapid small-scale column tests (RSSCTs) could also be used to predict the performance of pilot-scale adsorption columns.

There are a number of models commonly used to describe column adsorption, among the most popular of which are the Thomas model (Thomas, 1944), the Clark model (Clark, 1987), the Yoon-Nelson model (Yoon and Nelson, 1984), and the bed depth service time (BDST) model developed by Hutchins (Hutchins, 1973), based on an earlier model proposed by Bohart and Adams (Bohart and Adams, 1920). All of these models attempt to predict the performance of a filter column by studying the relationship between filter loading and effluent concentration, though in full-scale filters this relationship can be far from ideal. When a filter is intermittently loaded, as might be the case, for example, in sub-surface vertical flow constructed wetlands (Healy et al., 2007; Pant et al., 2001), intermittent sand filtration systems (Rodgers et al., 2005), or indeed even riparian buffer zones (Ulén and Etana, 2010; Vidon et al., 2010), the relationship between effluent concentration and running time can be strongly affected by pauses in filter loading. It has been noted by a great many researchers that such breaks in the continuity of loading potentially allows for the diffusion of

adsorbate molecules further into the adsorbent particles, thus resulting in a rejuvenation of the adsorbent surface prior to the next loading cycle (Ouvrard et al., 2002; DeMarco et al., 2003; Greenleaf and SenGupta, 2006; Sengupta and Pandit, 2011). This results in a non-uniform evolution of column effluent concentration with successive loadings, and means that the relationship between effluent concentration and loading is unlikely to follow one of the ideal breakthrough curves described by any of the aforementioned models. For example, the BDST model predicts an S-shaped curve, which is often not observed in laboratory studies, experimental data instead producing linear to convex curves associated with less ideal adsorption (Malkoc et al., 2006; Walker and Weatherley, 1997). Furthermore, this model is best suited to columns containing ideal adsorbents with continuous flow-through rates that are low enough to allow adsorptive equilibrium to be reached (Jusoh et al., 2007) – conditions which are not necessarily representative of real world conditions.

Considering that the ability to predict the point at which the effluent from an adsorptive filter exceeds a pre-defined contaminant concentration (i.e., the breakthrough point) is the principal objective of any column service time model (Deliyanni et al., 2009), the purpose of the current study was to develop a model capable of predicting filter breakthrough, while addressing the difficulties of modelling effluent concentration from an intermittently loaded filter. The proposed model works under the hypothesis that, if the relationship between filter media saturation and filter loading can be accurately described for an intermittently loaded filter, then effluent concentration can be obtained implicitly for any given influent concentration, and in the case of an intermittently loaded media, this approach is likely to be more successful than attempting to simply model the effluent concentration directly. To the best of our knowledge, this approach to predicting filter longevity has not been attempted before.

The proposed model was developed from rapid small-scale column tests, and its accuracy was confirmed using large-scale, laboratory-based filters which, in terms of media mass and loading, were two orders of magnitude larger than the experiment from which the model was derived. To test the model's adaptability to variations in operating conditions such as 1) removal of contaminants, 2) continuous loading, 3) treatment of complex sample matrices, 4) variations in contaminant concentration, and 5) variations in filter hydraulic retention time (HRT), the proposed model was fit to published data from a previous study (Claveau-Mallet et al., 2013).

The speed and ease with which the proposed experimental procedure may be performed, as well as the low costs associated with equipment and analysis, make this methodology an attractive complement to batch tests, as it provides an estimate of filter longevity in a similarly short timeframe to batch tests' provision of estimates of filter capacity. As is the case with the RSSCTs proposed by Crittenden et al. (1991), the proposed model makes rapid predictions of filter longevity without the need for any preceding kinetic or isotherm studies, and only a small volume of sample wastewater is required for collection of the experimental data necessary to construct the model. In contrast with RSSCTs, the proposed model focuses on filter media subject to intermittent loading, modelling media saturation instead of filter effluent concentration. Predictions of filter performance are greatly simplified by virtue of the proposed model's empirical nature, which circumvents the need to consider mechanistic factors such as solute transport mechanisms and intraparticle diffusivities.

4.2 Theory

Where a wastewater is loaded onto an adsorptive filter column, and the effluent collected in a number of containers, the relationship between the total volume of wastewater filtered and the mass of a contaminant adsorbed per unit mass of filter media is described by:

$$q_e = \sum_{i=1}^{n} \frac{(C_o - C_{e_i})V_i}{m} \quad (1)$$

where q_e is the cumulative mass of contaminant adsorbed per gram of filter media, n is the number of containers in which the total volume of effluent ($\sum$Vi) is collected, C_o is the influent contaminant concentration, $C_{e,i}$ is the effluent contaminant concentration in the i^{th} container, V_i is the volume of effluent contained in the i^{th} container, and m is the mass of filter media contained in the filter column.

The Freundlich adsorption isotherm (Freundlich, 1906) is an empirical model describing the relationship between the adsorption of a contaminant from a mobile phase to a solid phase across a range of contaminant concentrations. The equation is as follows:

$$q_e = K_f C^{\frac{1}{n}} \quad (2)$$

where q_e is the cumulative mass of contaminant adsorbed per gram of filter media, C is the

contaminant concentration of the supernatant at equilibrium, and K_f and n are the Freundlich constants. The Freundlich equation assumes that the heat of adsorption decreases in magnitude with increasing extent of adsorption, and that this decline in the heat of adsorption is logarithmic, thus implying an exponential distribution of adsorption sites and energies (Sheindorf et al., 1981; Thomas and Crittenden, 1998). There is much experimental evidence that the real energy distributions, while perhaps not being strictly exponential, are indeed roughly of this sort (Cooney, 1998). Being a characteristic of the media, the assumption of exponential distribution remains equally valid, regardless of whether the saturation of the media is due to batch or through-flow exposure to adsorbate molecules. In the case of a batch experiment, the mass of adsorbate bound to the surface of a filter media increases with increasing solute concentration. In the case of a column experiment, the mass of adsorbate bound to the surface of the media increases as more solution is passed through the filter. Column effluent concentration, C_e, increases as progressively more wastewater is passed through the adsorptive media in a filter column, and therefore C_e is a function of V, the volume treated by the filter. If that function of V were modeled after Eqn. 2, it could reasonably be hypothesized that there would be some values of A and B such that the following equation might hold true:

$$q_e = AV^{\frac{1}{B}} \qquad (3)$$

where B is a dimensionless constant of system heterogeneity, just as n is a heterogeneity factor in the Freundlich equation (Allen et al., 2004), and A is a constant of proportionality with units $(mg/g)(L)^{(-1/B)}$. This hypothesis was originally arrived at after noting the striking similarity between plots of q_e vs. V from column experiments and plots of q_e vs. C_e from batch experiments. Eqn. 3 should only be considered valid for B>1, as values of B<1 would imply that a greater adsorbate concentration in the filter media serves to enhance the free energies of further adsorption. If this were the case, it would contradict the earlier assertion that the heat of adsorption decreases in magnitude with increasing extent of adsorption. Eqn. 3 can be validated in the same manner as the Freundlich equation is validated for batch tests, i.e. by constructing a plot of experimental data and comparing it to the linearized version of the equation:

$$ln(q_e) = ln(A) + B^{-1}ln(V) \qquad (4)$$

If Eqn. 3 describes the experimental data, the plot of $ln(q_e)$ versus $ln(V)$ would then be linear,

meaning the model constants could be determined from the plot as follows: A=exp(intercept), and B = (slope)$^{-1}$. Should the linear plot have a coefficient of determination, R^2, close to unity, it would indicate that Eqn. 3 is a suitable empirical model to describe the relationship between filter loading and filter media saturation.

Were all the filter column effluent collected in a single container, the average effluent concentration up to any volume, V, would be given by substituting Eqn. 1 into Eqn. 3 to yield:

$$C_{e_{avg}} = C_o - AmV^{(\frac{1}{B}-1)} \qquad (5)$$

If, however, the effluent were collected in a number of sequentially filled containers, the theoretical concentration of a given effluent aliquot collected at any time over the duration of operation of a filter may be calculated using:

$$C_{e_{\Delta V}} = C_o - \frac{\Delta q_e m}{\Delta V} \qquad (6)$$

where ΔV is the volume the filter effluent collected in a container between some arbitrary volumes V_a and V_b, $C_{e\Delta V}$ is the theoretical concentration of the filter effluent volume ΔV, and Δq_e is the theoretical change in the mass of contaminant adsorbed per unit mass of filter media from V_a to V_b.

Assuming Eqn. 3 fits the experimental data with acceptable accuracy, Δq_e between V_a and V_b can be calculated as follows:

$$\Delta q_{e,mod} = AV_b^{\frac{1}{B}} - AV_a^{\frac{1}{B}} \qquad (7)$$

Substituting Eqn. 7 into Eqn. 6, and letting V_a equal V_b-ΔV therefore gives the following:

$$C_{e_{\Delta V}} = Co - \frac{Am[V_b^{\frac{1}{B}} - (V_b - \Delta V)^{\frac{1}{B}}]}{\Delta V} \qquad (8)$$

The concentration of effluent at a given cumulative flow-through volume, V, as opposed to the average concentration, as given by Eqn. 5, can then be estimated by obtaining the concentration across an infinitesimally small ΔV as follows:

$$C_{e_v} = \lim_{\Delta V \to 0} \left[C_o - \left(\frac{Am[V^{\frac{1}{B}} - (V-\Delta V)^{\frac{1}{B}}]}{\Delta V} \right) \right] \qquad (9)$$

This yields the following:

$$C_{e_V} = C_o - \frac{AmV^{(\frac{1}{B}-1)}}{B} \qquad (10)$$

Thus, to determine V_b, the volume at which any given breakthrough concentration, C_{eb}, is reached, Eqn. 10 can be rearranged as follows:

$$V_b = \left(\frac{(C_o - C_{eb})B}{Am} \right)^{-\frac{B}{B-1}} \qquad (11)$$

Eqn. 11 describes the breakthrough curve for all breakthrough effluent concentrations in the range $0<C_{eb}<C_o$, though it is important to note in Eqn. 10 that $V^{1/B-1} \rightarrow 0$ as $V \rightarrow \infty$, meaning the model will only asymptotically approach total breakthrough, $C_{eb}=C_o$. This should not pose a limitation at concentration ranges of practical interest, i.e $0<C_{eb}<0.9(C_o)$. Above this range filter media are commonly thought to have reached exhaustion (Han et al., 2006; Netpradit et al., 2004), and caution should be exercised when trying to utilise the model to predict effluent concentrations past this exhaustion point. The volume at which initial breakthrough occurs, $V_{b,0}$, is found by letting C_{eb}, in Eqn. 11 equal to 0 mg L^{-1}. Inputting a value less than $V_{b,0}$, into Eqn. 10 would result in a negative C_e (as $V^{1/B-1} \rightarrow -\infty$ as $V \rightarrow 0$) which should simply be taken as zero. Breakthrough curves can easily be predicted for any filter subjected to equivalent loading by simply multiplying Eqn. 11 by a scaling factor, M_2/M_1, where M_1 is the mass of the filter from which the data to derive Eqn.11 was obtained, and M_2 is the mass of the filter of interest. Eqn. 10 can also be rearranged to yield following linear relationship between C_e and V:

$$ln(C_o - C_e) = (\frac{1}{b} - 1)lnV + ln\frac{AM}{B} \qquad (12)$$

With Eqn. 12, the coefficients A and B can theoretically be obtained from the slope and intercept of a plot of $ln(C_o-C_e)$ vs $ln(V)$ as follows: A= B(exp(intercept)/(M)), and B = $(slope+1)^{-1}$. However, as discussed previously, for an intermittently loaded filter column, it is

hypothesized that attempting to model the saturation of the filter media would prove more successful than attempting to directly model column effluent concentration. To complement the explanations given in this section, Figure S4.1 shows the derivation of the breakthrough curve (Eqn. 11) from a mass balance analysis of a filter system.

4.3 Materials and Methods

4.3.1 Preparation of small bore adsorption columns

Small-bore adsorption columns were prepared using polycarbonate tubes with an internal diameter of 0.94 cm and lengths of 10, 15, 20, 30, and 40 cm. Sets of tubes (comprising one tube of each length without replication) were packed with four different adsorbent media. These media comprised mixtures containing (1) aluminium sulfate drinking water treatment residual (Al-WTR; oven dried for 24 h at 105 °C and ground to pass a 0.5 mm sieve) (2) ferric sulfate drinking water treatment residual (Fe-WTR; oven dried for 24 h at 105 °C and ground to pass a 0.5 mm sieve) (3) fine crushed concrete (pulverized with a mortar and pestle and ground to pass a 0.5 mm sieve), and (4) coarse crushed concrete (pulverized with a mortar and pestle and ground to pass a 1.18 mm sieve, but retained by a 0.5 mm sieve); these will henceforth be referred to as media A, B, C, and D, respectively. In a preliminary experiment (not reported here), the relationship between dry density and hydraulic conductivity was studied for each media. On this basis, polycarbonate tubes used in this study were packed with media at a dry density such that each of the columns had a saturated hydraulic conductivity of 0.14 cm s^{-1}. The physical characteristics of the different media were such that this value could be achieved for all four media, and this value of hydraulic conductivity is comparable to that found in constructed wetland substrates (Brix et al., 2001) and slow sand filters (Mauclaire et al., 2006; Rodgers et al., 2004). Plastic syringes with an internal diameter equal to that of the polycarbonate tubes' outside diameter were fastened, by friction fit, to either end of the columns, and a small quantity of acid-washed glass wool was placed at the top and bottom of each column to retain the filter media within the tube. Flexible silicone tubing was attached to the syringe ends to provide influent and effluent lines, and the columns were attached to a frame to maintain a stable vertical orientation throughout the duration of the experiment.

4.3.2 Operation of small bore adsorption columns

A peristaltic pump with a variable speed motor was used to pump influent water, with an ortho-phosphorus (PO_4-P) concentration of 1 mg L^{-1}, into the base of each small-bore adsorption column at an approximate flow rate of 202±30 ml hr^{-1}. The combination of using a low flow rate in up-flow mode, and the high ratio of the column diameter to adsorbent particle diameter was considered sufficient to preclude any channeling effects

(Vijayaraghavan et al., 2004). The influent was prepared by adding a small quantity of K_2HPO_4 to tap water, with the resulting solution having a pH of 8.09±0.37. The simple makeup of the influent precluded interfering chemical interactions, and phosphorus (P) was selected as an excellent example of a contaminant commonly targeted by adsorption filters; its precise quantification is also relatively simple and inexpensive. The pump was operated in twelve hour on/off cycles to achieve loading periods of 24 to 156 hours. The effluent from each column was collected in two-hour aliquots in separate containers using an auto-sampler. The effluent in each container was analyzed for dissolved PO_4-P using a nutrient analyzer (Konelab20, Thermo Clinical Lab systems, Finland) after APHA (1998) and the cumulative mass of P adsorbed by the filter media was calculated using Eqn. 1. The limit of detection was determined, after McNaught and Wilkinson (1997), to be 0.009 mg L^{-1}.

4.3.3 Preparation of full-scale filter units

The media which showed the highest and the lowest absorbencies in the small-bore column experiments – media A and media D, respectively – were studied in 0.65 m-deep laboratory filters with an internal diameter of 0.104 m. These filters were constructed in triplicate and were packed with filter media to a depth of 0.4 m from the bottom of each column. The free-board of 0.25 m in each column was to allow water to be poured onto the surface without spillage. As was the case in the small bore columns, the mass of media in each column was varied to achieve a packing density such that each of the columns had an approximate hydraulic conductivity of 0.14 cm s^{-1}.

4.3.4 Operation of full-scale filter units

The filter units were operated in a temperature-controlled room at 10°C, and were subjected to repeated synthetic wastewater loadings over one to three months (see Figure S4.1 of the supplementary information). The synthetic wastewater influent contained a PO_4-P concentration of 1 mg L^{-1}, and was loaded manually onto a baffle at the top of the filter media. Columns containing filter media D were loaded with 28 liters of synthetic wastewater per loading event 10 times over the course of one month. Columns containing filter media A were loaded with 28 liters of synthetic wastewater 17 times, and were subsequently loaded nine times with 56 liters, in order to hasten the P saturation of the media. This loading was carried out over the space of three months. For both media, each loading event took place over a period of 1.5 hours, and there was a minimum of one day's rest between each loading

event. (see Figure S4.1 of the supplementary information)

4.3.5 Processing of experimental data

During each loading event, the effluent from the filter units was collected in large HDPE containers and was analyzed for PO_4-P using a nutrient analyzer (Konelab20, Thermo Clinical Lab systems, Finland) after APHA (1998). The mass of phosphorus adsorbed per unit mass of filter media was calculated using Eqn. 1, and a graph of cumulative q_e versus cumulative collected effluent volume, V, was constructed. The observed values of q_e were then compared to values predicted by models created using coefficients calculated from the data collected during small-scale adsorption column experiments.

4.3.6 Verification of model's adaptability to variances in operating conditions

In their 2013 paper, "Removal of phosphorus, fluoride and metals from a gypsum mining leachate using steel slag filters", Claveau-Mallet et al. (2013) provided a supplementary file containing concentration and pH data for effluents from columns which were being used to treat reconstituted gypsum mining leachate. In the study, a total of ten columns were operated as five sets of two columns connected in series. These were continuously loaded with leachate for a period of 145-222 days, and effluent concentrations of fluoride (amongst other contaminants) were measured twice per week. Four of the columns were loaded with a low concentration leachate (L1), while the remaining six were fed with a higher concentration leachate (L2). The effluents of those columns fed with leachate L2 showed variations in pH of 4.15±2, while those of columns fed with leachate L1 showed variations of 1.29±0.67. Due to the effect that the large fluctuations in the pH of effluent from columns fed with leachate L2 had on the data, the model proposed in the current study was fit to the effluent fluoride concentration data from the columns fed with leachate L1. The columns were loaded continuously with an influent that had a fluoride concentration of 9 mg L^{-1}. Effluent fluoride concentrations were measured twice weekly, and using these data, averages of effluent concentration were used to determine the amount of fluoride removed by the filter media (q_e). Given that the columns were loaded at a continuous rate by a peristaltic pump, the volume of leachate filtered (V) was taken to be analogous to the time (T) for which the columns were running (as $V= \alpha T$, where α is the flow rate in L day^{-1}), and a plot of q_e versus V was developed from which the model coefficients, A and B, were computed from plots of Eqn. 4, as described previously. The difficulties of modeling non-ideal breakthrough curves was

discussed in detail by Sperlich et al. (2005), and to further validate our proposed model, a supplementary Excel file has been made available with this paper demonstrating our model's ability to describe and predict (using RSSCT data) the breakthrough curves observed in that study. The Excel file also contains a template to facilitate the fitting of our proposed model to other experimental data.

4.3.7 Determination of model error

The hybrid error function (HYBRID), developed by Porter et al. (1999), is a non-linear error function often employed when using non-linear regression methods to predict isotherm parameters. Chan et al. (2012) analyzed data relating to the adsorption of acid dyes onto charcoal, and of the five non-linear error functions studied, concluded that the HYBRID function was the most effective in determining isotherm parameters for the six isotherm equations used in their study. The HYBRID function was used in the current study as a metric for the comparison of the goodness of model fit to experimental data. The function is:

$$\frac{100}{n-p}\sum_{i=1}^{n}\frac{(q_{e,i,meas}-q_{e,i,calc})^2}{q_{e,i,meas}} \qquad (12)$$

where n is the number of experimental data points, p is the number of constants in the proposed model, $q_{e,i,meas}$ is the value of q_e obtained from Eqn. 1, and $q_{e,i,calc}$ is the value of q_e obtained from Eqn. 3. The mean percentage error (MPE) was also calculated to provide an easily comparable metric by which to assess the model's goodness of fit and its bias toward either over- or underestimation of predicted values compared to observed values. The MPE was calculated thus:

$$MPE = \frac{100\%}{n}\sum_{i=1}^{n}\frac{q_{e,i,meas}-q_{e,i,calc}}{q_{e,i,meas}} \qquad (13)$$

where n, $q_{e,i,meas}$, and $q_{e,i,calc}$ are the same as given for Eqn. 12. A negative MPE indicates that the model predictions tend to underestimate experimentally observed adsorption, whereas a positive error indicates an overestimation.

4.4 Results and Discussion

4.4.1 Verification of theory at bench scale.

For all four of the media studied, the relationship between filter loading and the mass of P adsorbed per unit mass of filter media, q_e, could be estimated with a very high degree of accuracy by the proposed model (Eqn.3). Figure 4.1 shows the goodness of fit of model predictions made using 36 hours of experimental data. The model coefficients, along with the R^2 values of the linear plots from which they were determined, are shown in Table S4.1. The experimental data fitted the linear expression of the model with a very high degree of accuracy, and the average linear regression coefficients observed for media A, B, C, and D were 0.997, 0.991, 0.963 and 0.997, respectively.

A column containing media A was loaded for 68 hours to study the effect of experimental runtime on the accuracy with which model coefficients could be determined. Revised estimates of model coefficients were determined from experimental data collected at two-hour increments, and a model using these coefficients was fitted to experimental data for the entirety of the period for which the filter was loaded. Figure S4.2a shows the HYBRID error of these models, against the time at which the model coefficients were determined. After an initial sharp drop-off in model error, there was little improvement in model fit past the 24-hour mark. Figure S4.2b shows the goodness of fit to experimental data of models using coefficients determined after 24 and 36 hours of data aggregation, demonstrating that there was little benefit to be gained from experimental run times in excess of 24 hours.

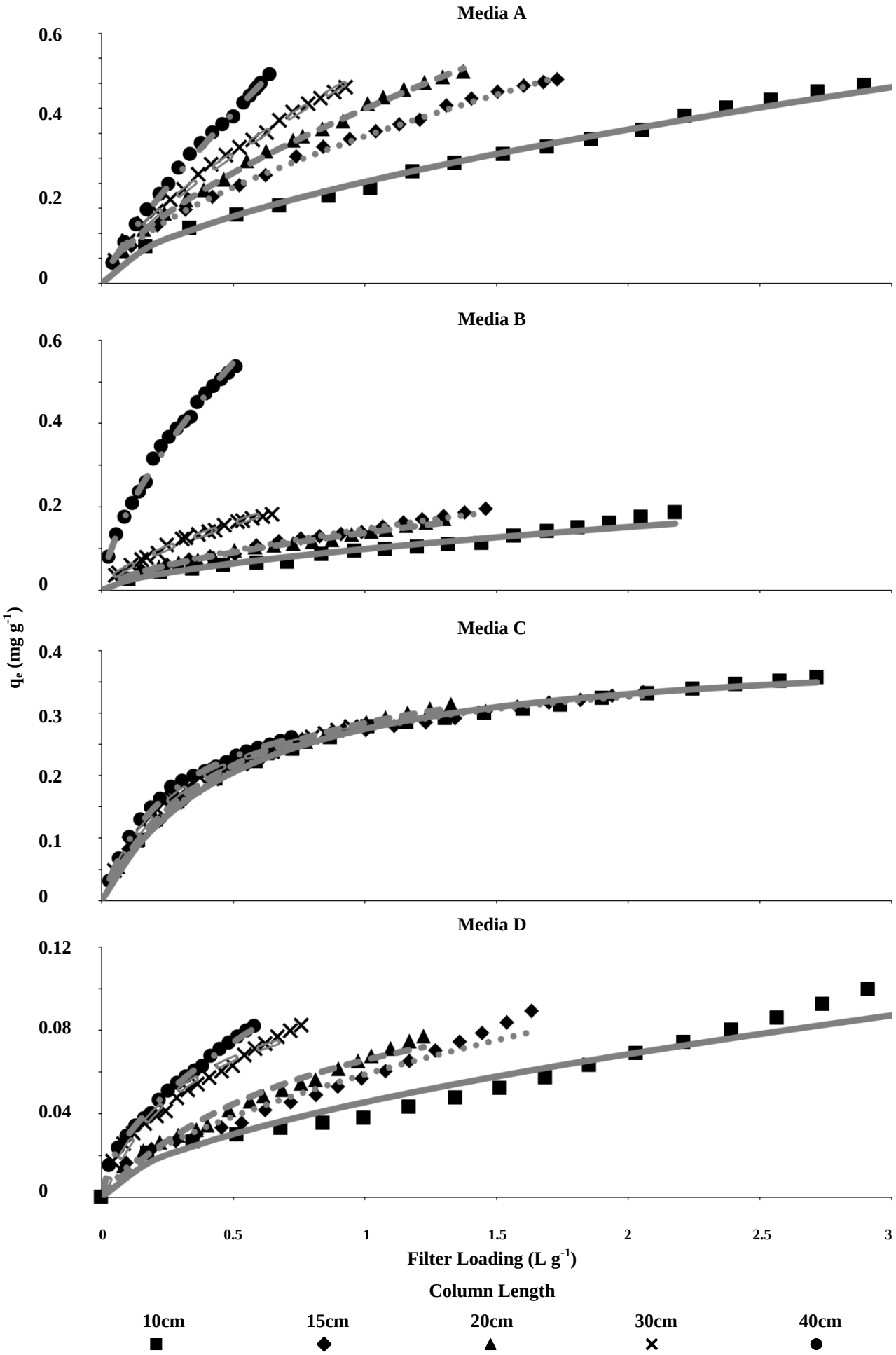

Figure 4.1 Filter media P adsorption (y-axis) vs. filter loading (x-axis), showing observed progressions of media saturation and the goodness of model fit for each media and column length.

To study the accuracy with which effluent concentration, average daily effluent concentration, and total P loss could be predicted, a small-bore adsorption column containing media A was operated for an extended period of 156 hours. All filter effluent was collected in two hour aliquots, and it was possible, using Eqn. 9, to predict the P concentration of any one of these aliquots at any given time. There were 12 hour rest-periods in between loading cycles, and these cessations in filter loading appear to have allowed the filter media to replenish some of its adsorptive potential. Increased P uptake at the beginning of each loading phase resulted in the effluent concentrations producing the cyclical 6-point pattern seen in Figure 4.2a, and this strongly suggests that intraparticle diffusion of P, driven by the concentration gradient within the media particles, resulted in rejuvenation of the media surface; this has also been observed by many others (DeMarco et al., 2003; Greenleaf and Sengupta, 2006; Sengupta and Pandit, 2011; Song et al., 2011). Model predictions of C_e describe the general trend of increasing effluent concentration with increasing volume well, though the model does not describe the cyclical pattern described previously. However, as can be seen in Figure 4.2b, it was possible to produce highly accurate model predictions of average daily effluent concentration; these values could be forecast with a mean error of just 0.59% ± 10.54%. Average daily effluent concentration is, arguably, a more useful metric for assessing the long-term performance of a filter media, and, as seen in Figure 4.2c, predictions of cumulative P loss made using predicted average daily effluent concentration had a mean error of just 3.74% ± 8.31%.

To ensure the results of the small-bore column experiments were replicable, 20 cm columns packed with media A were operated in triplicate for a period of 24 hours, and the model coefficients calculated from each column were compared. As can be seen in Figure S4.3a, the experimental data from each of the three columns fit the linear expression of the proposed model with a coefficient of determination, R^2, of 0.996±0.001. The model coefficients were determined as A = 0.109±0.003 and B = 1.480±0.043. Figure S4.3b demonstrates the effect of this variability in coefficients on the models produced. After 24 hours of operation, at which 0.5 liters of effluent had been collected, the mean q_e predicted by substituting V=5 litres into Eqn. 3 was 0.320±0.017 mg g^{-1}. The variability of model predictions being so slight would indicate that this method of determining model coefficients is highly replicable.

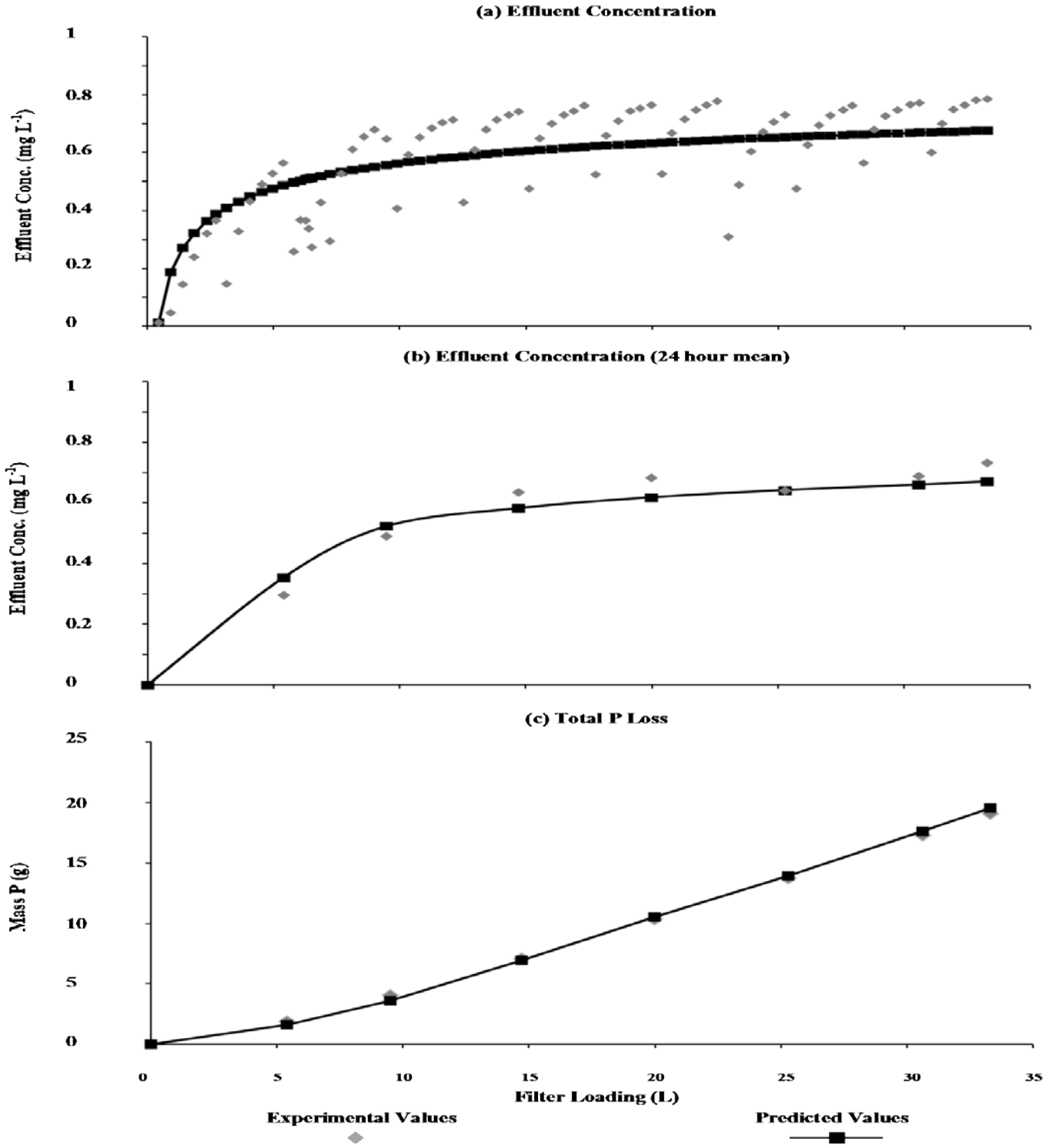

Figure 4.2 (a) Comparison of predicted and observed progressions of effluent concentration (y-axis) vs. cumulative filter loading (x-axis), with predictions and observations made on a bi-hourly basis.

Figure 4.2 (b) Comparison of predicted and observed daily mean effluent concentrations (y-axis) vs. cumulative filter loading (x-axis).

Figure 4.2 (c) Comparison of predicted and observed cumulative P loss in effluent (y-axis) vs. cumulative filter loading (x-axis).

4.4.2 Verification of theory at filter-scale.

Figure 4.3 shows the experimental data from large-scale experiments overlain by predictions made using models created from the small-bore adsorption column data. In the case of filter media A, the model obtained from the 24 hour small-bore adsorption study predicted the performance of the full-scale filter unit over three months with a very high degree of accuracy. Predicted values of q_e differed from observed values by just 2.94%±4.31%, and the model fit the observed values with a HYBRID error of just 0.074. In the case of filter media D, predicted values of q_e differed from observed values by 8.08%±11.49%, and the model fit the observed values with a HYBRID error of just 0.070. It was thus demonstrated that, in terms of media mass and loading, scaling the experiment up by approximately two orders of magnitude had very little negative impact on the ability of the model to predict filter performance, appearing to confirm the hypothesis that a small-scale, 24-hour experiment could be used to accurately predict large-scale filter performance over a much greater period. To further validate this assertion, RSSCT data from a study conducted by Sperlich et al. (2005) was used to construct a model which was then used to successfully predict the performance of a lab-scale filter that was over 700 times larger than the RSSCT in terms of filter media mass. This model and the data used in its construction can be found in the supplementary Excel file which has been made available with this paper.

4.4.3 Adaptability of model to varying conditions

Figure 4.4 shows the model proposed by this study fit to fluoride removal data published by Claveau-Mallet et al. (2013). As can be seen, the model described the evolution of fluoride concentrations in the filter effluent well for both those filters fed with a constant fluoride concentration of 9 mg L^{-1} (Figure 4.4, ‘A’ Columns), and those fed with a variable concentration from the effluent of the preceding filter in a series (Figure 4.4, ‘B’ Columns). This would appear to confirm the model's applicability to contaminants other than P, as well as to filter media other than those examined by this study. The complexity of the wastewater's composition did not appear to have a negative impact on the model's ability to describe the observed data, nor did continuous loading of the columns. Columns 1A, 1B, 4A, and 4B (Figure 4.4) had HRTs of 14.2, 18.2, 4.8, and 4.3 hours, respectively, though these variations in HRT appear to have had no significant impact on the goodness of model fit. Columns 1A and 4A were both loaded using wastewater with a constant fluoride concentration of 9 mg L^{-1}, while columns 1B and 4B were loaded with the effluents from columns 1A and 4A, thus

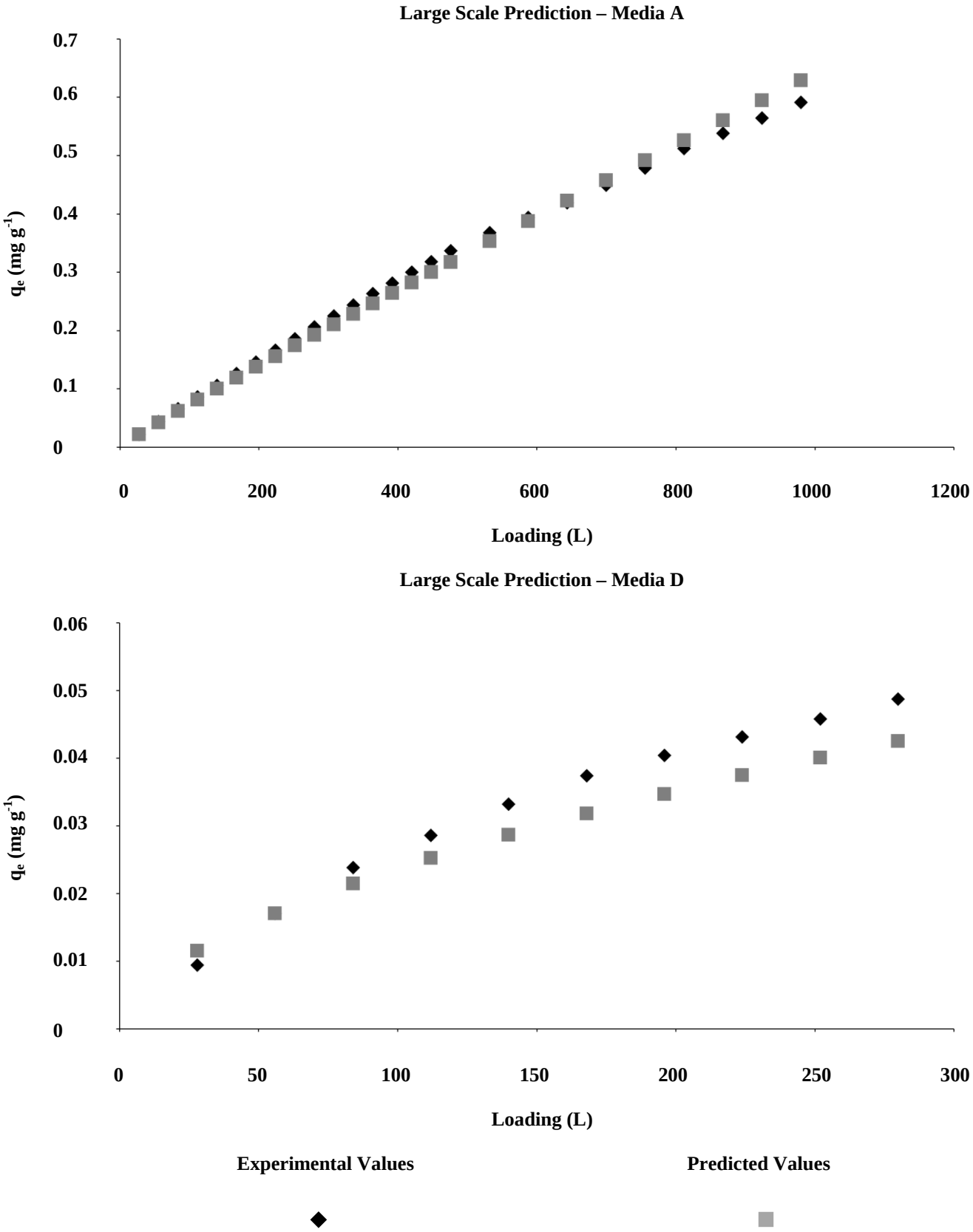

Figure 4.3 Comparison of predicted and observed q_e values (y-axis) vs. filter loading (x-axis), demonstrating the ability of the proposed model to predict large-scale filter performance.

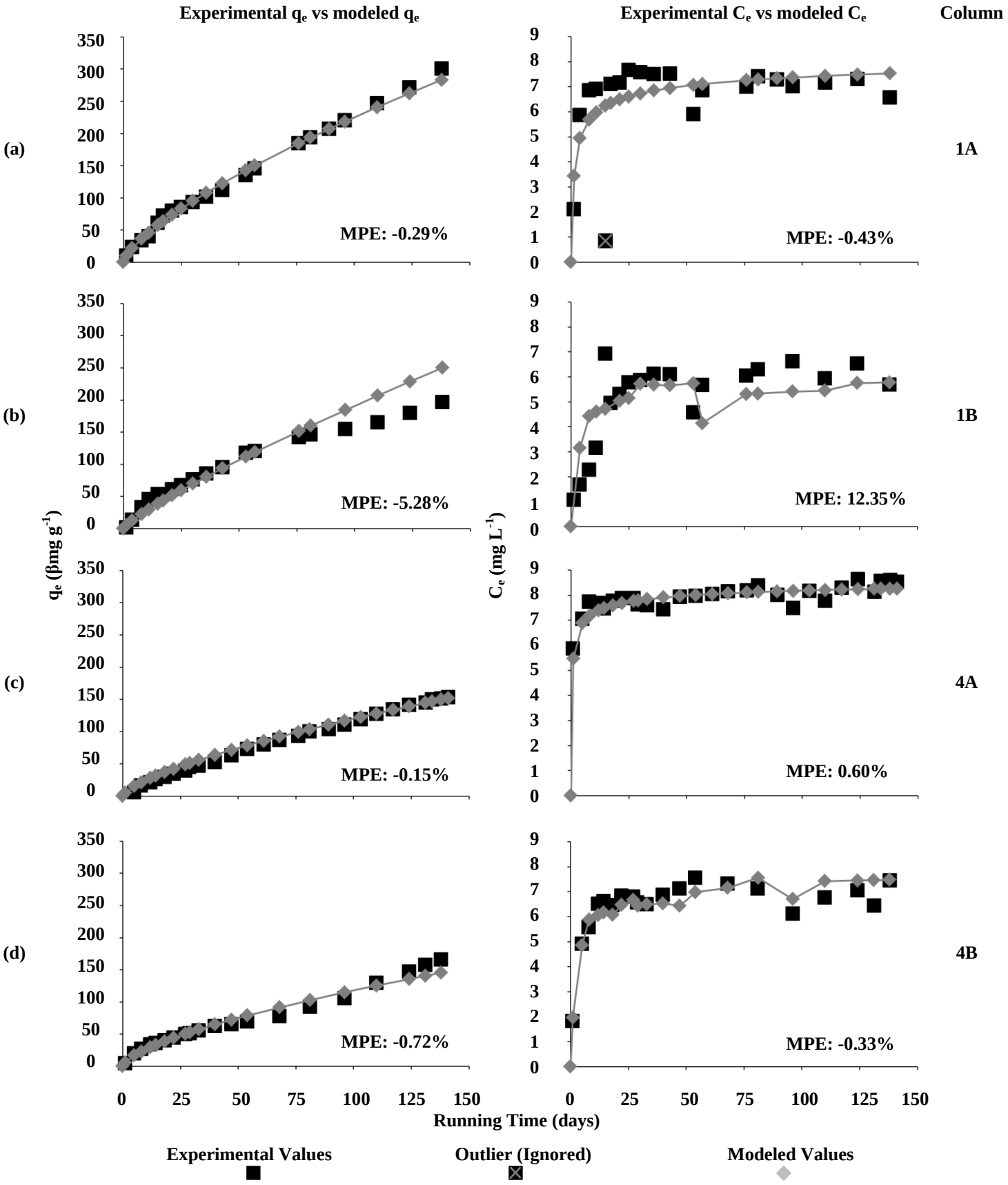

Figure 4.4 (a-d) Goodness of model fit to fluoride removal data reported by Claveau-Mallet et al. (2013).

receiving an influent with fluoride concentrations ranging from 0.85-7.66 and 5.86-8.63 mg L^{-1}, respectively. In general, higher MPEs were recorded for models fit to data from columns fed by an influent of varying concentration, and a greater variance in influent concentration resulted in a larger MPE. This would seem to indicate that variation in influent concentration had a negative impact on model fit, though with a maximum recorded MPE of 12.35% (Figure 4.5b), the model appeared to cope well with this variability nonetheless.

4.4.4 Practical implications

To be of the greatest utility, a method of filter media characterisation must be easy to use, quick to execute, and should replicate the performance of a field-scale system as closely as possible (Limousin et al., 2007). Many field-scale adsorption systems are loaded intermittently, and it was hypothesized that for such a system, a model which attempted to describe and predict filter media saturation would be more successful than a model which attempted to model filter column effluent directly. The model proposed by this study can be linearized in two ways, and the coefficients required to produce the model can be determined from linear plots of q_e or C_e data using linear plots of $ln q_e$ vs $ln V$ (method 1) and $ln(C_o-C_e)$ vs $ln V$ (method 2), respectively. The former attempts to model media saturation, while the later attempts to model column effluent directly. The suitability of an equation to model an adsorption system can be judged by the R^2 correlation coefficient of its linear plot, and when there are multiple methods of linearizing an equation to obtain model coefficients (e.g. as with the Langmuir isotherm) the R^2 can be used to determine the better method (Behnamfard and Salarirad, 2009). As can be seen in Figure 4.5, plots of $ln q_e$ vs $ln V$ produced graphs with higher linearity than plots of $ln(C_o-C_e)$ vs $ln V$ in all cases, suggesting that method 1 may be preferable to method 2. To further confirm this hypothesis, graphs of experimental data from small-bore columns containing filter media A were modeled using model coefficients determined using method 1 and method 2, respectively. Figure 4.6 shows the comparison of these models and their goodness of fit to values of q_e and C_e obtained experimentally. As can be concluded from analysis of Figure 4.6, coefficients determined using method 1 and method 2 described the evolution of filter effluent with similar accuracy, though method 2 gave marginally better accuracy. In contrast, method 1 was significantly better for producing accurate models of the evolution of filter saturation. This appears to confirm the hypothesis that to predict the performance of an intermittently loaded filter, modeling media saturation is a more successful approach than attempting to model filter effluent concentrations directly.

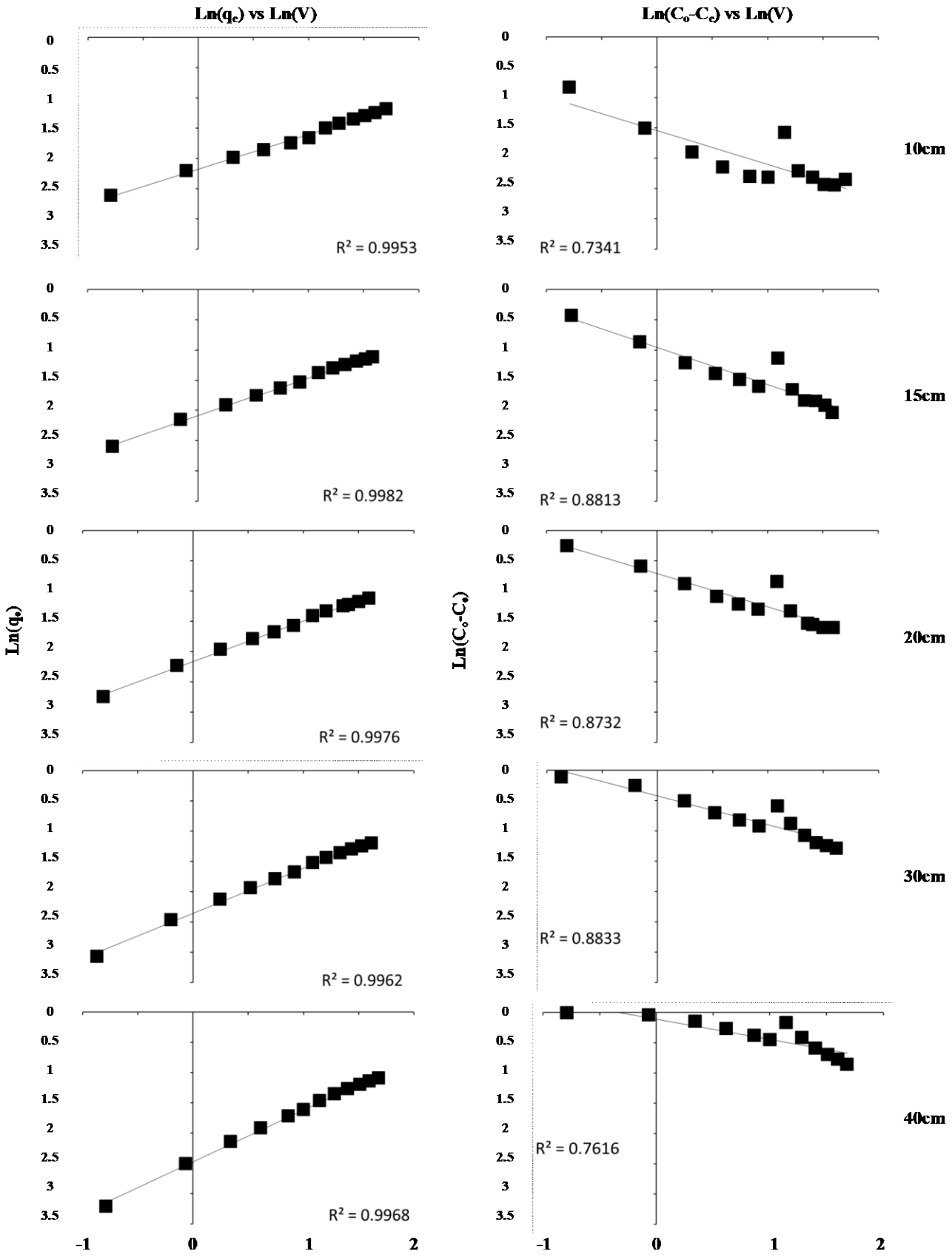

Figure 4.5 Comparison of the linearity of plots of $Ln(q_e)$ (left y-axis) vs. Ln(V) (x-axis), and $Ln(C_o-C_e)$ (right y-axis) vs. Ln(V) (x-axis). These plots are used to determine model coefficients by analysis of filter saturation or filter effluent concentration respectively.

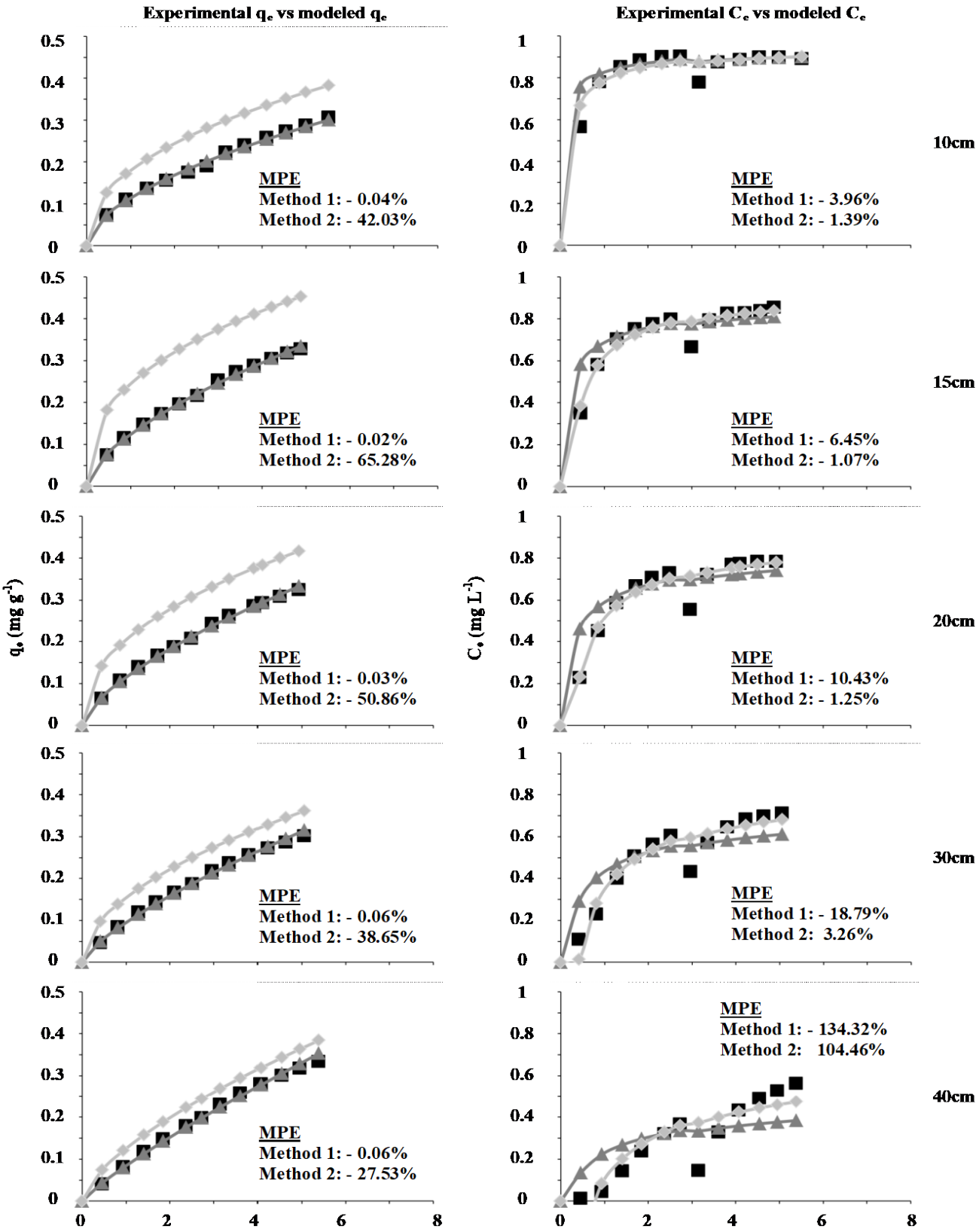

Figure 4.6 Plots of q_e (left y-axis) and C_e (right y-axis) vs. filtered volume (x-axis), demonstrating the effect that the method of coefficient determination (ie analysis of filter saturation or analysis of filter effluent concentration) has on model accuracy.

4.5 Conclusions

This study proposed a model capable of describing the non-ideal (i.e. non S-shaped, linear to convex) breakthrough curves often described by data from column experiments using low-cost adsorbents and soils.

- It was demonstrated that the model could be used to describe and predict the performance of multiple low-cost filter media, which were intermittently loaded with a wastewater containing 1 mg L^{-1} of PO_4-P.
- The model was fit to data from two independent studies, demonstrating its ability to describe the removal of contaminants other than phosphorus (fluoride and arsenate), and its adaptability to continuous loading conditions, complex wastewater compositions, and variations in HRT.
- It was shown that model parameters could be determined experimentally from both filter effluent data and media saturation data, with the latter approach being more successful when modelling intermittently loaded filters.
- The model was successfully used to predict the performance of lab-scale filter columns which were intermittently loaded over the course of a number of months.
- The model parameters required to predict the performance of the lab-scale filters were determined using data aggregated over a 24 hour period using small-scale column tests.

4.6 Acknowledgement

The first author would like to acknowledge the Irish Research Council for funding.

4.7 References

Ádám, K., Sovik, A.K., Krogstad, T., Heistad, A., 2007. Phosphorous removal by the filter materials light-weight aggregates and shellsand-a review of processes and experimental set-ups for improved design of filter systems for wastewater treatment. Vatten 63, 245.

Ali, I., Gupta, V.K., 2007. Advances in water treatment by adsorption technology. Nat. Protoc. 1, 2661–2667. doi:10.1038/nprot.2006.370

Allen, S.J., Mckay, G., Porter, J.F., 2004. Adsorption isotherm models for basic dye adsorption by peat in single and binary component systems. J. Colloid Interface Sci. 280, 322–333. doi:10.1016/j.jcis.2004.08.078

APHA (American Public Health Association), American Water Works Association., Water Environment Federation., 1998. Standard methods for the examination of water and wastewater. American Public Health Association, Washington, DC.

Babel, S., Kurniawan, T.A., 2003. Low-cost adsorbents for heavy metals uptake from contaminated water: a review. J. Hazard. Mater. 97, 219–243. doi:10.1016/S0304-3894(02)00263-7

Behnamfard, A., Salarirad, M.M., 2009. Equilibrium and kinetic studies on free cyanide adsorption from aqueous solution by activated carbon. J. Hazard. Mater. 170, 127–133. doi:10.1016/j.jhazmat.2009.04.124

Bohart, G.S., Adams, E.Q., 1920. Some Aspects of the Behavior of Charcoal with Respect to Chlorine. 1. J. Am. Chem. Soc. 42, 523–544. doi:10.1021/ja01448a018

Brix, H., Arias, C.A., Del Bubba, M., 2001. Media selection for sustainable phosphorus removal in subsurface flow constructed wetlands. Water Sci. Technol. 44, 47–54.

Buergisser, C.S., Cernik, M., Borkovec, M., Sticher, H., 1993. Determination of nonlinear adsorption isotherms from column experiments: an alternative to batch studies. Environ. Sci. Technol. 27, 943–948. doi:10.1021/es00042a018

Chan, L.S., Cheung, W.H., Allen, S.J., McKay, G., 2012. Error analysis of adsorption isotherm models for acid dyes onto bamboo derived activated carbon. Chin. J. Chem. Eng. 20, 535–542.

Clark, R.M., 1987. Evaluating the cost and performance of field-scale granular activated carbon systems. Environ. Sci. Technol. 21, 573–580. doi:10.1021/es00160a008

Claveau-Mallet, D., Wallace, S., Comeau, Y., 2013. Removal of phosphorus, fluoride and metals from a gypsum mining leachate using steel slag filters. Water Res. 47, 1512–1520. doi:10.1016/j.watres.2012.11.048

Cooney, D.O., 1998. Adsorption design for wastewater treatment. CRC Press

Crini, G., 2006. Non-conventional low-cost adsorbents for dye removal: a review. Bioresour. Technol. 97, 1061–1085.

Crini, G., Badot, P.-M., 2008. Application of chitosan, a natural aminopolysaccharide, for dye removal from aqueous solutions by adsorption processes using batch studies: A review of recent literature. Prog. Polym. Sci. 33, 399–447. doi:10.1016/j.progpolymsci.2007.11.001

Crittenden, J.C., Reddy, P.S., Arora, H., Trynoski, J., Hand, D.W., Perram, D.L., Summers, R.S., 1991. Predicting GAC Performance With Rapid Small-Scale Column Tests. J. Am. Water Works Assoc. 83, 77–87.

Cucarella, V., Renman, G., 2009. Phosphorus Sorption Capacity of Filter Materials Used for On-site Wastewater Treatment Determined in Batch Experiments-A Comparative Study. J. Environ. Qual. 38, 381–392. doi:10.2134/jeq2008.0192

Deliyanni, E.A., Peleka, E.N., Matis, K.A., 2009. Modeling the sorption of metal ions from aqueous solution by iron-based adsorbents. J. Hazard. Mater. 172, 550–558. doi:10.1016/j.jhazmat.2009.07.130

DeMarco, M.J., SenGupta, A.K., Greenleaf, J.E., 2003. Arsenic removal using a polymeric/inorganic hybrid sorbent. Water Res. 37, 164–176. doi:10.1016/S0043-1354(02)00238-5

Demirbas, A., 2008. Heavy metal adsorption onto agro-based waste materials: A review. J. Hazard. Mater. 157, 220–229. doi:10.1016/j.jhazmat.2008.01.024

Drizo, A., Comeau, Y., Forget, C., Chapuis, R.P., 2002. Phosphorus saturation potential: A parameter for estimating the longevity of constructed wetland systems. Environ. Sci. Technol. 36, 4642–4648.

Freundlich, 1906. Uber die adsorption in losungen. Z. Für Phys. Chem. 57, 384–470.

McKay, 1996. Use of adsorbents for the removal of pollutants from wastewaters. CRC Press, Boca Raton ; London.

Greenleaf, J.E., SenGupta, A.K., 2006. Environmentally Benign Hardness Removal Using Ion-Exchange Fibers and Snowmelt. Environ. Sci. Technol. 40, 370–376. doi:10.1021/es051702x

Grolimund, D., Borkovec, M., Federer, P., Sticher, H., 1995. Measurement of Sorption Isotherms with Flow-Through Reactors. Environ. Sci. Technol. 29, 2317–2321. doi:10.1021/es00009a025

Hamdaoui, O., Naffrechoux, E., 2007. Modeling of adsorption isotherms of phenol and chlorophenols onto granular activated carbon: Part II. Models with more than two parameters. J. Hazard. Mater. 147, 401–411.

Han, R., Zou, W., Li, H., Li, Y., Shi, J., 2006. Copper(II) and lead(II) removal from aqueous solution in fixed-bed columns by manganese oxide coated zeolite. J. Hazard. Mater. 137, 934–942. doi:10.1016/j.jhazmat.2006.03.016

Healy, M.G., Rodgers, M., Mulqueen, J., 2007. Treatment of dairy wastewater using constructed wetlands and intermittent sand filters. Bioresour. Technol. 98, 2268–2281. doi:10.1016/j.biortech.2006.07.036

Hutchins, R., 1973. New method simplifies design of activated carbon systems, Water Bed Depth Service Time analysis. J Chem Eng Lond 81, 133–138.

Johansson, L., 1999. Blast furnace slag as phosphorus sorbents — column studies. Sci. Total Environ. 229, 89–97. doi:10.1016/S0048-9697(99)00072-8

Jusoh, A., Su Shiung, L., Ali, N., Noor, M.J.M.M., 2007. A simulation study of the removal efficiency of granular activated carbon on cadmium and lead. Desalination, EuroMed 2006Conference on Desalination Strategies in South Mediterranean Countries 206, 9–16. doi:10.1016/j.desal.2006.04.048

Limousin, G., Gaudet, J.-P., Charlet, L., Szenknect, S., Barthès, V., Krimissa, M., 2007. Sorption isotherms: A review on physical bases, modeling and measurement. Appl. Geochem. 22, 249–275. doi:10.1016/j.apgeochem.2006.09.010

Malkoc, E., Nuhoglu, Y., Abali, Y., 2006. Cr(VI) adsorption by waste acorn of Quercus ithaburensis in fixed beds: Prediction of breakthrough curves. Chem. Eng. J. 119, 61–68. doi:10.1016/j.cej.2006.01.019

Mauclaire, L., Schürmann, A., Mermillod-Blondin, F., 2006. Influence of hydraulic conductivity on communities of microorganisms and invertebrates in porous media: a case study in drinking water slow sand filters. Aquat. Sci. 68, 100–108. doi:10.1007/s00027-005-0811-4

McNaught, A.D., Wilkinson, A., 1997. Compendium of chemical terminology. Blackwell Science Oxford.

Netpradit, S., Thiravetyan, P., Towprayoon, S., 2004. Evaluation of metal hydroxide sludge for reactive dye adsorption in a fixed-bed column system. Water Res. 38, 71–78. doi:10.1016/j.watres.2003.09.007

Ouvrard, S., Simonnot, M.-O., de Donato, P., Sardin, M., 2002. Diffusion-Controlled Adsorption of Arsenate on a Natural Manganese Oxide. Ind. Eng. Chem. Res. 41, 6194–6199. doi:10.1021/ie020269m

Pant, H.K., Reddy, K.R., Lemon, E., 2001. Phosphorus retention capacity of root bed media of sub-surface flow constructed wetlands. Ecol. Eng. 17, 345–355. doi:10.1016/S0925-8574(00)00134-8

Porter, J.F., McKay, G., Choy, K.H., 1999. The prediction of sorption from a binary mixture of acidic dyes using single- and mixed-isotherm variants of the ideal adsorbed solute theory. Chem. Eng. Sci. 54, 5863–5885. doi:10.1016/S0009-2509(99)00178-5

Pratt, C., Parsons, S.A., Soares, A., Martin, B.D., 2012. Biologically and chemically mediated adsorption and precipitation of phosphorus from wastewater. Curr. Opin. Biotechnol., Phosphorus biotechnology • Pharmaceutical biotechnology 23, 890–896. doi:10.1016/j.copbio.2012.07.003

Rodgers, M., Healy, M.G., Mulqueen, J., 2005. Organic carbon removal and nitrification of high strength wastewaters using stratified sand filters. Water Res. 39, 3279–3286. doi:10.1016/j.watres.2005.05.035

Rodgers, M., Mulqueen, J., Healy, M.G., 2004. Surface clogging in an intermittent stratified sand filter. Soil Sci. Soc. Am. J. 68, 1827–1832.

Sengupta, S., Pandit, A., 2011. Selective removal of phosphorus from wastewater combined with its recovery as a solid-phase fertilizer. Water Res. 45, 3318–3330. doi:10.1016/j.watres.2011.03.044

Seo, D.C., Cho, J.S., Lee, H.J., Heo, J.S., 2005. Phosphorus retention capacity of filter media for estimating the longevity of constructed wetland. Water Res. 39, 2445–2457. doi:10.1016/j.watres.2005.04.032

Sheindorf, C.H., Rebhun, M., Sheintuch, M., 1981. A Freundlich-type multicomponent isotherm. J. Colloid Interface Sci. 79, 136–142.

Song, X., Pan, Y., Wu, Q., Cheng, Z., Ma, W., 2011. Phosphate removal from aqueous solutions by adsorption using ferric sludge. Desalination 280, 384–390. doi:10.1016/j.desal.2011.07.028

Søvik, A.K., Kløve, B., 2005. Phosphorus retention processes in shell sand filter systems treating municipal wastewater. Ecol. Eng. 25, 168–182. doi:10.1016/j.ecoleng.2005.04.007

Sperlich, A., Werner, A., Genz, A., Amy, G., Worch, E., Jekel, M., 2005. Breakthrough behavior of granular ferric hydroxide (GFH) fixed-bed adsorption filters: modeling and experimental approaches. Water Res. 39, 1190–1198. doi:10.1016/j.watres.2004.12.032

Thomas, H.C., 1944. Heterogeneous Ion Exchange in a Flowing System. J. Am. Chem. Soc. 66, 1664–1666. doi:10.1021/ja01238a017

Thomas, W.J., Crittenden, B.D., 1998. Adsorption Technology and Design. Butterworth-Heinemann.

Ulén, B., Etana, A., 2010. Risk of phosphorus leaching from low input grassland areas. Geoderma 158, 359–365. doi:10.1016/j.geoderma.2010.06.003

Vidon, P., Allan, C., Burns, D., Duval, T.P., Gurwick, N., Inamdar, S., Lowrance, R., Okay, J., Scott, D., Sebestyen, S., 2010. Hot Spots and Hot Moments in Riparian Zones: Potential for Improved Water Quality Management1. JAWRA J. Am. Water Resour. Assoc. 46, 278–298. doi:10.1111/j.1752-1688.2010.00420.x

Vijayaraghavan, K., Jegan, J., Palanivelu, K., Velan, M., 2004. Removal of nickel(II) ions from aqueous solution using crab shell particles in a packed bed up-flow column. J. Hazard. Mater. 113, 223–230. doi:10.1016/j.jhazmat.2004.06.014

Von Post, L., 1922. Sveriges Geologiska Undersöknings torvinventering och n\a agra av dess hittills vunna resultat.

Vohla, C., Kõiv, M., Bavor, H.J., Chazarenc, F., Mander, Ü., 2011. Filter materials for phosphorus removal from wastewater in treatment wetlands—A review. Ecol. Eng., Special Issue: Enhancing ecosystem services on the landscape with created, constructed and restored wetlands 37, 70–89. doi:10.1016/j.ecoleng.2009.08.003

Walker, G.M., Weatherley, L.R., 1997. Adsorption of acid dyes on to granular activated carbon in fixed beds. Water Res. 31, 2093–2101. doi:10.1016/S0043-1354(97)00039-0

Yagub, M.T., Sen, T.K., Afroze, S., Ang, H.M., 2014. Dye and its removal from aqueous solution by adsorption: A review. Adv. Colloid Interface Sci. 209, 172–184. doi:10.1016/j.cis.2014.04.002

Yoon, Y.H., Nelson, J.H., 1984. Application of Gas Adsorption Kinetics I. A Theoretical Model for Respirator Cartridge Service Life. Am. Ind. Hyg. Assoc. J. 45, 509–516. doi:10.1080/15298668491400197

Supplement to Chapter 4

Table S4.1 Model coefficients and goodness of fit from 36 hour experiments

Filter Media	Length (cm)	Model Coefficients			$q_{e,calc}$ vs $q_{e,expt}$	
		R^2	A	B	R^2	slope
Media A	10	0.994	0.112	1.669	0.995	1.041
	15	0.998	0.125	1.626	0.998	1.005
	20	0.999	0.115	1.519	0.998	0.999
	30	0.997	0.096	1.410	0.998	0.988
	40	0.997	0.085	1.214	0.998	0.946
Media B	10	0.973	0.027	1.616	0.961	1.117
	15	0.995	0.030	1.584	0.993	1.031
	20	0.994	0.025	1.652	0.991	1.028
	30	0.996	0.032	1.517	0.993	0.974
	40	0.997	0.091	1.531	0.995	0.982
Media C	10	0.957	0.168	2.503	0.965	0.905
	15	0.959	0.134	2.193	0.958	0.895
	20	0.975	0.112	1.823	0.976	0.900
	30	0.970	0.095	1.819	0.976	0.898
	40	0.954	0.080	1.616	0.958	0.849
Media D	10	0.932	0.024	1.693	0.943	1.184
	15	0.976	0.023	1.651	0.977	1.107
	20	0.994	0.021	1.621	0.975	1.002
	30	0.997	0.028	1.856	0.971	0.977
	40	0.998	0.027	1.756	0.998	1.020

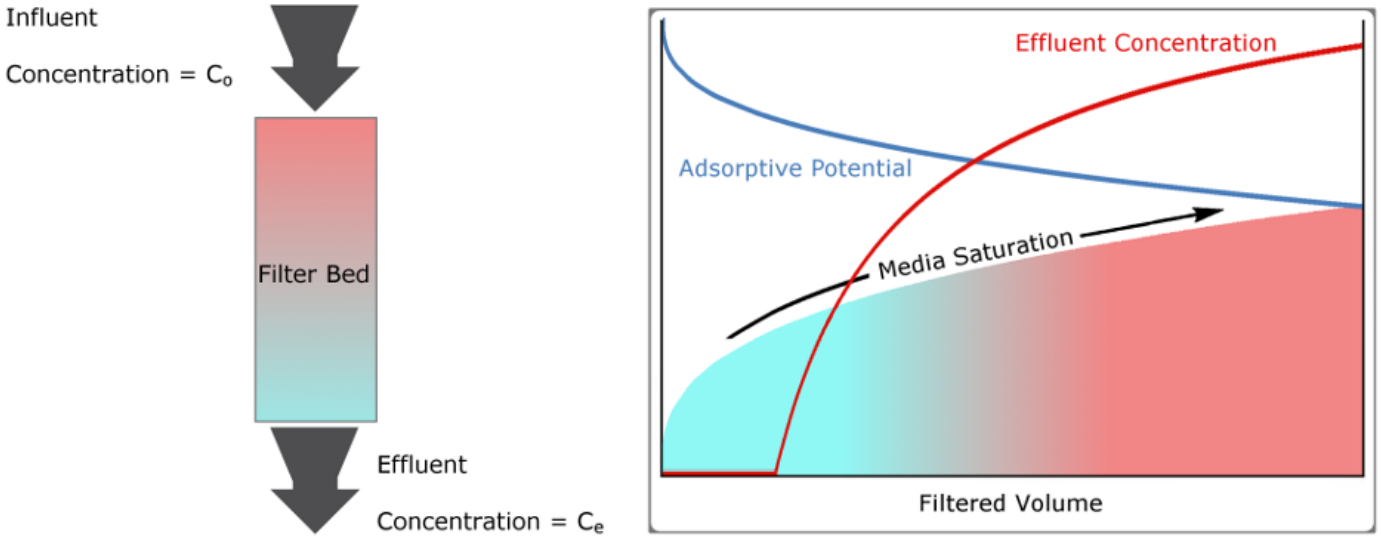

(a) Mass in/retained vs Filtered Volume, V

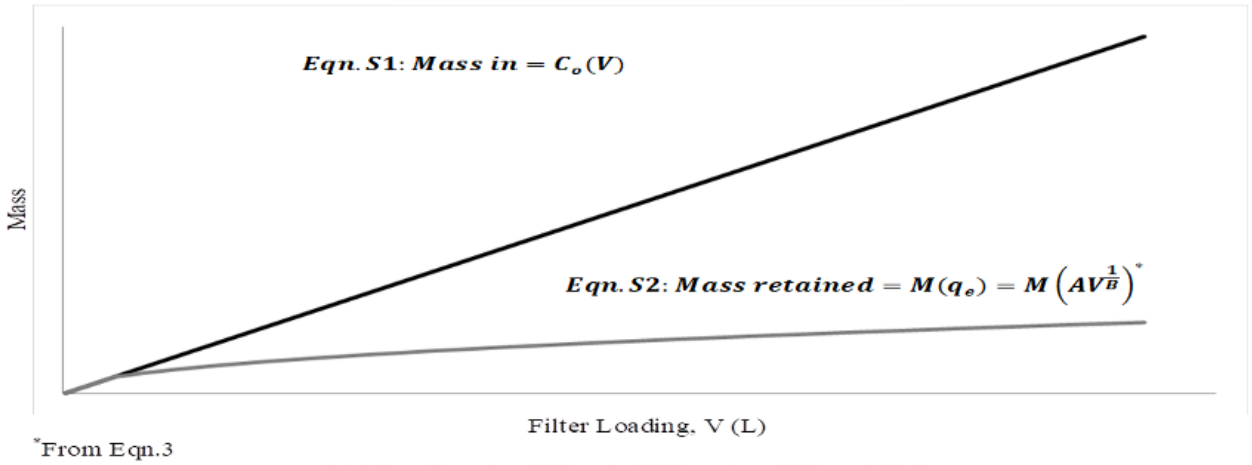

*From Eqn.3

(b) Mass Leaving Filter in Effluent vs. Filtered Volume

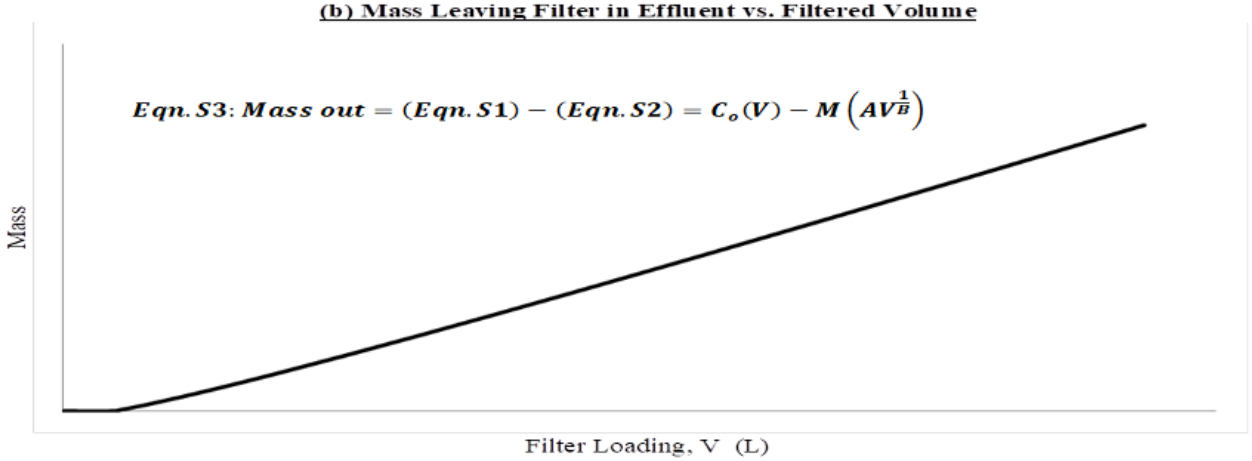

(c) Effluent Concentration, C_e, vs. Filter Loading, V

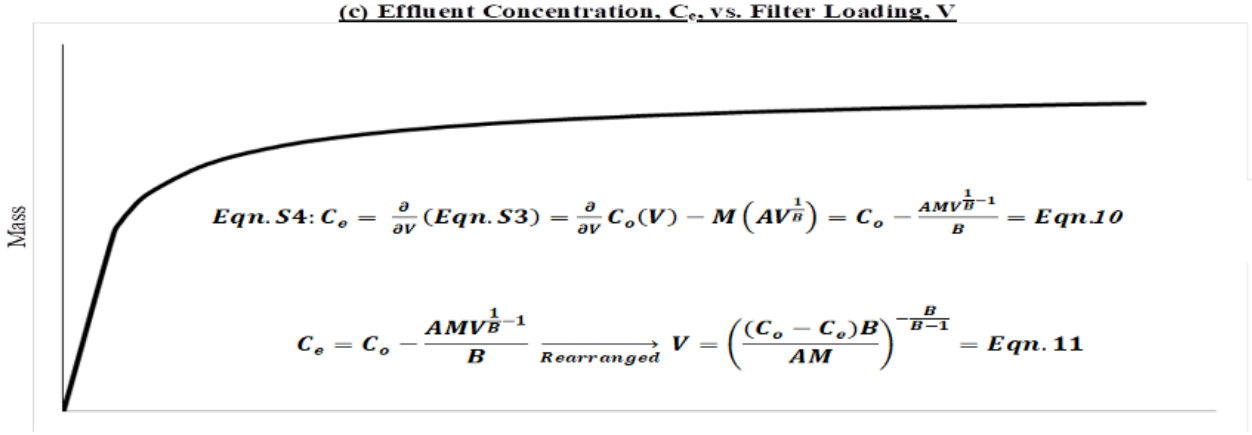

Figure S4.1

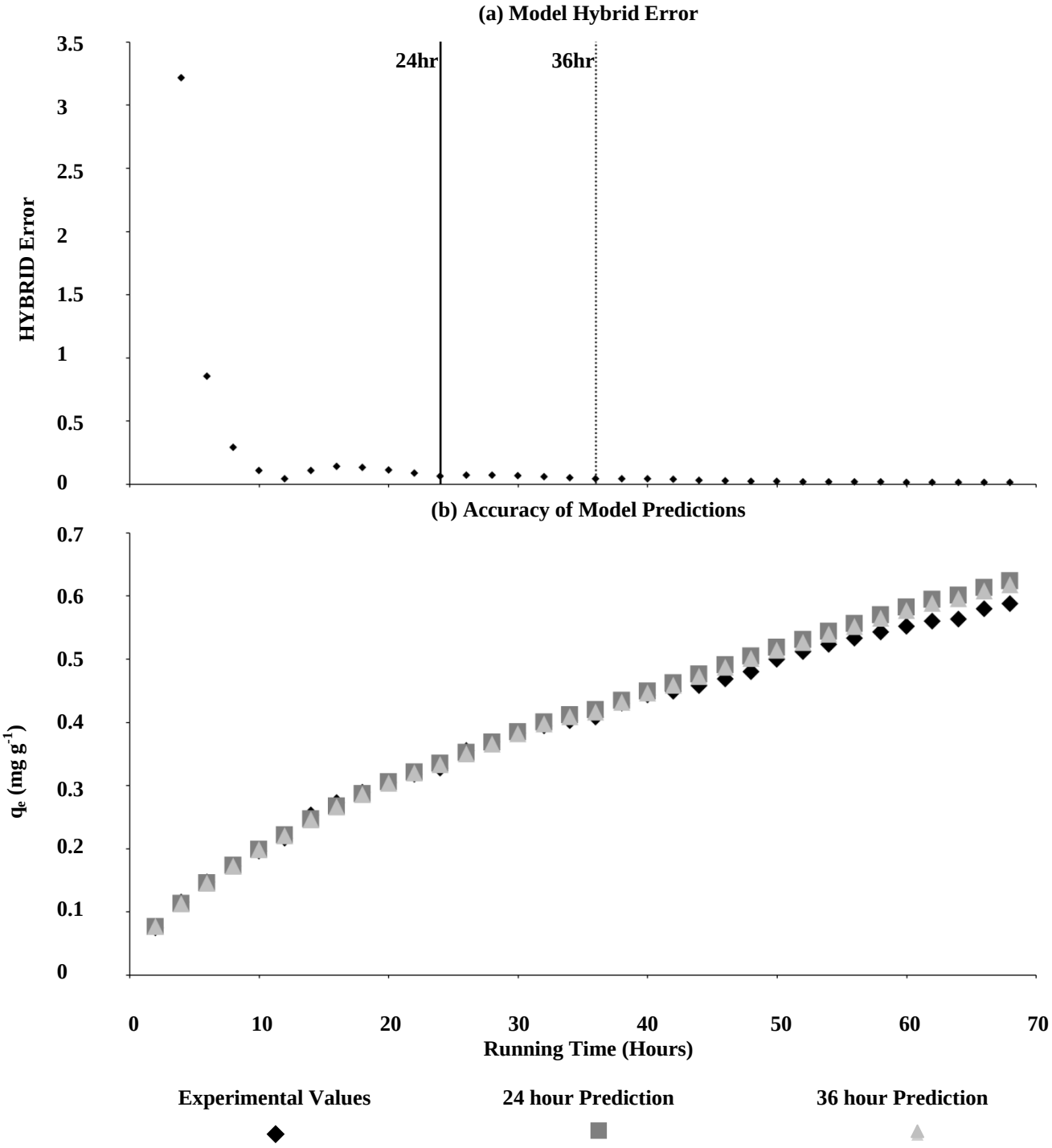

Figure S4.2 (a) HYBRID errors (y-axis) of models predicting 68 hours of adsorption column performance, against the time at which model predictions were made (x-axis). Model predictions were revised at two hour increments using increasingly more data as it was obtained.

Figure S4.2 (b) Comparison of predicted and observed progressions of filter media saturation (y-axis) vs. filter column loading time (x-axis). Two models were used to make predictions, with model coefficients determined after 24 and 36 hours respectively.

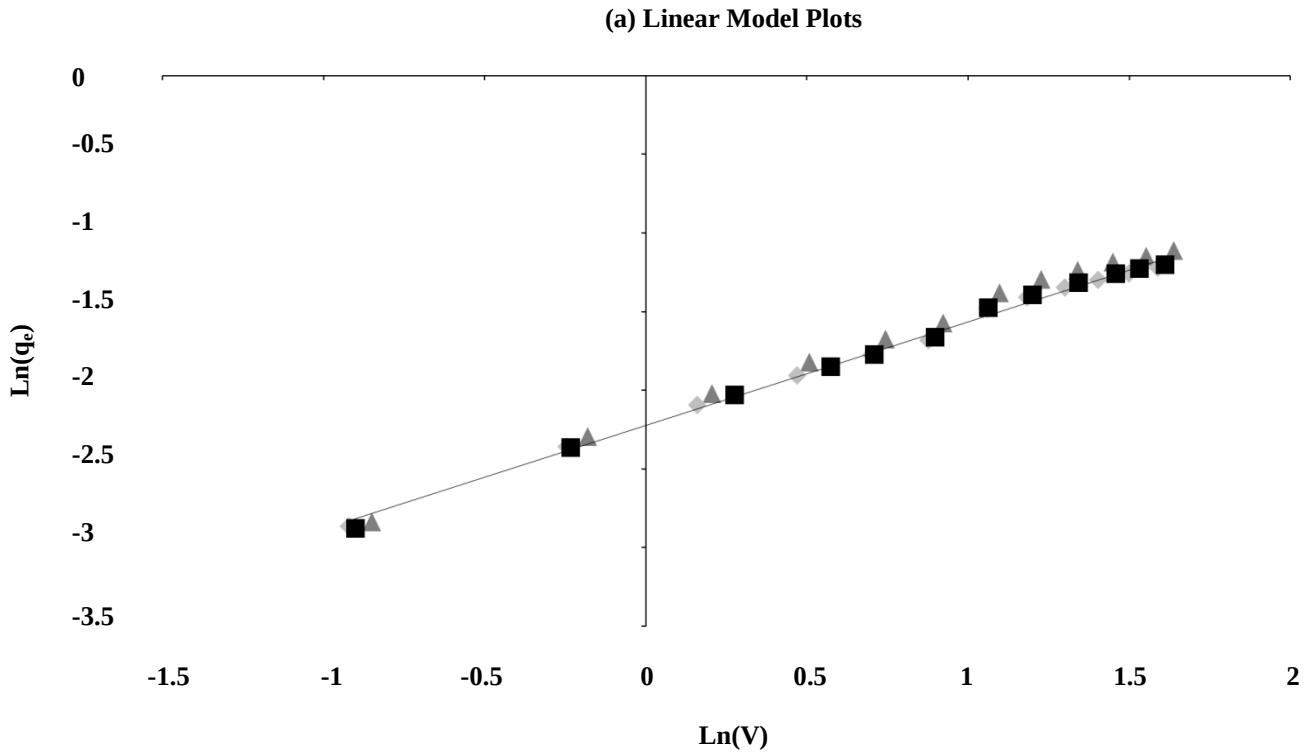
(a) Linear Model Plots
0
-0.5
-1
-1.5
-2
-2.5
-3
-3.5
Ln(qe)
-1.5
-1
-0.5
0
0.5
1
1.5
2
Ln(V)

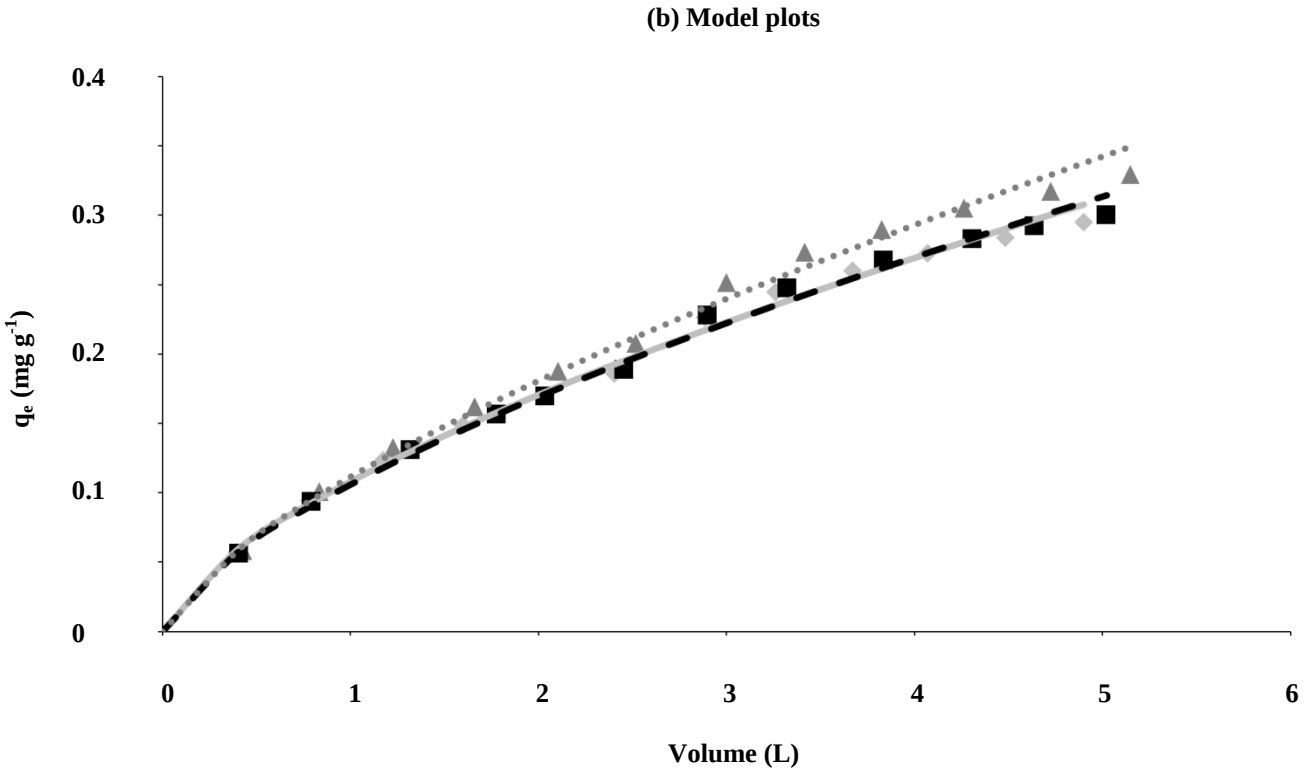
(b) Model plots
0.4
0.3
0.2
0.1
0
qe (mg g-1)
0
1
2
3
4
5
6
Volume (L)

Figure S4.3

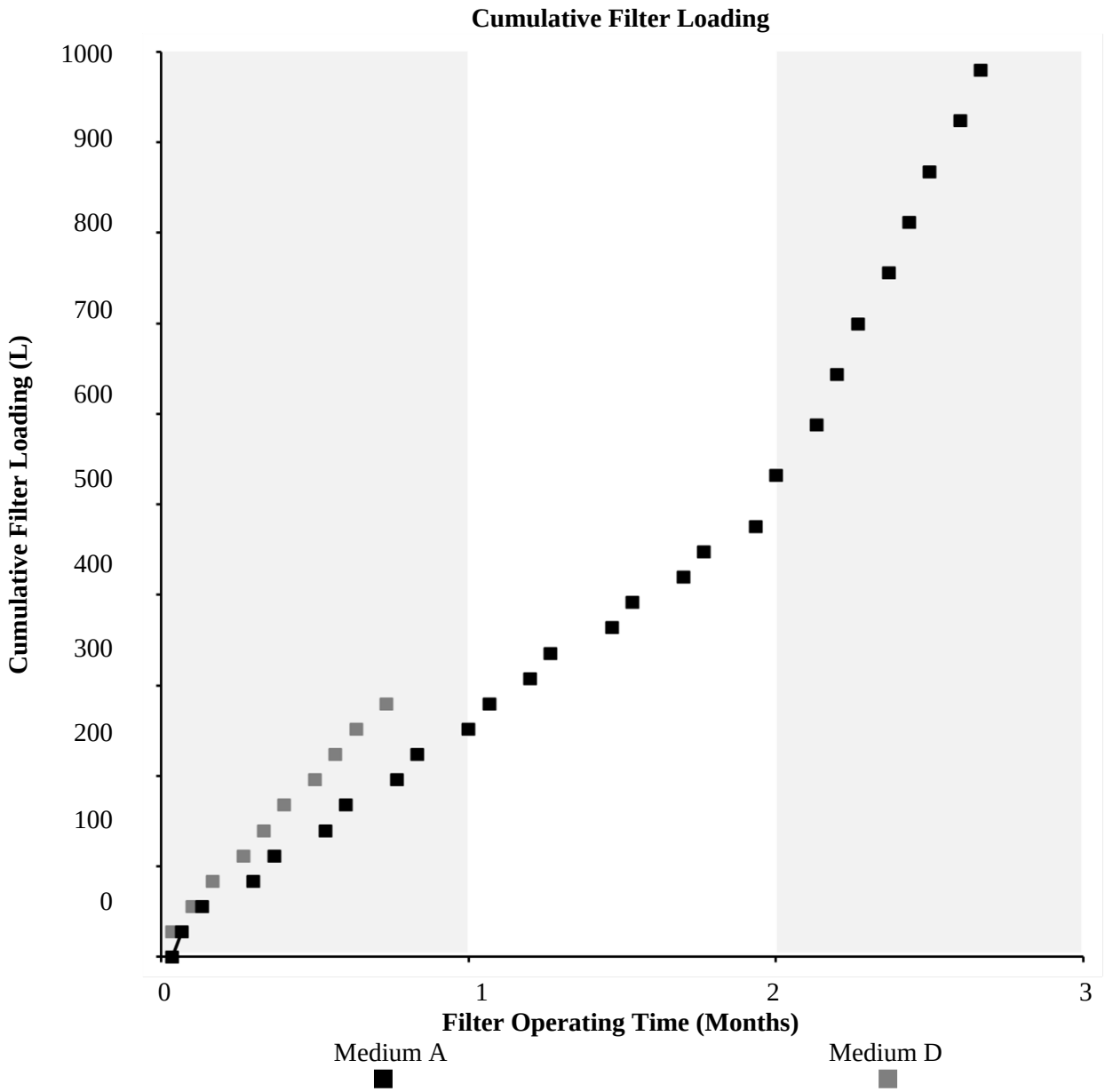
Cumulative Filter Loading
Cumulative Filter Loading (L)
1000
900
800
700
600
500
400
300
200
100
0
0
1
2
3
Filter Operating Time (Months)
Medium A
Medium D

Figure S4.4

Chapter 5

Chapter 4 detailed how rapid small-scale column tests (RSSCTs) and long-term large-scale column tests may be used to obtain similarly useful estimates of filter media longevity. Although the use of RSSCTs provides massive savings of time and cost compared to large-scale column tests, there is still a requirement to perform individual RSSCTs to predict the performances of individual large-scale column tests. This limitation can be addressed with the use of mathematical modeling techniques. However, current modeling methodologies are often unsuitable for the description of adsorption by low-cost adsorbents with highly variable chemical and physical characteristics, and novel methods are therefore required for this purpose. The third aim of this thesis was to address this knowledge gap.

In this chapter, a mathematical modelling approach was developed which related the pore concentrations and media saturation within a filter column to both the volume of wastewater filtered through the column, and the loading rate at which that wastewater was applied to the column. This addresses the third aim of the thesis. The model uses results from multiple small-scale column experiments to determine model coefficients which allow for the full description and prediction of the performances of filters of any size. To validate this approach, the model was fit to a number of independent data sets, and was found to successfully describe these data.

The contents of this chapter have been published in Water Research [Water Res. 123, 556–568 (2017)]. Oisín Callery designed and set up the experiment, carried out all testing and analysis, developed the mathematical approach used to model experimental data, and is the primary author of this publication. Dr. Mark G. Healy contributed to the experimental design and paper writing. The published paper is included in Appendix C.

Predicting the propagation of concentration and saturation fronts in fixed-bed filters

O. Callery, M.G. Healy

Civil Engineering, National University of Ireland, Galway, Co. Galway, Rep. of Ireland.

Abstract

The phenomenon of adsorption is widely exploited across a range of industries to remove contaminants from gases and liquids. Much recent research has focused on identifying low-cost adsorbents which have the potential to be used as alternatives to expensive industry standards like activated carbons. Evaluating these emerging adsorbents entails a considerable amount of labor intensive and costly testing and analysis. This study proposes a simple, low-cost method to rapidly assess the potential of novel media for potential use in large-scale adsorption filters. The filter media investigated in this study were low-cost adsorbents which have been found to be capable of removing dissolved phosphorus from solution, namely: i) aluminum drinking water treatment residual, and ii) crushed concrete. Data collected from multiple small-scale column tests were used to construct a model capable of describing and predicting the progression of adsorbent saturation and the associated effluent concentration breakthrough curves. This model was used to predict the performance of long-term, large-scale filter columns packed with the same media. The approach proved highly successful, and just 24-36 hours of experimental data from the small-scale column experiments were found to provide sufficient information to predict the performance of the large-scale filters for up to three months.

Nomenclature

a	Time constant in Eqn. 6/Eqn.13
a*	Time constant in Eqn. 7/Eqn.14
a**	Time constant in Eqn. 8/Eqn.15
A	Constant of proportionality in Eqn. 12 (mg g^{-1})
B	Constant of system heterogeneity in Eqn. 12
C	Sorbate concentration in bulk solution (mg L^{-1})
C_b	Breakthrough concentration (mg L^{-1})
C_e	Sorbate concentration of filter effluent (mg L^{-1})
C_o	Sorbate concentration of filter influent (mg L^{-1})
k_{BA}	Bohart-Adams rate constant (L mg^{-1} min^{-1})
M	Mass of adsorbent (g)
N	Residual sorption capacity of bed (mg L^{-1})
N′	Fractional residual sorption capacity (N/N_o)
N_o	Sorption capacity of bed at equilibrium (mg L^{-1})
N_t	Time dependent sorption capacity of bed (mg L^{-1})
Q	Filter loading rate (L min^{-1})
q_e	Equilibrium sorbate concentration per unit mass of adsorbent (mg g^{-1})
q_t	Time dependent sorbate concentration per unit mass of adsorbent (mg g^{-1})
t	Service time/operating time of bed (min)
t_b	Service time/operating time of bed at breakthrough (i.e. when $C_e = C_b$) (min)
U	Flow velocity of solution past adsorbent (cm min^{-1})
V	Volume of solution filtered (L)
V_B	Empty bed volumes of solution filtered
V_x	Filter-bed volume to a bed depth of ‘x’(L)
Z	Filter bed depth (cm)

5.1 Introduction

Adsorbents are used to remove contaminants from gases and liquids across a diverse range of industries including manufacturing, agriculture, mining, and the treatment of both drinking water and municipal wastewater (Dąbrowski, 2001). These industries are naturally interested achieving optimum treatment efficiency with minimal investment, and there has been a growing interest in 'low-cost adsorbents', which are emerging as alternatives to more expensive and well-established adsorbents such as activated carbons (Babel and Kurniawan, 2003; Crini, 2006). The term ‘low-cost adsorbent’ can be used to describe any abundantly available natural material, industrial byproduct, or waste material which, with minimal processing, has suitable physical and chemical properties to allow for its use in the adsorption of some contaminant of interest (Bailey et al., 1999). Such media often display lower adsorption affinities and saturation capacities than well-established adsorbents, like activated carbons and synthetic resins, but they can nonetheless replace these ostensibly 'better' media with the introduction of minor modifications to adsorption treatment processes (Brown et al., 2000; Reddad et al., 2002): for example, increasing the hydraulic residence time of a filter bed or increasing the adsorbent dose in a batch reactor. Therefore, despite the fact that low-cost adsorbents often display less favorable adsorption characteristics, their use is nonetheless a highly attractive option because of their ability to ultimately achieve equal treatment efficacy to established adsorbents, but at a greatly reduced cost.

The interaction between an adsorbent material and a dissolved contaminant is a highly complex one, influenced by a multitude of factors such as the physicochemical properties of the adsorbent and target adsorbate (Bockris et al., 1995), the composition and pH of the solution matrix (Faust and Aly, 1998), and the contact mechanism (i.e. batch or through-flow) between adsorbent and adsorbate (Goel et al., 2005). The complexity of these interactions makes characterizing the adsorptive properties of a medium for a given contaminant a vital first step in assessing its suitability for any intended treatment process. As low-cost adsorbents are often derived from locally sourced natural materials, industrial by-products, and waste materials, there is an inherent variability in their physical structure and chemical composition; no two low-cost adsorbents are exactly alike, and consequently, no two adsorbents will display identical adsorption characteristics. This problem is exacerbated by the fact that there is equal variability in waste streams, and hence there results an unavoidable necessity to characterize and assess every low-cost medium with respect to every

potential use.

This poses a significant challenge to researchers, as there is a substantial amount of work involved in characterizing an adsorptive medium prior to its utilization in a real world application. Batch studies, capable of providing a rough approximation of a medium's adsorptive properties, are a common first step in media characterization, and these are an attractive option by virtue of being cheap and easy to perform, with experimental methods well established and results easy to interpret (Crini and Badot, 2008). The primary disadvantage is that batch experimental conditions are radically different to through-flow conditions in real world filter-beds. These studies are, for this reason, unable to provide sufficient information to allow for the design of a full-scale adsorption filters (Søvik and Kløve, 2005). Accordingly, when media are to be used in filter-beds, large-scale field studies are widely considered to be the most reliable method of assessing their potential (Pratt et al., 2012). Such tests provide excellent insight into the behavior of real-world adsorption systems; however, the propriety of conducting such large-scale and costly investigations is questionable when using untested and unproven materials. The limitations of both batch studies and large-scale column studies have made rapid small-scale column tests (RSSCTs), of the kind proposed by Crittenden et al. (1986, 1987), an ideal option for initial media characterization, and it has been repeatedly demonstrated that such tests can provide excellent predictions as to the performances of real-world filter units (Crittenden et al., 1991). RSSCTs involve the use of scaling equations to select media particle sizes, hydraulic loading rates, and empty bed contact times (EBCT, defined as the empty bed volume divided by the flow rate) which will ensure exact similarity of operation between small- and large-scale adsorption filters. Providing exact similitude is achieved, the breakthrough curve (BTC) observed when operating a small-scale filter column should match that of a large-scale filter almost exactly. The advantages of RSSCT type experiments are numerous; they are fast and inexpensive to perform, they require minimal quantities of both adsorbent and adsorbate solution, and perhaps most importantly, they investigate the interaction between adsorbent and adsorbate under through-flow conditions which are representative of intended field conditions, providing insight into both adsorption capacity and kinetics simultaneously. The primary drawback of RSSCTs is that they only make reliable predictions for the very specific case for which they were designed; a single RSSCT corresponds to only one large-scale filter operated in an exactly similar manner (in terms of loading rate and empty bed contact time etc). Also, while it is easy to obtain different particle sizes of activated carbon (the material

for which the RSSCT methodology was originally proposed), it may not be possible to scale down many low-cost media due to their physical characteristics.

Mathematical models provide a means by which to make theoretical predictions for any fixed-bed system, and there are a great many mathematical models which have been developed in an attempt to predict the breakthrough behavior of adsorptive media. Xu et al. (2013) summarized some of the most widely used of these in a recent review, listing, amongst others, the Thomas model (Thomas, 1944), the Bohart-Adams (B-A) model (Bohart and Adams, 1920), and the Bed Depth Service Time (BDST) model (Hutchins, 1973). It is interesting to note that the B-A model is often erroneously referred to as the Thomas model; this has caused considerable confusion (Chu, 2010), even though the former predates the latter by a considerable margin. The B-A model is also the basis of the popular BDST model proposed by Hutchins (1973), which is, essentially, just a simplified rearrangement of the B-A model. It therefore seems reasonable to assert that the B-A model is quite possibly the most popular fixed-bed sorption model in current use. The basic form of the B-A model is as follows:

$$ln\left(\frac{C_O}{C_b}-1\right)=ln\left[exp\left(k_{BA}N_O\frac{Z}{U}\right)-1\right]-k_{BA}C_O t_b \quad (1)$$

where C_o is the influent concentration, C_b is the effluent breakthrough concentration at any time, t_b; k_{BA} is a kinetic constant associated with the B-A model, N_o is the adsorptive capacity of the medium per unit volume of the bed, Z is the depth of medium in the filter bed, and U is the linear flow velocity.

In practice, $\exp(K_{BA}N_oZ/U)$ is often much larger than one (Cooney, 1998; Al-Degs et al., 2009; Chu, 2010), and the equation can therefore be simplified by ignoring the unity term on the right hand side of Eqn.1 to yield:

$$ln\left(\frac{C_O}{C_b}-1\right)=k_{BA}N_O\frac{Z}{U}-k_{BA}C_O t_b \quad (2)$$

As stated earlier, Hutchins' BDST model is based on a rearrangement of the simplified B-A equation (Eqn.2), and proposes a linear relationship between filter-bed depth and filter service time to a given breakthrough concentration. The time to any breakthrough concentration is found by rearranging Eqn. 2 into form t=mx+c, to yield Hutchins' BDST equation (Hutchins, 1973) as follows:

$$t_b = \frac{N_o}{C_o U} z - \frac{1}{K_{BA} C_o} ln\left(\frac{C_o}{C_b} - 1\right) \quad (3)$$

Mathematical modelling offers more versatility in terms of predicting a wide range of potential fixed-bed arrangements, though this is arguably at the cost of the certainty and reliability that predictions based on experimental observations provide. It would therefore seem logical that a combination of both experimental observation and mathematical modelling would hold promise - providing the versatility of mathematical modelling as well as the certainty associated with experimental results. The BDST modeling approach is a widely implemented example of such a procedure. The BDST approach to filter design involves using experimental data from a number of filter columns to determine the coefficients N_o and K_{BA} in Eqn. 3. The BDST model then allows for designers to use interpolation and extrapolation to make predictions as to the behavior of adsorption systems with different flow rates, bed depths, and influent concentrations to those used to obtain the model coefficients.

The BDST model does not attempt to predict full BTCs, but instead predicts the time at which a certain breakthrough concentration will occur for a given filter depth and flow rate. Were the BDST equation rearranged in an attempt to predict the entire BTC, a sigmoidal function would be obtained, i.e. Eqn. 2. Therefore, the BDST model may fit experimental data at a single breakthrough point, but if extrapolations are made to different breakthrough concentrations, predicted BTCs may vary significantly from observed BTCs. This is particularly true in relation to low-cost adsorbents, which often produce BTCs that deviate significantly from the ideal symmetrical sigmoidal shape predicted by formulae such as that used in the BDST model.

Naturally, with the addition of enough modifying constants, a model can achieve an almost perfect fit to any dataset, but this detracts from the purpose of creating a model; a model should be simple enough to be of practical use, allowing for its easy application by those in industry, but sophisticated enough that the predictions it offers will be of practical use. Creating a model which adheres to these criteria will necessitate the adoption of various simplifications and assumptions, and depending on the assumptions made, the resultant model will almost certainly only be suitable for only certain adsorption systems (Xu et al., 2013). This is not a limitation, per se, rather just an unavoidable reality, one that necessitates the use of different models for different systems. Striving to create a ‘perfect’ model at the

expense of its ever being practically utilized is a wholly academic pursuit if its complexity is such that very few can effectively implement it. This is reflected by the popularity of the simple B-A model, which assumes a rectangular isotherm, while the Thomas model, which assumes a more realistic Langmuir isotherm, and often offers a better fit to experimental data, has seen much less use; Chu (2010) compared the Thomas model to the B-A model and described the former as being "computationally intractable".

In a recent paper, Callery et al. (2016) found that the long-term performance of large-scale filters packed with low-cost adsorbents could be predicted mathematically using a simple model, which was constructed using 24 hr of experimental data obtained from small-scale column tests. The methods used didn't require the use of scaling equations, as is generally the case with RSSCTs. Similitude was achieved by using the same media particle sizes and hydraulic loading rates in both the large and small-scale filters. In this way, the small columns were not so much scaled-down versions of large-scale filters, rather they could be considered cylindrical longitudinal-sections of hypothetical large-scale filter-beds. The BTCs obtained from these small-scale filters could be modeled, and extrapolations could be made to predict the performance of large-scale filters using the same media.

While dispensing with the necessity for scaling equations made this method simpler than the RSSCT approach, the advantages of RSSCTs were retained. So too was the disadvantage that there needed to be exact similarity between the small- and large-scale tests. For this reason, there is a necessity to develop this method further before it is capable of predicting the performance of filters with any bed depth operated at any loading rate, and this need is addressed by this study.

5.2 Theory

In through-flow adsorption systems, the mass of adsorbate retained by a filter medium is a function of the contact time between the adsorbent medium and the adsorbate solution. This means that having an understanding of an adsorbent's kinetic performance is of paramount importance when attempting to design any such system (Qiu et al., 2009). Changing the depth of a filter-bed (or adjusting the hydraulic loading rate) will affect the EBCT (used as a measure of the contact time between the adsorbent and the adsorbate solution) which will in turn affect the system's performance. The BDST model supposes that the relationship between bed depth (and therefore EBCT) and service time – the filter operating time to some defined breakthrough concentration - is a linear one (Hutchins, 1973). This assumption, while

often reasonable, was quickly shown to not be valid for all systems (Poots et al., 1976a, 1976b). Curved plots of bed depth vs. service time are not uncommon, and intraparticle diffusion can cause tailing of BTCs (Deokar and Mandavgane, 2015), and non-linear BDST plots which deviate from those predicted by Hutchins' BDST model (Ko et al., 2000, 2002). Internal diffusion of adsorbate molecules often becomes a significant factor as a medium's surface becomes increasingly saturated, or as a result of lengthy filter EBCTs. Hutchins' BDST model is based on the assumption that intraparticle diffusion and external mass resistance are negligible (Ayoob and Gupta, 2007); this is rarely the case in real-world adsorption systems, where adsorption is seldom controlled solely by surface chemical reactions between the adsorbent and adsorbate (Crini and Badot, 2010). This limitation has been noted before, and attempts have been made to modify the BDST model to make it more universally applicable (Ko et al., 2000, 2002).

In deriving their fixed-bed model, Bohart and Adams (1920) made the assumption that the rate of the adsorption reaction in a fixed bed filter is proportional to the fraction of the medium's adsorption capacity which is still retained, and the concentration of adsorbate in the solution being filtered. They described this relationship as follows:

$$\frac{\partial \mathrm{N}}{\partial \mathrm{t}} = -\mathrm{kNC} \qquad (4)$$

$$\frac{\partial C}{\partial Z} = \frac{-\mathrm{k}}{\mathrm{U}}\mathrm{NC} \qquad (5)$$

where C is the adsorbate concentration of the solution being filtered, t the time, Z the filter bed depth, U the flow velocity of the solution past the adsorbent, and k is a reaction rate constant; N is the residual adsorption capacity which is assumed to be some fraction, N′, of the adsorptive capacity of the adsorbent, N_o (i.e. $N'=N/N_o$, or $N=N_oN'$).

Eqns. 4 and 5 are based on the assumption that the filter bed has a definite sorption maximum, N_o, which is independent of bed contact time and the duration for which the filter has operated; at equilibrium Eqn. 4 reduces to a rectangular sorption isotherm (highly favorable, irreversible adsorption) (Chu, 2010). In reality, it is known that filter-bed adsorption capacity does change depending on the fluid residence time in the bed (Ko et al., 2000, 2002) and the duration of filter operation. Increases in bed depth, and consequent increases in EBCT and service time, allow adsorbate molecules to diffuse deeper into the adsorbent particles resulting in a consequent increase in bed capacity. To account for this, Ko

et al. (2000, 2002) proposed that a time dependent bed capacity term, N_t, could replace the standard bed capacity term of the BDST model, N_o, and presented two possible equations with which to determine this value:

$$N_t = N_o(1 - e^{-at}) \qquad (6)$$

$$N_t = N_o(1 - e^{-a^*\sqrt{t}}) \qquad (7)$$

where a and a* are first order and diffusional kinetic rate parameters respectively.

Regardless of the solid-liquid contact mechanism employed (i.e. batch or fixed bed), the equilibrium and kinetic characteristics of an adsorption system remain unchanged (Chu, 2010). With this in mind, just as Eqn. 6 is based on Lagergren's (1898) pseudo first-order model, following the work of Liu (2008), another possible expression for N_t is proposed, based on Ho and McKay's (1999) pseudo second-order model:

$$N_t = N_o \frac{t}{t + a^{**}} \qquad (8)$$

where a** is a fitting parameter associated with second order kinetics; the full derivation of Eqn. 8 can be found accompanying Figure S5.1 of the supplementary information. It is worth noting that (given the interdependence of bed depth, EBCT, and service time), with different values for the constants a, a*, and a**, EBCT could be used in the place of service time, t, in Eqns. 6 - 8. The primary advantage of this is that EBCT is an easily calculable property of a filter, whereas service time must be experimentally determined. This point is also expounded in Figure S5.1 of the supplementary file accompanying this text.

When N_t (as defined by one of Eqns. 6, 7 or 8, to be selected on the basis of best fit to the system in question) is substituted for N_o in Eqn. 3, a modified form of the BDST equation (one which can describe a non-linear relationship between bed depth and service time) is obtained:

$$t_b = \frac{N_t Z}{C_0 U} - \frac{1}{k_{BA} C_0} ln\left(\frac{C_0}{C_b} - 1\right) \qquad (9)$$

This equation can also be rearranged in the form of a modified BA equation to describe sigmoidal breakthrough curves:

$$ln\left(\frac{C_0}{C_b}-1\right)=\frac{k_{BA}N_tZ}{U}-k_{BA}C_0t_b \qquad (10)$$

Ko et al. (2000, 2002) demonstrated the utility of this modified BDST model (Eqn. 9), using Eqns. 6 and 7 to determine values for N_t (to the best of our knowledge, Eqn. 8 has not yet been used for this purpose), however, once the model is rearranged in the form of Eqn. 10 an inherent limitation becomes apparent: the model describes only sigmoidal curves, and is therefore poorly suited to the description of linear to convex BTCs which are commonly observed in fixed-bed studies using low-cost adsorbents.

To address this limitation, Callery et al. (2016) proposed the following model in a recent study:

$$\mathrm{C_e}=\mathrm{C_o}-\frac{\mathrm{q_eM}}{\mathrm{VB}} \qquad (11)$$

where C_e and C_o are the filter effluent and influent contaminant concentrations respectively, M is the mass of filter medium, V is the volume of solution loaded on to the filter, B is a model constant, and q_e is the mass of adsorbate adsorbed per unit mass of filter medium, as modeled by:

$$\mathrm{q_e}=\mathrm{A}V_B^{\left(\frac{1}{\mathrm{B}}\right)} \qquad (12)$$

where A is a model constant and V_B is the number of bed volumes of solution filtered.

Callery et al. (2016) found that Eqns. 11 and 12 were well suited to the modeling of non-sigmoidal BTCs, though a limitation of this model is that it does not provide any information regarding the bed depth service time relationship. It is hypothesized that this may be easily addressed; just as Ko et al. (2000, 2002) replaced N_o with N_t to modify the B-A/BDST model, q_e in Eqn. 11/12 could be replaced with an analogous time dependent parameter, q_t. Mirroring Eqns. 6-8, the following expressions for q_t are obtained:

$$q_t=q_e(1-e^{-at}) \qquad (13)$$

$$q_t=q_e(1-e^{-a^*\sqrt{t}}) \qquad (14)$$

$$q_t=q_e\frac{t}{t+a^{**}} \qquad (15)$$

Again, a, a*, and a** are model constants associated with first order, diffusional, and second

order kinetics respectively. Their value in the above equations will depend on whether service time or EBCT is used in the place of t; EBCT will be used in this study.

The adsorbate solution's concentration will reduce as it travels through the filter bed and, if the flow rate is constant, we can assume that at any depth within the filter, the pore concentrations will depend on the contact time that has elapsed between the solution and the filter medium, (as well as the duration for which the filter has been loaded). The solution adsorbate concentration at any filter depth (i.e. after any EBCT), C_t, as opposed to the filter effluent concentration, C_e, can be found by substituting q_t for q_e in Eqn 11/12:

$$C_t = C_o - \frac{q_t M}{VB} \qquad (16)$$

Given the linear relationship between filter depth and EBCT, Eqn. 16 can be used to calculate the filter pore concentrations of the adsorbate solution at any depth within the filter-bed after any filter loading, V, and can therefore describe the propagation of concentration fronts within the filter-bed.

Eqn. 16 can also be rearranged to yield a function with similar utility to Hutchins' BDST model, i.e. one that describes the relationship between bed depth and volume of solution treated to any breakthrough concentration, C_t, of interest:

$$V = \frac{q_t M}{B(C_o - C_t)} \qquad (17)$$

The filter service time can be found from Eqn. 17 by dividing the volume treated, V (L), by the loading rate (L s^{-1}).

In summary, sigmoidal BTCs and corresponding plots of bed depth vs. service time may be described by Eqns. 10 and 9 respectively, while linear to convex BTCS and corresponding plots of bed depth vs. service time may be described by Eqns. 17 and 16 respectively.

5.3 Materials and Methods

5.3.1 Preparation of filter columns

The low-cost adsorbents utilized in this study were aluminum water treatment residual (dried at 105°C for 24 hr and ground to pass a 0.5 mm sieve) and two grades of crushed concrete ("fine", ground to pass 0.5 mm sieve, and "coarse", ground to pass a 1.18 mm sieve but retained by a 0.5 mm sieve). Small bore filter columns of lengths 0.1, 0.15, 0.2, 0.3, and 0.4 m were constructed using HDPE tubing with an internal diameter of 0.0094 m. These columns were packed with each of the aforementioned media, with care being taken to ensure that an equal bulk density was achieved in each filter. Endcaps, consisting of PE syringe barrels packed with a small quantity of glass wool, were fastened by means of a friction fit to the ends of the filter columns, and silicone tubing was connected to the tip of these syringe barrels to provide inlet and outlet lines to the filter columns. Large bore filter columns of length 0.65 m were then constructed in triplicate using uPVC piping with an internal diameter of 0.104 m. These columns were packed to a bed depth of 0.4 m using the same media and same packing density as was used in the small-bore filters. Again, care was taken to ensure that an equal bulk density was achieved in each filter for each medium. Sampling ports were installed through the walls of the large-bore filter columns at bed depths of 0.05, 0.1, 0.18, and 0.25 m from the filter surface. Water samples could also be collected from the outlet at the base of each column.

5.3.2 Operation of filter units

A synthetic wastewater was produced by dissolving K_2HPO_4 in tap water to obtain a PO_4-P concentration of 1 mg L^{-1} [similar to forest drainage water (Finnegan et al., 2012)]. A peristaltic pump was used to supply this wastewater to the small-bore filter units at consistent flow rates of between 134 and 259 mL hr^{-1} [hydraulic loading rates similar to those found in high rate trickling filters (Spellman, 2013) or activated carbon adsorbers (Chowdhury, 2013)] to achieve a variety of filter bed contact times. The small-bore filters were operated intermittently, in 12 hour on/off cycles, and were fed from the bottom of the vertically oriented filters to preclude any incidence of wastewater bypassing the filter media. The effluent from the small-bore columns was collected in 2 hr aliquots using an auto-sampler. The large-bore filter columns were manually loaded 2-3 days per week with 28 L of the same synthetic wastewater as used in the small-bore filters. Water samples were collected from the

sampling ports at various intervals, and the effluent from each loading event was collected in large HDPE containers.

5.3.3 Data collection and analysis

Collected effluent samples were passed through 0.45 μm filters and analyzed with a Konelab nutrient analyzer in accordance with the standard methods (Eaton et al., 1998). With the influent and effluent PO_4-P concentrations determined, medium saturation, q_e, was calculated. Graphs of q_e vs V and C_e vs V were plotted, and Eqn.15 and Eqn.16 were fit to these experimental data by non-linear regression, using Microsoft Excel's solver add-in to minimize the sum of the squares of the errors (ERRSQ):

$$\sum_{i=1}^{p}\left(q_{e,calc} - q_{e,meas}\right)_i^2 \qquad (18)$$

where $q_{e,calc}$ is the model predicted equilibrium solid phase PO_4-P concentration and $q_{e,meas}$ is the measured equilibrium solid phase PO_4-P concentration.

5.3.4 Predicting large-scale filter performance

With the coefficients A, B, and a** determined from the small-scale column tests, Eqn. 16 was used to predict effluent concentrations and pore water concentrations at multiple depths within the large-scale filter columns. V_x, the volume of the large-scale filter to a depth of 'x' was calculated by multiplying 'x' by the area of the filter column (i.e. $\pi D^2/4$, where D is 0.104m, the internal diameter of the large-scale filter column). After some filter loading, V, the pore concentration at a filter-bed depth of 'x' (if predicting effluent concentration, x= Z, the full filter-bed depth), was predicted by inputing the following values into Eqn. 16: $V_B = V/V_x$, $M = \rho V_x$ (where ρ is the bulk density of the media in the filter column; this should be the same as used in the small-scale tests), and $t = V_x/Q$ (where Q is the loading rate applied to the large-scale filter).

5.3.5 Validation of model using independent data

To validate and further support the modelling strategy applied in this study, a literature review was carried out to identify column studies which utilized low-cost adsorbents and observed BTCs which tended towards a convex to linear shape, rather than the sigmoidal curve predicted by other models. The BTCs published in these studies were downloaded as raster images and converted to vector graphics, the ordinates of which could be exported as a

text file. The text files were imported into Microsoft Excel as x and y coordinates, which could then be processed in the same fashion as the experimental data. This method was validated using known data points, and it was found that the mean absolute percentage error between actual values and data points obtained in this manner was 0.18%.

Figure 5.1 shows a step-by-step schematic of the data collection and modelling procedure employed in this study.

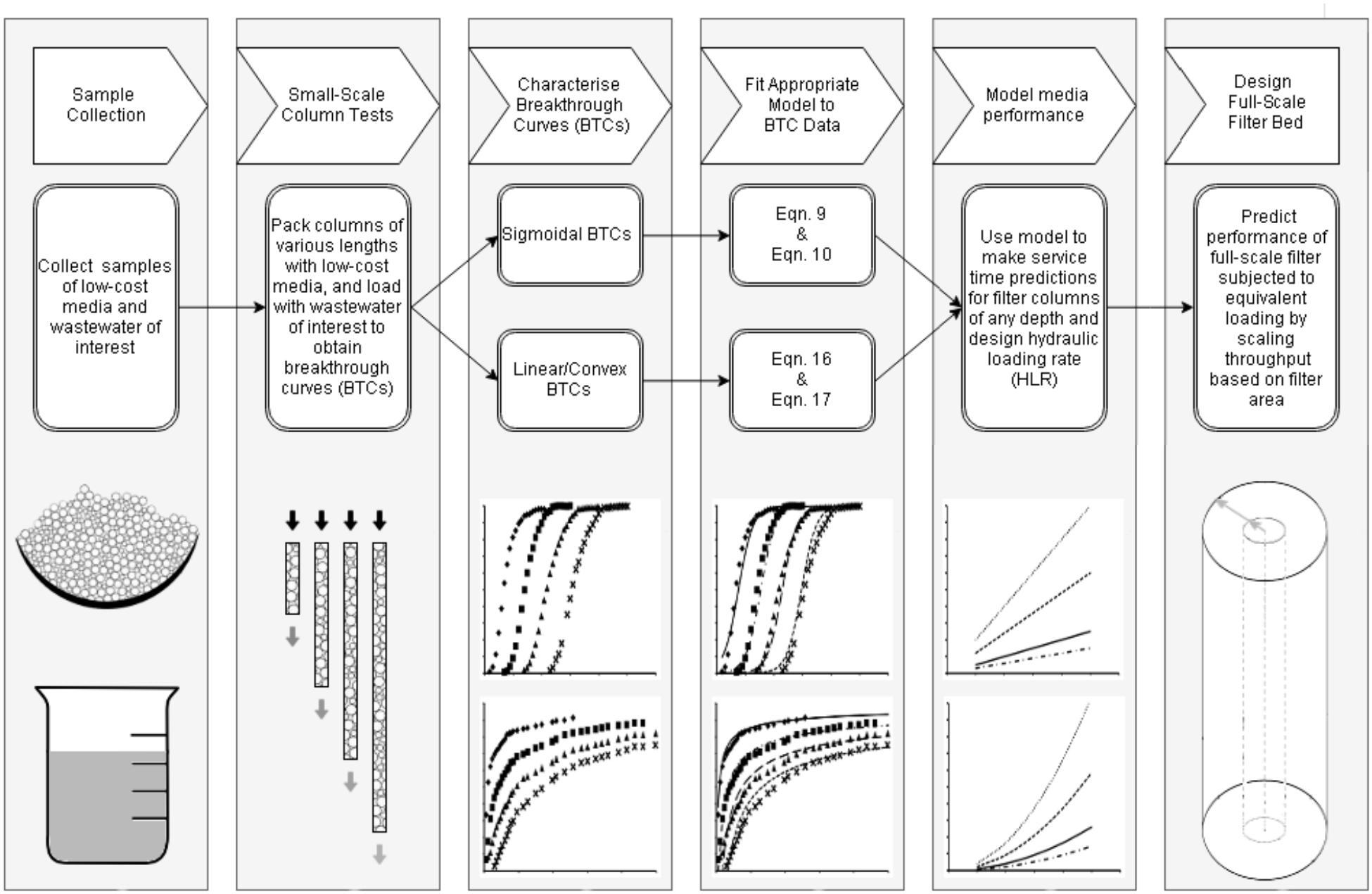

Figure 5.1 Step-by-step schematic of the data collection and modelling procedure employed in this study.

5.4 Results and Discussion

5.4.1 Predicting medium saturation in RSSCTs

Figure 5.2 shows plots of filter loading versus phosphorus retained by filter columns of various lengths. As can be seen, the relationship between filter loading and medium saturation could be accurately described by Eqn. 15. The ERRSQ function was used as a metric for goodness of model fit, with average ERRSQ values of 0.074, 0.057, and 0.008 obtained for small-scale filter columns containing Al-WTR, fine concrete, and coarse concrete, respectively. As described previously, q_t can be calculated in a number of ways; Figure S5.2 in the supplementary file compares graphs of the three functions from which a value for q_t may be obtained. Comparing the shapes of these functions, it can be seen that Eqn. 14, originally proposed by Ko et. al (2000, 2002) to account for diffusional adsorption, appears to very closely match the curve produced by Eqn. 15, based on second-order kinetics. This would seem to indicate that both functions might have similar utility, however the differences between the two can be considerable when the two are compared on a local scale, as can be seen from the inset in Figure S5.2. In constructing Figure 5.2, attempts were made to fit the experimental data from the small-scale column tests to each of Eqns.13, 14 and 15. As can be seen from Table 5.1, which compares ERRSQ values obtained using each of these equations, Eqn. 15 was found to be optimal for each of the media studied. As it provided the best fit to these initial data (and because Ko et al. (2000, 2002) have already explored the use of Eqns. 13 and 14), Eqn. 15 was used for the remainder of this study when fitting Eqns. 16 and 17 to experimental data.

Table 5.1 ERRSQ values obtained using Equations 13, 14, and 15 to model phosphorus retained by filter media vs. filter loading for small-scale filter columns of various lengths.

		Average model ERRSQ values		
Equation		Al-WTR	Fine Conc.	Coarse Conc.
$q_t = q_e(1 - e^{-at})$	(13)	0.0762	0.0687	0.0080
$q_t = q_e(1 - e^{-a^*\sqrt{t}})$	(14)	1.0534	0.0873	0.1028
$q_t = q_e \frac{t}{t+a^{**}}$	(15)	**0.0737**	**0.0568**	**0.0078**

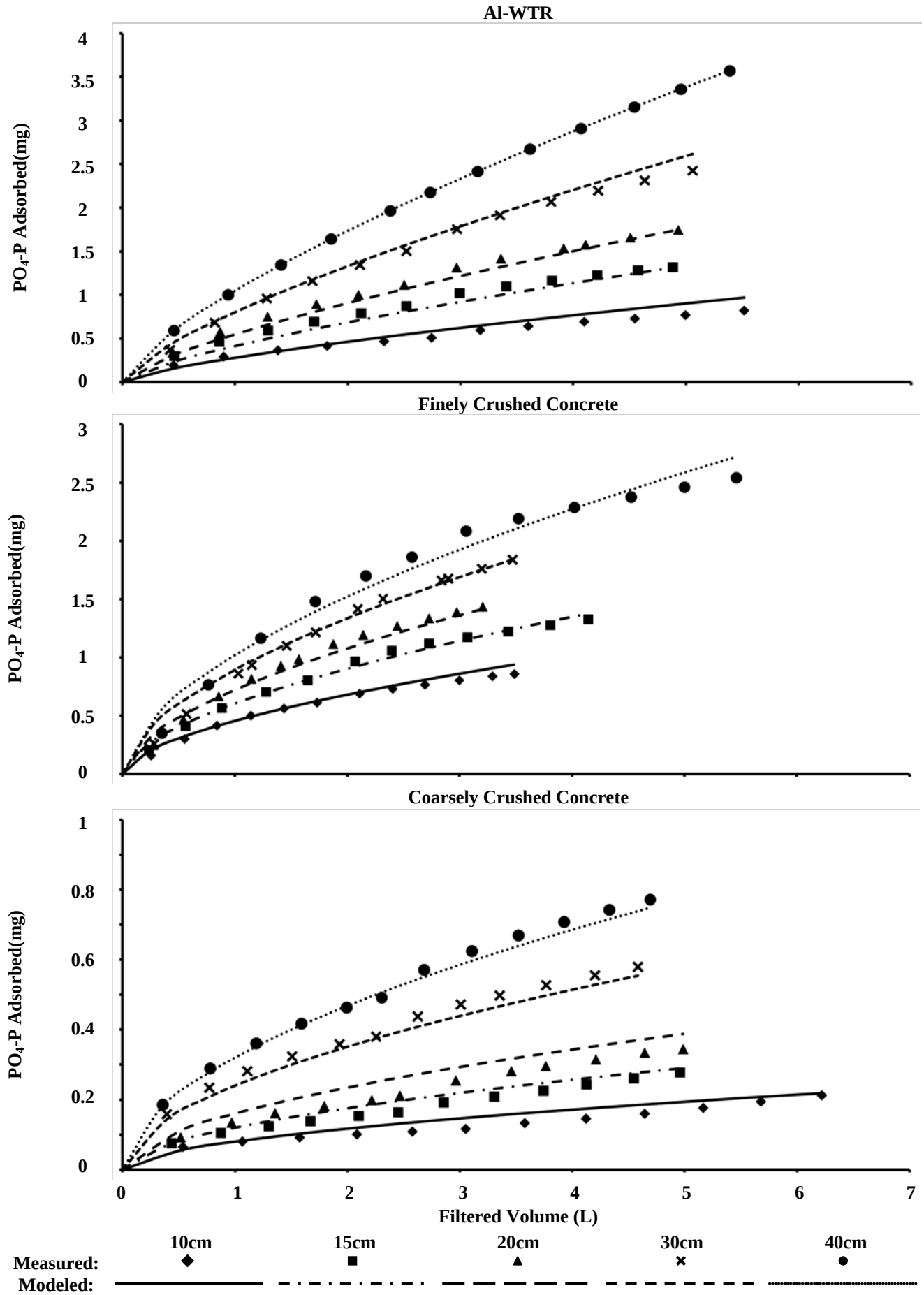

Figure 5.2 Phosphorus retained by filter media (y-axis) vs. filter loading (x-axis) for small scale filter columns of various lengths and predictions made by Equation 15.

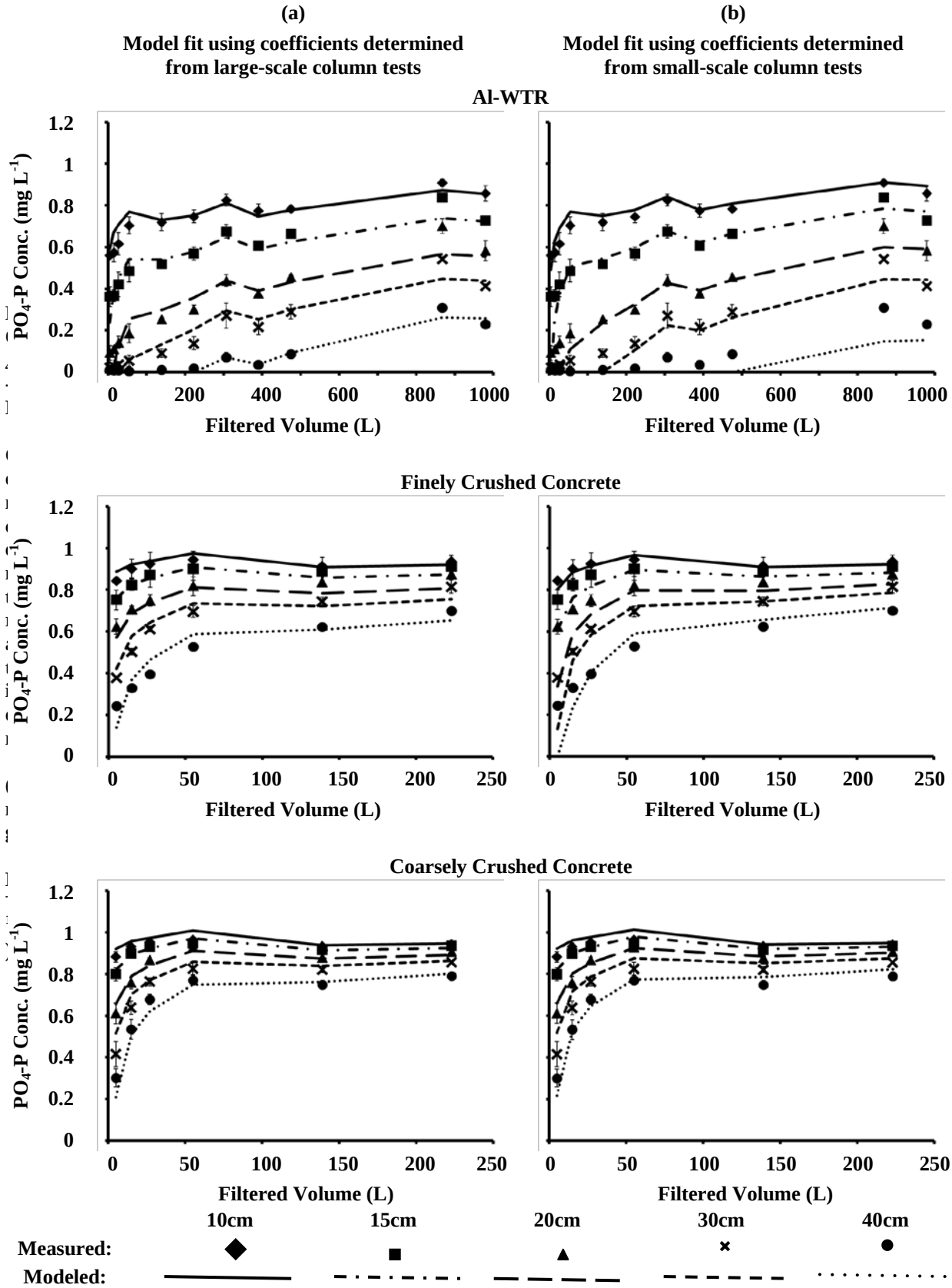

Figure 5.3 PO_4-P concentration (y-axis) vs. filter loading (x-axis) for large scale filter columns, showing (a) Equation 16 fit directly to large scale column data , and (b) predictions made by Equation 16 with model coefficients determined from small-scale column tests.

5.4.2 Predicting pore concentrations at multiple depths in large-scale filter columns

Once it was established that Eqn.15 was capable of describing and predicting the progression of medium saturation in small-scale filter columns of various lengths, it was hypothesized that Eqn.16 would also be able to predict pore PO_4-P concentrations at any bed depth within the filter bed of a large-scale column. To test this hypothesis, Eqn. 16 (with q_t determined using Eqn. 15) was fit, using the ERRSQ method, to the data obtained from depth samples taken from various depths within the large-scale filter columns. Figure 5.3(a) shows the fit of Eqn. 16 to these experimental data, and the associated ERRSQ values are shown in Table 5.2. Average ERRSQ values of 0.026, 0.011, and 0.005 were obtained for large-scale filter columns containing Al-WTR, fine concrete, and coarse concrete, respectively. It can be seen that the slight day-to-day variances in influent concentration had a marked influence on the shape of the observed BTCs. While Eqn.16 was initially proposed to be accurate with the assumption of constant influent concentration, it appeared to display good resilience to these fluctuations, and was nonetheless able to make accurate pore and effluent concentration predictions. With it established that the model could describe the performance of both small- and large-scale filter columns, it was further hypothesized that the coefficients determined from the small-scale columns could also be used to predict the performance of the large-scale filter columns. With these coefficients, the performance of small-scale filters of any depth operated at any HLR could be predicted, and equivalent loadings for large-scale columns subjected to the same HLR were calculated by scaling filter throughput based on the ratio of the small- and large-scale filter areas. Figure 5.3(b) shows data from the large-scale column tests fit to models created using data from the small-scale column tests, and the associated ERRSQ values are shown in Table 5.2. While not fitting quite as closely as when modeled directly on the large-scale column data, the level of precision achieved was still very good, with average ERRSQ values of 0.062, 0.054, and 0.008 obtained for filter columns containing Al-WTR, fine concrete, and coarse concrete, respectively. For practical purposes of preliminary filter design, this level of accuracy was considered more than sufficient, and it allowed for prediction of the adsorptive performance of the large-scale filter columns for the entire duration of their operation. It could reasonably be expected that loading the large-scale filters with a wastewater whose chemical composition was significantly different from that of the wastewater applied to the small-scale filters (in terms of pH, concentration of target contaminant, competing compounds etc.) would invalidate any model predictions of large-scale performance based on the small-scale experiments; a more complex modeling approach would be required to take account of such variations.

Table 5.2 Comparison of model coefficients and ERRSQ values obtained when (a) fitting Equation 16 directly to concentration data from the large-scale column experiments and (b) when fitting Eqn. 16 to concentration data from the large-scale column experiments using model coefficients determined from small-scale column tests.

		Model parameters determined from Large Column Data			Model parameters determined from Small Column Data		
		Al-WTR	Coarse Concrete	Fine Concrete	Al-WTR	Coarse Concrete	Fine Concrete
Model Parameters	A	0.0105	0.0062	0.0058	0.0163	0.0071	0.0124
	B	1.2370	1.6385	1.3733	1.3692	1.7606	1.7054
	a**	10.6786	9.1300	1.3525	10.1007	9.2322	1.2134
		Model ERRSQ values			Model ERRSQ values		
Filter Depth	5cm	0.0245	0.0028	0.0038	0.0210	0.0048	0.0026
	10cm	0.0328	0.0012	0.0027	0.1540	0.0011	0.0282
	18cm	0.0472	0.0032	0.0105	0.0596	0.0034	0.1034
	25cm	0.0209	0.0106	0.0144	0.0291	0.0189	0.0641
	40cm	0.0038	0.0074	0.0228	0.0463	0.0100	0.0735
	μ:	0.0259	0.0050	0.0108	0.0620	0.0076	0.0544

5.4.3 Validation of model using independent data

To further verify the validity and utility of Eqn. 16, it was fit to BTCs published in a number of independent studies. These results are shown in Figure 5.4, and it can be seen that the model fit these data very well. Poots (1976b) was the first author who attempted to apply Hutchins' (1973) BDST model to experimental results (according to the Web of Science™ citation index), and found that it was a poorly suited to describing the relationship between bed depth and service time in peat filters designed to remove Telon blue from aqueous solution. However, as can be seen in Figure 5.4(a), Eqn. 16 was able to describe the breakthrough behavior of Telon blue at all filter depths, accurately describing the non-linear relationship between bed depth and service time described by the BTCs. A recent study on phosphate adsorption (Nguyen et al., 2015) recorded BTCs from filters packed with a low cost adsorbent (zirconium-loaded okara) using phosphate concentrations an order of magnitude higher than those used in the present study; as can be seen from Figure 5.4(b), Eqn. 16 was well suited to the description of these curves. Finally, Han et al. (2009) investigated the ability of iron oxide-coated zeolite as an adsorbent for the removal of copper (II) from aqueous solution in filter beds of various depths, and, as shown in Figure 5.4(c), the BTCs obtained these can be suitably modeled by Eqn. 16.

(a) Adsorption of Telon Blue Dye on Peat (Poots et al., 1976b)

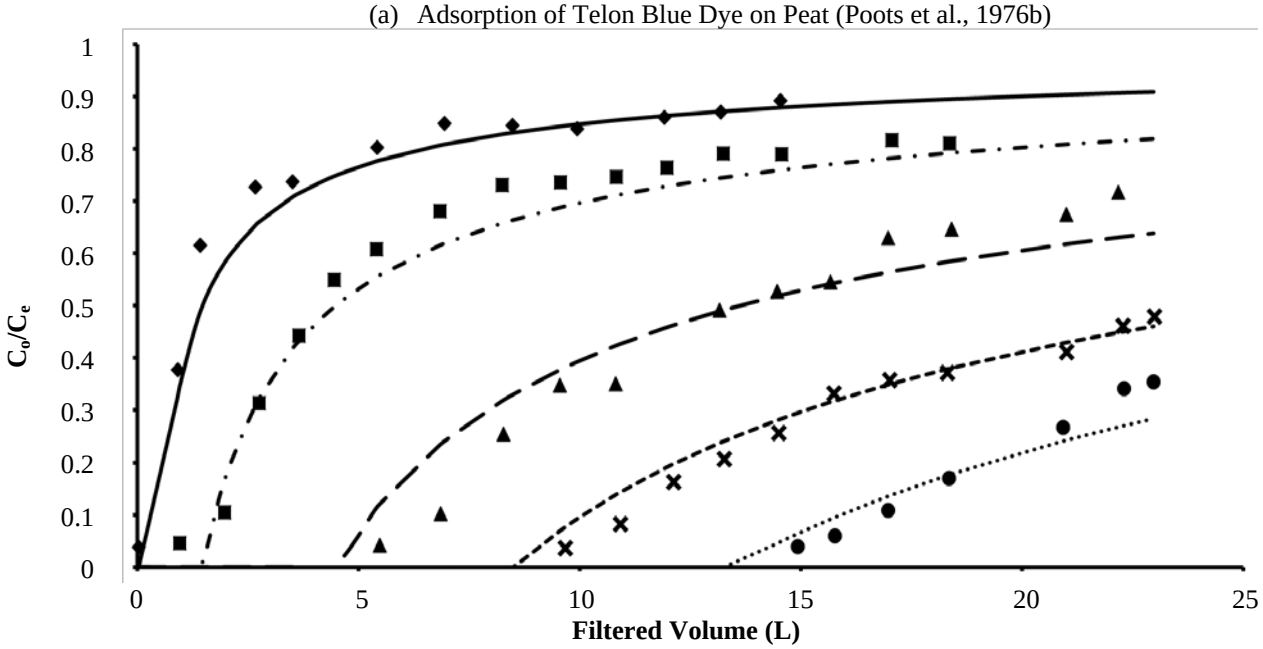

(b) Adsorption of Phosphate on Zirconium Loaded Okara (Nguyen et al., 2015)

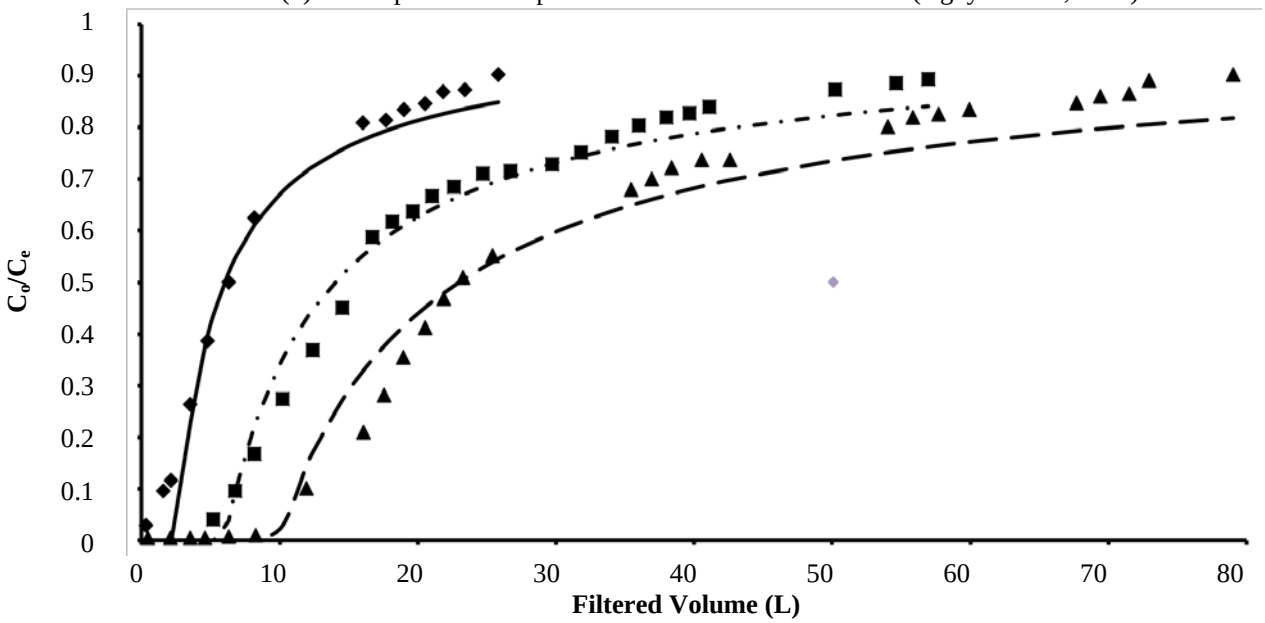

(c) Adsorption of Copper on Iron Oxide Coated Zeolite (Han et al., 2009)

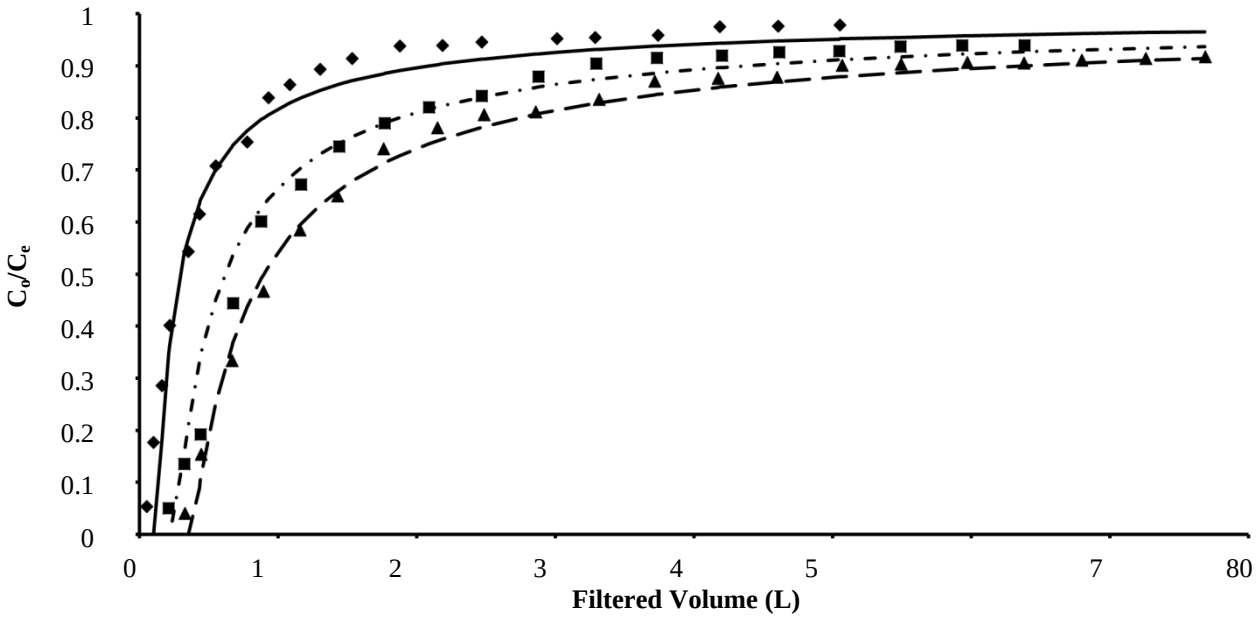

Figure 5.4 Equation 16 fit to independent data sets of normalised pore/effluent contaminant concentration (y-axis) vs. filter loading/operating time (x-axis).

5.4.4 Description of sigmoidal curves

Although Eqn.15 can describe many of the linear to convex BTCs commonly observed from fixed-bed studies using low-cost adsorbents, it is not suitable for the description of sigmoidal curves. This is perhaps the most commonly observed BTC shape observed in fixed-bed sorption studies (Gupta et al., 2000), and so, an attempt was made to model curves of this shape by modifying the B-A model (Eqn. 2) to obtain Eqn. 10, as described previously. Using Eqn. 8 (letting t in Eqn. 8 equal to EBCT) to determine a value for N_t, Eqn. 10 was fit to a number of independent data sets, as shown in Figure 5.5. In the B-A model, N_o serves a similar function to q_e in Eqn. 11, as both represent the sorption capacity of the media. The B-A model assumes a rectangular sorption isotherm (highly favorable, irreversible adsorption) and a definite sorption maximum, which is independent of the contact time and the duration for which the filter has operated. However, in reality, it is known that filter-bed adsorption capacity does change depending on contact time (Ko et al., 2002) and duration of operation. Eqn. 11 assumes that there is an exponential distribution of adsorption sites and energies, meaning that adsorption energies become exponentially weaker with increasing duration of filter operation and associated medium saturation; the bed's capacity increases with operating time and, though there is no defined maximum capacity, there are adsorption maxima for any given filter runtime. Making bed capacity dependent on empty bed contact time, i.e. substituting q_t for q_e, proved to be very successful, and similar success was found modifying Eqn. 2 by replacing N_o with N_t. This can be seen in Figure 5.5, in which Eqn.10 (with N_t determined from Eqn. 8) has been fit to six independent data sets. Ko et al. (2000, 2002) also implemented a similar approach, using Eqn. 6 and Eqn. 7 to modify the BDST model, which is itself derived from the B-A model.

5.4.5 Prediction of BDST relationship

The relationship between bed depth and service time is not necessarily a linear one; greater bed depths result in longer EBCTs, which in turn allow for increased adsorption due to increased intraparticle diffusion of adsorbate molecules. Figure S5.3 of the supplementary file shows some hypothetical BTCs, comparing a linear relationship between bed depth and service time, as proposed by Hutchins' arrangement of the B-A equation (Figure S5.3a), and a non-linear relationship between bed depth and service time as predicted by Eqn. 10, the B-A equation modified with Eqn. 8 (Figure S5.3b). The non-linear relationship between bed depth and service time as predicted by Eqns. 16 and 17 is also shown in Figure S5.3b,

illustrating that the BDST plot doesn't necessarily provide any information regarding the shape of the BTC; though the BTCs predicted by Eqn. 10 and Eqn. 16 are very different, both yield the same curved BDST plot.

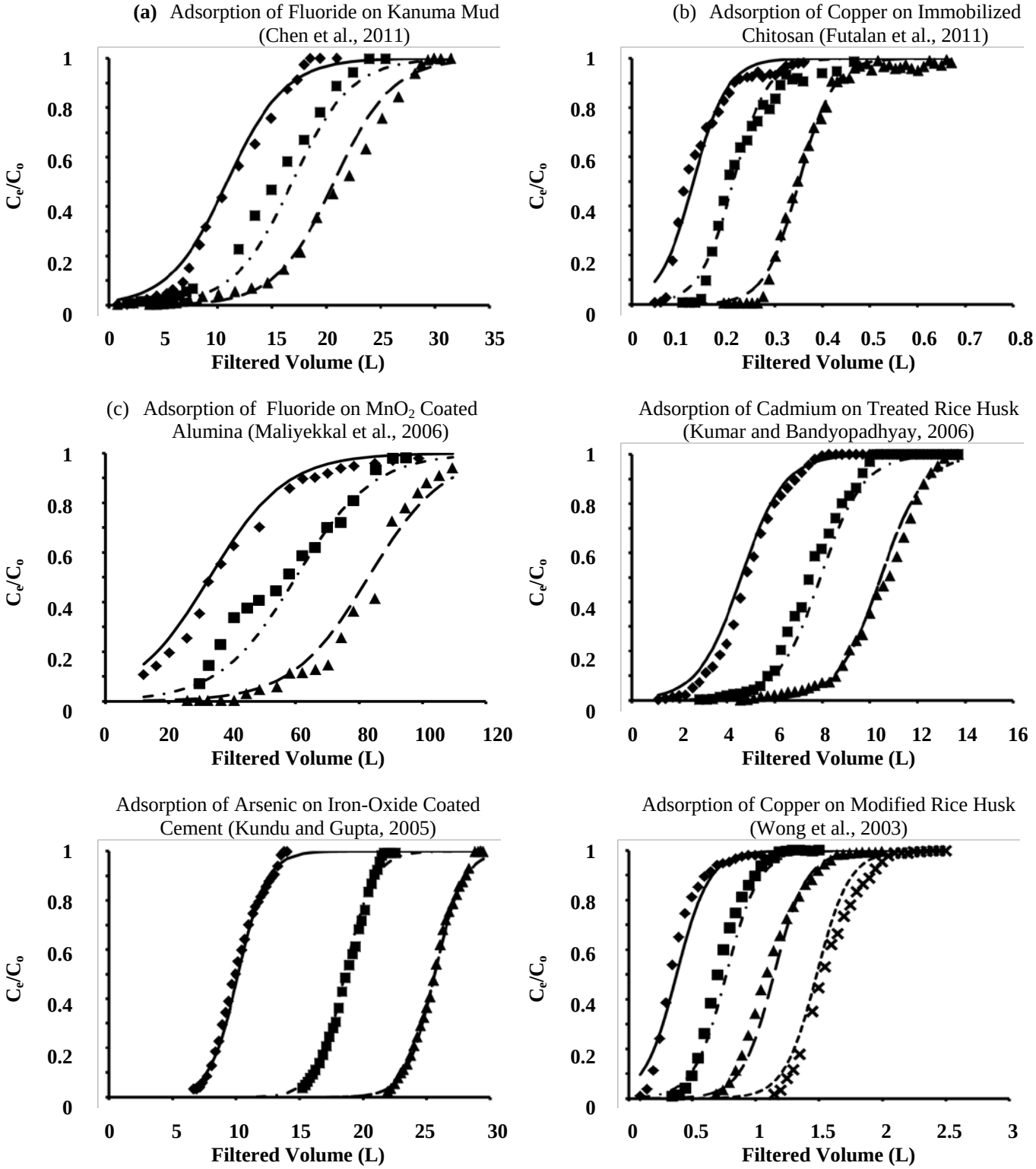

Figure 5.5 Equation 10 fit to independent data sets of normalised pore/effluent contaminant concentration (y-axis) vs. filter loading/operating time (x-axis).

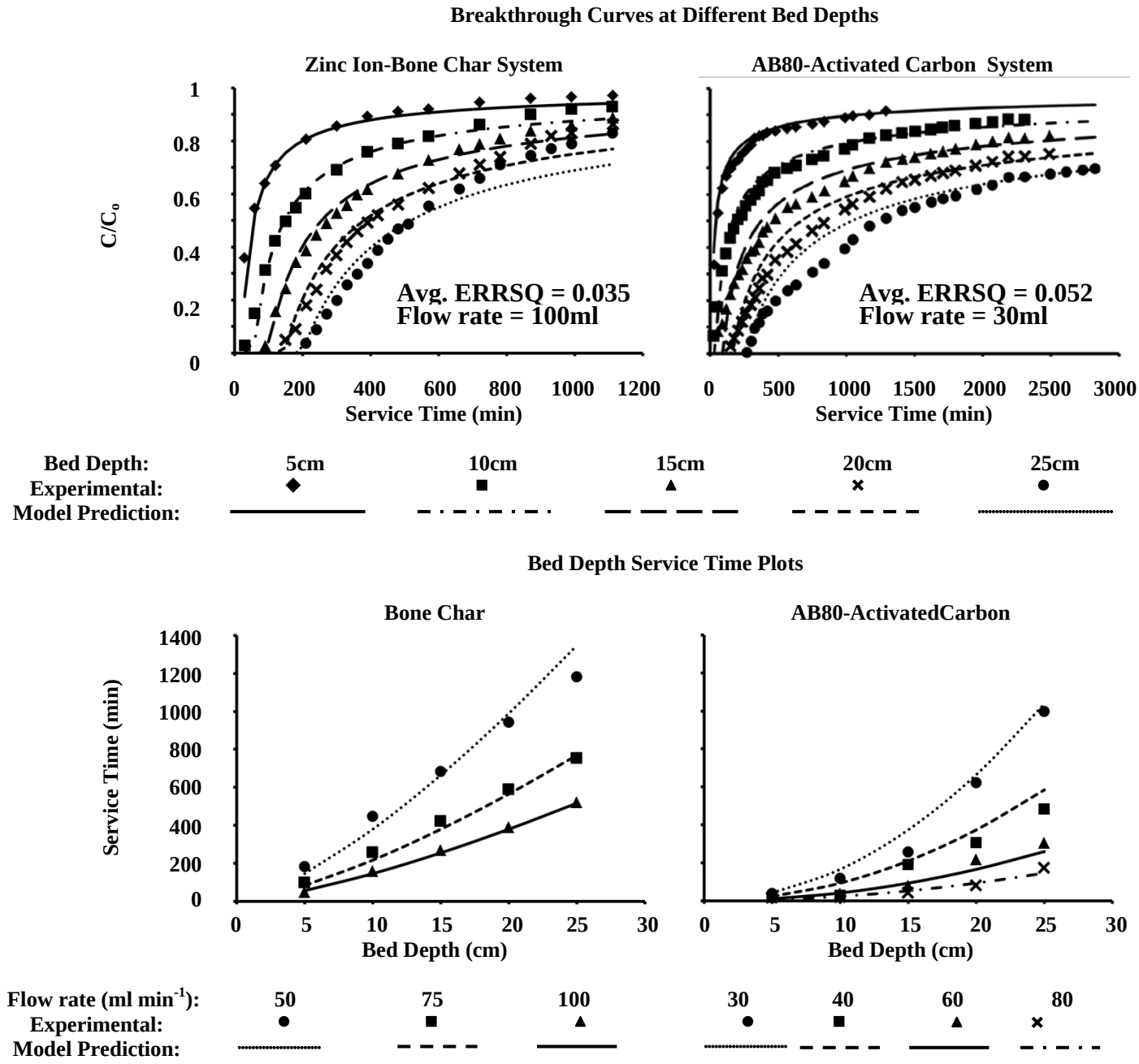

Figure 5.6 (a) Equation 16 fit to an independent data set (Ko et al., 2002) of normalised effluent contaminant concentration (y-axis) vs. filter operating time (x-axis) for various filter-bed depths, and (b) plots of filter service-time (y-axis) vs. filter-bed depth (x-axis) compared to predictions made by Equation 17 using the same model coefficients

Ko et al. (Ko et al., 2002) modified the BDST model using Eqn. 6 and Eqn. 7, and this made it possible to describe non-linear BDST plots. However, as can be seen in Figure 5.6, the BTCs observed in their study were not sigmoidal, and so, the B-A model on which the modified BDST model is based would not be appropriate for the description of entire BTCs. Eqn. 16 was fit to the data from this study, and, as can be seen in Figure 5.6, it was capable of describing not only the non-linear BDST relationship, but also the entire BTC for each filter-bed depth investigated. Eqn. 17 can therefore, in this case, be used to predict the BDST relationship at any breakthrough concentration of interest, as well as at any flow rate of interest, as demonstrated in Figure 5.6b.

5.5 Conclusions

This study described a testing and modelling methodology which uses results from short-term small-scale column tests to predict the long-term performance of large-scale fixed-bed filters.

- The proposed methodology was used to describe the adsorptive performance of small-scale and large-scale filter columns, successfully modelling medium saturation, as well as filter-pore and effluent concentration data.
- Predictions of large-scale filter performance based on small-scale filter performance were highly accurate.
- Two three-parameter models were investigated, and these allowed for the description and prediction of sigmoidal or convex breakthrough curves for multiple filters containing the same media, as well as concentration profiles across multiple depths within single filters.
- The proposed models also allow for the description of non-linear relationships between filter-bed depth and service time, as is commonly observed in fixed-bed systems which take a long time to reach equilibrium.
- The proposed modelling approach was applied to multiple independent data sets and was found to suitably describe the adsorption of various solutes including dyes, phosphate, metals (copper, cadmium, and zinc), fluoride, and arsenic.

5.6 Acknowledgement

The first author would like to acknowledge the Irish Research Council (GOIPG/2013/75) for funding.

5.7 References

Al-Degs, Y.S., Khraisheh, M.A.M., Allen, S.J., Ahmad, M.N., 2009. Adsorption characteristics of reactive dyes in columns of activated carbon. J. Hazard. Mater. 165, 944–949. doi:10.1016/j.jhazmat.2008.10.081

Ayoob, S., Gupta, A.K., 2007. Sorptive response profile of an adsorbent in the defluoridation of drinking water. Chem. Eng. J. 133, 273–281. doi:10.1016/j.cej.2007.02.013

Babel, S., Kurniawan, T.A., 2003. Low-cost adsorbents for heavy metals uptake from contaminated water: a review. J. Hazard. Mater. 97, 219–243. doi:10.1016/S0304-3894(02)00263-7

Bailey, S.E., Olin, T.J., Bricka, R.M., Adrian, D.D., 1999. A review of potentially low-cost sorbents for heavy metals. Water Res. 33, 2469–2479. doi:10.1016/S0043-1354(98)00475-8

Bockris, J.O.M., Conway, B.E., White, R.E., 1995. Modern aspects of electrochemistry Vol. 29. Springer.

Bohart, G.S., Adams, E.Q., 1920. Some Aspects of the Behavior of Charcoal with Respect to Chlorine. 1. J. Am. Chem. Soc. 42, 523–544. doi:10.1021/ja01448a018

Brown, P., Atly Jefcoat, I., Parrish, D., Gill, S., Graham, E., 2000. Evaluation of the adsorptive capacity of peanut hull pellets for heavy metals in solution. Adv. Environ. Res. 4, 19–29. doi:10.1016/S1093-0191(00)00004-6

Callery, O., Healy, M.G., Rognard, F., Barthelemy, L., Brennan, R.B., 2016. Evaluating the long-term performance of low-cost adsorbents using small-scale adsorption column experiments. Water Res. 101, 429–440. doi:10.1016/j.watres.2016.05.093

Chen, N., Zhang, Z., Feng, C., Li, M., Chen, R., Sugiura, N., 2011. Investigations on the batch and fixed-bed column performance of fluoride adsorption by Kanuma mud. Desalination 268, 76–82. doi:10.1016/j.desal.2010.09.053

Chowdhury, Z.K., 2013. Activated Carbon: Solutions for Improving Water Quality. American Water Works Association.

Chu, K.H., 2010. Fixed bed sorption: Setting the record straight on the Bohart–Adams and Thomas models. J. Hazard. Mater. 177, 1006–1012. doi:10.1016/j.jhazmat.2010.01.019

Cooney, D.O., 1998. Adsorption design for wastewater treatment. CRC Press.

Crini, G., 2006. Non-conventional low-cost adsorbents for dye removal: a review. Bioresour. Technol. 97, 1061–1085.

Crini, G., Badot, P.-M., 2010. Sorption Processes and Pollution: Conventional and Non-conventional Sorbents for Pollutant Removal from Wastewaters. Presses Univ. Franche-Comté.

Crini, G., Badot, P.-M., 2008. Application of chitosan, a natural aminopolysaccharide, for dye removal from aqueous solutions by adsorption processes using batch studies: A review of recent literature. Prog.Polym.Sci.33, 399–447. doi:10.1016/j.progpolymsci.2007.11.001

Crittenden, J.C., Berrigan, J.K., Hand, D.W., 1986. Design of rapid small-scale adsorption tests for a constant diffusivity. J. Water Pollut. Control Fed. 312–319.

Crittenden, J.C., Berrigan, J.K., Hand, D.W., Lykins, B., 1987. Design of rapid fixed-bed adsorption tests for nonconstant diffusivities. J. Environ. Eng. 113, 243–259.

Crittenden, J.C., Reddy, P.S., Arora, H., Trynoski, J., Hand, D.W., Perram, D.L., Summers, R.S., 1991. Predicting GAC Performance With Rapid Small-Scale Column Tests. J. Am. Water Works Assoc. 83, 77–87.

Dąbrowski, A., 2001. Adsorption — from theory to practice. Adv. Colloid Interface Sci. 93, 135–224. doi:10.1016/S0001-8686(00)00082-8

Deokar, S.K., Mandavgane, S.A., 2015. Estimation of packed-bed parameters and prediction of breakthrough curves for adsorptive removal of 2,4-dichlorophenoxyacetic acid using rice husk ash. J. Environ. Chem. Eng. 3, 1827–1836. doi:10.1016/j.jece.2015.06.025

Eaton, A.D., Clesceri, L.S., Greenberg, A.E., Franson, M.A.H., American Public Health Association., American Water Works Association., Water Environment Federation., 1998. Standard methods for the examination of water and wastewater. American Public Health Association, Washington, DC.

Faust, S.D., Aly, O.M., 1998. Chemistry of Water Treatment, Second Edition. CRC Press.

Finnegan, J., Regan, J.T., de Eyto, E., Ryder, E., Tiernan, D., Healy, M.G., 2012. Nutrient dynamics in a peatland forest riparian buffer zone and implications for the establishment of planted saplings. Ecol. Eng. 47, 155–164. doi:10.1016/j.ecoleng.2012.06.023

Futalan, C.M., Kan, C.-C., Dalida, M.L., Pascua, C., Wan, M.-W., 2011. Fixed-bed column studies on the removal of copper using chitosan immobilized on bentonite. Carbohydr. Polym. 83, 697–704. doi:10.1016/j.carbpol.2010.08.043

Goel, J., Kadirvelu, K., Rajagopal, C., Kumar Garg, V., 2005. Removal of lead(II) by adsorption using treated granular activated carbon: Batch and column studies. J. Hazard. Mater. 125, 211–220. doi:10.1016/j.jhazmat.2005.05.032

Gupta, V.K., Srivastava, S.K., Tyagi, R., 2000. Design parameters for the treatment of phenolic wastes by carbon columns (obtained from fertilizer waste material). Water Res. 34, 1543–1550. doi:10.1016/S0043-1354(99)00322-X

Han, R., Zou, L., Zhao, X., Xu, Y., Xu, F., Li, Y., Wang, Y., 2009. Characterization and properties of iron oxide-coated zeolite as adsorbent for removal of copper(II) from solution in fixed bed column. Chem. Eng. J. 149, 123–131. doi:10.1016/j.cej.2008.10.015

Ho, Y.S., McKay, G., 1999. Pseudo-second order model for sorption processes. Process Biochem. 34, 451–465. doi:10.1016/S0032-9592(98)00112-5

Hutchins, R., 1973. New method simplifies design of activated carbon systems, Water Bed Depth Service Time analysis. J Chem Eng Lond 81, 133–138.

Ko, D.C.K., Lee, V.K.C., Porter, J.F., McKay, G., 2002. Improved design and optimization models for the fixed bed adsorption of acid dye and zinc ions from effluents. J. Chem. Technol. Biotechnol. 77, 1289–1295. doi:10.1002/jctb.707

Ko, D.C.K., Porter, J.F., McKay, G., 2000. Optimised correlations for the fixed-bed adsorption of metal ions on bone char. Chem. Eng. Sci. 55, 5819–5829. doi:10.1016/S0009-2509(00)00416-4

Kumar, U., Bandyopadhyay, M., 2006. Fixed bed column study for Cd(II) removal from wastewater using treated rice husk. J. Hazard. Mater. 129, 253–259. doi:10.1016/j.jhazmat.2005.08.038

Kundu, S., Gupta, A.K., 2005. Analysis and modeling of fixed bed column operations on As(V) removal by adsorption onto iron oxide-coated cement (IOCC). J. Colloid Interface Sci. 290, 52–60. doi:10.1016/j.jcis.2005.04.006

Lagergren, S., 1898. About the theory of so-called adsorption of soluble substances.

Liu, Y., 2008. New insights into pseudo-second-order kinetic equation for adsorption. Colloids Surf. Physicochem. Eng. Asp. 320, 275–278. doi:10.1016/j.colsurfa.2008.01.032

Maliyekkal, S.M., Sharma, A.K., Philip, L., 2006. Manganese-oxide-coated alumina: A promising sorbent for defluoridation of water. Water Res. 40, 3497–3506. doi:10.1016/j.watres.2006.08.007

Nguyen, T.A.H., Ngo, H.H., Guo, W.S., Pham, T.Q., Li, F.M., Nguyen, T.V., Bui, X.T., 2015. Adsorption of phosphate from aqueous solutions and sewage using zirconium loaded okara (ZLO): Fixed-bed column study. Sci. Total Environ. 523, 40–49. doi:10.1016/j.scitotenv.2015.03.126

Poots, V.J.P., McKay, G., Healy, J.J., 1976a. The removal of acid dye from effluent using natural adsorbents—II Wood. Water Res. 10, 1067–1070. doi:10.1016/0043-1354(76)90037-3

Poots, V.J.P., McKay, G., Healy, J.J., 1976b. The removal of acid dye from effluent using natural adsorbents—I peat. Water Res. 10, 1061–1066. doi:10.1016/0043-1354(76)90036-1

Pratt, C., Parsons, S.A., Soares, A., Martin, B.D., 2012. Biologically and chemically mediated adsorption and precipitation of phosphorus from wastewater. Curr. Opin. Biotechnol., Phosphorus biotechnology • Pharmaceutical biotechnology 23, 890–896. doi:10.1016/j.copbio.2012.07.003

Qiu, H., Lv, L., Pan, B., Zhang, Qing-jian, Zhang, W., Zhang, Quan-xing, 2009. Critical review in adsorption kinetic models. J. Zhejiang Univ. Sci. A 10, 716–724. doi:10.1631/jzus.A0820524

Reddad, Z., Gerente, C., Andres, Y., Le Cloirec, P., 2002. Adsorption of Several Metal Ions onto a Low-Cost Biosorbent: Kinetic and Equilibrium Studies. Environ. Sci. Technol. 36, 2067–2073. doi:10.1021/es0102989

Søvik, A.K., Kløve, B., 2005. Phosphorus retention processes in shell sand filter systems treating municipal wastewater. Ecol. Eng. 25, 168–182. doi:10.1016/j.ecoleng.2005.04.007

Spellman, F.R., 2013. Handbook of Water and Wastewater Treatment Plant Operations, Third Edition. CRC Press.

Thomas, H.C., 1944. Heterogeneous Ion Exchange in a Flowing System. J. Am. Chem. Soc. 66, 1664–1666. doi:10.1021/ja01238a017

Wong, K.K., Lee, C.K., Low, K.S., Haron, M.J., 2003. Removal of Cu and Pb from electroplating wastewater using tartaric acid modified rice husk. Process Biochem. 39, 437–445. doi:10.1016/S0032-9592(03)00094-3

Xu, Z., Cai, J., Pan, B., 2013. Mathematically modeling fixed-bed adsorption in aqueous systems. J. Zhejiang Univ. Sci. A 14, 155–176.

Supplement to Chapter 5

Figure S5.1 Comparison, using data from Ko et al. (2000), showing equal efficacy of correlating time dependent bed capacity, N_t, with either service time, t, or empty bed contact time, EBCT.

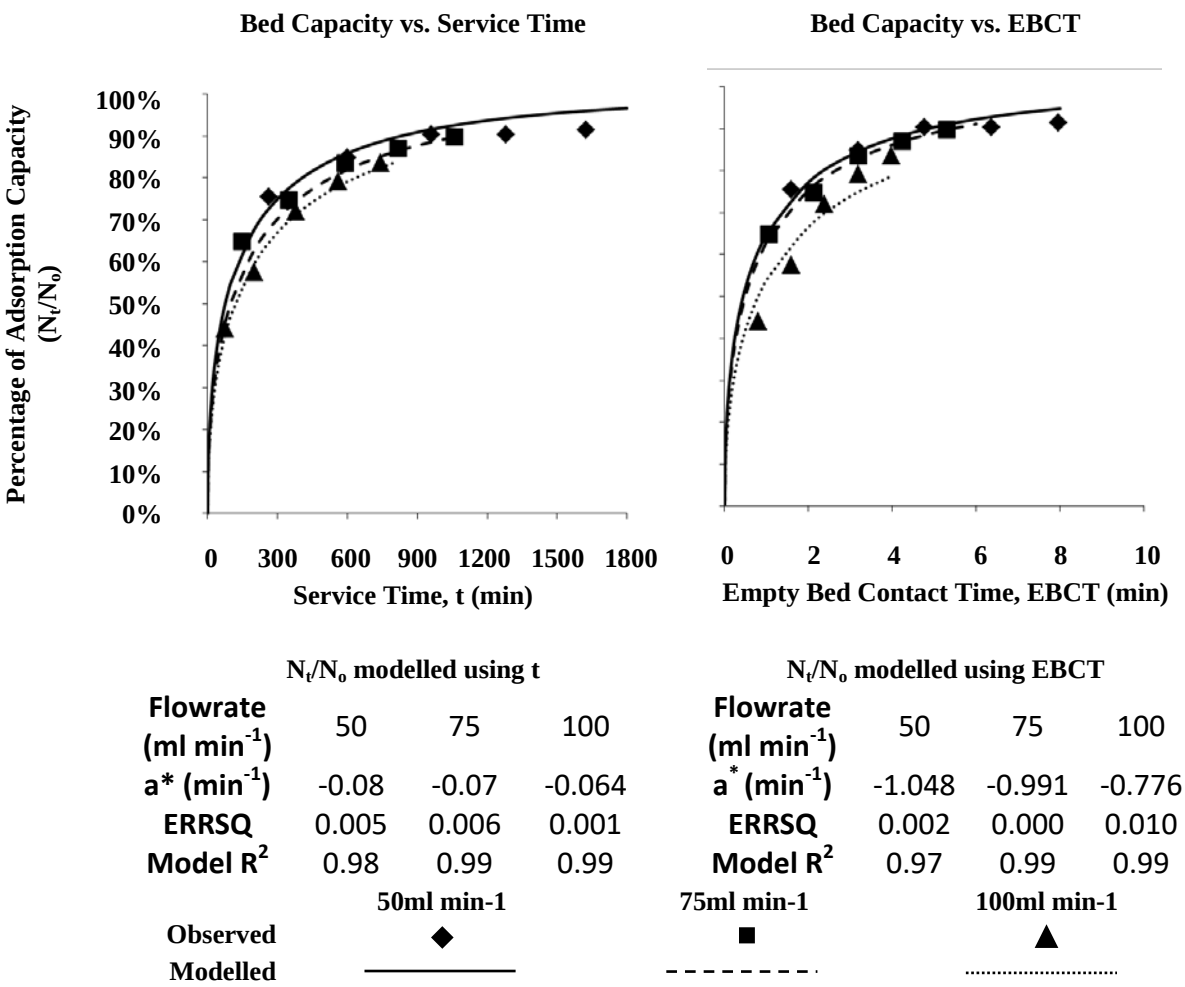

<u>Regarding the derivation of an expression for N_t from second order kinetics (Eqn.8):</u>

Lagergren's (1898) pseudo first-order model can be written as follows: $\frac{dN_t}{dt} = a(N_o - N_t)$

Where N_t is the amount of adsorption (mg g^{-1}) at time, t, N_o is the adsorption capacity at equilibrium (mg g^{-1}), and a is the first-order rate constant.
Integrating this, we get Eqn. 6, as given in the manuscript: $N_t = N_o(1 - e^{-at})$
We can also use the same logic to derive an expression for N_t based on second-order kinetics; Ho and McKay's (1999) pseudo second-order can be written as follows: $\frac{dN_t}{dt} = k_2(N_o - N_t)^2$
Where k_2 is the second-order rate constant. When integrated, this yields the following:
$N_t = \frac{tN_o^2 k_2}{tk_2N_o+1}$
Dividing both sides by N_o we get: $\frac{N_t}{N_o} = \frac{tN_o k_2}{tk_2N_o+1}$
Divide every term on RHS by $N_o k_2$: $\frac{N_t}{N_o} = \frac{t}{t+\frac{1}{N_o k_2}}$
Let $a^{**} = 1/N_o k_2$, and cross-multiply to get Eqn. 8, as given in the manuscript: $N_t = N_o \frac{t}{t+a^{**}}$

Figure S5.2 Contact time (x-axis) vs fractional uptake, q_t/q_e, (y-axis) as predicted by Eqns. 13, 14, and 15.

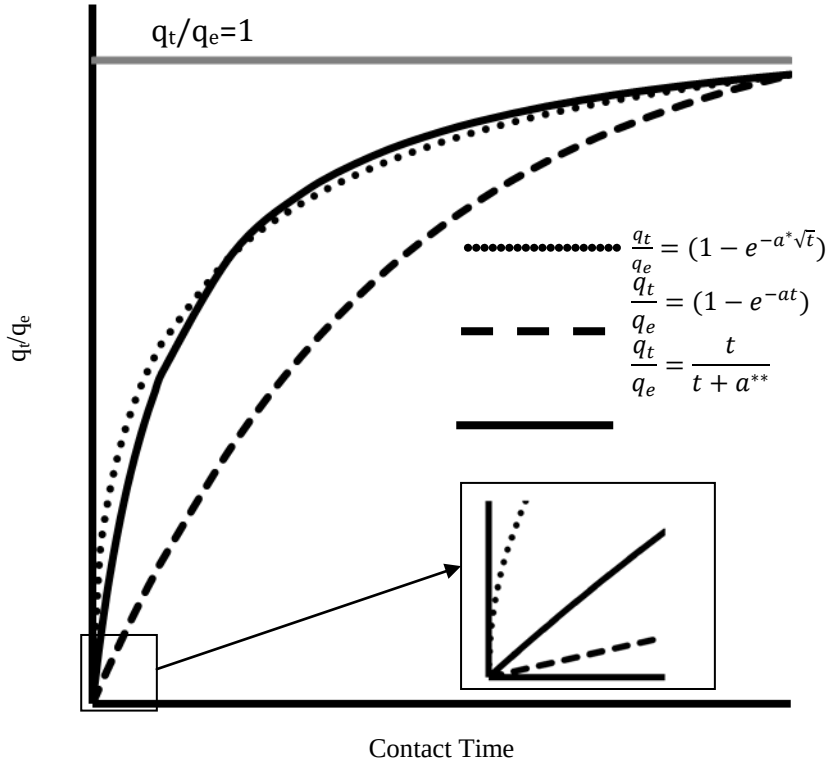

Figure S5.3 Comparison of breakthrough curve shapes and bed-depth service-time plots as predicted by (a) the B-A model (Eqn. 2) and Hutchins' BDST model (Eqn. 3), and (b) the modified B-A model (Eqn. 10), modified BDST model (Eqn. 9), and Eqns. 16 and 17.

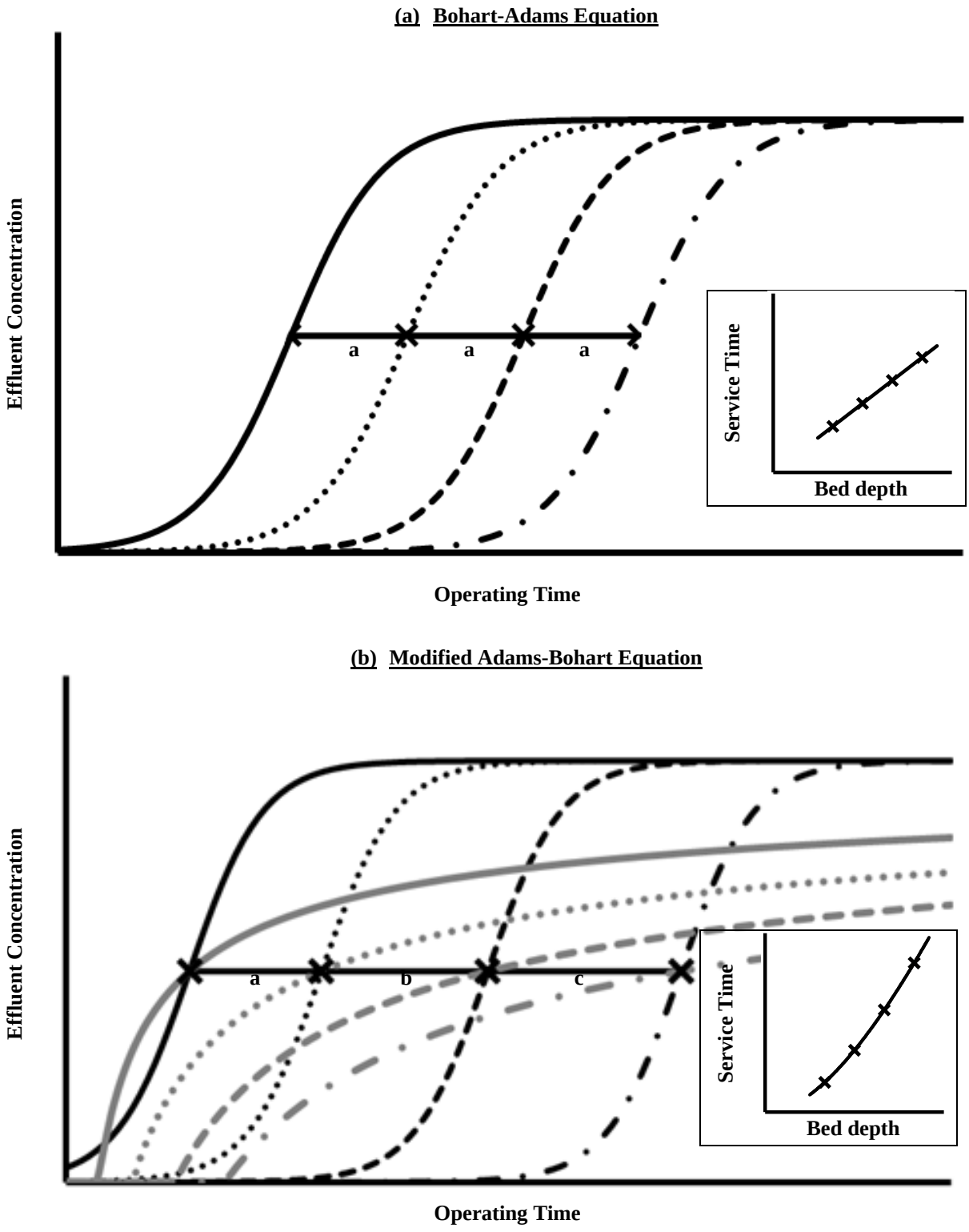

Chapter 6

To assess the potential longevity of a filter medium, flow-through experiments must be performed using real wastewater, as (1) interactions between adsorbents and wastewaters are extremely complex with each adsorbent-wastewater system requiring individual assessment, as discussed in Chapter 3, and (2) the results of batch experiments are not necessarily indicative of in-field media performance. In this chapter, the RSSCT methodology developed in Chapter 4 was used in conjunction with the mathematical modelling techniques developed in Chapter 5 to assess the potential of aluminium water treatment residual and crushed concrete for use in pilot-scale in-field filters intended to remove phosphorus from peatland forestry runoff and dairy soiled water. The study described in this chapter also investigated any potential pollution swapping issues that might preclude the use of these media in the treatment of either wastewater. Addressing this knowledge gap was the fourth thesis aim identified in Chapter 1.

The contents of this chapter have been submitted to an international journal for publication. Oisín Callery designed and set up the experiment, carried out all of the testing and analysis, and is the primary author of this publication. Dr. Mark G. Healy contributed to the experimental design and paper writing.

A novel method to rapidly assess the suitability of low-cost adsorbents for the mitigation of point and nonpoint source phosphorus losses

O. Callery, M.G. Healy

Civil Engineering, National University of Ireland, Galway, Co. Galway, Rep. of Ireland.

Abstract

Freshwater ecosystems worldwide are at risk of becoming degraded as a result of excessive inputs of phosphorus associated with human terrestrial activities. This study (1) assesses the potential of two low-cost adsorbents, aluminum drinking water treatment residual (Al-WTR) and crushed concrete (CC), to remove phosphorus (P) from dairy-soiled water (DSW) and forestry runoff - wastewaters which are representative of point and nonpoint P pollution sources, respectively; (2) examines potential risks, such as elevated pH and release of metals, associated with their use, and (3) applies two models to determine the performance and longevity of these media in large-scale filters. The results of this study indicate that, in terms of ability to remove P, both CC and Al-WTR show promise for use in treating forestry runoff; however, the raised pH of effluent from CC filters may be of environmental concern. Al-WTR showed greater promise for the treatment of DSW due to its higher adsorption capacity at high concentrations. Small cumulative releases of aluminum and copper were observed from both media when treating forestry runoff, and Al-WTR also released a small amount of nickel. The majority of metal release occurred immediately after filter loading began, indicating that pre-washing of the media might prevent metal losses. In summary, these results indicate that field-scale tests are warranted for the treatment of both wastewaters with Al-WTR; however, CC is likely to be unsuitable for either forestry runoff or DSW due to its effects on pH and its relatively low lifespan, respectively.

Nomenclature

a**	Time constant in Eqn. 3 and Eqn. 11
A	Constant of proportionality in Eqn. x (mg g^{-1})
B	Constant of system heterogeneity in Eqn. x
C_b	Breakthrough concentration (mg L^{-1})
C_e	Sorbate concentration of filter effluent (mg L^{-1})
C_o	Sorbate concentration of filter influent (mg L^{-1})
k	Bohart-Adams rate constant (L mg^{-1} min^{-1})
m	Mass of adsorbent (g)
N_o	Sorption capacity of bed (mg L^{-1})
N_t	Time dependent sorption capacity of bed (mg L^{-1})
q_t	Time dependent sorbate concentration per unit mass of adsorbent (mg g^{-1})
t	Empty bed contact time (min)
t_b	Service time/operating time of bed at breakthrough (i.e. when $C_e = C_b$) (min)
U	Flow velocity of solution past adsorbent (cm min^{-1})
V	Volume of solution filtered (L)
V_x	Volume of filter bed (L)
Z	Filter bed depth (cm)

6.1 Introduction

Excessive nutrient enrichment of surface waters results in optimal conditions for the overgrowth of algae and many species of noxious aquatic plants. The proliferation of these nuisance species causes serious damage to aquatic ecosystems, both in terms of long-term losses of biodiversity, as well as the more immediate concern posed by the sudden influx of large volumes of biomass into aquatic ecosystems. Sources of nutrient pollution may be divided into two categories: point sources and nonpoint sources. Discreet, easily identifiable point sources such as outlets from municipal wastewater treatment plants and drains from livestock housing and farmyards are usually comparatively low-volume, high-concentration nutrient waste streams (Eaton et al., 1995). By comparison, nonpoint sources such as runoff from pastures, arable lands, and forestry plantations represent high-volume, low-concentration nutrient pollution streams (Acreman, 2012). Nonpoint sources are particularly difficult to control for a number of reasons, though the primary challenge is simply that the pollution source is spread across a large area for which it is extremely challenging to implement effective runoff treatment strategies (Rao et al., 2009).

A multitude of technologies and management practices have been developed to curtail the loss of nutrients, primarily phosphorus (P) and nitrogen (N), from point and nonpoint sources, though the focus has been largely on P, as it is the limiting nutrient in freshwater environments (Blomqvist et al., 2004; Correll, 1999; Hilton et al., 2006; Schoumans et al., 2014). There is evidence to suggest that controlling N inputs alone can have a deleterious effect by favoring a shift in algal communities towards more objectionable nitrogen fixing cyanobacteria (blue-green algae) (Schindler et al., 2008), further supporting the assertion that P control is of primary importance to the prevention of eutrophication (Schindler et al., 2016; Sharpley et al., 2003).

In the case of point sources, P is usually removed at centralized wastewater treatment facilities using well-advanced technologies such as metal precipitation and adsorption, enhanced biological P removal, and, more recently, struvite crystallization (de-Bashan and Bashan, 2004). Phosphorus losses from nonpoint sources are usually addressed at source through the implementation of sound management practices: balancing fertilizer application in relation to crop requirements, matching animal feed P inputs to the nutritional requirements of livestock, reducing particulate P losses by minimizing erosion, and, where P must be applied, timing applications to minimize losses in runoff. Many mitigation strategies

targeting nonpoint source P losses take advantage of the fact that a large portion of total P is present as particulate bound P, and hence trapping sediments in settling ponds, constructed wetlands, and riparian buffer zones is often an effective strategy.

There are, however, still many instances where conventional techniques and management practices such as these fail to produce desired results, or where their implementation is not practicable. In the case of nonpoint source pollution, a problematic example is P losses from forestry harvesting on blanket peat soils. Riparian buffer zones are the recommended best management practice to control such P losses, but these have been shown to be largely ineffective at removing dissolved P released during clearfelling due to low P retention capacity of low-mineral soils and insufficient uptake by vegetation (Rodgers et al., 2010). Reducing inputs of P is not a feasible option either, given that much of the P lost during forest harvesting originates from the brash (tree harvesting residues) materials, and hence is already present on site (Finnegan et al., 2014). In the case of point source pollution, a potentially troublesome source of nutrients is improperly managed dairy soiled water (DSW) (Dunne et al., 2005). Farms often lack the prohibitive amount of space required for treatment with a constructed wetland, and climatic/soil conditions often preclude land spreading (Ruane et al., 2011), as to do so would simply transmute a point source problem to a nonpoint source problem.

In cases such as these, where source control is neither feasible nor effective and/or where traditional onsite treatment methods are not possible, alternative remedial strategies must be implemented in order to prevent unacceptable P losses. Phosphorus-sorbing materials may offer a solution, and there has been a great deal of recent interest in identifying low-cost adsorbents suitable for use in on-site wastewater treatment systems (Cucarella and Renman, 2009). More recently, adsorbents are also being used to remove dissolved P from surface and ground waters (Buda et al., 2012), and numerous technologies are being investigated, using adsorptive materials (1) applied as soil amendments (Stout et al., 2000) (2) as substrates in constructed wetlands (Vohla et al., 2005), or (3) as filter media in permeable reactive barriers (Baker et al., 1997) and in-drain filters (Penn et al., 2007).

Once a prospective adsorptive media has been identified, its suitability for an in-field trial must be fully assessed. Commonly, this involves laboratory-based evaluation of the media's adsorptive capacity using batch tests, though there is a growing body of research which indicates that results of these tests are not suitable for the purposes of estimating media

lifespan (Drizo et al., 2002; Guo et al., 2017; Penn and McGrath, 2011; Pratt and Shilton, 2009; Seo et al., 2005; Søvik and Kløve, 2005). To determine filter lifespan, flow-through experiments are often performed (Ali and Gupta, 2007), and in conjunction with predictive modeling, these can give at least an indicative estimate of potential media longevity (Shiue et al., 2011). This is an obviously important first step before costly and time-consuming field studies are performed, though many flow-through methodologies can be time consuming in their own right, lasting many weeks (Razali et al., 2007), months (Bowden et al., 2009; Heal et al., 2003), or even years (Baker et al., 1998).

The aim of this study was to assess the potential usefulness of two low-cost adsorbents, namely aluminum drinking water treatment residual (Al-WTR) and crushed concrete (CC), as filter media intended to remove P from DSW and forestry runoff. These wastewaters are representative sources of point and nonpoint P losses, respectively, and the two low-cost media have shown past promise as P-sorbing materials (Babatunde et al., 2009; Callery et al., 2015; Egemose et al., 2012). A major concern with novel low-cost adsorbents is that they may be potential sources of metals (Velghe et al., 2012). To address this concern, the final effluent from both filter media were also analyzed for metals. The potential of the materials for use as filter media was assessed using a recently-developed methodology which uses a combination of rapid small-scale filter experiments and modeling techniques to make predictive estimates of the performance and longevity of hypothetical large-scale filters (Callery et al., 2016; Callery and Healy, 2017). The methodology used assesses the media under flow-through conditions similar to those experienced in-field, but produces results in as little as 24 hours, similar to batch tests.

6.2 Materials and Methods

6.2.1 Sample collection and preparation

The two low-cost adsorbents investigated in this study were Al-WTR and CC. The Al-WTR, which had an initial dry solids content of approximately 20%, was first passed through a 1 mm mesh to remove any coarse particles. The strained sludge was then oven dried at 105°C for 24 hr, before being ground with a mortar and pestle and sieved; the fraction which was retained by a 0.5 mm sieve after passing a 1 mm sieve was stored in airtight high density polyethylene (HDPE) containers for use in the adsorption columns. The concrete was pulverized using a mortar and pestle, and dried in an oven at 105°C for 24 hr before being

sieved; similarly, the fraction which was retained by a 0.5 mm sieve after passing a 1 mm sieve was stored in airtight HDPE containers until use in the adsorption columns.

6.2.2 Preparation of filter columns

For each medium, filter column sets, comprising four columns with lengths of 0.4 m, 0.3 m, 0.2 m, and 0.1 m, were prepared using low density polyethylene (LDPE) tubing with an internal diameter of 9.5 mm. The filter columns were packed with filter media, and syringe barrels (i.e. syringes with the plungers removed), packed with a small quantity of glass wool, were fastened to the top and bottom of each filter column. The columns were fixed to a frame to maintain a vertical orientation throughout the experiment, and silicone tubing with an internal diameter of 3.1 mm was attached to the syringe ends at the bottom and top of the filter columns to provide influent and effluent lines.

6.2.3 Operation of filter columns

Coarse straining filters, comprising a syringe barrel packed with a small quantity of glass wool, were attached to the ends of the influent lines, and these were submerged in a feed tank filled with either forestry runoff or DSW. A Masterflex peristaltic pump was used to supply influent the base of each filter column at flow rates of 105-205 mL hr^{-1}, corresponding to hydraulic loading rates (HLRs) of 1.47-2.88 m hr^{-1}, rates typical of activated carbon adsorption filters (Chowdhury, 2013) and tricking filters (Spellman, 2013), and HLRs that have been used in reactive filters for P removal (Erickson et al., 2012). The effluent from each filter column was collected in 2 hr aliquots using an autosampler. The filter columns were operated in 12 hr on/off cycles to replicate the intermittent loading conditions that would be expected on site, thus allowing time for intra-particle diffusion of adsorbate molecules and associated rejuvenation of the media surface. The collected aliquots were weighed to determine the volume of solution filtered, and subsamples of each aliquot were passed through a 0.45 μm filter before being analyzed for P concentrations after APHA (Eaton et al., 1998). Subsamples of the aliquots were acidified to a pH<2 with nitric acid and metal concentrations were determined by ICP-MS after U.S. EPA method 6020A (U. S. Environmental Protection Agency, 2007). Metal analyses were only performed on effluent samples from the 0.4 m filter columns, as testing samples from all columns was cost-prohibitive.

6.2.4 Data collection and analyses

For each filter column, after any filter loading, V, the mass of P removed per gram of filter medium, was calculated by:

$$q_t = \sum_{i=1}^{n} \frac{(C_o - C_e)V_i}{m} \quad (1)$$

where q_t is the mass of P retained per gram of filter medium (dependent on the contact time between the solution and the filter media), C_o is the P concentration of the influent, C_e is the P concentration of the i^{th} aliquot of filter effluent, V_i is the volume of the i^{th} aliquot (of a total number of aliquots, n, whose combined volume is V), and m is the mass of media in the adsorption column.

In a recent paper, Callery and Healy (2017) proposed that the performance of multiple adsorption columns could be described with one of two models. The first of these, which is best suited to the description of sigmoidal breakthrough curves, is based on a modification of the popular Bohart-Adams model (Bohart and Adams, 1920):

$$ln\left(\frac{C_0}{C_b} - 1\right) = kN_t\frac{Z}{U} - kC_0t_b \quad (2)$$

where k is a model constant, Z is the filter-bed depth, U is the linear flow velocity, t_b is the filter-bed service time at which the concentration C_b occurs, and N_t is the time-dependent bed capacity, defined as follows:

$$N_t = N_o\frac{t}{t + a^{**}} \quad (3)$$

where t is the filter empty bed contact time (EBCT), N_o is the maximum adsorption capacity of the filter bed per unit volume of filter medium, and a** is a model constant sometimes referred to as the 'time of relaxation', i.e. the time taken for the adsorptive medium to reach half of its adsorptive potential.

Rearranging Eqn. 2, we get an expression for C_b at any filter loading, V:

$$C_b = \frac{C_o}{1 + e^{-k\left(C_o t_b - N_t\frac{Z}{U}\right)}} \quad (4)$$

Eqn. 4 may also be rearranged to determine the time at which a given breakthrough concentration will occur:

$$t_b = \frac{N_t Z}{C_0 U} - \frac{1}{kC_0} ln\left(\frac{C_0}{C_b} - 1\right) \qquad (5)$$

Assuming that the influent concentration remains constant, the total mass of P loaded onto the adsorption column can be defined as follows:

$$mass\ loading = \int_0^V C_o\ dV \qquad (6)$$

The total mass of P lost in filter effluent can be defined as the integral from 0 to t_b of Eqn. 4:

$$\int_0^{t_b} C_b\ dV = \frac{\ln\left(e^{C_o k t_b} + e^{\frac{kN_t Z}{U}}\right)}{k} - \frac{\ln\left(1 + e^{\frac{kN_t Z}{U}}\right)}{k} \qquad (7)$$

Given that at the time of breakthrough, the volume treated can be defined as $V = t_b * Q$ (where Q is the loading rate in L hr^{-1}). The total mass retained by the filter media, $q_t m$, can therefore be described by making this substitution and subtracting Eqn. 7 from Eqn. 6:

$$q_t m = C_o t_b Q - \frac{\ln\left(e^{C_o k t_b} + e^{\frac{kN_t Z}{U}}\right)}{k} + \frac{\ln\left(1 + e^{\frac{kN_t Z}{U}}\right)}{k} \qquad (8)$$

q_e can be determined dividing both sides of Eqn. 8 by the filter medium mass, m, which after some simplification yields:

$$q_t = \frac{C_o t_b Q}{m} - \frac{\ln\left(\left(e^{C_o k t_b} + e^{\frac{kN_t Z}{U}}\right)\left(1 + e^{\frac{kN_t Z}{U}}\right)\right)}{mk} \qquad (9)$$

The second model, proposed by Callery and Healy (2017), is best suited to the description of non-sigmoidal, convex to linear breakthrough curves of the type often observed in flow-through studies using low-cost adsorbents. This model is as follows:

$$\mathrm{C_b} = \mathrm{C_o} - \frac{\mathrm{q_t} m}{\mathrm{VB}} \qquad (10)$$

where B is a model constant and q_t is a EBCT-dependent term for the mass of P adsorbed at a filter loading of V per unit mass of filter bed, described by:

$$q_t = \mathrm{AV_b}^{\left(\frac{1}{\mathrm{B}}\right)} \frac{t}{t + a^{**}} \qquad (11)$$

where A is a model constant of proportionality and V_b is the number of empty bed volumes filtered. As with Eqn. 9, Eqn. 11 may be rearranged to find the filter loading, V, at which any given breakthrough concentration occurs:

$$V = \frac{q_t m}{B(C_o - C_t)} \qquad (12)$$

Substituting Eqn. 11 for q_t in Eqn 12., we obtain the following:

$$V = \left(\frac{B(C_o - C_e)(t+k)}{V_x^{-\left(\frac{1}{B}\right)} Amt} \right)^{\frac{B}{1-B}} \qquad (13)$$

where V_x is the volume of the filter bed.

With experimental values for q_t determined from Eqn 1, an attempt was made to fit both Eqn. 9 and Eqn. 11 to the data using nonlinear regression. Values for the model were obtained using the Solver tool in Microsoft Excel by minimizing the value obtained by the sum of the squared errors (ERRSQ) function:

$$ERRSQ = \sum_{i=1}^{n} \left(q_{t,i,meas} - q_{t,i,calc} \right)^2 \qquad (14)$$

where $q_{t,i,meas}$ is the measured value of q_t obtained using Eqn. 9, and $q_{t,i,calc}$ is the value of q_t predicted by either Eqn. 9 or Eqn. 11.

The mean percentage error (MPE), which can be negative or positive depending on whether the model over- or underestimated experimental values respectively, was also calculated by:

$$MPE = \frac{100\%}{n} \sum_{i=1}^{n} \frac{q_{t,i,meas} - q_{t,i,calc}}{q_{t,i,meas}} \qquad (15)$$

The MPE provides a more an intuitive metric of goodness of model fit, providing information both on how closely a model fits experimental data, as well as whether modeled values over- or underestimate actual values.

Using the model coefficients obtained from the small-scale columns, the performance of full-scale pilot filters could be estimated with either Eqn. 5 or Eqn.13, depending on which of Eqn. 9 or Eqn. 11 best fit the small-scale data. If using Eqn. 5, the volume at which a given breakthrough concentration, C_b, occurs may be found by multiplying t_b by the volumetric flow through the large-scale filter. If using Eqn. 13, the volume at breakthrough is found by

using the mass of adsorbent in the large-scale column in the place of 'M', and the volume of the large-scale column in the place of V_x.

6.3 Results and Discussion

6.3.1 Phosphorus retention

Graphs of P retention against filter column loading can be seen in Figure 6.1. When filtering forestry runoff, the maximum amount of P retained by Al-WTR and CC was 0.349 and 0.142 mg g^{-1}, respectively, and when filtering DSW, the maximum amount of P removed by Al-WTR and crushed concrete was 3.673 and 1.333 mg g^{-1}, respectively. These values do not represent saturated adsorption capacities, and had the columns been loaded for longer, further adsorption would almost certainly have taken place; however, 24-36 hr of loading was sufficient to fit Eqns. 9 and 11 to experimental data (Callery et al., 2016). Though Al-WTR displayed a higher overall adsorption capacity when filtering forestry runoff, it also displayed a faster breakthrough (assuming breakthrough to be when the column effluent reaches 10% of the influent concentration (Ahmad and Hameed, 2010; Netpradit et al., 2004)). Crushed concrete's high performance at low concentrations indicates that it has a higher adsorption affinity than Al-WTR (Hinz, 2001), even though it had a lesser adsorption capacity.

The media saturation, q_t, for each media-wastewater combination was modeled using Eqn. 9 (the modified Bohart-Adams equation) and Eqn. 11 (the Callery-Healy model). When used to treat forestry runoff, it was found that crushed concrete's performance could be best modeled by Eqn. 9, which fit the experimental data with a MPE of 1.02% (Table 6.1). Eqn. 11 offered a better fit to experimental data from Al-WTR used to treat forestry runoff, concrete used to treat DSW, and Al-WTR used to treat DSW, with modeled values having MPEs of -4.03%, -0.27%, and -2.69%, respectively (Table 6.1). The negative MPEs obtained when fitting Eqn. 11 to experimental data indicate that model predictions were, on average, slightly higher than observed values, and the positive MPE obtained when fitting Eqn. 9 to experimental data indicated that model predictions were, on average, slightly higher; this indicates that both models tended to slightly under- or overestimate the adsorptive performance of each media, though not significantly.

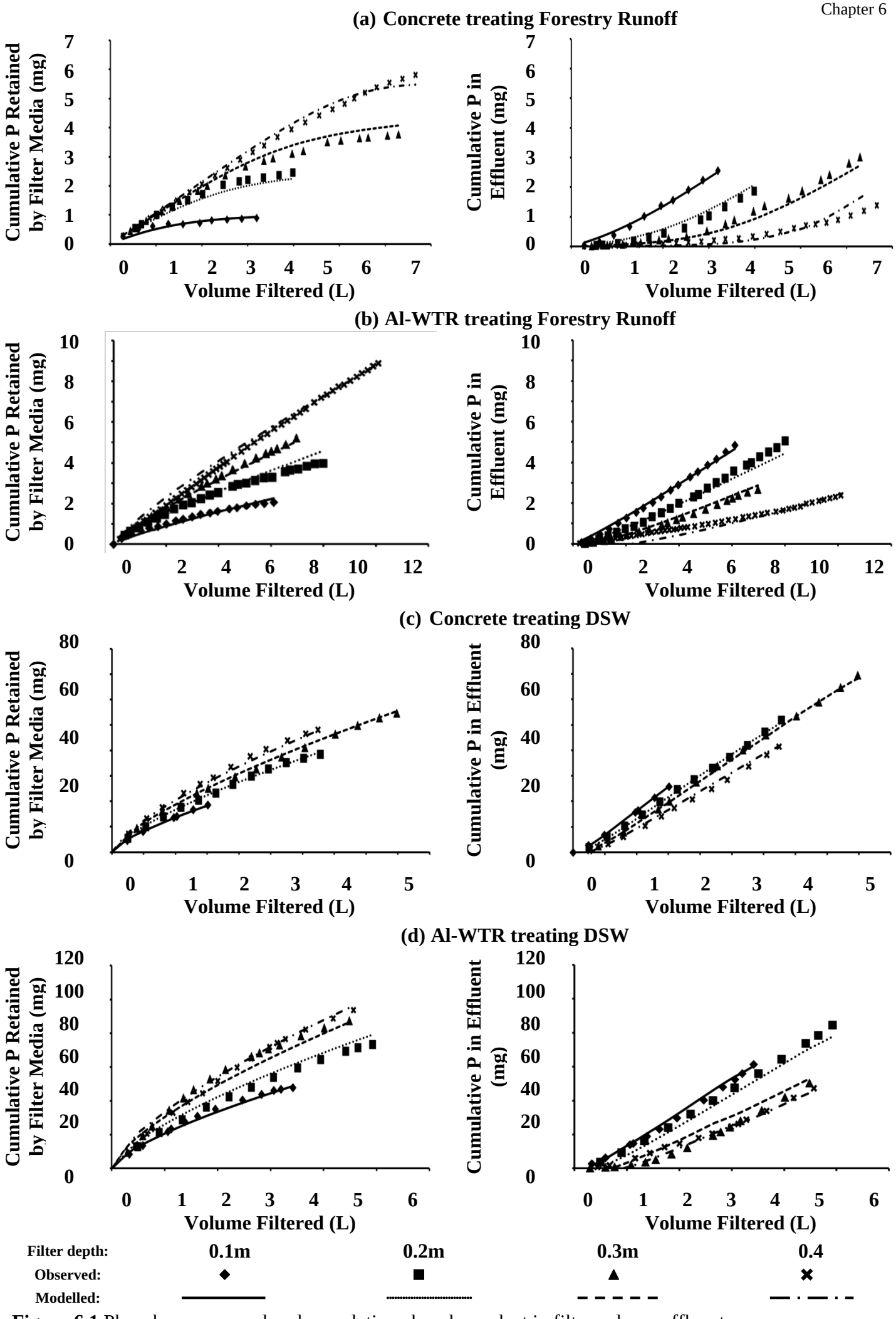

Figure 6.1 Phosphorus removal and cumulative phosphorus lost in filter column effluent

6.3.2 Metals release

In general, there was no significant release of metals from either media when filtering DSW. However, both media released small amounts copper (Cu) and aluminum (Al) when filtering forestry runoff, and Al-WTR also released a very small amount of nickel (0.16 µg g^{-1}). Figure 6.2 shows the relationship between cumulative metals release from the 0.4 m columns and filter loading for each media/wastewater combination studied. The total cumulative metal loss from 0.4 m filter columns of each media and wastewater combination investigated is summarized in Table 6.2, and Table 6.3 shows metal concentrations in the influent to the filter columns alongside maximum metal concentrations measured in the effluent from the 0.4 m filter columns.

When CC was used to filter forestry runoff, there was an initial small release of chromium (Cr) and lead (Pb) - though there was subsequent uptake of these metals, resulting in net removal over the course of the experiment; manganese (Mn), zinc (Zn), and iron (Fe) were removed from the influent. There was a net removal of all metals tested when CC was used to filter DSW, though there was an initial period where concentrations of Cu and Cr were slightly elevated. When filtering forestry water, Al-WTR released small amounts of Mn, though subsequent uptake resulted in net removal of Mn from the influent. Al-WTR also removed Cr, Zn, Pb, and Fe from the forestry runoff influent, and though Al was released initially, filter effluent concentrations quickly leveled off, indicating that a state of equilibrium had been reached, and further release was unlikely. Al-WTR removed all of the metals tested from DSW, though there was an initial small release of nickel prior to this uptake.

A commonly observed phenomenon for all media was that there was a brief initial period of metal release for many metals. This was often followed either by a cessation in further release or often even subsequent uptake by the media, resulting in a net removal of metals over the duration of filter loading. This suggests that an initial washing of the filter media would be highly advisable to rinse off any loosely bound media particles and easily solubilized metals. This would likely help to prevent or significantly reduce any release of metals associated with extreme pH values and loss of particulate matter.

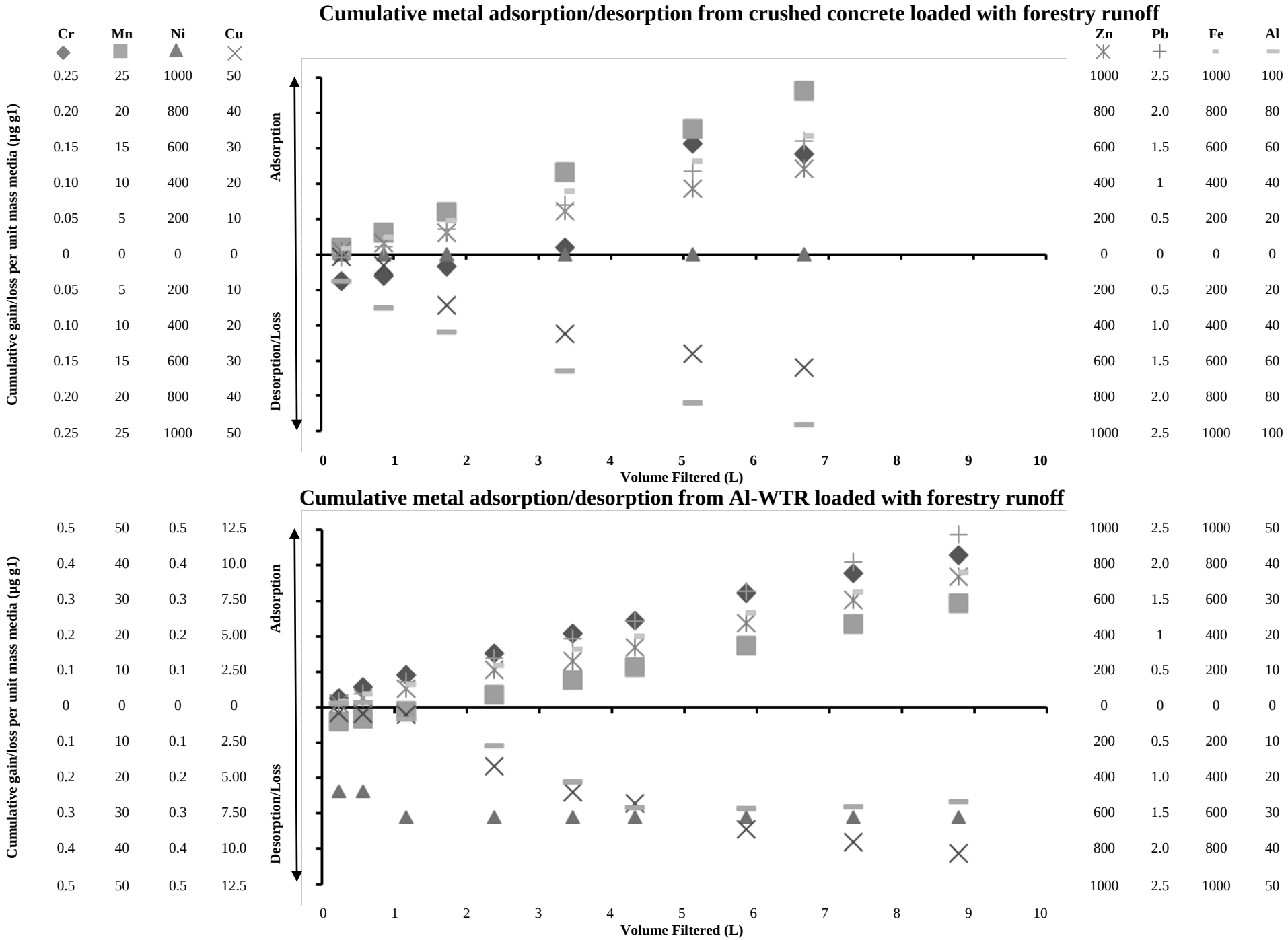

Figure 6.2 (a) Cumulative metal release/uptake by 0.4 m filter columns.

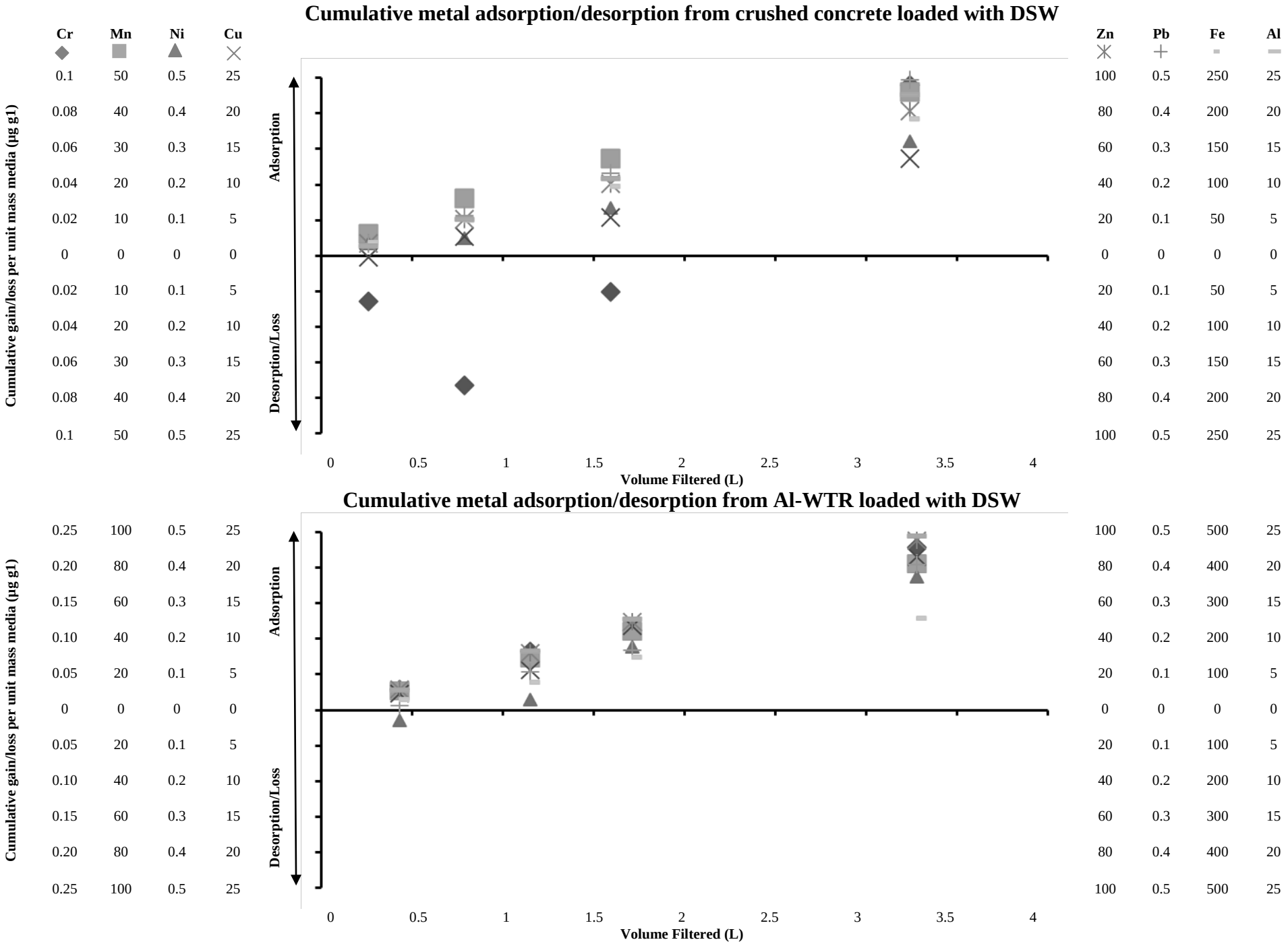

Figure 6.2 (b) Cumulative metal release/uptake by 0.4 m filter columns.

Table 6.1 MPEs obtained fitting Eqn. 9 and Eqn. 11 to small-scale adsorption column data using minimization of the ERRSQ function (Eqn. 14).

	MPE of modelled vs. observed data			
	Forestry Runoff		DSW	
	Concrete	Al-WTR	Concrete	Al-WTR
Equation 9	**1.02%**	-14.77%	4.01%	-4.09%
Equation 11	-5.24%	**-4.03%**	**-0.27%**	**-2.69%**

Values in bold indicate lowest MPE

Table 6.2 Cumulative release of metals from 0.4m filter columns.

		Cumulative metals release (µg g^{-1} filter media)								
		Cr	Mn	Ni	Cu	Zn	Cd	Pb	Fe	Al
FOR	CC	-	-	-	31.90	-	-	-	-	96.17
	Al-WTR	-	-	0.16	5.25	-	-	-	-	13.63
DSW	CC	-	-	-	-	-	-	-	-	-
	Al-WTR	-	-	-	-	-	-	-	-	-

Table 6.3 Maximum observed metal concentrations in filter effluents from 0.4m columns.

		Maximum filter influent and effluent concentrations (µg L^{-1})								
		Cr	Mn	Ni	Cu	Zn	Cd	Pb	Fe	Al
Forestry Runoff	Influent	2.14	96.37	0.00	30.26	1888.02	0.00	7.05	3230	194
	CC	**5.60**	9.72	0.00	**356.84**	43.76	0.00	**10.96**	829	**1560**
	Al-WTR	1.42	**432.14**	**20.25**	**93.45**	921.24	0.00	1.47	1630	**389**
DSW	Influent	3.36	671.74	11	326.66	825.05	0.00	5.49	2690	241
	CC	**5.82**	382.83	10.3	**344.31**	193.15	0.00	2.12	1220	109
	Al-WTR	2.26	169.69	**12.35**	229.19	242.58	0.00	4.89	1270	102

Values in bold indicate elevated effluent

6.3.3 Filter effluent pH

Differences between filter influents and effluents were more pronounced for filters treating forestry runoff compared to filters treating DSW (Figure 6.3). This was unsurprising, as the forestry runoff was collected from a blanket peat catchment in an area which is known to have surface waters with low alkalinity and poor buffering capacities (Johnson et al., 2008). Crushed concrete initially raised the pH of the forestry runoff from an average of 6.62±0.11 to a maximum value of 11.18. The magnitude of this increase in pH depended greatly on the contact time between the runoff and the CC, with shorter columns showing lesser elevations and a quicker leveling off of pH values. After the full duration of filter loading had elapsed, the effluent from the 0.1 m, 0.2 m and 0.3 m filter columns had dropped below the upper recommended surface water environmental quality pH standard (EQS) (EPA, 2001) of 9, and the pH of the effluent from the 0.4 m column was only slightly above this level. This indicates that approximately 240 bed volumes of wastewater had to pass through the crushed concrete filter media prior to pH reaching acceptable levels (pH≤9); this requirement may preclude its use in the treatment of forestry runoff.

Al-WTR, by comparison, had a much smaller impact on the pH of the forestry runoff. Filter effluents showed an initial decrease in pH compared to that of the filter influent, with a minimum pH of 5.45 observed - slightly below the lower recommended surface water pH EQS of 6 (EPA, 2001). The contact time between the Al-WTR and the forestry runoff had a much less marked effect on observed changes in pH and, excluding the pH measurements from the first effluent aliquots, the effluent from all columns quickly stabilized to an average pH of 7.31±0.36.

When treating DSW, effluent from both crushed concrete and Al-WTR stabilized very quickly at pHs of 8.00±0.10 and 7.87±0.23, respectively (excluding the pH values from the first aliquot). All effluent from filters treating DSW was within the recommended surface water EQS range of 6 to 9.

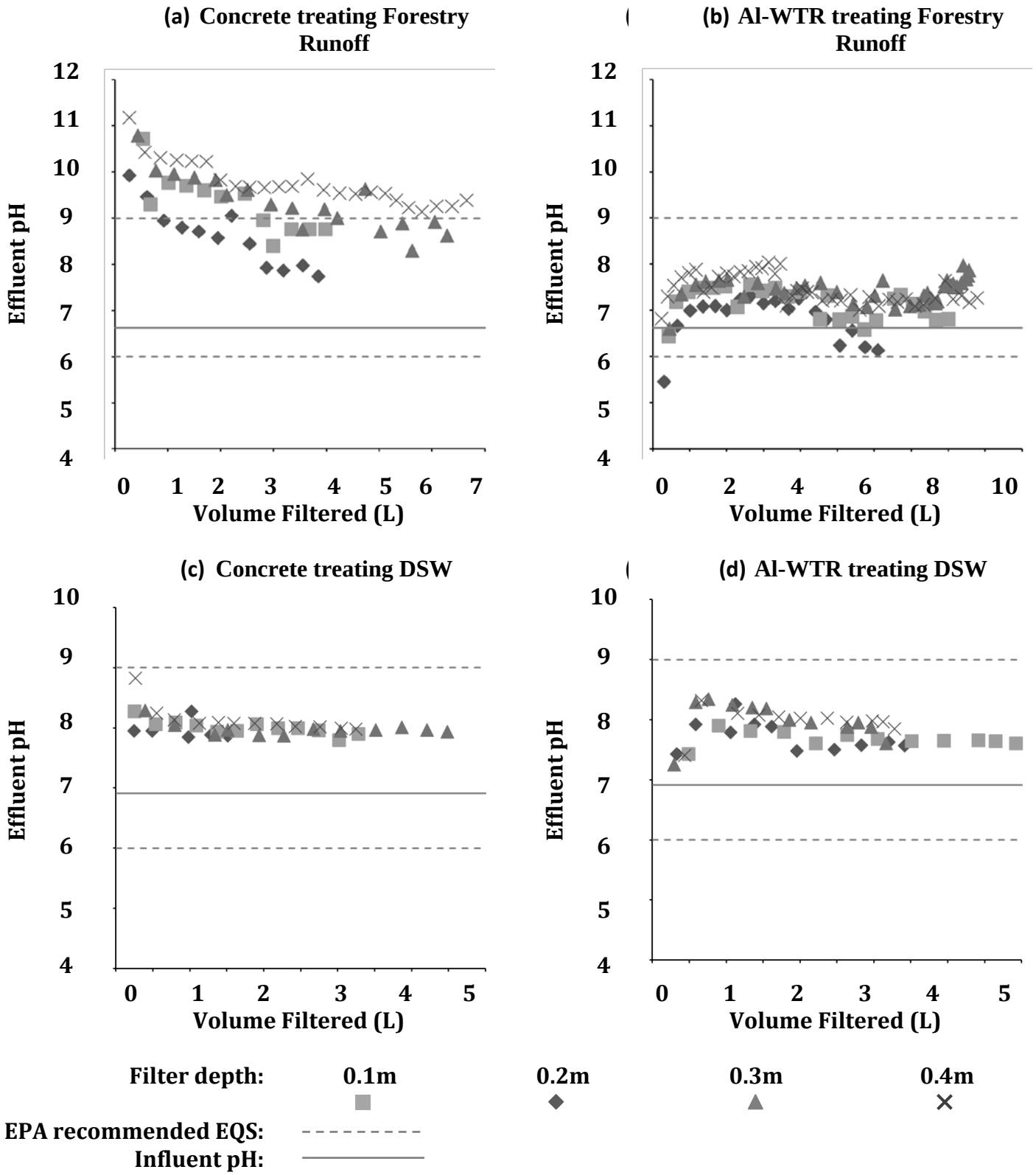

Figure 6.3 Filter column influent and effluent pH and their relationship to EPA recommended environmental quality standards (EPA 2001).

6.3.4 Potential for use in full-scale filters

Figure 6.4 shows indicative lifespans of full-scale filters to a breakthrough concentration of 10% filter influent concentration; these were prepared using Eqns. 5 and 12, depending on which best modeled media performance in the small-scale column tests. The charts show design curves for filters of bed depths ranging from 0.5 m to 2 m, although curves for intermediate bed depths may be interpolated, if desired. The purpose of these charts is to give the user the ability to roughly estimate media longevity and filter performance over the course of a hypothetical filter's lifespan, thus aiding with the decision of proceeding to field-scale trials. As would be expected, the charts indicated that increases in filter depth could be expected to result in increases in filter life span. The high P adsorption affinity of CC led to greater adsorption at low concentrations, meaning CC filters would, in theory, have a longer lifespan when treating forestry runoff.

In general, lower loading rates could be expected to result in longer filter lifespans due to increased EBCTs, allowing for more complete treatment. The high adsorption affinity of CC led to rapid adsorption of P, implying that the HLR applied to CC filters was of less importance in determining filter lifespan. This is evidenced in the less pronounced curvature of the lifespan curves for CC in relation to HLR (Figure 6.4d). Similarly, the high concentration of DSW drove more rapid adsorption of P by Al-WTR, as shown by the less pronounced curvature of the lifespan curves in Figure 6.4d.

As evident from comparison of Figure 6.4c and Figure 6.4d, the lifespans of filters utilizing Al-WTR to treat DSW could be expected to be much greater than those of filters containing CC. This indicates that field-scale testing of Al-WTR could be expected to yield much better results than field-scale testing of CC.

Characterization methodologies like the one described in this paper are a critical first step in evaluating novel P-sorbing materials; however, subsequent full-scale in-field testing is still critical to investigate potential issues concomitant with in-field use, e.g. the formation of preferential flow pathways, surface clogging, effects of animal activity and vegetation etc. (Buda et al., 2012).

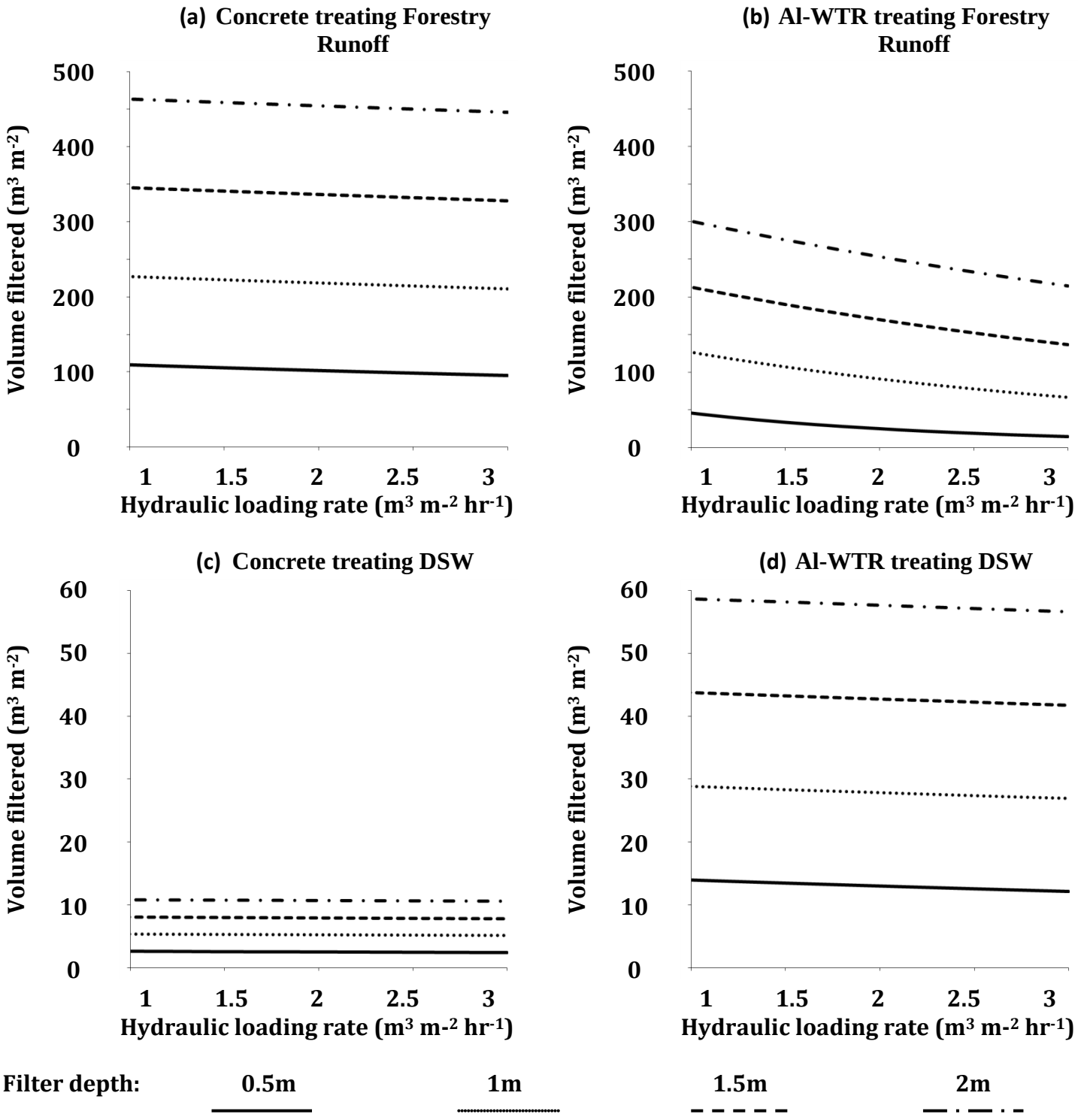

Figure 6.4 Indicative full-scale filter lifespan to effluent breakthrough concentration of 10% filter influent concentration for filter-beds of various depths subject to HLRs of 1-3 m hr^{-1}.

6.4 Conclusions

Crushed concrete and aluminum water treatment residual (Al-WTR) were investigated as potential filter media for use in filters intended to remove dissolved phosphorus from forestry runoff and dairy soiled water (DSW). The primary study findings were as follows:

- The adsorptive performance of small-scale adsorption columns could be described with great accuracy using two recently developed models.
- Model extrapolations to full-scale filters imply that, for a treatment standard of 90% phosphorus removal,
  - both crushed concrete and Al-WTR show promise for the treatment of forestry runoff, though crushed concrete may have slightly greater longevity as a filter media due to its higher phosphorus adsorption affinity at low concentrations;
  - for the treatment of DSW, filters containing Al-WTR would, due to its higher phosphorus adsorption capacity, likely have much greater longevity than filters containing crushed concrete.
- When utilized in small-scale filters, crushed concrete and Al-WTR both released small quantities of aluminum and copper when filtering forestry runoff; filters containing Al-WTR also released a small amount of nickel. There was no cumulative metal loss from either media when filtering DSW.
- The pH of effluents from small-scale filters utilizing crushed concrete to treat forestry runoff were above recommended EPA environmental quality standards, and this may preclude the use of crushed concrete in a peat forestry environment.

6.5 Acknowledgement

The first author would like to acknowledge the Irish Research Council (GOIPG/2013/75) for funding.

6.6 References

Acreman, M., 2012. The Hydrology of the UK: A Study of Change. Routledge.

Ahmad, A.A., Hameed, B.H., 2010. Fixed-bed adsorption of reactive azo dye onto granular activated carbon prepared from waste. J. Hazard. Mater. 175, 298–303. doi:10.1016/j.jhazmat.2009.10.003

Ali, I., Gupta, V.K., 2007. Advances in water treatment by adsorption technology. Nat. Protoc. 1, 2661–2667. doi:10.1038/nprot.2006.370

Babatunde, A.O., Zhao, Y.Q., Burke, A.M., Morris, M.A., Hanrahan, J.P., 2009. Characterization of aluminium-based water treatment residual for potential phosphorus removal in engineered wetlands. Environ. Pollut. 157, 2830–2836. doi:10.1016/j.envpol.2009.04.016

Baker, M.J., Blowes, D.W., Placek, C.J., 1997. Phosphorous adsorption and precipitation in a permeable reactive wall: applications for wastewater disposal systems. USDOE, Washington, DC (United States).

Baker, M.J., Blowes, D.W., Ptacek, C.J., 1998. Laboratory Development of Permeable Reactive Mixtures for the Removal of Phosphorus from Onsite Wastewater Disposal Systems. Environ. Sci. Technol. 32, 2308–2316. doi:10.1021/es970934w

Blomqvist, S., Gunnars, A., Elmgren, R., 2004. Why the limiting nutrient differs between temperate coastal seas and freshwater lakes: A matter of salt. Limnol. Oceanogr. 49, 2236–2241. doi:10.4319/lo.2004.49.6.2236

Bohart, G.S., Adams, E.Q., 1920. Some Aspects of the Behavior of Charcoal with Respect to Chlorine. 1. J. Am. Chem. Soc. 42, 523–544. doi:10.1021/ja01448a018

Bowden, L.I., Jarvis, A.P., Younger, P.L., Johnson, K.L., 2009. Phosphorus Removal from Waste Waters Using Basic Oxygen Steel Slag. Environ. Sci. Technol. 43, 2476–2481. doi:10.1021/es801626d

Buda, A.R., Koopmans, G.F., Bryant, R.B., Chardon, W.J., 2012. Emerging Technologies for Removing Nonpoint Phosphorus from Surface Water and Groundwater: Introduction. J. Environ. Qual. 41, 621–627. doi:10.2134/jeq2012.0080

Callery, O., Brennan, R.B., Healy, M.G., 2015. Use of amendments in a peat soil to reduce phosphorus losses from forestry operations. Ecol. Eng. 85, 193–200. doi:10.1016/j.ecoleng.2015.10.016

Callery, O., Healy, M.G., 2017. Predicting the propagation of concentration and saturation fronts in fixed-bed filters. Water Res. 123, 556–568. doi:10.1016/j.watres.2017.07.010

Callery, O., Healy, M.G., Rognard, F., Barthelemy, L., Brennan, R.B., 2016. Evaluating the long-term performance of low-cost adsorbents using small-scale adsorption column experiments. Water Res. 101, 429–440. doi:10.1016/j.watres.2016.05.093

Chowdhury, Z.K., 2013. Activated Carbon: Solutions for Improving Water Quality. American Water Works Association.

Correll, D.L., 1999. Phosphorus: a rate limiting nutrient in surface waters. Poult. Sci. 78, 674–682.

Cucarella, V., Renman, G., 2009. Phosphorus Sorption Capacity of Filter Materials Used for On-site Wastewater Treatment Determined in Batch Experiments-A Comparative Study. J. Environ. Qual. 38, 381–392. doi:10.2134/jeq2008.0192

de-Bashan, L.E., Bashan, Y., 2004. Recent advances in removing phosphorus from wastewater and its future use as fertilizer (1997–2003). Water Res. 38, 4222–4246. doi:10.1016/j.watres.2004.07.014

Drizo, A., Comeau, Y., Forget, C., Chapuis, R.P., 2002. Phosphorus saturation potential: A parameter for estimating the longevity of constructed wetland systems. Environ. Sci. Technol. 36, 4642–4648.

Dunne, E.J., Culleton, N., O'Donovan, G., Harrington, R., Olsen, A.E., 2005. An integrated constructed wetland to treat contaminants and nutrients from dairy farmyard dirty water. Ecol. Eng. 24, 219–232. doi:10.1016/j.ecoleng.2004.11.010

Eaton, A.D., Clesceri, L.S., Greenberg, A.E., Franson, M.A.H., American Public Health Association., American Water Works Association., Water Environment Federation., 1998. Standard methods for the examination of water and wastewater. American Public Health Association, Washington, DC.

Egemose, S., Sønderup, M.J., Beinthin, M.V., Reitzel, K., Hoffmann, C.C., Flindt, M.R., 2012. Crushed concrete as a phosphate binding material: A potential new management tool. J. Environ. Qual. 41, 647–653.

EPA, 2001. Parameters of Water Quality: Interpretation and Standards.

Erickson, A.J., Gulliver, J.S., Weiss, P.T., 2012. Capturing phosphates with iron enhanced sand filtration. Water Res. 46, 3032–3042. doi:10.1016/j.watres.2012.03.009

Guo, W.J., Zhao, L.Y., Zhao, W.H., Li, Q.Y., Wu, Z.B., 2017. Phosphorus Sorption Capacities of Steel Slag in Pilot-Scale Constructed Wetlands for Treating Urban Runoff: Saturation Potential and Longevity. IOP Conf. Ser. Earth Environ. Sci. 51, 012021. doi:10.1088/1742-6596/51/1/012021

Heal, K., Younger, P.L., Smith, K., Glendinning, S., Quinn, P., Dobbie, K., 2003. Novel use of ochre from mine water treatment plants to reduce point and diffuse phosphorus pollution. Land Contam. Reclam. 11, 145–152.

Hilton, J., O'Hare, M., Bowes, M.J., Jones, J.I., 2006. How green is my river? A new paradigm of eutrophication in rivers. Sci. Total Environ., Monitoring and modelling the impacts of global change on European freshwater ecosystems 365, 66–83. doi:10.1016/j.scitotenv.2006.02.055

Hinz, C., 2001. Description of sorption data with isotherm equations. Geoderma 99, 225–243. doi:10.1016/S0016-7061(00)00071-9

Johnson, J., Farrell, E., Baars, J.-R., Cruikshanks, R., Matson, R., Kelly-Quinn, M., 2008. Literature review: Forests and surface water acidification. Water Framew. Dir. West. River Basin Dist.

Netpradit, S., Thiravetyan, P., Towprayoon, S., 2004. Evaluation of metal hydroxide sludge for reactive dye adsorption in a fixed-bed column system. Water Res. 38, 71–78. doi:10.1016/j.watres.2003.09.007

Penn, C.J., Bryant, R.B., Kleinman, P.J.A., Allen, A.L., 2007. Removing dissolved phosphorus from drainage ditch water with phosphorus sorbing materials. J. Soil Water Conserv. 62, 269–276.

Penn, C.J., McGrath, J.M., 2011. Predicting phosphorus sorption onto steel slag using a flow-through approach with application to a pilot scale system. J. Water Resour. Prot. 3, 235.

Pratt, C., Shilton, A., 2009. Suitability of adsorption isotherms for predicting the retention capacity of active slag filters removing phosphorus from wastewater. Water Sci. Technol. 59, 1673–1678. doi:10.2166/wst.2009.163

Rao, N.S., Easton, Z.M., Schneiderman, E.M., Zion, M.S., Lee, D.R., Steenhuis, T.S., 2009. Modeling watershed-scale effectiveness of agricultural best management practices to reduce phosphorus loading. J. Environ. Manage. 90, 1385–1395. doi:10.1016/j.jenvman.2008.08.011

Razali, M., Zhao, Y.Q., Bruen, M., 2007. Effectiveness of a drinking-water treatment sludge in removing different phosphorus species from aqueous solution. Sep. Purif. Technol. 55, 300–306.

Rodgers, M., O'Connor, M., Healy, M.G., O'Driscoll, C., Asam, Z.-Z., Nieminen, M., Poole, R., Müller, M., Xiao, L., 2010. Phosphorus release from forest harvesting on an upland blanket peat catchment. For. Ecol. Manag. 260, 2241–2248.

Ruane, E.M., Murphy, P.N.C., Healy, M.G., French, P., Rodgers, M., 2011. On-farm treatment of dairy soiled water using aerobic woodchip filters. Water Res. 45, 6668–6676. doi:10.1016/j.watres.2011.09.055

Schindler, D.W., Carpenter, S.R., Chapra, S.C., Hecky, R.E., Orihel, D.M., 2016. Reducing Phosphorus to Curb Lake Eutrophication is a Success. Environ. Sci. Technol. 50, 8923–8929. doi:10.1021/acs.est.6b02204

Schindler, D.W., Hecky, R.E., Findlay, D.L., Stainton, M.P., Parker, B.R., Paterson, M.J., Beaty, K.G., Lyng, M., Kasian, S.E.M., 2008. Eutrophication of lakes cannot be controlled by reducing nitrogen input: Results of a 37-year whole-ecosystem experiment. Proc. Natl. Acad. Sci. 105, 11254–11258. doi:10.1073/pnas.0805108105

Schoumans, O.F., Chardon, W.J., Bechmann, M.E., Gascuel-Odoux, C., Hofman, G., Kronvang, B., Rubæk, G.H., Ulén, B., Dorioz, J.-M., 2014. Mitigation options to reduce phosphorus losses from the agricultural sector and improve surface water quality: A review. Sci. Total Environ. 468, 1255–1266. doi:10.1016/j.scitotenv.2013.08.061

Seo, D.C., Cho, J.S., Lee, H.J., Heo, J.S., 2005. Phosphorus retention capacity of filter media for estimating the longevity of constructed wetland. Water Res. 39, 2445–2457. doi:10.1016/j.watres.2005.04.032

Sharpley, A.N., Daniel, T., Sims, T., Lemunyon, J., Stevens, R., Parry, R., 2003. Agricultural phosphorus and eutrophication. US Dep. Agric. Agric. Res. Serv. ARS–149 44.

Shiue, A., Den, W., Kang, Y.-H., Hu, S.-C., Jou, G., Lin, C.H., Hu, V., Lin, S.I., 2011. Validation and application of adsorption breakthrough models for the chemical filters used in the make-up air unit (MAU) of a cleanroom. Build. Environ. 46, 468–477. doi:10.1016/j.buildenv.2010.08.010

Søvik, A.K., Kløve, B., 2005. Phosphorus retention processes in shell sand filter systems treating municipal wastewater. Ecol. Eng. 25, 168–182. doi:10.1016/j.ecoleng.2005.04.007

Spellman, F.R., 2013. Handbook of Water and Wastewater Treatment Plant Operations, Third Edition. CRC Press.

Stout, W.L., Sharpley, A.N., Landa, J., 2000. Effectiveness of coal combustion by-products in controlling phosphorus export from soils. J. Environ. Qual. 29, 1239–1244.

U. S. Environmental Protection Agency, 2007. Method 6020A Revision 1: Inductively Coupled Plasma-Mass Spectrometry. Method 6020A Revis. 1 Inductively Coupled Plasma-Mass Spectrom.

Velghe, I., Carleer, R., Yperman, J., Schreurs, S., D'Haen, J., 2012. Characterisation of adsorbents prepared by pyrolysis of sludge and sludge/disposal filter cake mix. Water Res. 46, 2783–2794. doi:10.1016/j.watres.2012.02.034

Vohla, C., PÕLDVERE, E., NOORVEE, A., KUUSEMETS, V., MANDER, Ü., 2005. Alternative Filter Media for Phosphorous Removal in a Horizontal Subsurface Flow Constructed Wetland. J. Environ. Sci. Health Part A 40, 1251–1264. doi:10.1081/ESE-200055677

Chapter 7 - Conclusions and Recommendations

7.1 Overview and context

Because of the complex and unique interactions between adsorbents and a given wastewater, there is a need to investigate each adsorbent-wastewater system on an individual basis. Though low-cost adsorbents have shown great promise at removing phosphorus (P) from a variety of point and nonpoint source wastewaters, their potential to reduce P losses associated with clearfelling of peatland forestry has not be explored; this was the first knowledge gap identified in this study. Hence, the first aim of this study was to identify materials which would be effective at removing phosphorus (P) from peatland forestry runoff, using a wastewater which replicated the chemistry of such runoff by having peat soil incorporated into the solution. To achieve this aim, the interaction between peat and six potential materials was examined. The materials used were (1) aluminium water treatment residual (Al-WTR) (2) crushed concrete (3) gypsum (4) magnesium hydroxide $Mg(OH)_2$ (5) magnesium oxide (MgO), and (6) steel wool. The results of these investigations are presented in **Chapter 3**. The first study aim was addressed by the key findings of this chapter, which were that the presence of peat in solution enhanced the ability of Al-WTR and steel wool to remove P from solution at low concentrations, i.e. those most pertinent to low-concentration forestry runoff, and when the ratio of amendment to peat in solution was high (1:2), P removal by crushed concrete was largely unaffected; at ratios of 1:4 and 1:10, P removal by crushed concrete decreased. Peat had a negative impact on the P removal ability of gypsum, and also $Mg(OH)_2$ at an amendment to peat ratio of 1:10, though at ratios of 1:4 and 1:2 P removal by $Mg(OH)_2$ improved. Any improved removal by $Mg(OH)_2$ was offset, however, by significant increases in solution pH, and final solution pHs of approximately 10-10.5 were observed. Phosphorus removal by MgO was largely unaffected by the presence of peat; however, at all amendment to peat ratios, MgO also raised the solution pH to approximately 11.5, indicating that the peat had little ability to buffer the solution against the influence of either $Mg(OH)_2$ or MgO on pH.

In the context of their in-field use, these results indicate that gypsum would be a poor choice of P sorbing soil amendment in a peat environment due to the negative effect of peat on gypsum's ability to remove P. The results also indicate that, were they to be used as soil amendments, MgO and $Mg(OH)_2$ would increase the pH the soil to an unacceptable degree (>9), and, in the case of $Mg(OH)_2$ at least, effective P removal appeared to be predicated on

this change of soil/solution pH. In contrast, the ability of Al-WTR and steel wool to remove P was increased by the presence of peat in solution, with neither having an unacceptable effect on the solution pH (final pH <9). The results of tests with crushed concrete were somewhat inconclusive, as the ratio of peat to amendment in solution played an important role in crushed concrete's ability to remove P. At high amendment to peat ratios, crushed concrete's removal of P was unhindered by the presence of peat, and its effect on solution pH (final pH of approximately 8) would not preclude its in-field use. Although these batch experiments provide valuable insight into the interaction between these P sorbing materials, they could not provide estimates of in-field media longevity.

To address the question of media longevity, a follow-on study was conducted using small- and large-scale filter column experiments. Current rapid small-scale column test (RSSCT) methodologies are often unsuitable for use with low-cost adsorbents which are highly variable in terms of physical and chemical makeup, hence the second knowledge gap identified by this study was that there is a need for RSSCT methodologies which can (1) be applied to highly variable low-cost materials and (2) yield similarly useful results to large-scale column studies. The second aim of this study was therefore to develop such a methodology and demonstrate that the results from these tests were equivalent to those obtained from long-term, large-scale columns tests. **Chapter 4** addresses this aim, and the key findings of the chapter were that rapid small-scale column studies could indeed be excellent predictors of large-scale filter performance. Small-scale experiments had numerous advantages over large-scale experiments in terms of the timeframe in which results could be obtained and the materials and labour required to perform the necessary investigations. Furthermore, a mathematical model, which allowed for the prediction of small- and large-scale column media saturation, was presented in **Chapter 4**, and this further increased the speed at which estimations of media longevity could be obtained, as it made it unnecessary to operate filters to complete saturation to estimate lifespan. Initial small-scale filter tests with steel wool identified a critical limitation to its application in flow-through scenarios, as accumulation of iron oxides and hydroxides in the columns rapidly caused filter clogging and rendered it unusable as a filter media. Ferric drinking water treatment residual (Fe-WTR) was therefore substituted as an iron based adsorbent, but its comparatively poor performance in small-scale columns, as detailed in **Chapter 4**, eliminated it from consideration in large-scale filters.

The main practical implications of these findings relate to the speed at which an initial media assessment could be completed. Large-scale column studies can take weeks, months, or even years to complete, and this has resulted in an over-reliance by researchers on fast and convenient batch tests. As detailed in **Chapter 3**, these batch studies are an invaluable aid to media selection; however, the general consensus of the research community is that the results of these tests are an insufficient basis for the estimation of media longevity. Though it had been demonstrated that rapid small-scale tests were effective for this purpose, or at least as effective as large-scale column tests, there was still the major limitation that individual small-scale tests would be required to predict the performance of individual large-scale filters. This potentially necessitates large amounts of experimentation, which, to some degree, lessens the appeal of the methodology developed in **Chapter 4**. This limitation highlighted the need for a mathematical modelling approach which could expand the usefulness of the small-scale flow-through experiments to the point that it was possible to predict the performance of any large-scale filter subject to any reasonable loading. This was the third knowledge gap identified by this study.

Therefore, the third aim of this study was to develop a mathematical modelling approach to expand the usefulness of small-scale filter experiments to enable performance predictions of any large-scale filter column to be made. This aim was addressed as detailed in **Chapter 5**. In this chapter, a modelling approach was developed which related the pore concentrations and media saturation within a filter column to both the volume of wastewater filtered through the column, and the loading rate at which that wastewater was applied to the column. The model uses results from multiple small-scale column experiments to determine model coefficients which allow for the full description and prediction of the performances of filters of any size. To validate the model, it was fit to a number of independent data sets, and was found to successfully describe these data (see **Chapter 5**).

In **Chapters 4 and 5**, a synthetic wastewater was used to demonstrate the relationship between small- and large-scale filter columns. This was an unavoidable necessity as the large-scale column tests required thousands of litres of influent, and the regular collection of such large volumes of wastewater from site was not practicable. The media which had shown greatest promise, i.e. Al-WTR and crushed concrete, therefore needed to be assessed with the aid of the modelling approach developed in **Chapter 5,** but using real wastewater. As had been demonstrated in **Chapter 32**, the relationship between a material's ability to remove P

from solution was highly dependent on the unique interactions between a given wastewater and filter media. The fourth knowledge gap identified by this study was therefore that there was a need to perform flow-through experiments with real wastewater to both (1) assess the longevity of the media and (2) determine if there is a risk of a pollution-swapping effect associated with their in-field use - i.e. the possibility that the materials might have some polluting effect on the environment through the release of metals or an unacceptable filter effluent pH.

The fourth aim of this study was to address this knowledge gap by using the RSSCT and modelling approaches developed in **Chapters 4 and 5** to assess the potential of Al-WTR and crushed concrete for uses in the treatment of forestry runoff. This aim was addressed in **Chapter 6.** The findings of **Chapter 6** confirmed that Al-WTR was successful in removing P from forestry runoff and furthermore demonstrated that it also held great promise for the treatment of dairy-soiled water (DSW), a wastewater with a P concentration approximately 30 times that of peatland forestry runoff. The pollution swapping potential of Al-WTR did not preclude its usefulness for either application. When used to treat forestry runoff, the effluents from filters containing crushed concrete were deemed to have an unacceptably high pH; the potential of this being an issue had been raised in **Chapter 3**, though batch results were inconclusive. It was also indicated that, for the treatment of DSW, filters containing crushed concrete would have a significantly lower useful lifespan than those containing Al-WTR, and for these reasons, studies using pilot-scale in-field filters for the treatment of either wastewater were not recommended in the case of crushed concrete.

7.2 Conclusions

The main study conclusions are as follows:

- Small- and large-scale laboratory filter studies demonstrated that Al-WTR was effective at removing P from synthetic wastewater, and the results of initial batch tests indicated that the material's P sorption capacity may actually be increased in a peat soil environment (**Chapter 3**). This suggested that Al-WTR would perform well as a P-sorbing peat soil amendment or as media in filters treating peatland forestry runoff, a hypothesis which was confirmed using small-scale adsorption columns, which were loaded with runoff from a recently clearfelled stand of coniferous peatland forestry (**Chapter 6**). Al-WTR's usefulness was found not to be limited to the removal of P

from forestry runoff, and the results of small-scale column tests indicated that it also shows promise for the treatment of DSW, a point source wastewater containing P concentrations that are orders of magnitude greater than those found in peatland forestry runoff (**Chapter 6**). Furthermore, these small-scale column tests indicated that there was no significant impediments to the use of Al-WTR for the treatment of either wastewater, as any release of metals was very small and occurred only in the 'first flush' through the filter; this issue may be resolved by washing the media prior to its placement in pilot-scale in-field filters. Furthermore, Al-WTR also removed various metals from both the forestry runoff and the DSW, further highlighting the potential for its usefulness for applications beyond the scope of this research.

- It was demonstrated that rapid small-scale column tests could be used to evaluate the performance of potential phosphorus sorbing filter media with equal efficacy to long-term large-scale column tests (**Chapter 4**). Moreover, small-scale tests had numerous advantages compared to large-scale tests in that they (1) required smaller quantities of media and wastewater (2) produced results in 24 to 36 hours (3) had much lower material costs for apparatus (4) required less sample analysis, resulting in reductions in cost and labour (5) were largely automated, further reducing labour requirements, and (6) had a much smaller footprint in the laboratory.

- With the aid of novel mathematical modelling techniques, the results of small-scale column tests can be used to predict the propagation of saturation and concentration fronts in large-scale filters with a high degree of accuracy. This potentially allows researchers to predict the long-term performances of large-scale filters of any size subjected to any loading using a methodology that takes no longer than commonly used batch adsorption tests (**Chapter 5**), which, by comparison, cannot provide insight into potential media longevity.

- The modelling strategies used in **Chapter 5** were found to be applicable to a number of independent data sets, suggesting that the experimental and modelling methodologies developed in **Chapter 5** are not only applicable to P removal, but can also describe the treatment of wastewaters containing contaminants such as metals, dyes, and other pollutants such as arsenic and fluoride.

7.3 Recommendations

The experiments carried out in this study are intended as a rapid means of assessing the in-field potential of filter media. They were performed under controlled laboratory conditions necessary for accurate modelling media performance. In-field conditions are highly variable, and in-field filters would be subjected to variations in volumetric loading, influent wastewater concentration, and a host of other external influences, including the effects of weathering, biological activity and sediment loads. The recommendations arising from this project may be summarised as follows:

- Because of the positive results obtained from laboratory-scale tests, in-field pilot-scale filters containing Al-WTR should be investigated for their potential to treat peatland forestry runoff.

- Because of the positive results observed at laboratory-scale when using Al-WTR to treat DSW, it is recommended that in-field pilot-scale filters be tested for the treatment of DSW and other P-rich wastewaters.

- Phosphorus is a valuable and limited resource. The third recommendation of this study is therefore that the possibility of recovering P from the spent media should be evaluated.

- Whether or not the P in the saturated media can be recovered, the fourth recommendation of this study is that an environmentally benign end-of-life use be found for the spent filter media. This may potentially be found in the recovery of P from the media, resulting in its rejuvenation for further use as a filter media.

- Closely linked to this fourth recommendation, the fifth recommendation of this study is that life-cycle analyses be performed on the use of Al-WTR for the treatment of various wastewaters to assess whether these applications are economically feasible.

Appendix A

Ecological Engineering 85 (2015) 193–200

Contents lists available at ScienceDirect

Ecological Engineering

journal homepage: www.elsevier.com/locate/ecoleng

Use of amendments in a peat soil to reduce phosphorus losses from forestry operations

O. Callery, R.B. Brennan*, M.G. Healy

Civil Engineering, National University of Ireland, Galway, Co. Galway, Ireland

ARTICLE INFO

Article history:
Received 19 March 2015
Received in revised form 6 October 2015
Accepted 7 October 2015
Available online 18 October 2015

Keywords:
Phosphorus
Forestry
Peat
Clearfelling
Harvesting
Buffer zones
Adsorption

ABSTRACT

Forestry harvesting on peats is known to result in significant losses of soil phosphorus (P) to adjacent waters, and the issue is becoming an increasingly serious concern as peatland forest stocks mature and reach harvestable age. One potential solution could be the use of low-cost P recovery techniques based on the chemical precipitation and/or adsorption of the dissolved fraction of soil P, which would otherwise be lost. Such recovery techniques have shown promise in similar applications on mineral soils. However, the interaction of peat with P adsorbing materials can significantly alter their adsorptive characteristics, and it is consequentially not known what materials might be suitable for this application. This study compared the performance of six potential soil amendments (aluminum water treatment residual (Al-WTR), crushed concrete, gypsum, magnesium hydroxide, magnesium oxide, and steel wool) in removing P from aqueous solution in the presence of a typical forest peat soil. Comparison of adsorption isotherms plotted from these batch adsorption studies showed that the observed P adsorption maxima of Al-WTR and steel wool were increased by the presence of peat, from 10.6 mg g^{-1} and 20.4 mg g^{-1}, to 11.8 mg g^{-1} and 52.5 mg g^{-1}, respectively. In contrast, the observed P adsorption maxima of crushed concrete, gypsum, and magnesium oxide were reduced in the presence of peat, by 44%, 87%, and 37%, respectively. The maximum P adsorption achieved by magnesium hydroxide was increased from 29.8 mg g^{-1} to 59 mg g^{-1} at an amendment to peat–solid ratio of 1:4, but decreased from 73.9 mg g^{-1} to 23.6 mg g^{-1} at an amendment to peat–solid ratio of 1:10. It was concluded that Al-WTR, in particular, shows considerable promise for use as a soil amendment for P immobilization in a peat environment.

1. Introduction

Ireland's forestry stock of 731,000 ha covers about 10.5% of the country, of which 44% is planted on peats (National Forest Inventory, 2012). Peats, especially ombrotrophic upland blanket peats, are generally lacking in minerals like aluminum (Al) and iron (Fe), and consequently have extremely low soil phosphorus (P) sorption capacities (Renou et al., 2000). As a result, any P released by the forestry operations, such as clearfelling and afforestation, is liable to leach unimpeded into adjacent receiving waters, even with the application of current best management practices targeted at preventing such pollution (Finnegan et al., 2014).

Nutrient enrichment, or eutrophication, of inland waters is recognized as Ireland's most serious environmental pollution problem (Department of the Environment, 2002). As P has been identified as the primary nutrient limiting eutrophication in freshwaters (Carpenter et al., 1998; Boesch et al., 2001), preventing its migration from soil to aquatic environments is paramount. The oligotrophic nature of Ireland's upland catchments, and the unique flora and fauna present in these waters, make them particularly sensitive to eutrophication (Mainstone and Parr, 2002; Hutton et al., 2008). These forested peat catchments are headwaters for many of Ireland's river systems, a great number of which contain important salmonid populations (Giller and O'Halloran, 2004), as well as other species protected under European Union (EU) legislation (O'Driscoll et al., 2012; Reid et al., 2013). Consequentially, pollution from diffuse, low concentration sources of P, such as forestry, is capable of causing considerable environmental damage to an area much larger than that which is forested.

The sustained release of P following forestry harvesting has been highlighted as an issue of particular concern, as much of Ireland's current peatland forestry stock was planted between the 1950s and the 1990s (Renou and Farrell, 2005) and has now reached, or is reaching, harvestable age (Rodgers et al., 2010). Clearfelling is the harvesting technique most prevalent in Ireland, and accounted for

Abbreviation: Al-WTR, aluminum water treatment residual.

* Corresponding author.
E-mail address: raymond.brennan@nuigalway.ie (R.B. Brennan).

http://dx.doi.org/10.1016/j.ecoleng.2015.10.016
0925-8574/

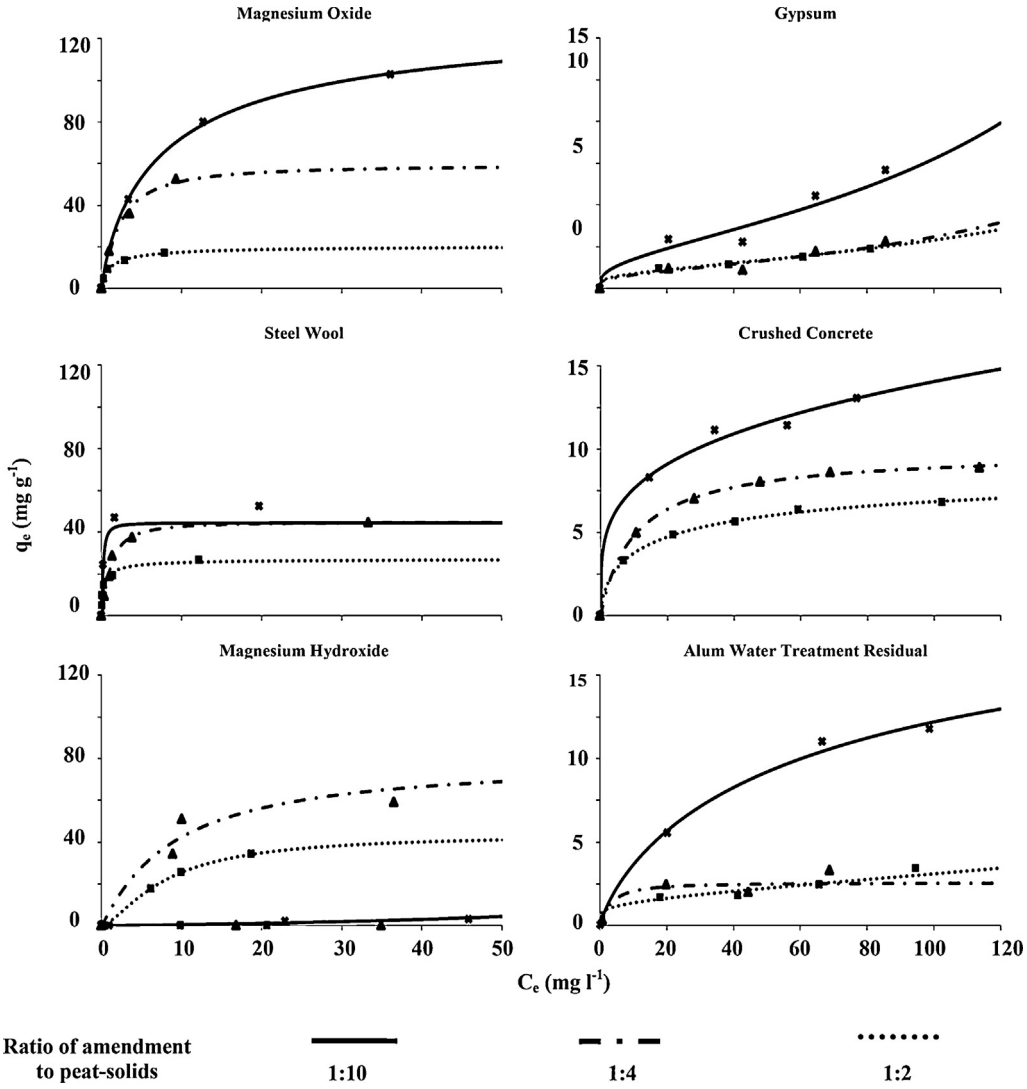

Fig. 1. Best fit Koble–Corrigan adsorption isotherm models derived using non-linear regression methods for (a) magnesium oxide, (b) gypsum, (c) steel wool, (d) crushed concrete, (e) magnesium hydroxide, and (f) Al-WTR, at amendment to peat–solid ratios of 1:10, 1:4, and 1:2.

76.6% of timber felled between 2006 and 2012 (National Forest Inventory, 2012). Clearfelling involves the removal from site of the commercially viable portions of the forestry crop (i.e. tree trunks), leaving large amounts of P to remain onsite, present both in the soil and in the non-commercial logging residues, or 'brash'. This brash accounts for a considerable percentage of the above ground nutrients contained in a typical coniferous tree (Moffat et al., 2006), and it has been shown to release these nutrients for many years following its deposition (Titus and Malcolm, 1999; Hyvönen et al., 2000). To compound the issue, the use of brash mats to form temporary driving surfaces for heavy felling machinery is an essential management practice, as it prevents serious damage to the underlying soil (Moffat et al., 2006). Clearfelling completely disrupts natural P cycling in a forest ecosystem, with the deposition of brash mats resulting in increased P availability, while the concurrent removal of trees from site results in decreased P uptake and sequestration – a situation which greatly increases the threat of P leaching to aquatic ecosystems (Schaller et al., 2015).

While rates of afforestation on blanket peats have been in decline in recent years (National Forest Inventory, 2012), the harvesting of presently established forest is inevitable, as are the resulting water quality issues, if effective pollution mitigation measures are not implemented. Current best management practices advocate the use of riparian buffer strips between forestry and adjacent aquatic zones (Forest Service, 2000). Previous research has found the use of suitably large riparian buffer zones on peat soils to be largely successful in protecting surface waters from influxes of suspended sediments and associated particulate nutrients (Nieminen et al., 2005). However, with peat's low P adsorption capacity, the performance of these buffer zones in satisfactorily mitigating the flow of dissolved P off site varies greatly. Moreover, it has been found that these buffer zones' effect can be anywhere from positive, with total retention of released P (Vaananen et al., 2008), to negative, compounding the issue with additional P release (Vasander et al., 2003; Liljaniemi et al., 2003).

There has been increasing interest in the use of soil amendments to control P losses from diffuse sources, such as land spreading of manure from dairy cattle (Brennan et al., 2011a,b) and pigs (O'Flynn et al., 2012), land spreading of dairy waste water from washing of milking parlors (Serrenho et al., 2012), and construction of wetlands on sites previously used for agriculture (Ann et al., 1999). The use of chemical amendments has shown much promise in these instances, though there has been little to no investigation into the practice's potential in abating the loss of P from peatland forestry.

Table 1
Peat and amendment characteristics.

Material	Total exchange capacity (meq 100 g^{-1})	pH	Organic matter (%)	P[a] (mg kg^{-1})	Bray II P (mg kg^{-1})	Ca[a] (mg kg^{-1})	Mg[a] (mg kg^{-1})	Fe[a] (mg kg^{-1})	Al[a] (mg kg^{-1})
Peat	11.45	3.8	100	5	3	228	142	152	47
Al-WTR	16.78	7	21.62	2	<1	2983	32	154	2159
Gypsum	64.3	8.8	1.85	6	14	11,858	296	111	66
Crushed concrete	145.15	11.7	0.82	<1	<1	27,593	622	405	441
MgO	267.55	10	1.04	<1	<1	2734	29,760	77	<1
$Mg(OH)_2$	247.78	9.8	23.53	<1	<1	739	28,660	57	<1

[a] Mehlich-3 extractable.

The performance of chemical amendments in this context has the potential to be quite different, as the interaction of amendments with the complex chemistry of peat can significantly alter their P removal performance (James et al., 1992).

This study tested the hypothesis that chemical amendments could immobilize P in a forest peat soil. To address this hypothesis, the aim of this study was to identify and compare potential soil amendments which function well in a peat chemistry environment and, when mixed with peat onsite, could increase the adsorptive capacity of the soil to the point where P losses from a forestry site would no longer pose a risk to receiving surface waters. Specifically, the objectives of this study were to: (1) identify chemical amendments capable of removing P from an aqueous solution which mimics the chemistry of runoff/ground water on a forested peat site; (2) compare the performance of each amendment and identify the amendment most ideally suited to application in a forested peat site; (3) analyze the effect of peat on the performance of each amendment in terms of its adsorptive capacity.

2. Materials and methods

2.1. Collection and characterization of peat samples

Samples of blanket peat were collected from a recently clear-felled riparian buffer zone, located near the town of Oughterard, County Galway, Ireland (approx. coordinates 53.375 N, −9.419 E). The peat was collected from a stratum of homogeneous composition, at a depth of 5–25 cm from the surface (the surface layer of vegetation and semi-decayed sphagnum moss was discarded, along with any larger roots and plant fibers). Before testing, the samples were homogenized by repeatedly folding and kneading the peat until its texture and water content were entirely uniform. Once homogenized, peat samples were sealed in airtight Ziploc® bags and stored in a temperature-controlled room at 11 °C until testing commenced. The water content of the homogenized peat was determined to be 89.7% ± 0.08% by oven drying the peat for 24 h at 105 °C (BSI, 1990).

2.2. Sourcing and characterization of amendments

The following amendments were used in this study (Table 1): dewatered aluminum sulphate water treatment residual (Al-WTR; oven dried for 24 h at 105 °C and ground to pass a 0.5 mm sieve), crushed concrete cubes (pulverized with a mortar and pestle and ground to pass a 0.5 mm sieve), gypsum (sourced from recycled plasterboard, supplied as a powder, and passed through a 0.5 mm sieve to ensure uniformity), magnesium oxide (MgO; sourced from seawater, supplied as a powder, and passed through a 0.5 mm sieve to ensure uniformity), magnesium hydroxide ($Mg(OH)_2$; sourced from seawater, supplied as a paste, and passed through a 0.5 mm sieve to ensure uniformity) and steel wool (grade 00, fiber diameter approx. 0.04 mm).

2.3. Batch test procedure

Samples were prepared comprising two grams (wet weight) of the homogenized peat, mixed with each of the six amendments, at amendment to peat–solid ratios of 1:10, 1:4 and 1:2. These masses provided a material to solution ratio that was small enough to ensure non-zero equilibrium concentrations, thus allowing the determination of the entire isotherm curve. The material to solution ratio used in the current study was comparable to ratios used in similar studies (Li et al., 2006; Chardon et al., 2012). The samples were placed in separate 50 ml conical flasks and overlain by 25 ml of deionized water, with ortho-phosphorus (PO_4-P) concentrations (prepared by adding various amounts of K_2HPO_4 to deionized water) of 0, 25, 50, 75, 100, and 150 mg P L^{-1}. This range of P concentrations was determined to be sufficiently wide to account for the variation in the amendments' adsorptive capacities, and the dependence of adsorption capacity on the initial concentration (Seo et al., 2005). The flasks were sealed with Parafilm and shaken in a reciprocal shaker (250 rpm) at room temperature (25 °C) for 24 h. After 24 h had elapsed, the samples were centrifuged at 14,500 rpm for 5 min, and the supernatant water was passed through a 0.45 μm filter. Dissolved P concentrations of the supernatant water were determined using a nutrient analyzer (Konelab 20, Thermo Clinical Lab systems, Finland) after APHA (1998). Experiments were conducted at neutral pH to ensure that all observed changes in pH could be attributed to the addition of peat to the solution. The same procedure was also carried out using identical masses of amendment but without the addition of peat.

2.4. Analysis of experimental data

The mass of P adsorbed per gram of adsorbent, q_e, at equilibrium was calculated by:

$$q_e = \frac{V(C_o - C_e)}{m} \quad (1)$$

where C_o and C_e are the initial and final PO_4-P concentrations of the solution (mg L^{-1}), V is the volume of solution (L), and m is the dry weight of adsorbent (g). For the purpose of these calculations, the PO_4-P adsorbency of the peat was considered to be negligible, and for solutions containing peat and amendment, only the dry weight of the amendment was considered in Eq. (1).

The C_e and q_e data obtained from the batch tests were fitted to the Koble–Corrigan equation, which was chosen for its ability to model adsorption over a wide range of data, as well as for its being more universally applicable than the commonly used

Table 2
Koble–Corrigan fitting coefficients, HYBRID errors, and values of slope and R^2 obtained from plots of $q_{e\,calc}$ vs $q_{e\,exp}$ for all amendments studied.

Amendment	Mass of amendment (g)	Mass of peat (g)	Koble–Corrigan parameters			Hybrid error	$q_{e\,calc}$ vs $q_{e\,exp}$	
			A_{kc}	B_{kc}	p		R^2	Slope
Al-WTR	0.021	–	0.004	0.000	1.748	26.161	0.980	0.994
	0.051	–	0.002	0.001	1.844	21.142	0.870	1.016
	0.103	–	0.029	0.010	1.090	8.652	0.814	0.988
	0.021	2.000	0.710	0.032	0.795	4.725	0.995	1.001
	0.051	2.000	0.669	0.259	1.201	15.625	0.822	1.039
	0.103	2.000	0.001	−0.999	0.000	5.526	0.911	1.041
Crushed concrete	0.021	–	1.031	−0.072	0.446	0.045	1.000	1.000
	0.051	–	0.510	0.020	0.873	33.659	0.881	1.016
	0.103	–	1.929	0.205	0.514	8.719	0.903	1.003
	0.021	2.000	3.964	−0.099	0.210	3.408	0.969	0.998
	0.051	2.000	1.087	0.109	0.935	0.187	0.997	1.000
	0.103	2.000	1.625	0.169	0.585	0.230	0.996	1.000
Gypsum	0.021	–	0.191	0.002	1.722	1.816	1.000	1.000
	0.051	–	0.004	0.000	2.841	8.108	0.998	0.999
	0.103	–	0.089	−0.950	0.016	72.056	0.963	1.007
	0.021	2.000	0.504	−0.381	0.176	23.740	0.963	0.981
	0.051	2.000	0.000	−0.999	0.000	10.299	0.962	1.011
	0.103	2.000	0.000	−0.999	0.000	0.826	0.994	0.998
Magnesium oxide	0.021	–	1.686	0.012	2.406	742.198	0.895	1.036
	0.051	–	27.452	0.442	1.438	41.918	0.975	1.008
	0.103	–	17.694	0.252	0.520	17.290	0.986	1.000
	0.021	2.000	23.555	0.177	0.827	4.847	1.000	1.000
	0.051	2.000	24.286	0.407	1.197	34.473	0.994	1.000
	0.103	2.000	18.636	0.895	0.774	3.136	0.996	1.000
Magnesium hydroxide	0.021	–	1.214	−0.159	0.379	287.793	0.933	0.999
	0.051	–	0.055	0.001	1.474	60.942	0.949	1.007
	0.103	–	0.152	−0.939	0.011	21.583	0.933	1.006
	0.021	2.000	0.047	−0.009	1.011	35.254	0.997	0.992
	0.051	2.000	7.849	0.098	1.065	408.260	0.937	0.932
	0.103	2.000	2.075	0.047	1.473	0.003	1.000	1.000
Steel wool	0.021	–	2.921	0.159	1.484	42.332	0.968	1.009
	0.051	–	4.128	0.411	0.996	0.870	0.999	1.001
	0.103	–	1.181	0.156	1.001	617.693	0.520	1.453
	0.021	2.000	434.832	9.756	1.352	137.919	0.715	1.003
	0.051	2.000	41.715	0.926	1.313	32.093	0.980	0.996
	0.103	2.000	68.370	2.490	0.728	62.409	0.959	0.975

Langmuir and Freundlich equations (Koble and Corrigan, 1952). The Koble–Corrigan equation is as follows:

$$q_e = \frac{A_{KC} C_e^p}{1 + B_{KC} C_e^p} \tag{2}$$

where A_{KC}, B_{KC} and p are the Koble–Corrigan isotherm constants determined by using an iterative approach to minimize the value returned by the hybrid fractional error function (HYBRID), an error function used to fit Eq. (2) to the observed data (Porter et al., 1999):

$$\frac{100}{n-p} \sum_{i=1}^{n} \frac{(q_{e,i,meas} - q_{e,i,calc})^2}{q_{e,i,meas}} \tag{3}$$

where n is the number of experimental data points, p is the number of isotherm constants in the Koble–Corrigan equation (Eq. (2)), $q_{e,i,meas}$ is the value of q_e obtained from Eq. (1), and $q_{e,i,calc}$ is the value of q_e obtained from Eq. (2). By fitting the experimental data for each adsorbent to the Koble–Corrigan equation, it was possible to make predictions for values of C_e and q_e for any given C_o. Substituting Eq. (1) into Eq. (2) gives:

$$\frac{V(c_o - c_e)}{m} = \frac{A_{KC} C_e^p}{1 + B_{KC} C_e^p} \tag{4}$$

An iterative approach, using Microsoft Excel's Solver™, was then used to determine values of C_e for any given value of C_o. The impact of peat on the amendments' performance was evaluated using:

$$\phi = \frac{q_{e,a}^{calc}}{q_{e,b}^{calc}} \tag{5}$$

where $q_{e,a}^{calc}$ is the modeled mass of P adsorbed by the amendment in a solution containing peat, and $q_{e,b}^{calc}$ is the modeled mass of P adsorbed by the amendment in a solution containing no peat. Calculated values of $\Phi > 1$ indicate a synergistic effect was obtained by exposing an amendment to peat, i.e. the influence of peat chemistry was favorable for P adsorption, while values of $\Phi < 1$ suggest the opposite, i.e. that the effect was antagonistic. In this way, ϕ could be considered to be a coefficient of synergy.

3. Results and discussion

All of the amendments were effective at removing P from aqueous solution, both with and without the presence of peat in solution. The addition of peat did, however, influence the behavior of all amendments, leading to either improved or diminished adsorptive performance.

3.1. Equilibrium adsorption isotherms

Fig. 1 shows the adsorption isotherms obtained by fitting the Koble–Corrigan model to each of the peat amendment-mixtures.

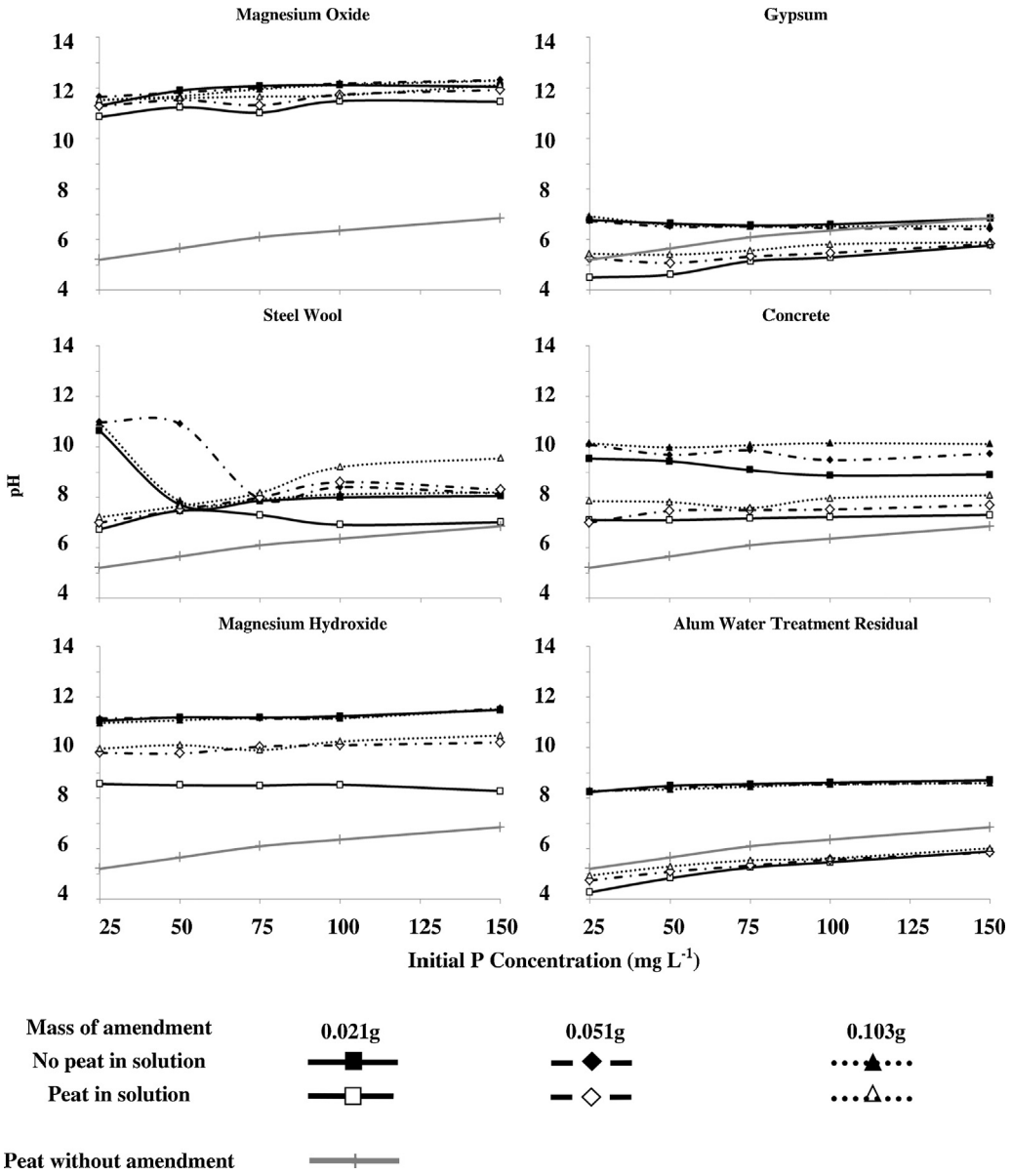

Fig. 2. Effect of peat on pH at equilibrium.

The Koble–Corrigan fitting coefficients (A_{kc}, B_{kc}, and p) as well as slope, and R^2 values obtained from plots of $q_{e\,calc}$ (calculated using the Koble–Corrigan equation) vs $q_{e\,exp}$, are shown in Table 2. The Koble–Corrigan model fitted the experimental data well, and there was a very good correlation (average $R^2 = 0.94 \pm 0.1$) between predicted and experimental values. In general, higher values of q_e were observed when the ratio of adsorbent to solution was smaller. This is in agreement with a review conducted by Cucarella and Renman (2009), who reported that smaller adsorbent-to-solution ratios may lead to higher concentrations of P sorbed to the adsorbent material. Al-WTR, in particular, showed a much larger increase in P adsorption capacity (maximum observed $q_e = 11.8\ mg\ g^{-1}$) when added to peat-containing solutions at an amendment to peat–solid ratio of 1:10, compared to amendment to peat–solid ratios of 1:4 and 1:2 (maximum observed $q_e = 3.3\ mg\ g^{-1}$ and $3.6\ mg\ g^{-1}$, respectively).

Maximum q_e values observed for concrete were $15\ mg\ g^{-1}$, $8.9\ mg\ g^{-1}$, and $6.8\ mg\ g^{-1}$ at amendment to peat–solid ratios of 1:10, 1:4, and 1:2, which were similar to q_e values of $26.8\ mg\ g^{-1}$, $15.1\ mg\ g^{-1}$, and $6.6\ mg\ g^{-1}$ observed for the same masses of concrete, but without the addition of peat. These values are all comparable to the q_e range of 5.1–19.6 $mg\ g^{-1}$ observed by Egemose et al. (2012). With respect to gypsum, the presence of peat in solution resulted in greatly reduced maximum observed q_e values of $10.8\ mg\ g^{-1}$, $4.4\ mg\ g^{-1}$, and $3.6\ mg\ g^{-1}$ at amendment to peat–solid ratios of 1:10, 1:4, and 1:2, compared to values of $84.8\ mg\ g^{-1}$, $58.4\ mg\ g^{-1}$, and $34\ mg\ g^{-1}$ observed for the same masses without the addition of peat.

Magnesium oxide and $Mg(OH)_2$ displayed the highest P adsorption capacities, with MgO having the greatest of the two, with a maximum q_e of $102.7\ mg\ g^{-1}$ observed at an amendment to peat–solid ratio of 1:10. Liu et al. (2011) found that removal of As(III) from aqueous solution by MgO was due to the in situ formation of $Mg(OH)_2$ by reaction of the MgO with water, followed by subsequent adsorption/reaction of the newly formed $Mg(OH)_2$ with the As(III) anion. Liu et al. (2011) also reported that the adsorptive performance of $Mg(OH)_2$ formed in situ was greater than that of pre-formed $Mg(OH)_2$, at least partially as a result of the former's larger specific surface area, which was almost 5.5 times greater than that of the latter ($58.4\ m^2\ g^{-1}$ vs. $10.7\ m^2\ g^{-1}$, respectively).

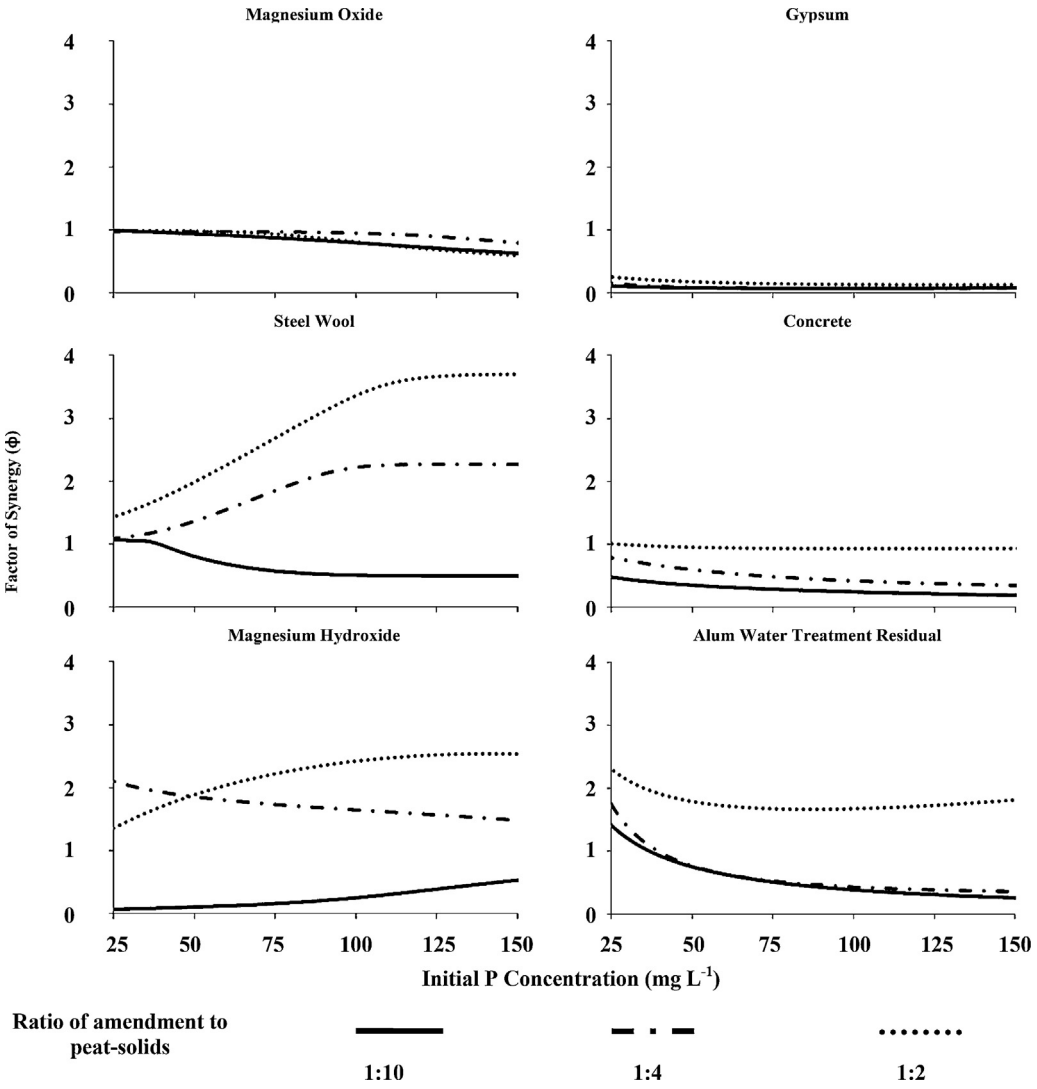

Fig. 3. Synergistic effect of peat on P adsorption (refer to Eq. (5)).

The results of our study indicate that $Mg(OH)_2$ formed in situ also had a greater adsorptive capacity for PO_4-P compared to that of preformed $Mg(OH)_2$. Stoichiometrically, MgO contains approximately 45% more Mg per unit weight than $Mg(OH)_2$; however, its P adsorption capacity was observed to be up to 120% greater than that of preformed $Mg(OH)_2$ in solutions where peat was absent (data not shown).

When steel wool was examined, P adsorption was observed to be inhibited at high initial PO_4-P concentrations (C_o), both with and without the addition of peat. This appeared to be the result of high PO_4-P concentrations inhibiting the formation of the iron oxides/hydroxides responsible for P removal, and it was observed that much less of the steel wool had rusted in these comparatively high concentration solutions. Similar observations were made by Pryor and Cohen (1953), who found that solutions of orthophosphate passivate iron; i.e. iron became less reactive due to presence of a micro coating in the presence of dissolved air, and Harahuc et al. (2000), who found that phosphate at or above concentrations of 25 mmol inhibited the solubilization of iron.

3.2. pH effects

Fig. 2 summarizes the effect the addition of peat had on the pH of the solution at equilibrium (after 24 h). The peat displayed a strong buffering capacity, and its addition altered the final pH of the solution at equilibrium in all cases. In real-world applications, an amendment that has a strong effect on pH may not be desirable, as large fluctuations in pH may have a deleterious impact on the environment. For example, the addition of an amendment which increases the soil's pH may increase soil nitrate (NO_3) concentrations, and the risk of NO_3 leaching could be particularly great during the clearfelling of forestry (Wickström, 2002). After shaking for 24 h, the pH of samples containing peat mixed with Al-WTR was found to be closest to those of a solution containing peat only. The performances of P adsorbent materials are known to be strongly affected by pH, and in acidic soils such as peats, Al and Fe are known to be responsible for the sorption of P (Sato et al., 2005), while binding by calcium (Ca) and magnesium (Mg) is responsible for P immobilization in alkaline soils (Faulkner and Richardson, 1989; Reddy et al., 1999).

3.3. Synergistic effects

The results indicate that, at certain initial PO_4-P concentrations, a degree of synergy exists between the peat and certain amendments; i.e. their adsorption performance was better in an environment whose chemistry was influenced by peat (Fig. 3). Al-WTR and steel wool, in particular, showed improved performance

across a large range of concentrations, while concrete, gypsum, and MgO showed largely diminished efficacy. The effect of peat on P adsorption by $Mg(OH)_2$ varied from beneficial to detrimental, depending on the ratio of peat to amendment in solution.

One mechanism by which an amendment's P sorption performance may improve when in a peat environment is as a result of the interaction of humic substances with soluble metal ions. Humic substances facilitate the removal of P through reactions with Al and Fe ions, which results in the formation of insoluble phosphate complexes (Bloom, 1981; Renou et al., 2000). Conversely, humic materials inhibit the removal of P by precipitation with Ca by competing with the phosphate anion for Ca, with this effect being more exaggerated at lower pH (Alvarez et al., 2004; Song et al., 2006; Cao et al., 2007). The formation of humic complexes may therefore contribute both to the observed improvement in Al-WTR and steel wool's adsorptive performance, as well as the diminished performance of concrete and gypsum. Phosphorus sorption by gypsum, for example, is directly related to its solubility, as its P removal is largely due to precipitation reactions (Penn et al., 2007) and thus the availability of Ca for the formation of calcium phosphates (Kordlaghari and Rowell, 2006).

The concrete used in this study had significantly higher levels of Al and Fe present than the gypsum (Table 1), which may explain why its P removal performance was not as adversely affected as gypsum's. Oğuz et al. (2003) found that P removal by concrete was by precipitation of metallic PO_4 salts, which were adsorbed onto the surface of the concrete, and $AlPO_4$ appeared to be the main product adsorbed onto the surface of the gas concrete examined in their study. This result suggests that the Al and Fe content of the concrete examined in this study, perhaps more so than its Ca content, plays a crucial role in P adsorption. Berg et al. (2005) reported that P removal by crushed gas concrete was not affected by the presence of organic matter in the form of dissolved organic carbon. However, as concrete's adsorption of P is strongly related to pH, and improves with increasing pH (Oğuz et al., 2003), it appears that the acidification of the solution by the peat is at least partially responsible for the observed reduction in performance.

The pH buffering action of the peat is also likely to have contributed to the observed synergistic effects by lowering the solution pH, which can improve Al-WTR's P adsorption, as observed by Yang et al. (2006), and promote corrosion of the steel wool to form P adsorbing iron oxide/hydroxides. Consequently, the peat had a stronger effect on pH at this rate, with the final solution pH ranging from 8.3–8.6, compared to 9.8–10.2 and 9.9–10.5 at amendment to peat–solid ratios of 1:4 and 1:2, respectively. It was also observed that when $Mg(OH)_2$ was added at an amendment to peat–solid ratio of 1:10, recorded q_e values were much lower than solutions containing $Mg(OH)_2$ at amendment to peat–solid ratios of 1:4 and 1:2. While the reason for this is not entirely clear, the marked difference in pH accompanied by the significant drop in P adsorption strongly suggests that the pH buffering effect of the peat may also be responsible for reducing the P adsorbency of $Mg(OH)_2$ at this lowest rate of amendment. Xie et al. (2013) reported that fulvic and humic acids had a slight negative effect on PO_4 adsorption by a magnesium oxide nanoflake-modified diatomite adsorbent, and attributed this observation to the effects of competitive adsorption. It is quite possible that at low $Mg(OH)_2$ to peat ratios this effect is more exaggerated.

4. Conclusions

This study found that the presence of peat in solution increased the P adsorption capacities of Al-WTR and steel wool, while the adsorptive capacities of crushed concrete, gypsum, and magnesium oxide were decreased. Magnesium hydroxide showed both increased and decreased adsorptive capacity, depending on the ratio of peat to amendment in solution. Throughout the study, peat displayed considerable ability to buffer the peat-amendment mixture pH. However, the equilibrium pH of solutions containing Al-WTR and gypsum were observed to be closest to the peat's natural pH, indicating that these amendments were best suited to the peat environment. Taking these factors into consideration, the results of this study indicate that Al-WTR, in particular, holds great promise for utilization in the mitigation of P runoff caused by forestry operations on blanket peat sites. Previous research into the use of Al-WTR has shown it to be effective in preventing P runoff when used as a soil amendment in an agricultural context, and this study's findings demonstrate that the chemistry of a peat forest environment is likely to interact with Al-WTR in such a manner as to improve its P removal performance at low P concentrations. As a waste material, an additional benefit lies in the fact that it does not have the production costs associated with other high performing amendments studied, i.e. steel wool and $Mg(OH)_2$.

Acknowledgement

The first author would like to acknowledge the Irish Research Council for funding.

References

Alvarez, R., Evans, L.A., Milham, P.J., Wilson, M.A., 2004. Effects of humic material on the precipitation of calcium phosphate. Geoderma 118, 245–260.

Ann, Y., Reddy, K.R., Delfino, J.J., 1999. Influence of chemical amendments on phosphorus immobilization in soils from a constructed wetland. Ecol. Eng. 14, 157–167.

American Public Health Association (APHA), American Water Works Association, and Water Environment Federation, 1998. Standard Methods for the Examination of Water and Wastewater. American Public Health Association, Washington, DC.

Berg, U., Donnert, D., Ehbrecht, A., Bumiller, W., Kusche, I., Weidler, P.G., Nüesch, R., 2005. "Active filtration" for the elimination and recovery of phosphorus from waste water. Colloids Surf. A 265, 141–148.

Bloom, P.R., 1981. Phosphorus adsorption by an aluminum-peat complex. Soil Sci. Soc. Am. J. 45, 267.

Boesch, D.F., Brinsfield, R.B., Magnien, R.E., 2001. Chesapeake bay eutrophication. J. Environ. Qual. 30, 303–320.

Brennan, R.B., Fenton, O., Grant, J., Healy, M.G., 2011a. Impact of chemical amendment of dairy cattle slurry on phosphorus, suspended sediment and metal loss to runoff from a grassland soil. Sci. Total Environ. 409, 5111–5118.

Brennan, R.B., Fenton, O., Rodgers, M., Healy, M.G., 2011b. Evaluation of chemical amendments to control phosphorus losses from dairy slurry. Soil Use Manage. 27, 238–246.

British Standards Institution (BSI), 1990. British Standard Methods of Test for Soils for Civil Engineering Purposes. British Standards Institution, Milton Keynes, England.

Cao, X., Harris, W.G., Josan, M.S., Nair, V.D., 2007. Inhibition of calcium phosphate precipitation under environmentally-relevant conditions. Sci. Total Environ. 383, 205–215.

Carpenter, S.R., Caraco, N.F., Correll, D.L., Howarth, R.W., Sharpley, A.N., Smith, V.H., 1998. Nonpoint pollution of surface waters with phosphorus and nitrogen. Ecol. Appl. 8, 559–568.

Chardon, W.J., Groenenberg, J.E., Temminghoff, E.J., Koopmans, G.F., 2012. Use of reactive materials to bind phosphorus. J. Environ. Qual. 41, 636–646.

Cucarella, V., Renman, G., 2009. Phosphorus sorption capacity of filter materials used for on-site wastewater treatment determined in batch experiments—a comparative study. J. Environ. Qual. 38, 381–392.

Department of the Environment, Community and Local Government, 2002. Making Ireland's Development Sustainable Review, Assessment and Future Action, Available at: http://www.environ.ie/en/Environment/SustainableDevelopment/PublicationsDocuments/FileDownLoad,1847,en.pdf (verified 09.11.14).

Egemose, S., Sønderup, M.J., Beinthin, M.V., Reitzel, K., Hoffmann, C.C., Flindt, M.R., 2012. Crushed concrete as a phosphate binding material: a potential new management tool. J. Environ. Qual. 41, 647–653.

Faulkner, S.P., Richardson, C.J., 1989. Physical and chemical characteristics of freshwater wetland soils. In: Hammer, D.A. (Ed.), Constructed Wetlands for Wastewater Treatment. CRC Press, Boca Raton, FL, pp. 41–72.

Finnegan, J., Regan, J.T., O'Connor, M., Wilson, P., Healy, M.G., 2014. Implications of applied best management practice for peatland forest harvesting. Ecol. Eng. 63, 12–26.

Forest Service, 2000. Code of Best Forest Practice, Available at: http://www.agriculture.gov.ie/forestservice/publications/codeofbestforestpractice/ (verified 10.11.14).
Giller, P.S., O'Halloran, J., 2004. Forestry and the aquatic environment: studies in an Irish context. Hydrol. Earth Syst. Sci. 8, 314–326.
Harahuc, L., Lizama, H.M., Suzuki, I., 2000. Selective inhibition of the oxidation of ferrous iron or sulfur in *Thiobacillus ferrooxidans*. Appl. Environ. Microbiol. 66, 1031–1037.
Hutton, S., Harrison, S., O'Halloran, J., 2008. An Evaluation of the Role of Forests and Forest Practices in the Eutrophication and Sedimentation of Receiving Waters, Available at: http://www.wfdireland.net/docs/22_ForestAndWater/Forest%20and%20Water_UCC_Draft%20Final%20Report.pdf (verified 09.05.14).
Hyvönen, R., Olsson, B.A., Lundkvist, H., Staaf, H., 2000. Decomposition and nutrient release from *Picea abies* (L.) Karst. and *Pinus sylvestris* L. logging residues. For. Ecol. Manage. 126, 97–112.
James, B.R., Rabenhorst, M.C., Frigon, G.A., 1992. Phosphorus sorption by peat and sand amended with iron oxides or steel wool. Water Environ. Res. 64, 699–705.
Koble, R.A., Corrigan, T.E., 1952. Adsorption isotherms for pure hydrocarbons. Ind. Eng. Chem. 44, 383–387.
Kordlaghari, M.P., Rowell, D.L., 2006. The role of gypsum in the reactions of phosphate with soils. Geoderma 132, 105–115.
Li, Y., Liu, C., Luan, Z., Peng, X., Zhu, C., Chen, Z., Zhang, Z., Fan, J., Jia, Z., 2006. Phosphate removal from aqueous solutions using raw and activated red mud and fly ash. J. Hazard. Mater. 137, 374–383.
Liljaniemi, P., Vuori, K.-M., Tossavainen, T., Kotanen, J., Haapanen, M., Lepistö, A., Kenttämies, K., 2003. Effectiveness of constructed overland flow areas in decreasing diffuse pollution from forest drainages. Environ. Manage. 32, 602–613.
Liu, Y., Li, Q., Gao, S., Shang, J.K., 2011. Exceptional As(III) sorption capacity by highly porous magnesium oxide nanoflakes made from hydrothermal synthesis. J. Am. Ceram. Soc. 94, 217–223.
Mainstone, C.P., Parr, W., 2002. Phosphorus in rivers – ecology and management. Sci. Total Environ. 282–283, 25–47.
Moffat, A.J., Jones, B.M., Mason, W.L., Britain, G., 2006. Managing Brash on Conifer Clearfell Sites. Forestry Commission, http://www.forestry.gov.uk/pdf/FCPN013.pdf/$FILE/FCPN013.pdf (verified 26.11.14).
National Forest Inventory, 2012. National Forest Inventory. Available at: https://www.agriculture.gov.ie/nfi/nfisecondcycle2012/nationalforestinventorypublications2012/[inventorypublications2012/] (verified 09.05.14).
Nieminen, M., Ahti, E., Nousiainen, H., Joensuu, S., Vuollekoski, M., 2005. Capacity of riparian buffer zones to reduce sediment concentrations in discharge from peatlands drained for forestry. Silva Fennica 39, 331–339.
O'Driscoll, C., de Eyto, E., Rodgers, M., O'Connor, M., Asam, Z.-Z., Xiao, L., 2012. Diatom assemblages and their associated environmental factors in upland peat forest rivers. Ecol. Indic. 18, 443–451.
O'Flynn, C.J., Fenton, O., Healy, M.G., 2012. Evaluation of amendments to control phosphorus losses in runoff from pig slurry applications to land. CLEAN – Soil Air Water 40, 164–170.
Oğuz, E., Gürses, A., Canpolat, N., 2003. Removal of phosphate from wastewaters. Cement Concrete Res. 33, 1109–1112.
Penn, C.J., Bryant, R.B., Kleinman, P.J.A., Allen, A.L., 2007. Removing dissolved phosphorus from drainage ditch water with phosphorus sorbing materials. J. Soil Water Conserv. 62, 269–276.
Porter, J.F., McKay, G., Choy, K.H., 1999. The prediction of sorption from a binary mixture of acidic dyes using single- and mixed-isotherm variants of the ideal adsorbed solute theory. Chem. Eng. Sci. 54, 5863–5885.
Pryor, M.J., Cohen, M., 1953. The inhibition of the corrosion of iron by some anodic inhibitors. J. Electrochem. Soc. 100, 203–215.
Reddy, K.R., Kadlec, R.H., Flaig, E., Gale, P.M., 1999. Phosphorus retention in streams and wetlands: a review. Crit. Rev. Environ. Sci. Technol. 29, 83–146.
Reid, N., Keys, A., Preston, J.S., Moorkens, E., Roberts, D., Wilson, C.D., 2013. Conservation status and reproduction of the critically endangered freshwater pearl mussel (*Margaritifera margaritifera*) in Northern Ireland. Aquat. Conserv: Mar. Freshw. Ecosyst. 23, 571–581.
Renou, F., Farrell, E.P., 2005. Reclaiming Peatlands for Forestry: The Irish Experience. Restoration of Boreal and Temperate Forests. CRC Press, Boca Raton, pp. 541–557.
Renou, F., Jones, S., Farrell, E.P., 2000. Leaching of phosphorus fertilizer applied on cutaway peatland forests recently established in central Ireland. Sustain. Peatl. 2, 984–990.
Rodgers, M., O'Connor, M., Healy, M.G., O'Driscoll, C., Asam, Z.-Z., Nieminen, M., Poole, R., Müller, M., Xiao, L., 2010. Phosphorus release from forest harvesting on an upland blanket peat catchment. Forest Ecol. Manage. 260 (12), 2241–2248.
Sato, S., Solomon, D., Hyland, C., Ketterings, Q.M., Lehmann, J., 2005. Phosphorus speciation in manure and manure-amended soils using XANES spectroscopy. Environ. Sci. Technol. 39, 7485–7491.
Seo, D.C., Cho, J.S., Lee, H.J., Heo, J.S., 2005. Phosphorus retention capacity of filter media for estimating the longevity of constructed wetland. Water Res. 39, 2445–2457.
Serrenho, A., Fenton, O., Murphy, P.N.C., Grant, J., Healy, M.G., 2012. Effect of chemical amendments to dairy soiled water and time between application and rainfall on phosphorus and sediment losses in runoff. Sci. Total Environ. 430, 1–7.
Schaller, J., Tischer, A., Struyf, E., Bremer, M., Belmonte, D.U., Potthast, K., 2015. Fire enhances phosphorus availability in topsoils depending on binding properties. Ecology 96, 1598–1606.
Song, Y., Hahn, H.H., Hoffmann, E., Weidler, P.G., 2006. Effect of humic substances on the precipitation of calcium phosphate. J. Environ. Sci. 18, 852–857.
Titus, B.D., Malcolm, D.C., 1999. The long-term decomposition of Sitka spruce needles in brash. Forestry 72 (3), 207–221.
Vaananen, R., Nieminen, M., Vuollekoski, M., Nousiainen, H., Sallantaus, T., Tuittila, E., Ilvesniemi, H., 2008. Retention of phosphorus in peatland buffer zones at six forested catchments in southern Finland. Silva Fennica 42 (2), 211.
Vasander, H., Tuittila, E.-S., Lode, E., Lundin, L., Ilomets, M., Sallantaus, T., Heikkilä, R., Pitkänen, M.-L., Laine, J., 2003. Status and restoration of peatlands in northern Europe. Wetlands Ecol. Manage. 11, 51–63.
Wickström, H., 2002. Action Plan to Counteract Soil Acidification and to Promote Sustainable Use of Forestland. National Board of Forestry, Jönköping, Available at: http://shop.skogsstyrelsen.se/shop/9098/art63/4645963-efc63c-1546.pdf (verified 26.11.14).
Xie, F., Wu, F., Liu, G., Mu, Y., Feng, C., Wang, H., Giesy, J.P., 2013. Removal of phosphate from eutrophic lakes through adsorption by in situ formation of magnesium hydroxide from diatomite. Environ. Sci. Technol. 48, 582–590.
Yang, Y., Zhao, Y.Q., Babatunde, A.O., Wang, L., Ren, Y.X., Han, Y., 2006. Characteristics and mechanisms of phosphate adsorption on dewatered alum sludge. Sep. Purif. Technol. 51, 193–200.

Appendix B

Water Research 101 (2016) 429–440

Contents lists available at ScienceDirect

Water Research

journal homepage: www.elsevier.com/locate/watres

Evaluating the long-term performance of low-cost adsorbents using small-scale adsorption column experiments

O. Callery [a], M.G. Healy [a], F. Rognard [b], L. Barthelemy [c], R.B. Brennan [a, *]

[a] Civil Engineering, National University of Ireland, Galway, Co. Galway, Ireland
[b] Université François Rabelais de Tours, Tours, France
[c] École Nationale du Génie de l'Eau et de l'Environnement de Strasbourg, Strasbourg, France

ARTICLE INFO

Article history:
Received 21 March 2016
Received in revised form
5 May 2016
Accepted 30 May 2016
Available online 31 May 2016

Keywords:
Adsorption
Column
Phosphorus
Low-cost adsorbent
Modeling

ABSTRACT

This study investigated a novel method of predicting the long-term phosphorus removal performance of large-scale adsorption filters, using data derived from short-term, small-scale column experiments. The filter media investigated were low-cost adsorbents such as aluminum sulfate drinking water treatment residual, ferric sulfate drinking water treatment residual, and fine and coarse crushed concretes. Small-bore adsorption columns were loaded with synthetic wastewater, and treated column effluent volume was plotted against the mass of phosphorus adsorbed per unit mass of filter media. It was observed that the curve described by the data strongly resembled that of a standard adsorption isotherm created from batch adsorption data. Consequently, it was hypothesized that an equation following the form of the Freundlich isotherm would describe the relationship between filter loading and media saturation. Moreover, the relationship between filter loading and effluent concentration could also be derived from this equation. The proposed model was demonstrated to accurately predict the performance of large-scale adsorption filters over a period of up to three months with a very high degree of accuracy. Furthermore, the coefficients necessary to produce said model could be determined from just 24 h of small-scale experimental data.

1. Introduction

Adsorption and surface precipitation are fast, cost-effective, and therefore highly attractive water treatment techniques that are applicable to the removal of a broad range of contaminants. In particular, there is considerable interest in low-cost adsorbents, which may be suitable for use in the treatment of water contaminated by pollutants such as heavy metals, industrial dyes, and nutrients (Demirbas, 2008; Vohla et al., 2011; Yagub et al., 2014). Natural materials, as well as industrial and agricultural wastes, are ideal in this regard, due to their low cost, local availability, and the added economic value associated with avoiding disposal routes such as landfill and incineration (Babel and Kurniawan, 2003; Crini, 2006).

When assessing the suitability of a potential filter medium, batch adsorption experiments are the most commonly utilized test, favored by researchers for their convenience and low cost (Crini and Badot, 2008). In fact, a large proportion of studies (arguably erroneously) rely solely on batch experiments to make inferences as to the behaviour of media in real-world filters (Ali and Gupta, 2007). The data from these batch adsorption tests are used in the construction of adsorption isotherms - curves that describe the removal of a contaminant from a mobile (liquid or gaseous) phase by its binding to a solid phase, across a range of contaminant concentrations. The determination of these isotherms is considered a critical step in the design and optimization of any adsorption process (Behnamfard and Salarirad, 2009; Hamdaoui and Naffrechoux, 2007), and there are a multitude of models describing these equilibrium curves.

Whilst important in the characterisation of potential adsorptive materials, it has been noted that batch adsorption tests have a number of potential shortcomings. Data obtained from batch studies are heavily influenced by factors such as initial solution concentration (Drizo et al., 2002), pH (Cucarella and Renman, 2009), and contact time (McKay, 1996), as well as by experimental conditions which are sometimes very different to real world applications - for example the use of unrealistic solid-to-solution ratios, and the agitation of batch samples (Ádám et al., 2007;

* Corresponding author.
E-mail address: raymond21brennan@gmail.com (R.B. Brennan).

http://dx.doi.org/10.1016/j.watres.2016.05.093
0043-1354/

Søvik and Kløve, 2005).

Adsorption isotherms may also be determined using flow-through experiments, and the utilization of such methodologies, while not offering a 'solve-all solution', may help to address many of the shortcomings associated with batch studies. Buergisser et al. (1993) note that the solid-to-liquid ratio used when determining sorption isotherms with flow-through experiments is much closer to ratios that might be found in real-life systems where the adsorption of contaminants plays an important role in the treatment of contaminated waters (e.g. wastewater filtration units, constructed wetland substrates, and riparian buffer zones). Grolimund et al. (1995) also highlighted a number of other advantages of flow-through methodologies, such as the ease of pre-washing the media under investigation, the reduced cost of the equipment necessary to perform the analysis, and the mitigation of experimental errors caused by the shaking motions used in batch experiments. A question still remains, however, regarding the applicability of the obtained isotherm to real-world situations. The isotherm alone provides no useful information regarding the longevity of a system (Seo et al., 2005), and when considering potential practical applications, predicting the lifespan of a given filter media is of paramount importance (Johansson, 1999).

Pratt et al. (2012) argue that the only reliable method of predicting the long-term performance of a filter media is full-scale field testing. While this may be true, it is obviously impractical to conduct such a study with an unproven material, and it is therefore desirable to perform short-term, laboratory-based experiments prior to undertaking any such large-scale study. Therefore, to address the question of adsorbent longevity, flow-through experiments in large-scale, laboratory-based columns are the most commonly utilised method, though Crittenden et al. (1991) demonstrated that rapid small-scale column tests (RSSCTs) could also be used to predict the performance of pilot-scale adsorption columns.

There are a number of models commonly used to describe column adsorption, among the most popular of which are the Thomas model (Thomas, 1944), the Clark model (Clark, 1987), the Yoon-Nelson model (Yoon and Nelson, 1984), and the bed depth service time (BDST) model developed by Hutchins (Hutchins, 1973), based on an earlier model proposed by Bohart and Adams (Bohart and Adams, 1920). All of these models attempt to predict the performance of a filter column by studying the relationship between filter loading and effluent concentration, though in full-scale filters this relationship can be far from ideal. When a filter is intermittently loaded, as might be the case, for example, in sub-surface vertical flow constructed wetlands (Healy et al., 2007; Pant et al., 2001), intermittent sand filtration systems (Rodgers et al., 2005), or indeed even riparian buffer zones (Ulén and Etana, 2010; Vidon et al., 2010), the relationship between effluent concentration and running time can be strongly affected by pauses in filter loading. It has been noted by a great many researchers that such breaks in the continuity of loading potentially allows for the diffusion of adsorbate molecules further into the adsorbent particles, thus resulting in a rejuvenation of the adsorbent surface prior to the next loading cycle (Ouvrard et al., 2002; DeMarco et al., 2003; Greenleaf and SenGupta, 2006; Sengupta and Pandit, 2011). This results in a non-uniform evolution of column effluent concentration with successive loadings, and means that the relationship between effluent concentration and loading is unlikely to follow one of the ideal breakthrough curves described by any of the aforementioned models. For example, the BDST model predicts an S-shaped curve, which is often not observed in laboratory studies, experimental data instead producing linear to convex curves associated with less ideal adsorption (Malkoc et al., 2006; Walker and Weatherley, 1997). Furthermore, this model is best suited to columns containing ideal adsorbents with continuous flow-through rates that are low enough to allow adsorptive equilibrium to be reached (Jusoh et al., 2007) – conditions which are not necessarily representative of real world conditions.

Considering that the ability to predict the point at which the effluent from an adsorptive filter exceeds a pre-defined contaminant concentration (i.e., the breakthrough point) is the principal objective of any column service time model (Deliyanni et al., 2009), the purpose of the current study was to develop a model capable of predicting filter breakthrough, while addressing the difficulties of modeling effluent concentration from an intermittently loaded filter. The proposed model works under the hypothesis that, if the relationship between filter media saturation and filter loading can be accurately described for an intermittently loaded filter, then effluent concentration can be obtained implicitly for any given influent concentration, and in the case of an intermittently loaded media, this approach is likely to be more successful than attempting to simply model the effluent concentration directly. To the best of our knowledge, this approach to predicting filter longevity has not been attempted before.

The proposed model was developed from rapid small-scale column tests, and its accuracy was confirmed using large-scale, laboratory-based filters which, in terms of media mass and loading, were two orders of magnitude larger than the experiment from which the model was derived. To test the model's adaptability to variations in operating conditions such as 1) removal of contaminants, 2) continuous loading, 3) treatment of complex sample matrices, 4) variations in contaminant concentration, and 5) variations in filter hydraulic retention time (HRT), the proposed model was fit to published data from a previous study (Claveau-Mallet et al., 2013).

The speed and ease with which the proposed experimental procedure may be performed, as well as the low costs associated with equipment and analysis, make this methodology an attractive complement to batch tests, as it provides an estimate of filter longevity in a similarly short timeframe to batch tests' provision of estimates of filter capacity. As is the case with the RSSCTs proposed by Crittenden et al. (1991), the proposed model makes rapid predictions of filter longevity without the need for any preceding kinetic or isotherm studies, and only a small volume of sample wastewater is required for collection of the experimental data necessary to construct the model. In contrast with RSSCTs, the proposed model focuses on filter media subject to intermittent loading, modeling media saturation instead of filter effluent concentration. Predictions of filter performance are greatly simplified by virtue of the proposed model's empirical nature, which circumvents the need to consider mechanistic factors such as solute transport mechanisms and intraparticle diffusivities.

2. Theory

Where a wastewater is loaded onto an adsorptive filter column, and the effluent collected in a number of containers, the relationship between the total volume of wastewater filtered and the mass of a contaminant adsorbed per unit mass of filter media is described by:

$$q_e = \sum_{i=1}^{n} \frac{(C_o - C_{e_i})V_i}{m} \quad (1)$$

where q_e is the cumulative mass of contaminant adsorbed per gram of filter media, n is the number of containers in which the total volume of effluent ($\sum$Vi) is collected, C_o is the influent contaminant concentration, $C_{e,i}$ is the effluent contaminant concentration in the

ith container, V_i is the volume of effluent contained in the ith container, and m is the mass of filter media contained in the filter column.

The Freundlich adsorption isotherm (Freundlich, 1906) is an empirical model describing the relationship between the adsorption of a contaminant from a mobile phase to a solid phase across a range of contaminant concentrations. The equation is as follows:

$$q_e = K_f C^{\frac{1}{n}} \tag{2}$$

where q_e is the cumulative mass of contaminant adsorbed per gram of filter media, C is the contaminant concentration of the supernatant at equilibrium, and K_f and n are the Freundlich constants. The Freundlich equation assumes that the heat of adsorption decreases in magnitude with increasing extent of adsorption, and that this decline in the heat of adsorption is logarithmic, thus implying an exponential distribution of adsorption sites and energies (Sheindorf et al., 1981; Thomas and Crittenden, 1998). There is much experimental evidence that the real energy distributions, while perhaps not being strictly exponential, are indeed roughly of this sort (Cooney, 1998). Being a characteristic of the media, the assumption of exponential distribution remains equally valid, regardless of whether the saturation of the media is due to batch or through-flow exposure to adsorbate molecules. In the case of a batch experiment, the mass of adsorbate bound to the surface of a filter media increases with increasing solute concentration. In the case of a column experiment, the mass of adsorbate bound to the surface of the media increases as more solution is passed through the filter. Column effluent concentration, C_e, increases as progressively more wastewater is passed through the adsorptive media in a filter column, and therefore C_e is a function of V, the volume treated by the filter. If that function of V were modeled after Eqn. (2), it could reasonably be hypothesized that there would be some values of A and B such that the following equation might hold true:

$$q_e = AV^{\frac{1}{B}} \tag{3}$$

where B is a dimensionless constant of system heterogeneity, just as n is a heterogeneity factor in the Freundlich equation (Allen et al., 2004), and A is a constant of proportionality with units $(mg/g)(L)^{(-1/B)}$. Eqn. (3) should only be considered valid for $B > 1$, as values of $B < 1$ would imply that a greater adsorbate concentration in the filter media serves to enhance the free energies of further adsorption. If this were the case, it would contradict the earlier assertion that the heat of adsorption decreases in magnitude with increasing extent of adsorption. Eqn. (3) can be validated in the same manner as the Freundlich equation is validated for batch tests, i.e. by constructing a plot of experimental data and comparing it to the linearized version of the equation:

$$\ln(q_e) = \ln(A) + B^{-1} \ln(V) \tag{4}$$

If Eqn. (3) describes the experimental data, the plot of $\ln(q_e)$ versus $\ln(V)$ would then be linear, meaning the model constants could be determined from the plot as follows: $A = \exp(\text{intercept})$, and $B = (\text{slope})^{-1}$. Should the linear plot have a coefficient of determination, R^2, close to unity, it would indicate that Eqn. (3) is a suitable empirical model to describe the relationship between filter loading and filter media saturation.

Were all the filter column effluent collected in a single container, the average effluent concentration up to any volume, V, would be given by substituting Eqn. (1) into Eqn. (3) to yield:

$$C_{e_{avg}} = C_o - AmV^{\left(\frac{1}{B}-1\right)} \tag{5}$$

If, however, the effluent were collected in a number of sequentially filled containers, the theoretical concentration of a given effluent aliquot collected at any time over the duration of operation of a filter may be calculated using:

$$C_{e_{\Delta V}} = C_o - \frac{\Delta q_e M}{\Delta V} \tag{6}$$

where ΔV is the volume the filter effluent collected in a container between some arbitrary volumes V_a and V_b, $C_{e\Delta V}$ is the theoretical concentration of the filter effluent volume ΔV, and Δq_e is the theoretical change in the mass of contaminant adsorbed per unit mass of filter media from V_a to V_b.

Assuming Eqn. (3) fits the experimental data with acceptable accuracy, Δq_e between V_a and V_b can be calculated as follows:

$$\Delta q_{e,mod} = AV_b^{\frac{1}{B}} - AV_a^{\frac{1}{B}} \tag{7}$$

Substituting Eqn. (7) into Eqn. (6), and letting V_a equal V_b-ΔV therefore gives the following:

$$C_{e_{\Delta V}} = Co - \frac{AM\left[V_b^{\frac{1}{B}} - (V_b - \Delta V)^{\frac{1}{B}}\right]}{\Delta V} \tag{8}$$

The concentration of effluent at a given cumulative flow-through volume, V, as opposed to the average concentration, as given by Eqn. (5), can then be estimated by obtaining the concentration across an infinitesimally small ΔV as follows:

$$C_{e_v} = \lim_{\Delta V \to 0}\left[C_o - \left(\frac{AM\left[V^{\frac{1}{B}} - (V - \Delta V)^{\frac{1}{B}}\right]}{\Delta V}\right)\right] \tag{9}$$

This yields the following:

$$C_{e_V} = C_o - \frac{AMV^{\left(\frac{1}{B}-1\right)}}{B} \tag{10}$$

Thus, to determine V_b, the volume at which any given breakthrough concentration, C_{eb}, is reached, Eqn. (10) can be rearranged as follows:

$$V_b = \left(\frac{(C_o - C_{eb})B}{AM}\right)^{-\frac{B}{B-1}} \tag{11}$$

Eqn. (11) describes the breakthrough curve for all breakthrough effluent concentrations in the range $0<C_{eb} < C_o$, though it is important to note in Eqn. (10) that $V^{1/B-1} \to 0$ as $V \to \infty$, meaning the model will only asymptotically approach total breakthrough, $C_{eb} = C_o$. This should not pose a limitation at concentration ranges of practical interest, i.e $0 < C_{eb} < 0.9(C_o)$. Above this range filter media are commonly thought to have reached exhaustion (Han et al., 2006; Netpradit et al., 2004), and caution should be exercised when trying to utilise the model to predict effluent concentrations past this exhaustion point. The volume at which initial breakthrough occurs, $V_{b,0}$, is found by letting C_e, in Eqn. (11) equal to 0 mg L^{-1}. Inputting a value less than $V_{b,0}$, into by Eqn. (10) would result in a negative C_e (as $V^{1/B-1} \to -\infty$ as $V \to 0$) which should simply be taken as zero. Breakthrough curves can easily be predicted for any filter subjected to equivalent loading by simply multiplying Eqn. (11) by a scaling factor, M_2/M_1, where M_1 is the mass of the filter from which the data to derive Eqn. (11) was obtained, and M_2 is the mass of the filter of interest. Eqn. (10) can also be rearranged to yield following linear relationship between C_e and V:

$$\ln(C_o - C_e) = \left(\frac{1}{b} - 1\right)\ln V + \ln\frac{AM}{B} \quad (12)$$

With Eqn. (12), the coefficients A and B can theoretically be obtained from the slope and intercept of a plot of $\ln(C_o - C_e)$ vs $\ln(V)$ as follows: A = B(exp(intercept)/(M)), and B = (slope + 1)$^{-1}$. However, as discussed previously, for an intermittently loaded filter column, it is hypothesized that attempting to model the saturation of the filter media would prove more successful than attempting to directly model column effluent concentration. To complement the explanations given in this section, Figure S1 shows the derivation of the breakthrough curve (Eqn. (11)) from a mass balance analysis of a filter system.

3. Materials and methods

3.1. Preparation of small bore adsorption columns

Small bore adsorption columns were prepared using polycarbonate tubes with an internal diameter of 0.94 cm and lengths of 10, 15, 20, 30, and 40 cm. Sets of tubes (comprising one tube of each length without replication) were packed with four different adsorbent media. These media comprised mixtures containing (1) aluminium sulfate drinking water treatment residual (Al-WTR; oven dried for 24 h at 105 °C and ground to pass a 0.5 mm sieve) (2) ferric sulfate drinking water treatment residual (Fe-WTR; oven dried for 24 h at 105 °C and ground to pass a 0.5 mm sieve) (3) fine crushed concrete (pulverized with a mortar and pestle and ground to pass a 0.5 mm sieve), and (4) coarse crushed concrete (pulverized with a mortar and pestle and ground to pass a 1.18 mm sieve, but retained by a 0.5 mm sieve); these will henceforth be referred to as media A, B, C, and D, respectively. In a preliminary experiment (not reported here), the relationship between dry bulk density and hydraulic conductivity was studied for each media, and the polycarbonate tubes used in this study were packed with media at a dry bulk density such that each of the columns had a saturated hydraulic conductivity of 0.14 cm s^{-1}. The physical characteristics of the different media were such that this value could be achieved for all four media, and this value of hydraulic conductivity is comparable to that found in constructed wetland substrates (Brix et al., 2001) and slow sand filters (Mauclaire et al., 2006; Rodgers et al., 2004). Plastic syringes with an internal diameter equal to that of the polycarbonate tubes' outside diameter were fastened, by friction fit, to either end of the columns, and a small quantity of acid-washed glass wool was placed at the top and bottom of each column to retain the filter media within the tube. Flexible silicone tubing was attached to the syringe ends to provide influent and effluent lines, and the columns were attached to a frame to maintain a stable vertical orientation throughout the duration of the experiment.

3.2. Operation of small bore adsorption columns

A peristaltic pump with a variable speed motor was used to pump influent water, with an ortho-phosphorus (PO_4P) concentration of 1 mg L^{-1}, into the base of each small-bore adsorption column at an approximate flow rate of 202 ± 30 ml h^{-1}. The combination of using a low flow rate in up-flow mode, and the high ratio of the column diameter to adsorbent particle diameter was considered sufficient to preclude any channeling effects (Vijayaraghavan et al., 2004). The influent was prepared by adding a small quantity of K_2HPO_4 to tap water, with the resulting solution having a pH of 8.09 ± 0.37. The simple makeup of the influent precluded interfering chemical interactions, and phosphorus (P) was selected as an excellent example of a contaminant commonly targeted by adsorption filters; its precise quantification is also relatively simple and inexpensive. The pump was operated in 12 h on/off cycles to achieve loading periods of 24–156 h. The effluent from each column was collected in 2-h aliquots in separate containers using an auto-sampler. The effluent in each container was analyzed for dissolved PO_4-P using a nutrient analyzer (Konelab20, Thermo Clinical Lab systems, Finland) after APHA (1998) and the cumulative mass of P adsorbed by the filter media was calculated using Eqn. (1). The limit of detection was determined, after McNaught and Wilkinson (1997), to be 0.009 mg L^{-1}.

3.3. Preparation of full-scale filter units

The media which showed the highest and the lowest absorbencies in the small-bore column experiments – media A and media D, respectively – were studied in 0.65 m-deep laboratory filters with an internal diameter of 0.104 m. These filters were constructed in triplicate and were packed with filter media to a depth of 0.4 m from the bottom of each column. The free-board of 0.25 m in each column was to allow water to be poured onto the surface without spillage. As was the case in the small bore columns, the mass of media in each column was varied to achieve a packing density such that each of the columns had an approximate hydraulic conductivity of 0.14 cm s^{-1}.

3.4. Operation of full-scale filter units

The filter units were operated in a temperature-controlled room at 10 °C, and were subjected to repeated synthetic wastewater loadings over one to three months. The synthetic wastewater influent contained a PO_4-P concentration of 1 mg L^{-1}, and was loaded manually onto a baffle at the top of the filter media. Columns containing filter media D were loaded with 28 L of synthetic wastewater per loading event 10 times over the course of one month. Columns containing filter media A were loaded with 28 L of synthetic wastewater 17 times, and were subsequently loaded nine times with 56 L, in order to hasten the P saturation of the media. This loading was carried out over the space of three months. For both media, each loading event took place over a period of 1.5 h, and there was a minimum of one day's rest between each loading event.

3.5. Processing of experimental data

During each loading event, the effluent from the filter units was collected in large HDPE containers and was analyzed for PO_4-P using a nutrient analyzer (Konelab20, Thermo Clinical Lab systems, Finland) after APHA (1998). The mass of phosphorus adsorbed per unit mass of filter media was calculated using Eqn. 1, and a graph of cumulative q_e versus cumulative collected effluent volume, V, was constructed. The observed values of q_e were then compared to values predicted by models created using coefficients calculated from the data collected during small-scale adsorption column experiments.

3.6. Verification of model's adaptability to variances in operating conditions

In their 2013 paper, "Removal of phosphorus, fluoride and metals from a gypsum mining leachate using steel slag filters", Claveau-Mallet et al. (2013) provided a supplementary file containing concentration and pH data for effluents from columns which were being used to treat reconstituted gypsum mining leachate. In the study, a total of ten columns were operated as five

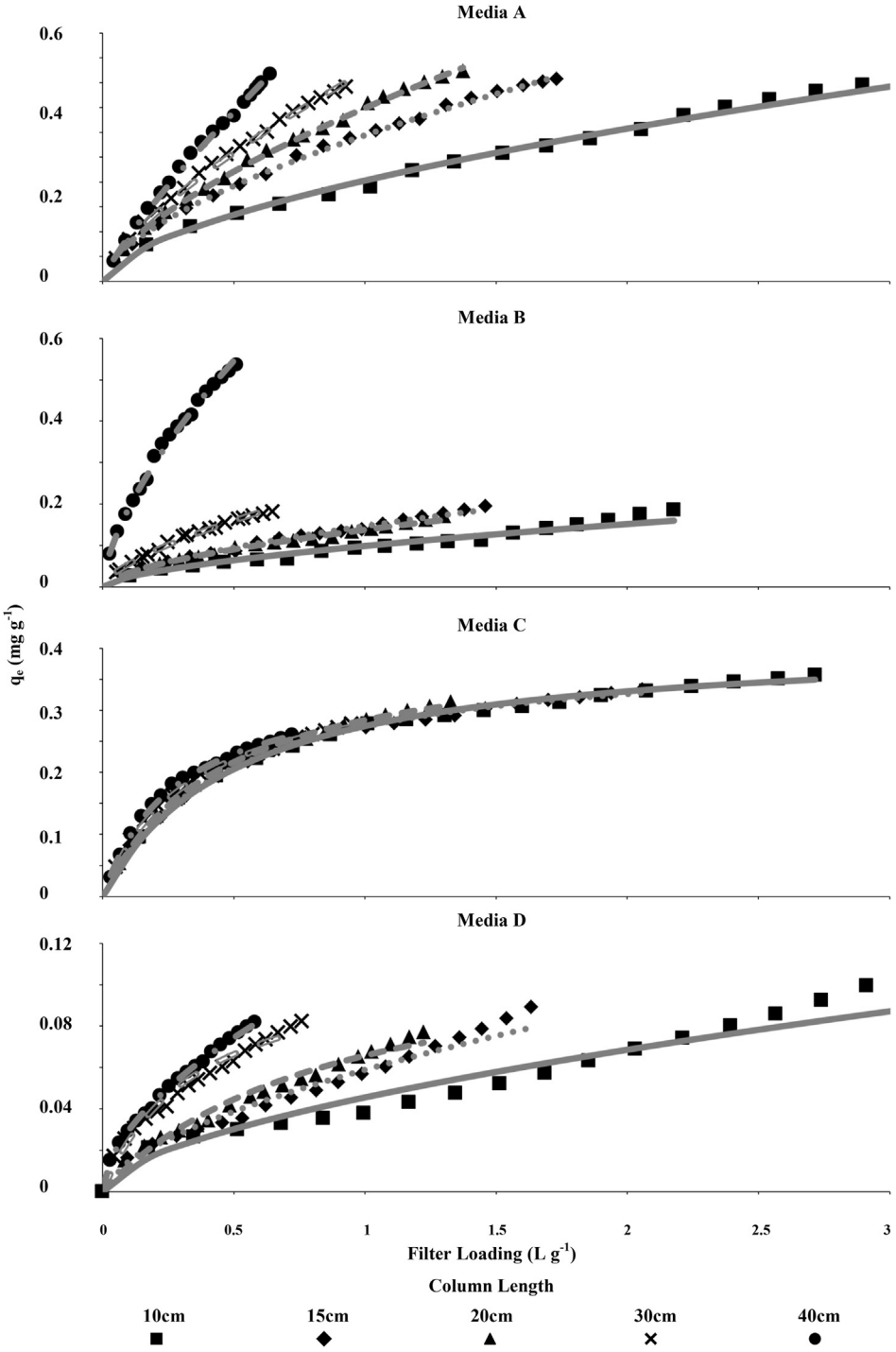

Fig. 1. Filter media P adsorption (y-axis) vs. filter loading (x-axis), showing observed progressions of media saturation and the goodness of model fit for each media and column length.

sets of two columns connected in series. These were continuously loaded with leachate for a period of 145–222 days, and effluent concentrations of fluoride (amongst other contaminants) were measured twice per week. Four of the columns were loaded with a low concentration leachate (L1), while the remaining six were fed with a higher concentration leachate (L2). The effluents of those columns fed with leachate L2 showed variations in pH of 4.15 ± 2, while those of columns fed with leachate L1 showed variations of 1.29 ± 0.67. Due to the effect that the large fluctuations in the pH of effluent from columns fed with leachate L2 had on the data, the model proposed in the current study was fit to the effluent fluoride concentration data from the columns fed with leachate L1. The columns were loaded continuously with an influent that had a fluoride concentration of 9 mg L^{-1}. Effluent fluoride concentrations were measured twice weekly, and using these data, averages of effluent concentration were used to determine the amount of fluoride removed by the filter media (q_e). Given that the columns were loaded at a continuous rate by a peristaltic pump, the volume

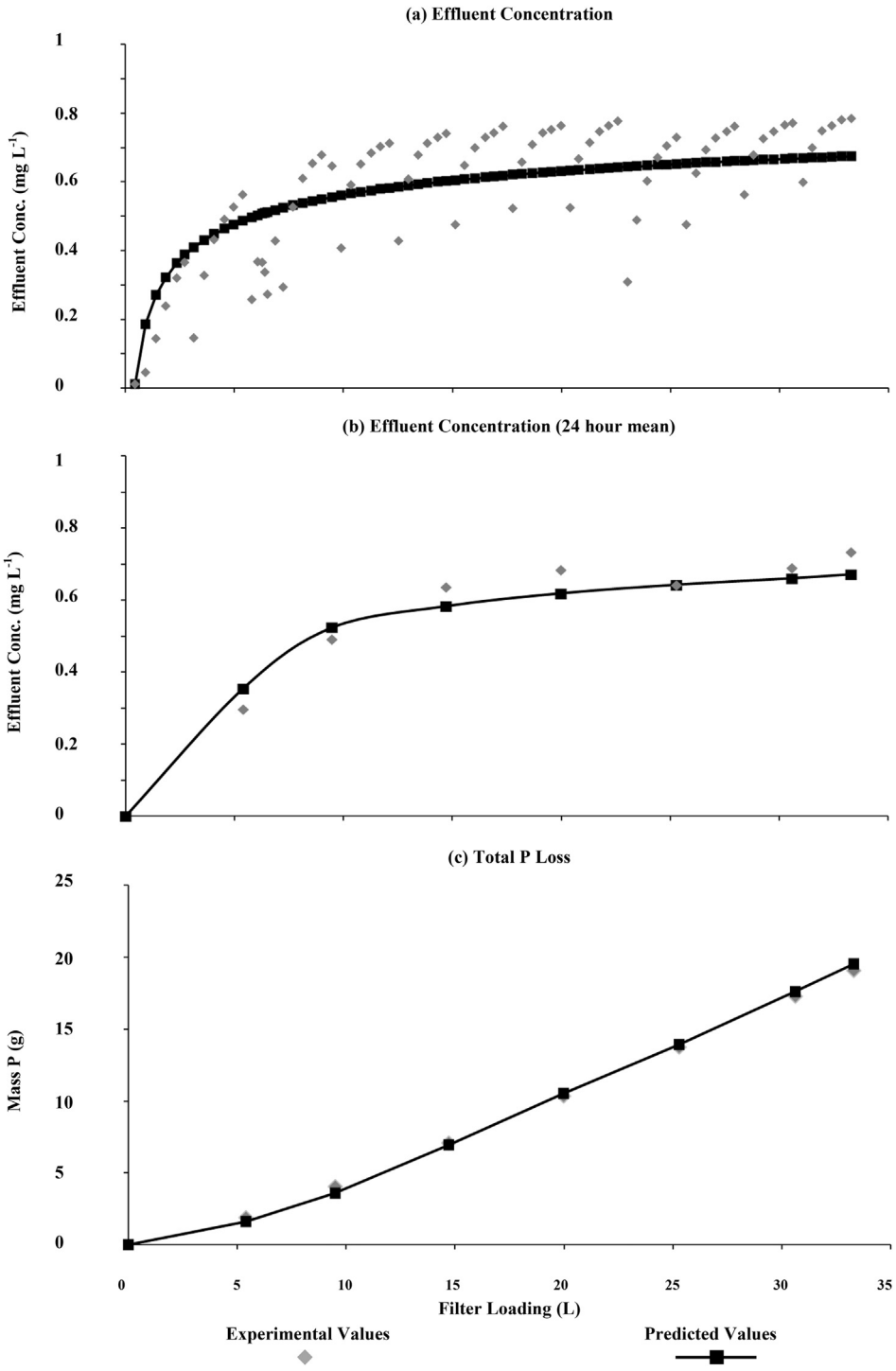

Fig. 2. **(a)** Comparison of predicted and observed progressions of effluent concentration (y-axis) vs. cumulative filter loading (x-axis), with predictions and observations made on a bi-hourly basis. **(b)** Comparison of predicted and observed daily mean effluent concentrations (y-axis) vs. cumulative filter loading (x-axis). **(c)** Comparison of predicted and observed cumulative P loss in effluent (y-axis) vs. cumulative filter loading (x-axis).

of leachate filtered (V) was taken to be analogous to the time (T) for which the columns were running (as $V = \alpha T$, where α is the flow rate in L day^{-1}), and a plot of q_e versus V was developed from which the model coefficients, A and B, were computed from plots of Eqn. (4), as described previously. The difficulties of modeling non-ideal breakthrough curves was discussed in detail by Sperlich et al. (2005), and to further validate our proposed model, a supplementary Excel file has been made available with this paper demonstrating our model's ability to describe and predict (using RSSCT data) the breakthrough curves observed in that study. The Excel file also contains a template to facilitate the fitting of our proposed model to other experimental data.

3.7. Determination of model error

The hybrid error function (HYBRID), developed by Porter et al.

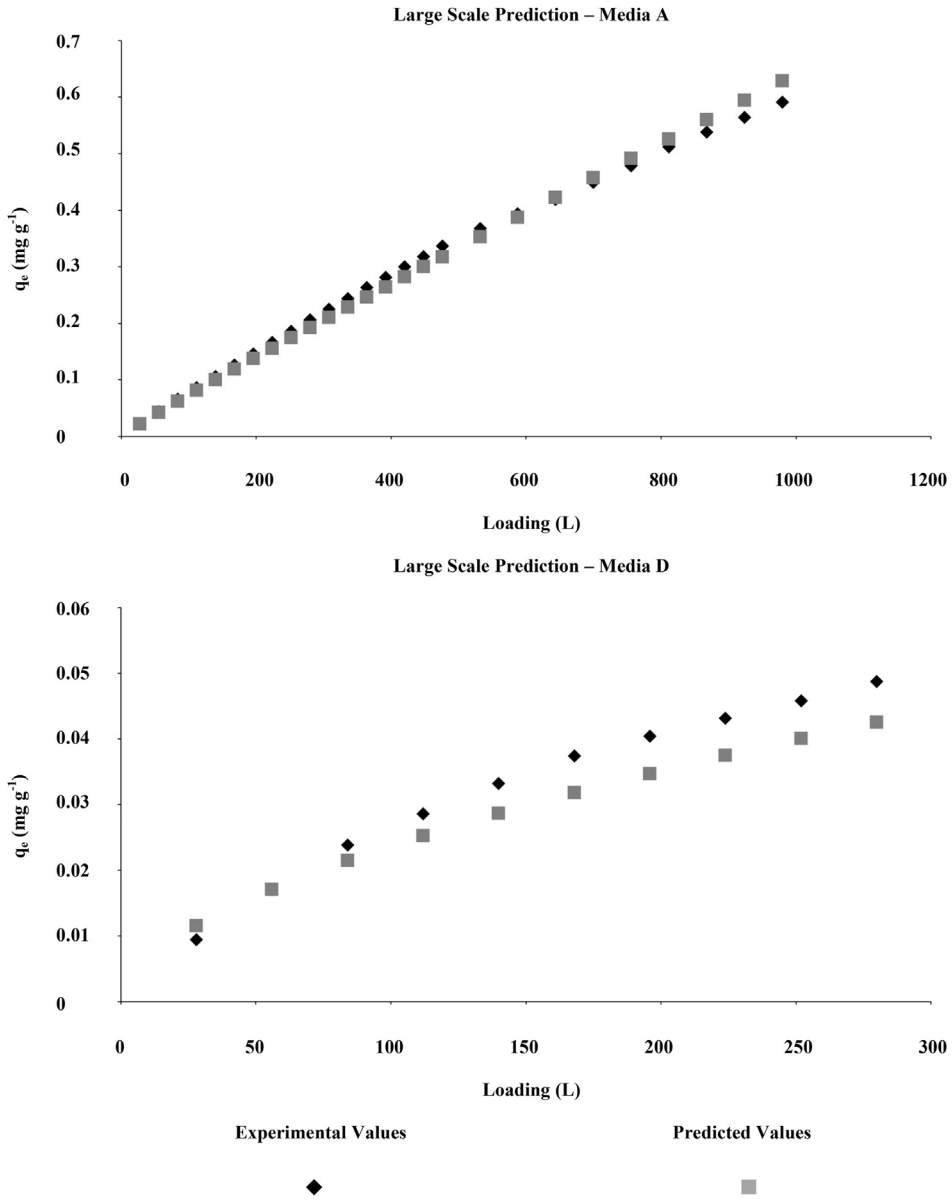

Fig. 3. Comparison of predicted and observed q_e values (y-axis) vs. filter loading (x-axis), demonstrating the ability of the proposed model to predict large-scale filter performance.

(1999), is a non-linear error function often employed when using non-linear regression methods to predict isotherm parameters. Chan et al. (2012) analyzed data relating to the adsorption of acid dyes onto charcoal, and of the five non-linear error functions studied, concluded that the HYBRID function was the most effective in determining isotherm parameters for the six isotherm equations used in their study. The HYBRID function was used in the current study as a metric for the comparison of the goodness of model fit to experimental data. The function is:

$$\frac{100}{n-p}\sum_{i=1}^{n}\frac{\left(q_{e,i,meas}-q_{e,i,calc}\right)^2}{q_{e,i,meas}} \tag{13}$$

where n is the number of experimental data points, p is the number of constants in the proposed model, $q_{e,i,meas}$ is the value of q_e obtained from Eqn. (1), and $q_{e,i,calc}$ is the value of q_e obtained from Eqn. (3). The mean percentage error (MPE) was also calculated to provide an easily comparable metric by which to assess the model's goodness of fit and its bias toward either over- or underestimation of predicted values compared to observed values. The MPE was calculated thus:

$$MPE = \frac{100\%}{n}\sum_{i=1}^{n}\frac{q_{e,i,meas}-q_{e,i,calc}}{q_{e,i,meas}} \tag{14}$$

where n, $q_{e,i,meas}$, and $q_{e,i,calc}$ are the same as given for Eqn. (13). A negative MPE indicates that the model predictions tend to underestimate experimentally observed adsorption, whereas a positive error indicates an overestimation.

4. Results and discussion

4.1. Verification of theory at bench scale

For all four of the media studied, the relationship between filter

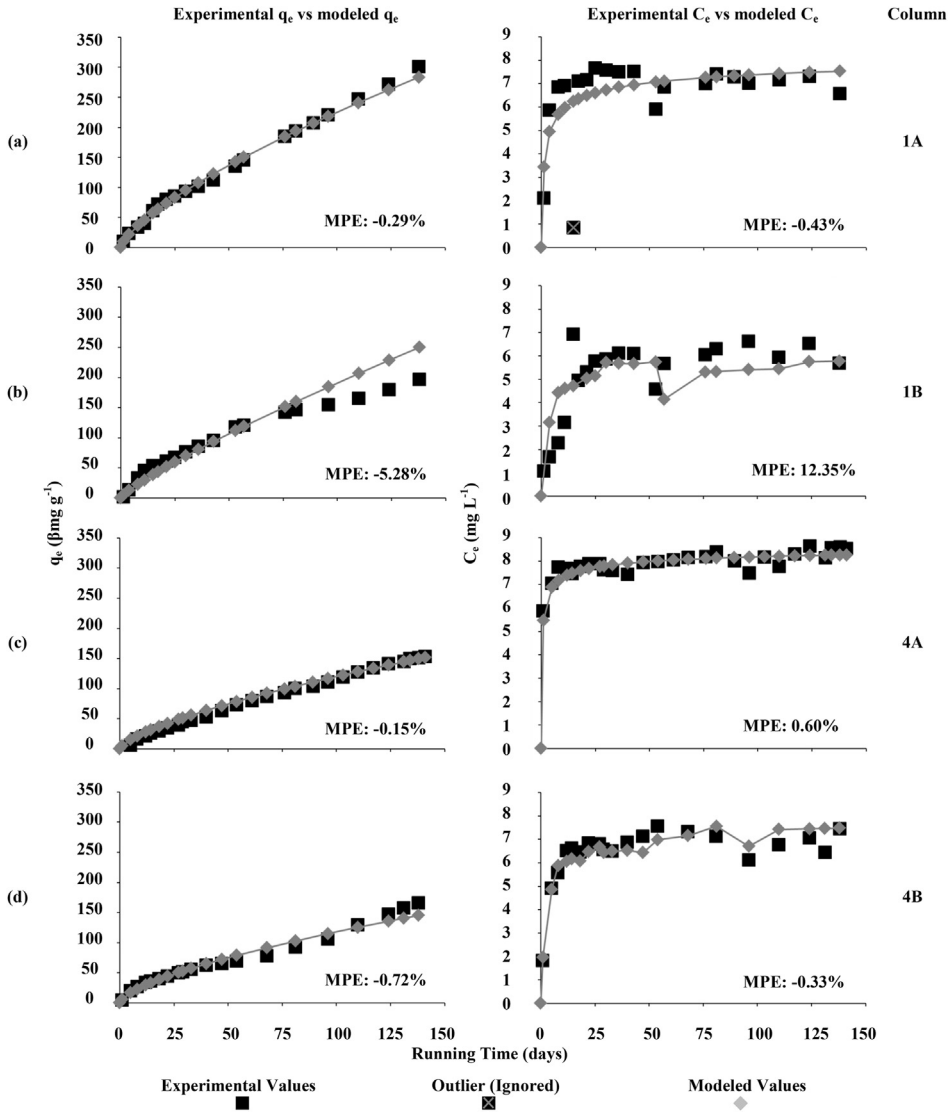

Fig. 4. (a-d) Goodness of model fit to fluoride removal data reported by Claveau-Mallet et al. (2013).

loading and the mass of P adsorbed per unit mass of filter media, q_e, could be estimated with a very high degree of accuracy by the proposed model (Eqn. (3)). Fig. 1 shows the goodness of fit of model predictions made using 36 h of experimental data. The model coefficients, along with the R^2 values of the linear plots from which they were determined, are shown in Table S1. The experimental data fitted the linear expression of the model with a very high degree of accuracy, and the average linear regression coefficients observed for media A, B, C, and D were 0.997, 0.991, 0.963 and 0.997, respectively.

A column containing media A was loaded for 68 h to study the effect of experimental runtime on the accuracy with which model coefficients could be determined. Revised estimates of model coefficients were determined from experimental data collected at 2-h increments, and a model using these coefficients was fitted to experimental data for the entirety of the period for which the filter was loaded. Figure S2a shows the HYBRID error of these models, against the time at which the model coefficients were determined. After an initial sharp drop-off in model error, there was little improvement in model fit past the 24-h mark. Figure S2b shows the goodness of fit to experimental data of models using coefficients determined after 24 and 36 h of data aggregation, demonstrating that there was little benefit to be gained from experimental run times in excess of 24 h.

To study the accuracy with which effluent concentration, average daily effluent concentration, and total P loss could be predicted, a small-bore adsorption column containing media A was operated for an extended period of 156 h. All filter effluent was collected in 2 h aliquots, and it was possible, using Eqn. (9), to predict the P concentration of any one of these aliquots at any given time. There were 12 h rest-periods in between loading cycles, and these cessations in filter loading appear to have allowed the filter media to replenish some of its adsorptive potential. Increased P uptake at the beginning of each loading phase resulted in the effluent concentrations producing the cyclical 6-point pattern seen in Fig. 2a, and this strongly suggests that intraparticle diffusion of P, driven by the concentration gradient within the media particles, resulted in rejuvenation of the media surface; this has also been observed by many others (DeMarco et al., 2003; Greenleaf and SenGupta, 2006; Sengupta and Pandit, 2011; Song et al., 2011). Model predictions of C_e describe the general trend of increasing effluent concentration with increasing volume well, though the

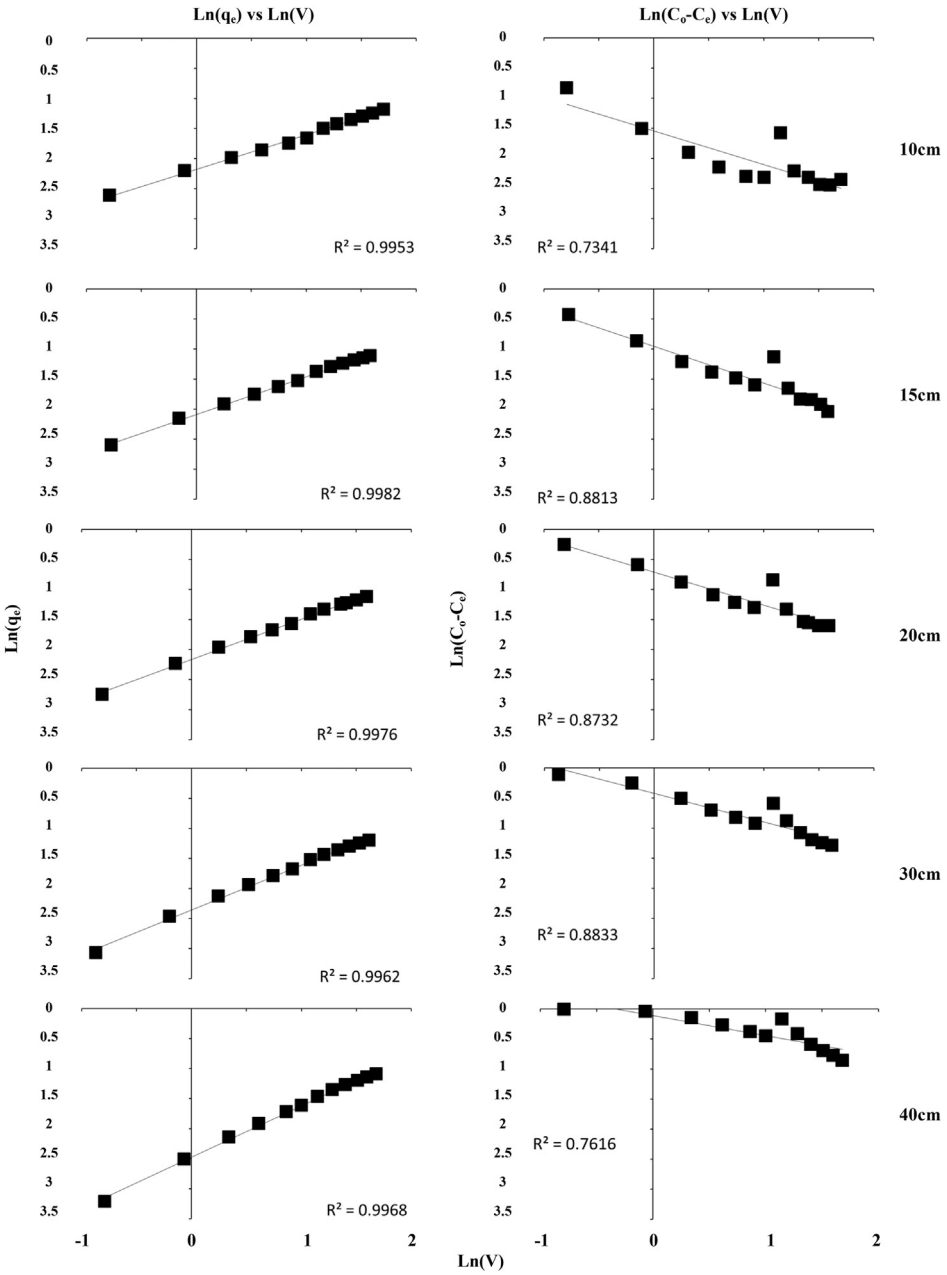

Fig. 5. Comparison of the linearity of plots of $Ln(q_e)$ (left y-axis) vs. Ln(V) (x-axis), and $Ln(C_o-C_e)$ (right y-axis) vs. Ln(V) (x-axis). These plots are used to determine model coefficients by analysis of filter saturation or filter effluent concentration respectively.

model does not describe the cyclical pattern described previously. However, as can be seen in Fig. 2b, it was possible to produce highly accurate model predictions of average daily effluent concentration; these values could be forecast with a mean error of just 0.59% ± 10.54%. Average daily effluent concentration is, arguably, a more useful metric for assessing the long-term performance of a filter media, and, as seen in Fig. 2c, predictions of cumulative P loss made using predicted average daily effluent concentration had a mean error of just 3.74% ± 8.31%.

To ensure the results of the small-bore column experiments were replicable, 20 cm columns packed with media A were operated in triplicate for a period of 24 h, and the model coefficients calculated from each column were compared. As can be seen in Figure S3a, the experimental data from each of the three columns fit the linear expression of the proposed model with a coefficient of determination, R^2, of 0.996 ± 0.001. The model coefficients were determined as A = 0.109 ± 0.003 and B = 1.480 ± 0.043. Figure S3b demonstrates the effect of this variability in coefficients on the models produced. After 24 h of operation, at which 0.5 L of effluent had been collected, the mean q_e predicted by substituting V = 5 L into Eqn. (3) was 0.320 ± 0.017 mg g^{-1}. The variability of model predictions being so slight would indicate that this method of determining model coefficients is highly replicable.

4.2. Verification of theory at filter-scale

Fig. 3 shows the experimental data from large-scale experiments overlain by predictions made using models created from the small-bore adsorption column data. In the case of filter media A, the model obtained from the 24 h small-bore adsorption study

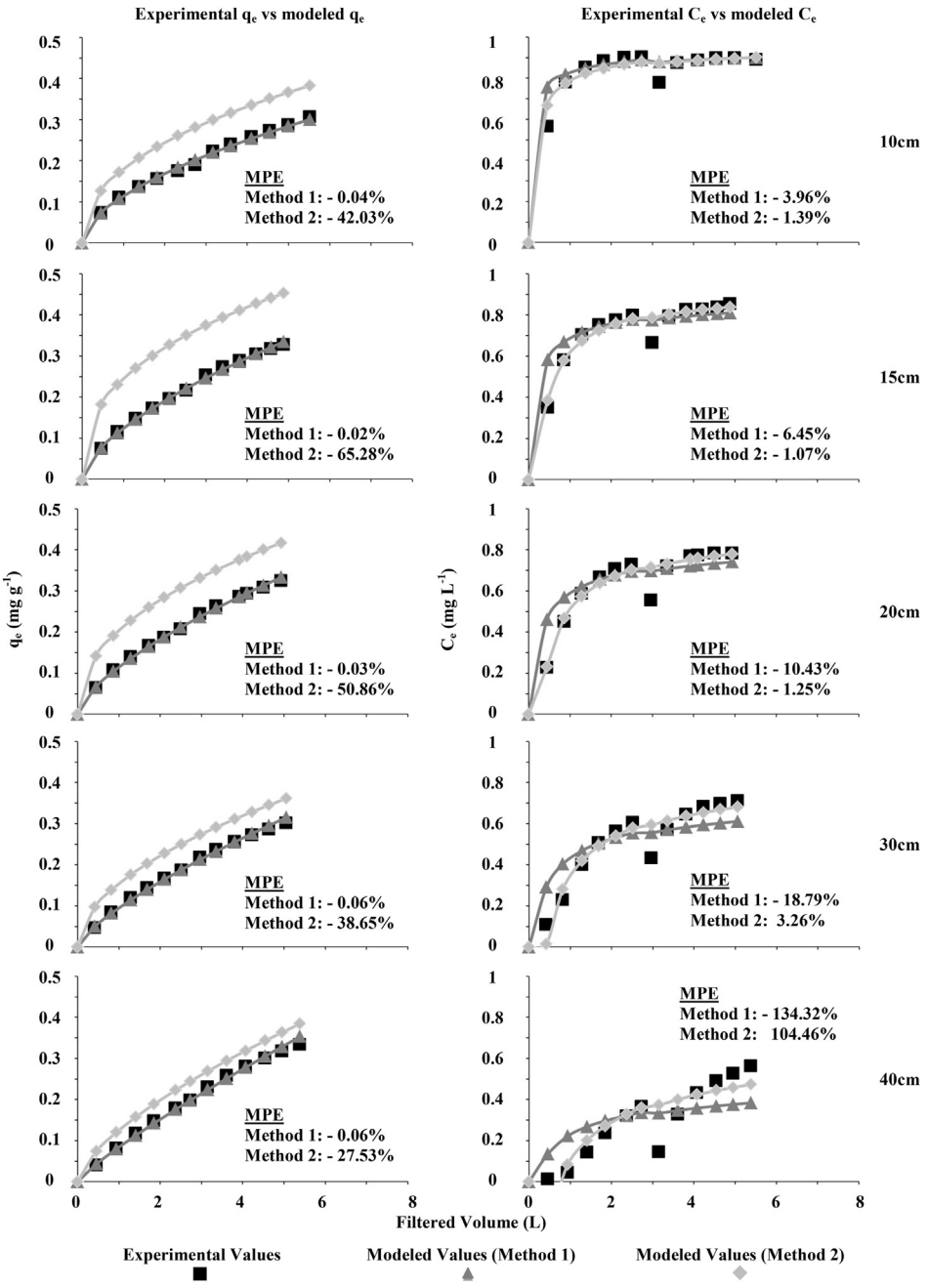

Fig. 6. Plots of q_e (left y-axis) and C_e (right y-axis) vs. filtered volume (x-axis), demonstrating the effect that the method of coefficient determination (ie analysis of filter saturation or analysis of filter effluent concentration) has on model accuracy.

predicted the performance of the full-scale filter unit over three months with a very high degree of accuracy. Predicted values of q_e differed from observed values by just 2.94% ± 4.31%, and the model fit the observed values with a HYBRID error of just 0.074. In the case of filter media D, predicted values of q_e differed from observed values by 8.08% ± 11.49%, and the model fit the observed values with a HYBRID error of just 0.070. It was thus demonstrated that, in terms of media mass and loading, scaling the experiment up by approximately two orders of magnitude had very little negative impact on the ability of the model to predict filter performance, appearing to confirm the hypothesis that a small-scale, 24-h experiment could be used to accurately predict large-scale filter performance over a much greater period. To further validate this assertion, RSSCT data from a study conducted by Sperlich et al. (2005) was used to construct a model which was then used to successfully predict the performance of a lab-scale filter that was over 700 times larger than the RSSCT in terms of filter media mass. This model and the data used in its construction can be found in the supplementary Excel file which has been made available with this paper.

4.3. Adaptability of model to varying conditions

Fig. 4 shows the model proposed by this study fit to fluoride removal data published by Claveau-Mallet et al. (2013). As can be seen, the model described the evolution of fluoride

concentrations in the filter effluent well for both those filters fed with a constant fluoride concentration of 9 mg L^{-1} (Fig. 4, 'A' Columns), and those fed with a variable concentration from the effluent of the preceding filter in a series (Fig. 4, 'B' Columns). This would appear to confirm the model's applicability to contaminants other than P, as well as to filter media other than those examined by this study. The complexity of the wastewater's composition did not appear to have a negative impact on the model's ability to describe the observed data, nor did continuous loading of the columns. Columns 1A, 1B, 4A, and 4B (Fig. 4) had HRTs of 14.2, 18.2, 4.8, and 4.3 h, respectively, though these variations in HRT appear to have had no significant impact on the goodness of model fit. Columns 1A and 4A were both loaded using wastewater with a constant fluoride concentration of 9 mg L^{-1}, while columns 1B and 4B were loaded with the effluents from columns 1A and 4A, thus receiving an influent with fluoride concentrations ranging from 0.85 to 7.66 and 5.86–8.63 mg L^{-1}, respectively. In general, higher MPEs were recorded for models fit to data from columns fed by an influent of varying concentration, and a greater variance in influent concentration resulted in a larger MPE. This would seem to indicate that variation in influent concentration had a negative impact on model fit, though with a maximum recorded MPE of 12.35% (Fig. 5b), the model appeared to cope well with this variability nonetheless.

4.4. Practical implications

To be of the greatest utility, a method of filter media characterisation must be easy to use, quick to execute, and should replicate the performance of a field-scale system as closely as possible (Limousin et al., 2007). Many field-scale adsorption systems are loaded intermittently, and it was hypothesized that for such a system, a model which attempted to describe and predict filter media saturation would be more successful than a model which attempted to model filter column effluent directly. The model proposed by this study can be linearized in two ways, and the coefficients required to produce the model can be determined from linear plots of q_e or C_e data using linear plots of $\ln q_e$ vs lnV (method 1) and $\ln(C_o - C_e)$ vs *ln*V (method 2), respectively. The former attempts to model media saturation, while the later attempts to model column effluent directly. The suitability of an equation to model an adsorption system can be judged by the R^2 correlation coefficient of its linear plot, and when there are multiple methods of linearizing an equation to obtain model coefficients (e.g. as with the Langmuir isotherm) the R^2 can be used to determine the better method (Behnamfard and Salarirad, 2009). As can be seen in Fig. 5, plots of $\ln q_e$ vs *ln*V produced graphs with higher linearity than plots of $\ln(C_o - C_e)$ vs *ln*V in all cases, suggesting that method 1 may be preferable to method 2. To further confirm this hypothesis, graphs of experimental data from small-bore columns containing filter media A were modeled using model coefficients determined using method 1 and method 2, respectively. Fig. 6 shows the comparison of these models and their goodness of fit to values of q_e and C_e obtained experimentally. As can be concluded from analysis of Fig. 6, coefficients determined using method 1 and method 2 described the evolution of filter effluent with similar accuracy, though method 2 gave marginally better accuracy. In contrast, method 1 was significantly better for producing accurate models of the evolution of filter saturation. This appears to confirm the hypothesis that to predict the performance of an intermittently loaded filter, modeling media saturation is a more successful approach than attempting to model filter effluent concentrations directly.

5. Conclusions

This study proposed a model capable of describing the non-ideal (i.e. non s-shaped, linear to convex) breakthrough curves often described by data from column experiments using low-cost adsorbents and soils.

- It was demonstrated that the model could be used to describe and predict the performance of multiple low-cost filter media, which were intermittently loaded with a wastewater containing 1 mg L^{-1} of PO_4P.
- The model was fit to data from two independent studies, demonstrating its ability to describe the removal of contaminants other than phosphorus (fluoride and arsenate), and its adaptability to continuous loading conditions, complex wastewater compositions, and variations in HRT.
- It was shown that model parameters could be determined experimentally from both filter effluent data and media saturation data, with the latter approach being more successful when modeling intermittently loaded filters.
- The model was successfully used to predict the performance of lab-scale filter columns which were intermittently loaded over the course of a number of months.
- The model parameters required to predict the performance of the lab-scale filters were determined using data aggregated over a 24 h period using small-scale column tests.

Acknowledgement

The first author would like to acknowledge the Irish Research Council (GOIPG/2013/75) for funding.

Appendix A. Supplementary data

Supplementary data related to this article can be found at http://dx.doi.org/10.1016/j.watres.2016.05.093.

References

Ádám, K., Sovik, A.K., Krogstad, T., Heistad, A., 2007. Phosphorous removal by the filter materials light-weight aggregates and shellsand-a review of processes and experimental set-ups for improved design of filter systems for wastewater treatment. Vatten 63, 245.

Ali, I., Gupta, V.K., 2007. Advances in water treatment by adsorption technology. Nat. Protoc. 1, 2661–2667. http://dx.doi.org/10.1038/nprot.2006.370.

Allen, S.J., Mckay, G., Porter, J.F., 2004. Adsorption isotherm models for basic dye adsorption by peat in single and binary component systems. J. Colloid Interface Sci. 280, 322–333. http://dx.doi.org/10.1016/j.jcis.2004.08.078.

APHA (American Public Health Association), American Water Works Association, Water Environment Federation, 1998. Standard Methods for the Examination of Water and Wastewater. American Public Health Association, Washington, DC.

Babel, S., Kurniawan, T.A., 2003. Low-cost adsorbents for heavy metals uptake from contaminated water: a review. J. Hazard. Mater 97, 219–243. http://dx.doi.org/10.1016/S0304-3894(02)00263-7.

Behnamfard, A., Salarirad, M.M., 2009. Equilibrium and kinetic studies on free cyanide adsorption from aqueous solution by activated carbon. J. Hazard. Mater 170, 127–133. http://dx.doi.org/10.1016/j.jhazmat.2009.04.124.

Bohart, G.S., Adams, E.Q., 1920. Some aspects of the behavior of charcoal with respect to chlorine. 1. J. Am. Chem. Soc. 42, 523–544. http://dx.doi.org/10.1021/ja01448a018.

Brix, H., Arias, C.A., Del Bubba, M., 2001. Media selection for sustainable phosphorus removal in subsurface flow constructed wetlands. Water Sci. Technol. 44, 47–54.

Buergisser, C.S., Cernik, M., Borkovec, M., Sticher, H., 1993. Determination of nonlinear adsorption isotherms from column experiments: an alternative to batch studies. Environ. Sci. Technol. 27, 943–948. http://dx.doi.org/10.1021/es00042a018.

Chan, L.S., Cheung, W.H., Allen, S.J., McKay, G., 2012. Error analysis of adsorption isotherm models for acid dyes onto bamboo derived activated carbon. Chin. J. Chem. Eng. 20, 535–542.

Clark, R.M., 1987. Evaluating the cost and performance of field-scale granular activated carbon systems. Environ. Sci. Technol. 21, 573–580. http://dx.doi.org/10.1021/es00160a008.

Claveau-Mallet, D., Wallace, S., Comeau, Y., 2013. Removal of phosphorus, fluoride and metals from a gypsum mining leachate using steel slag filters. Water Res. 47, 1512–1520. http://dx.doi.org/10.1016/j.watres.2012.11.048.
Cooney, D.O., 1998. Adsorption Design for Wastewater Treatment. CRC Press.
Crini, G., 2006. Non-conventional low-cost adsorbents for dye removal: a review. Bioresour. Technol. 97, 1061–1085.
Crini, G., Badot, P.-M., 2008. Application of chitosan, a natural aminopolysaccharide, for dye removal from aqueous solutions by adsorption processes using batch studies: a review of recent literature. Prog. Polym. Sci. 33, 399–447. http://dx.doi.org/10.1016/j.progpolymsci.2007.11.001.
Crittenden, J.C., Reddy, P.S., Arora, H., Trynoski, J., Hand, D.W., Perram, D.L., Summers, R.S., 1991. Predicting GAC performance with rapid small-scale column tests. J. Am. Water Works Assoc. 83, 77–87.
Cucarella, V., Renman, G., 2009. Phosphorus sorption capacity of filter materials used for on-site wastewater treatment determined in batch experiments-a comparative study. J. Environ. Qual. 38, 381–392. http://dx.doi.org/10.2134/jeq2008.0192.
Deliyanni, E.A., Peleka, E.N., Matis, K.A., 2009. Modeling the sorption of metal ions from aqueous solution by iron-based adsorbents. J. Hazard. Mater 172, 550–558. http://dx.doi.org/10.1016/j.jhazmat.2009.07.130.
DeMarco, M.J., SenGupta, A.K., Greenleaf, J.E., 2003. Arsenic removal using a polymeric/inorganic hybrid sorbent. Water Res. 37, 164–176. http://dx.doi.org/10.1016/S0043-1354(02)00238-5.
Demirbas, A., 2008. Heavy metal adsorption onto agro-based waste materials: a review. J. Hazard. Mater 157, 220–229. http://dx.doi.org/10.1016/j.jhazmat.2008.01.024.
Drizo, A., Comeau, Y., Forget, C., Chapuis, R.P., 2002. Phosphorus saturation potential: a parameter for estimating the longevity of constructed wetland systems. Environ. Sci. Technol. 36, 4642–4648.
Freundlich, 1906. Uber die adsorption in losungen. Z. Für Phys. Chem. 57, 384–470.
Greenleaf, J.E., SenGupta, A.K., 2006. Environmentally benign hardness removal using ion-exchange fibers and snowmelt. Environ. Sci. Technol. 40, 370–376. http://dx.doi.org/10.1021/es051702x.
Grolimund, D., Borkovec, M., Federer, P., Sticher, H., 1995. Measurement of sorption isotherms with flow-through reactors. Environ. Sci. Technol. 29, 2317–2321. http://dx.doi.org/10.1021/es00009a025.
Hamdaoui, O., Naffrechoux, E., 2007. Modeling of adsorption isotherms of phenol and chlorophenols onto granular activated carbon: Part II. Models with more than two parameters. J. Hazard. Mater 147, 401–411.
Han, R., Zou, W., Li, H., Li, Y., Shi, J., 2006. Copper(II) and lead(II) removal from aqueous solution in fixed-bed columns by manganese oxide coated zeolite. J. Hazard. Mater 137, 934–942. http://dx.doi.org/10.1016/j.jhazmat.2006.03.016.
Healy, M.G., Rodgers, M., Mulqueen, J., 2007. Treatment of dairy wastewater using constructed wetlands and intermittent sand filters. Bioresour. Technol. 98, 2268–2281. http://dx.doi.org/10.1016/j.biortech.2006.07.036.
Hutchins, R., 1973. New method simplifies design of activated carbon systems, water bed depth service time analysis. J. Chem. Eng. Lond 81, 133–138.
Johansson, L., 1999. Blast furnace slag as phosphorus sorbents — column studies. Sci. Total Environ. 229, 89–97. http://dx.doi.org/10.1016/S0048-9697(99)00072-8.
Jusoh, A., Su Shiung, L., Ali, N., Noor, M.J.M.M., 2007. A simulation study of the removal efficiency of granular activated carbon on cadmium and lead. Desalination 206, 9–16. http://dx.doi.org/10.1016/j.desal.2006.04.048. EuroMed 2006 Conference on Desalination Strategies in South Mediterranean Countries.
Limousin, G., Gaudet, J.-P., Charlet, L., Szenknect, S., Barthès, V., Krimissa, M., 2007. Sorption isotherms: a review on physical bases, modeling and measurement. Appl. Geochem 22, 249–275. http://dx.doi.org/10.1016/j.apgeochem.2006.09.010.
Malkoc, E., Nuhoglu, Y., Abali, Y., 2006. Cr(VI) adsorption by waste acorn of Quercus ithaburensis in fixed beds: prediction of breakthrough curves. Chem. Eng. J. 119, 61–68. http://dx.doi.org/10.1016/j.cej.2006.01.019.
Mauclaire, L., Schürmann, A., Mermillod-Blondin, F., 2006. Influence of hydraulic conductivity on communities of microorganisms and invertebrates in porous media: a case study in drinking water slow sand filters. Aquat. Sci. 68, 100–108. http://dx.doi.org/10.1007/s00027-005-0811-4.
McKay, 1996. Use of Adsorbents for the Removal of Pollutants from Wastewaters. CRC Press, Boca Raton, London.
McNaught, A.D., Wilkinson, A., 1997. Compendium of Chemical Terminology. Blackwell Science Oxford.
Netpradit, S., Thiravetyan, P., Towprayoon, S., 2004. Evaluation of metal hydroxide sludge for reactive dye adsorption in a fixed-bed column system. Water Res. 38, 71–78. http://dx.doi.org/10.1016/j.watres.2003.09.007.
Ouvrard, S., Simonnot, M.-O., de Donato, P., Sardin, M., 2002. Diffusion-controlled adsorption of arsenate on a natural manganese oxide. Ind. Eng. Chem. Res. 41, 6194–6199. http://dx.doi.org/10.1021/ie020269m.
Pant, H.K., Reddy, K.R., Lemon, E., 2001. Phosphorus retention capacity of root bed media of sub-surface flow constructed wetlands. Ecol. Eng. 17, 345–355. http://dx.doi.org/10.1016/S0925-8574(00)00134-8.
Porter, J.F., McKay, G., Choy, K.H., 1999. The prediction of sorption from a binary mixture of acidic dyes using single- and mixed-isotherm variants of the ideal adsorbed solute theory. Chem. Eng. Sci. 54, 5863–5885. http://dx.doi.org/10.1016/S0009-2509(99)00178-5.
Pratt, C., Parsons, S.A., Soares, A., Martin, B.D., 2012. Biologically and chemically mediated adsorption and precipitation of phosphorus from wastewater. Curr. Opin. Biotechnol 23, 890–896. http://dx.doi.org/10.1016/j.copbio.2012.07.003. Phosphorus biotechnology • Pharmaceutical biotechnology.
Rodgers, M., Mulqueen, J., Healy, M.G., 2004. Surface clogging in an intermittent stratified sand filter. Soil Sci. Soc. Am. J. 68, 1827–1832.
Rodgers, M., Healy, M.G., Mulqueen, J., 2005. Organic carbon removal and nitrification of high strength wastewaters using stratified sand filters. Water Res. 39, 3279–3286. http://dx.doi.org/10.1016/j.watres.2005.05.035.
Sengupta, S., Pandit, A., 2011. Selective removal of phosphorus from wastewater combined with its recovery as a solid-phase fertilizer. Water Res. 45, 3318–3330. http://dx.doi.org/10.1016/j.watres.2011.03.044.
Seo, D.C., Cho, J.S., Lee, H.J., Heo, J.S., 2005. Phosphorus retention capacity of filter media for estimating the longevity of constructed wetland. Water Res. 39, 2445–2457. http://dx.doi.org/10.1016/j.watres.2005.04.032.
Sheindorf, C.H., Rebhun, M., Sheintuch, M., 1981. A Freundlich-type multicomponent isotherm. J. Colloid Interface Sci. 79, 136–142.
Song, X., Pan, Y., Wu, Q., Cheng, Z., Ma, W., 2011. Phosphate removal from aqueous solutions by adsorption using ferric sludge. Desalination 280, 384–390. http://dx.doi.org/10.1016/j.desal.2011.07.028.
Søvik, A.K., Kløve, B., 2005. Phosphorus retention processes in shell sand filter systems treating municipal wastewater. Ecol. Eng. 25, 168–182. http://dx.doi.org/10.1016/j.ecoleng.2005.04.007.
Sperlich, A., Werner, A., Genz, A., Amy, G., Worch, E., Jekel, M., 2005. Breakthrough behavior of granular ferric hydroxide (GFH) fixed-bed adsorption filters: modeling and experimental approaches. Water Res. 39, 1190–1198. http://dx.doi.org/10.1016/j.watres.2004.12.032.
Thomas, H.C., 1944. Heterogeneous ion exchange in a flowing system. J. Am. Chem. Soc. 66, 1664–1666. http://dx.doi.org/10.1021/ja01238a017.
Thomas, W.J., Crittenden, B.D., 1998. Adsorption Technology and Design. Butterworth-Heinemann.
Ulén, B., Etana, A., 2010. Risk of phosphorus leaching from low input grassland areas. Geoderma 158, 359–365. http://dx.doi.org/10.1016/j.geoderma.2010.06.003.
Vidon, P., Allan, C., Burns, D., Duval, T.P., Gurwick, N., Inamdar, S., Lowrance, R., Okay, J., Scott, D., Sebestyen, S., 2010. Hot spots and hot moments in riparian zones: potential for improved water quality management 1. JAWRA J. Am. Water Resour. Assoc. 46, 278–298. http://dx.doi.org/10.1111/j.1752-1688.2010.00420.x.
Vijayaraghavan, K., Jegan, J., Palanivelu, K., Velan, M., 2004. Removal of nickel(II) ions from aqueous solution using crab shell particles in a packed bed up-flow column. J. Hazard. Mater 113, 223–230. http://dx.doi.org/10.1016/j.jhazmat.2004.06.014.
Vohla, C., Kõiv, M., Bavor, H.J., Chazarenc, F., Mander, Ü., 2011. Filter materials for phosphorus removal from wastewater in treatment wetlands—a review. Ecol. Eng. 37, 70–89. http://dx.doi.org/10.1016/j.ecoleng.2009.08.003. Special Issue: Enhancing ecosystem services on the landscape with created, constructed and restored wetlands.
Walker, G.M., Weatherley, L.R., 1997. Adsorption of acid dyes on to granular activated carbon in fixed beds. Water Res. 31, 2093–2101. http://dx.doi.org/10.1016/S0043-1354(97)00039-0.
Yagub, M.T., Sen, T.K., Afroze, S., Ang, H.M., 2014. Dye and its removal from aqueous solution by adsorption: a review. Adv. Colloid Interface Sci. 209, 172–184. http://dx.doi.org/10.1016/j.cis.2014.04.002.
Yoon, Y.H., Nelson, J.H., 1984. Application of gas adsorption kinetics I. A theoretical model for respirator cartridge service life. Am. Ind. Hyg. Assoc. J. 45, 509–516. http://dx.doi.org/10.1080/15298668491400197.

Appendix C

Water Research 123 (2017) 556–568

Contents lists available at ScienceDirect

Water Research

journal homepage: www.elsevier.com/locate/watres

Predicting the propagation of concentration and saturation fronts in fixed-bed filters

O. Callery, M.G. Healy*

Civil Engineering, National University of Ireland, Galway, Co., Galway, Ireland

ARTICLE INFO

Article history:
Received 28 February 2017
Received in revised form
27 June 2017
Accepted 4 July 2017
Available online 5 July 2017

Keywords:
Low-cost adsorbents
Adsorption
Phosphorus
Wastewater treatment

ABSTRACT

The phenomenon of adsorption is widely exploited across a range of industries to remove contaminants from gases and liquids. Much recent research has focused on identifying low-cost adsorbents which have the potential to be used as alternatives to expensive industry standards like activated carbons. Evaluating these emerging adsorbents entails a considerable amount of labor intensive and costly testing and analysis. This study proposes a simple, low-cost method to rapidly assess the potential of novel media for potential use in large-scale adsorption filters. The filter media investigated in this study were low-cost adsorbents which have been found to be capable of removing dissolved phosphorus from solution, namely: i) aluminum drinking water treatment residual, and ii) crushed concrete. Data collected from multiple small-scale column tests was used to construct a model capable of describing and predicting the progression of adsorbent saturation and the associated effluent concentration breakthrough curves. This model was used to predict the performance of long-term, large-scale filter columns packed with the same media. The approach proved highly successful, and just 24–36 h of experimental data from the small-scale column experiments were found to provide sufficient information to predict the performance of the large-scale filters for up to three months.

1. Introduction

Adsorbents are used to remove contaminants from gases and liquids across a diverse range of industries including manufacturing, agriculture, mining, and the treatment of both drinking water and municipal wastewater (Dąbrowski, 2001). These industries are naturally interested achieving optimum treatment efficiency with minimal investment, and there has been a growing interest in 'low-cost adsorbents', which are emerging as alternatives to more expensive and well-established adsorbents such as activated carbons (Babel and Kurniawan, 2003; Crini, 2006). The term 'low-cost adsorbent' can be used to describe any abundantly available natural material, industrial byproduct, or waste material which, with minimal processing, has suitable physical and chemical properties to allow for its use in the adsorption of some contaminant of interest (Bailey et al., 1999). Such media often display lower adsorption affinities and saturation capacities than well-established adsorbents, like activated carbons and synthetic resins, but they can nonetheless replace these ostensibly 'better' media with the introduction of minor modifications to adsorption treatment processes (Brown et al., 2000; Reddad et al., 2002) - for example, increasing the hydraulic residence time of a filter bed or increasing the adsorbent dose in a batch reactor. Therefore, despite the fact that low-cost adsorbents often display less favorable adsorption characteristics, their use is nonetheless a highly attractive option because of their ability to ultimately achieve equal treatment efficacy to established adsorbents, but at a greatly reduced cost.

The interaction between an adsorbent material and a dissolved contaminant is a highly complex one, influenced by a multitude of factors such as the physicochemical properties of the adsorbent and target adsorbate (Bockris et al., 1995), the composition and pH of the solution matrix (Faust and Aly, 1998), and the contact mechanism (i.e. batch or through-flow) between adsorbent and adsorbate (Goel et al., 2005). The complexity of these interactions makes characterizing the adsorptive properties of a medium for a given contaminant a vital first step in assessing its suitability for any intended treatment process. As low-cost adsorbents are often derived from locally sourced natural materials, industrial by-products, and waste materials, there is an inherent variability in

* Corresponding author.
E-mail address: mark.healy@nuigalway.ie (M.G. Healy).

http://dx.doi.org/10.1016/j.watres.2017.07.010
0043-1354/

Nomenclature

a	Time constant in Eqn. (6)/Eqn. (13)
a*	Time constant in Eqn. (7)/Eqn. (14)
a**	Time constant in Eqn. (8)/Eqn. (15)
A	Constant of proportionality in Eqn. (12) (mg g^{-1})
B	Constant of system heterogeneity in Eqn. (12)
C	Sorbate concentration in bulk solution (mg L^{-1})
C_b	Breakthrough concentration (mg L^{-1})
C_e	Sorbate concentration of filter effluent (mg L^{-1})
C_o	Sorbate concentration of filter influent (mg L^{-1})
k_{BA}	Bohart-Adams rate constant (L mg^{-1} min^{-1})
M	Mass of adsorbent (g)
N	Residual sorption capacity of bed (mg L^{-1})
N′	Fractional residual sorption capacity (N/N_o)
N_o	Sorption capacity of bed at equilibrium (mg L^{-1})
N_t	Time dependent sorption capacity of bed (mg L^{-1})
Q	Filter loading rate (L min^{-1})
q_e	Equilibrium sorbate concentration per unit mass of adsorbent (mg g^{-1})
q_t	Time dependent sorbate concentration per unit mass of adsorbent (mg g^{-1})
t	Service time/operating time of bed (min)
t_b	Service time/operating time of bed at breakthrough (i.e. when $C_e = C_b$) (min)
U	Flow velocity of solution past adsorbent (cm min^{-1})
V	Volume of solution filtered (L)
V_B	Empty bed volumes of solution filtered
V_x	Filter-bed volume to a bed depth of 'x'(L)
Z	Filter bed depth (cm)

their physical structure and chemical composition; no two low-cost adsorbents are exactly alike, and consequently, no two adsorbents will display identical adsorption characteristics. This problem is exacerbated by the fact that there is equal variability in waste streams, and hence there results an unavoidable necessity to characterize and assess every low-cost medium with respect to every potential use.

This poses a significant challenge to researchers, as there is a substantial amount of work involved in characterizing an adsorptive medium prior to its utilization in a real world application. Batch studies, capable of providing a rough approximation of a medium's adsorptive properties, are a common first step in media characterization, and these are an attractive option by virtue of their being cheap and easy to perform, with experimental methods being well established and results being easy to interpret (Crini and Badot, 2008). The primary disadvantage is that batch experimental conditions are radically different to through-flow conditions in real world filter-beds. These studies are, for this reason, unable to provide sufficient information to allow for the design of full-scale adsorption filters (Søvik and Kløve, 2005). Accordingly, when media are to be used in filter-beds, large-scale field studies are widely considered to be the most reliable method of assessing their potential (Pratt et al., 2012). Such tests provide excellent insight into the behavior of real-world adsorption systems; however, the propriety of conducting such large-scale and costly investigations is questionable when using untested and unproven materials. The limitations of both batch studies and large-scale column studies have made rapid small-scale column tests (RSSCTs), of the kind proposed by Crittenden et al. (1986, 1987), an ideal option for initial media characterization, and it has been repeatedly demonstrated that such tests can provide excellent predictions as to the performances of real-world filter units (Crittenden et al., 1991). RSSCTs involve the use of scaling equations to select media particle sizes, hydraulic loading rates, and empty bed contact times (EBCT, defined as the empty bed volume divided by the flow rate) which will ensure exact similarity of operation between small- and large-scale adsorption filters. Providing exact similitude is achieved, the breakthrough curve (BTC) observed when operating a small-scale filter column should match that of a large-scale filter almost exactly. The advantages of RSSCT type experiments are numerous; they are fast and inexpensive to perform, they require minimal quantities of both adsorbent and adsorbate solution, and perhaps most importantly, they investigate the interaction between adsorbent and adsorbate under through-flow conditions which are representative of intended field conditions, providing insight into both adsorption capacity and kinetics simultaneously. The primary drawback of RSSCTs is that they only make reliable predictions for the very specific case for which they were designed; a single RSSCT corresponds to only one large-scale filter operated in an exactly similar manner (in terms of loading rate and empty bed contact time etc). Also, while it is easy to obtain different particle sizes of activated carbon (the material for which the RSSCT methodology was originally proposed), it may not be possible to scale down many low-cost media due to their physical characteristics.

Mathematical models provide a means by which to make theoretical predictions for any fixed-bed system, and there are a great many mathematical models which have been developed in an attempt to predict the breakthrough behavior of adsorptive media. Xu et al. (2013) summarized some of the most widely used of these in a recent review, listing, amongst others, the Thomas model (Thomas, 1944), the Bohart-Adams (B-A) model (Bohart and Adams, 1920), and the Bed Depth Service Time (BDST) model (Hutchins, 1973). It is interesting to note that the B-A model is often erroneously referred to as the Thomas model; this has caused considerable confusion (Chu, 2010), even though the former predates the latter by a considerable margin. The B-A model is also the basis of the popular BDST model proposed by Hutchins (1973), which is, essentially, just a simplified rearrangement of the B-A model. It therefore seems reasonable to assert that the B-A model is quite possibly the most popular fixed-bed sorption model in current use. The basic form of the B-A model is as follows:

$$ln\left(\frac{C_O}{C_b}-1\right)=ln\left[exp\left(k_{BA}N_O\frac{Z}{U}\right)-1\right]-k_{BA}C_Ot_b \quad (1)$$

Where C_o is the influent concentration, C_b is the effluent breakthrough concentration at any time, t_b; K_{BA} is a kinetic constant associated with the B-A model, N_o is the adsorptive capacity of the medium per unit volume of the bed, Z is the depth of medium in the filter bed, and U is the linear flow velocity.

In practice, $\exp(K_{BA}N_oZ/U)$ is often much larger than one (Al-Degs et al., 2009), and the equation can therefore be simplified by ignoring the unity term on the right hand side of Eqn. (1) to yield:

$$ln\left(\frac{C_O}{C_b}-1\right)=k_{BA}N_O\frac{Z}{U}-k_{BA}C_Ot_b \quad (2)$$

As stated earlier, Hutchins' BDST model is based on a rearrangement of the simplified B-A equation (Eqn. (2)), and proposes a linear relationship between filter-bed depth and filter service time to a given breakthrough concentration. The time to any

breakthrough concentration is found by rearranging Eqn. (2) into form t = mx + c, to yield Hutchins' BDST equation (Hutchins, 1973) as follows:

$$t_b = \frac{N_o}{C_o U} z - \frac{1}{K_{BA} C_o} ln\left(\frac{C_o}{C_b} - 1\right) \quad (3)$$

Mathematical modelling offers more versatility in terms of predicting a wide range of potential fixed-bed arrangements, though this is arguably at the cost of the certainty and reliability that predictions based on experimental observations provide. It would therefore seem logical that a combination of both experimental observation and mathematical modelling would hold promise - providing the versatility of mathematical modelling as well as the certainty associated with experimental results. The BDST modeling approach is a widely implemented example of such a procedure. The BDST approach to filter design involves using experimental data from a number of filter columns to determine the coefficients N_o and K_{BA} in Eqn. (3). The BDST model then allows for designers to use interpolation and extrapolation to make predictions as to the behavior of adsorption systems with different flow rates, bed depths, and influent concentrations to those used to obtain the model coefficients.

The BDST model does not attempt to predict full BTCs, but instead predicts the time at which a certain breakthrough concentration will occur for a given filter depth and flow rate. Were the BDST equation rearranged in an attempt to predict the entire BTC, a sigmoidal function would be obtained, i.e. Eqn. (2). Therefore, the BDST model may fit experimental data at a single breakthrough point, but if extrapolations are made to different breakthrough concentrations, predicted BTCs may vary significantly from observed BTCs. This is particularly true in relation to low-cost adsorbents, which often produce BTCs that deviate significantly from the ideal symmetrical sigmoidal shape predicted by formulae such as that used in the BDST model.

Naturally, with the addition of enough modifying constants, a model can achieve an almost perfect fit to any dataset, but this detracts from the purpose of creating a model; a model should be simple enough to be of practical use, allowing for its easy application by those in industry, but sophisticated enough that the predictions it offers will be of practical use. Creating a model which adheres to these criteria will necessitate the adoption of various simplifications and assumptions, and depending on the assumptions made, the resultant model will almost certainly only be suitable for only certain adsorption systems (Xu et al., 2013). This is not a limitation, per se, rather just an unavoidable reality, one that necessitates the use of different models for different systems. Striving to create a 'perfect' model at the expense of its ever being practically utilized is a wholly academic pursuit if its complexity is such that very few can effectively implement it. This is reflected by the popularity of the simple B-A model, which assumes a rectangular isotherm, while the Thomas model, which assumes a more realistic Langmuir isotherm, and often offers a better fit to experimental data, has seen much less use; Chu (2010) compared the Thomas model to the B-A model and described the former as being "computationally intractable".

In a recent paper, Callery et al. (2016) found that the long-term performance of large-scale filters packed with low-cost adsorbents could be predicted mathematically using a simple model, which was constructed using 24 h of experimental data obtained from small-scale column tests. The methods used didn't require the use of scaling equations, as is generally the case with RSSCTs. Similitude was achieved by using the same media particle sizes and hydraulic loading rates in both the large and small-scale filters. In this way, the small columns were not so much scaled-down versions of large-scale filters, rather they could be considered cylindrical longitudinal-sections of hypothetical large-scale filter-beds. The BTCs obtained from these small-scale filters could be modeled, and extrapolations could be made to predict the performance of large-scale filters using the same media.

While dispensing with the necessity for scaling equations made this method simpler than the RSSCT approach, the advantages of RSSCTs were retained. So too was the disadvantage that there needed to be exact similarity between the small- and large-scale tests. For this reason, there is a necessity to develop this method further before it is capable of predicting the performance of filters with any bed depth operated at any loading rate, and this need is addressed by this study.

1.1. Theory

In through-flow adsorption systems, the mass of adsorbate retained by a filter medium is a function of the contact time between the adsorbent medium and the adsorbate solution. This means that having an understanding of an adsorbent's kinetic performance is of paramount importance when attempting to design any such system (Qiu et al., 2009). Changing the bed depth of a filter-bed (or adjusting the hydraulic loading rate) will affect the EBCT (used as a measure of the contact time between the adsorbent and the adsorbate solution) which will in turn affect the system's performance. The BDST model supposes that the relationship between bed depth (and therefore EBCT) and service time – the filter operating time to some defined breakthrough concentration - is a linear one (Hutchins, 1973). This assumption, while often reasonable, was quickly shown to not be valid for all systems (Poots et al., 1976a, 1976b). Curved plots of bed depth vs. service time are not uncommon, and intraparticle diffusion can cause tailing of BTCs (Deokar and Mandavgane, 2015), and non-linear BDST plots which deviate from those predicted by Hutchins' BDST model (Ko et al., 2000, 2002). Internal diffusion of adsorbate molecules often becomes a significant factor as a medium's surface becomes increasingly saturated, or as a result of lengthy filter EBCTs. Hutchins' BDST model is based on the assumption that intraparticle diffusion and external mass resistance are negligible (Ayoob and Gupta, 2007); this is rarely the case in real-world adsorption systems, where adsorption is seldom controlled solely by surface chemical reactions between the adsorbent and adsorbate (Crini and Badot, 2010). This limitation has been noted before, and attempts have been made to modify the BDST model to make it more universally applicable (Ko et al., 2000, 2002).

In deriving their fixed-bed model, Bohart and Adams (1920) made the assumption that the rate of the adsorption reaction in a fixed bed filter is proportional to the fraction of the medium's adsorption capacity which is still retained, and the concentration of adsorbate in the solution being filtered. They described this relationship as follows:

$$\frac{\partial N}{\partial t} = -kNC \quad (4)$$

$$\frac{\partial C}{\partial Z} = \frac{-k}{U} NC \quad (5)$$

Where C is the adsorbate concentration of the solution being filtered, t the time, Z the filter bed depth, U the flow velocity of the solution past the adsorbent, and k is a reaction rate constant; N is the residual adsorption capacity which is assumed to be some fraction, N′, of the adsorptive capacity of the adsorbent, N_o (i.e. $N' = N/N_o$, or $N = N_o N'$).

Eqns. (4) and (5) are based on the assumption that the filter bed

has a definite sorption maximum, N_o, which is independent of bed contact time and the duration for which the filter has operated; at equilibrium Eqn. (4) reduces to a rectangular sorption isotherm (highly favorable, irreversible adsorption) (Chu, 2010). In reality, it is known that filter-bed adsorption capacity does change depending on the fluid residence time in the bed (Ko et al., 2000, 2002) and the duration of filter operation. Increases in bed depth, and consequent increases in EBCT and service time, allow adsorbate molecules to diffuse deeper into the adsorbent particles resulting in a consequent increase in bed capacity. To account for this, Ko et al. (2000, 2002) proposed that a time dependent bed capacity term, N_t, could replace the standard bed capacity term of the BDST model, N_o, and presented two possible equations with which to determine this value:

$$N_t = N_o\left(1 - e^{-at}\right) \tag{6}$$

$$N_t = N_o\left(1 - e^{-a^*\sqrt{t}}\right) \tag{7}$$

where a and a* are first order and diffusional kinetic rate parameters respectively.

Regardless of the solid-liquid contact mechanism employed (i.e. batch or fixed bed), the equilibrium and kinetic characteristics of an adsorption system remain unchanged (Chu, 2010). With this in mind, just as Eqn. (6) is based on Lagergren (1898) pseudo first-order model, following the work of Liu (2008), another possible expression for N_t is proposed, based on Ho and McKay (1999) pseudo second-order model:

$$N_t = N_o\frac{t}{t + a^{**}} \tag{8}$$

Where a** is a fitting parameter associated with second order kinetics; the full derivation of Eqn. (8) can be found accompanying Fig. S1 of the supplementary information. It is worth noting that (given the interdependence of bed depth, EBCT, and service time), with different values for the constants a, a*, and a**, EBCT could be used in the place of service time, t, in Eqns. (6)–(8). The primary advantage of this being that EBCT is an easily calculable property of a filter, whereas service time must be experimentally determined. This point is also expounded in Fig. S1 of the supplementary file accompanying this text.

When N_t (as defined by one of Eqns. (6) and (7) or (8), to be selected on the basis of best fit to the system in question) is substituted for N_o in Eqn. (3), a modified form of the BDST equation (one which can describe a non-linear relationship between bed depth and service time) is obtained:

$$t_b = \frac{N_t Z}{C_0 U} - \frac{1}{k_{BA}C_0} ln\left(\frac{C_0}{C_b} - 1\right) \tag{9}$$

This equation can also be rearranged in the form of a modified BA equation to describe sigmoidal breakthrough curves:

$$ln\left(\frac{C_0}{C_b} - 1\right) = \frac{k_{BA}N_t Z}{U} - k_{BA}C_0 t_b \tag{10}$$

Ko et al. (2000, 2002) demonstrated the utility of this modified BDST model (Eqn. (9)), using Eqns. (6) and (7) to determine values for N_t (to the best of our knowledge, Eqn. (8) has not yet been used for this purpose), however, once the model is rearranged in the form of Eqn. (10) an inherent limitation becomes apparent: the model describes only sigmoidal curves, and is therefore poorly suited to the description of linear to convex BTCs which are commonly observed in fixed-bed studies using low-cost adsorbents.

To address this limitation, Callery et al. (2016) proposed the following model in a recent study:

$$C_e = C_o - \frac{q_e M}{VB} \tag{11}$$

Where C_e and C_o are the filter effluent and influent contaminant concentrations respectively, M is the mass of filter medium, V is the volume of solution loaded on to the filter, B is a model constant, and q_e is the mass of adsorbate adsorbed per unit mass of filter medium, as modeled by:

$$q_e = AV_B^{\left(\frac{1}{B}\right)} \tag{12}$$

where A is a model constant and V_B is the number of bed volumes of solution filtered.

Callery et al. (2016) found that Eqns. (11) and (12) were well suited to the modeling of non-sigmoidal BTCs, though a limitation of this model is that it does not provide any information regarding the bed depth service time relationship. It is hypothesized that this may be easily addressed; just as Ko et al. (2000, 2002) replaced N_o with N_t to modify the B-A/BDST model, q_e in Eqn. (11)/(12) could be replaced with an analogous time dependent parameter, q_t. Mirroring Eqns. (6)–(8), the following expressions for q_t are obtained:

$$q_t = q_e\left(1 - e^{-at}\right) \tag{13}$$

$$q_t = q_e\left(1 - e^{-a^*\sqrt{t}}\right) \tag{14}$$

$$q_t = q_e\frac{t}{t + a^{**}} \tag{15}$$

Again, a, a*, and a** are model constants associated with first order, diffusional, and second order kinetics respectively. Their value in the above equations will depend on whether service time or EBCT is used in the place of t; EBCT will be used in this study.

The adsorbate solution's concentration will reduce as it travels through the filter bed and, if the flow rate is constant, we can assume that at any depth within the filter, the pore concentrations will depend on the contact time that has elapsed between the solution and the filter medium (as well as the duration for which the filter has been loaded). The solution adsorbate concentration at any filter depth (i.e. after any EBCT), C_t, as opposed to the filter effluent concentration, C_e, can be found by substituting q_t for q_e in Eqn (11)/(12):

$$C_t = C_o - \frac{q_t M}{VB} \tag{16}$$

Given the linear relationship between filter depth and EBCT, Eqn. (16) can be used to calculate the filter pore concentrations of the adsorbate solution at any depth within the filter-bed after any filter loading, V, and can therefore describe the propagation of concentration fronts within the filter-bed.

Eqn. (16) can also be rearranged to yield a function with similar utility to Hutchins' BDST model, i.e. one that describes the relationship between bed depth and volume of solution treated to any breakthrough concentration, C_t, of interest:

$$V = \frac{q_t M}{B(C_o - C_t)} \tag{17}$$

The filter service time can be found from Eqn. (17) by dividing

the volume treated, V (L), by the loading rate (L s^{-1}).

In summary, sigmoidal BTCs and corresponding plots of bed depth vs. service time may be described by Eqns. (10) and (9) respectively, while linear to convex BTCS and corresponding plots of bed depth vs. service time may be described by Eqns. (17) and (16) respectively.

2. Materials and methods

2.1. Preparation of filter columns

The low-cost adsorbents utilized in this study were aluminum water treatment residual (dried at 105 °C for 24 h and ground to pass a 0.5 mm sieve) and two grades of crushed concrete ("fine", ground to pass 0.5 mm sieve, and "coarse", ground to pass a 1.18 mm sieve but retained by a 0.5 mm sieve). Small bore filter columns of lengths 0.1, 0.15, 0.2, 0.3, and 0.4 m were constructed using HDPE tubing with an internal diameter of 0.0094 m. These columns were packed with each of the aforementioned media, with care being taken to ensure that an equal bulk density was achieved in each filter. Endcaps, consisting of PE syringe barrels packed with a small quantity of glass wool, were fastened by means of a friction fit to the ends of the filter columns, and silicone tubing was connected to the tip of these syringe barrels to provide inlet and outlet lines to the filter columns. Large bore filter columns of length 0.65 m were then constructed in triplicate using uPVC piping with an internal diameter of 0.104 m. These columns were packed to a bed depth of 0.4 m using the same media and same packing density as was used in the small-bore filters. Again, care was taken to ensure that an equal bulk density was achieved in each filter for each medium. Sampling ports were installed through the walls of the large-bore filter columns at bed depths of 0.05, 0.1, 0.18, and 0.25 m from the filter surface. Water samples could also be collected from the outlet at the base of each column.

2.2. Operation of filter units

A synthetic wastewater was produced by dissolving K_2HPO_4 in tap water to obtain a PO_4-P concentration of 1 mg L^{-1} [similar to forest drainage water (Finnegan et al., 2012)]. A peristaltic pump was used to supply this wastewater to the small-bore filter units at consistent flow rates of between 134 and 259 mL h^{-1} [hydraulic loading rates similar to those found in high rate trickling filters (Spellman, 2013) or activated carbon adsorbers (Chowdhury, 2013)] to achieve a variety of filter bed contact times. The small-bore filters were operated intermittently, in 12 h on/off cycles, and were fed from the bottom of the vertically oriented filters to preclude any incidence of wastewater bypassing the filter media. The effluent from the small-bore columns was collected in 2 h aliquots using an auto-sampler. The large-bore filter columns were manually loaded 2–3 days per week with 28 L of the same synthetic wastewater as used in the small-bore filters. Water samples were collected from the sampling ports at various intervals, and the effluent from each loading event was collected in large HDPE containers.

2.3. Data collection and analysis

Collected effluent samples were passed through 0.45 μm filters and analyzed with a Konelab nutrient analyzer in accordance with the standard methods (Eaton et al., 1998). With the influent and effluent PO_4-P concentrations determined, medium saturation, q_e, was calculated. Graphs of q_e vs V and C_e vs V were plotted, and Eqn. (15) and Eqn. (16) were fit to these experimental data by non-linear regression, using Microsoft Excel's solver add-in to minimize the sum of the squares of the errors (ERRSQ):

$$\sum_{i=1}^{p}\left(q_{e,calc}-q_{e,meas}\right)_i^2 \tag{18}$$

where $q_{e,calc}$ is the model predicted equilibrium solid phase PO_4-P concentration and $q_{e,meas}$ is the measured equilibrium solid phase PO_4-P concentration.

2.4. Predicting large-scale filter performance

With the coefficients A, B, and a** determined from the small-scale column tests, Eqn. (16) was used to predict effluent concentrations and pore water concentrations at multiple depths within the large-scale filter columns. V_x, the volume of the large-scale filter to a depth of 'x' was calculated by multiplying 'x' by the area of the filter column (i.e. $\pi D^2/4$, where D is 0.104 m, the internal diameter of the large-scale filter column). After some filter loading, V, the pore concentration at a filter-bed depth of 'x' (if predicting effluent concentration, x = Z, the full filter-bed depth), was predicted by inputting the following values into Eqn. (16): $V_B = V/V_x$, $M = \rho V_x$ (where ρ is the bulk density of the media in the filter column; this should be the same as used in the small-scale tests), and $t = V_x/Q$ (where Q is the loading rate applied to the large-scale filter).

2.5. Validation of model using independent data

To validate and further support the modelling strategy applied in this study, a literature review was carried out to identify column studies which utilized low-cost adsorbents and observed BTCs which tended towards a convex to linear shape, rather than the sigmoidal curve predicted by other models. The BTCs published in these studies were downloaded as raster images and converted to vector graphics, the ordinates of which could be exported as a text file. The text files were imported into Microsoft Excel as x and y coordinates, which could then be processed in the same fashion as the experimental data. This method was validated using known data points, and it was found that the mean absolute percentage error between actual values and data points obtained in this manner was 0.18%.

Fig. 1 shows a step-by-step schematic of the data collection and modelling procedure employed in this study.

3. Results and discussion

3.1. Predicting medium saturation in RSSCTs

Fig. 2 shows plots of filter loading versus phosphorus retained by filter columns of various lengths. As can be seen, the relationship between filter loading and medium saturation could be accurately described by Eqn. (15). The ERRSQ function was used as a metric for goodness of model fit, with average ERRSQ values of 0.074, 0.057, and 0.008 obtained for small-scale filter columns containing Al-WTR, fine concrete, and coarse concrete, respectively. As described previously, q_t can be calculated in a number of ways; Fig. S2 in the supplementary file compares graphs of the three functions from which a value for q_t may be obtained. Comparing the shapes of these functions, it can be seen that Eqn. (14), originally proposed by Ko et al. (2000, 2002) to account for diffusional adsorption, appears to very closely match the curve produced by Eqn. (15), based on second-order kinetics. This would seem to indicate that both functions might have similar utility, however the differences between the two can be considerable when the two are compared on a local scale, as can be seen from the inset in Fig. S2. In

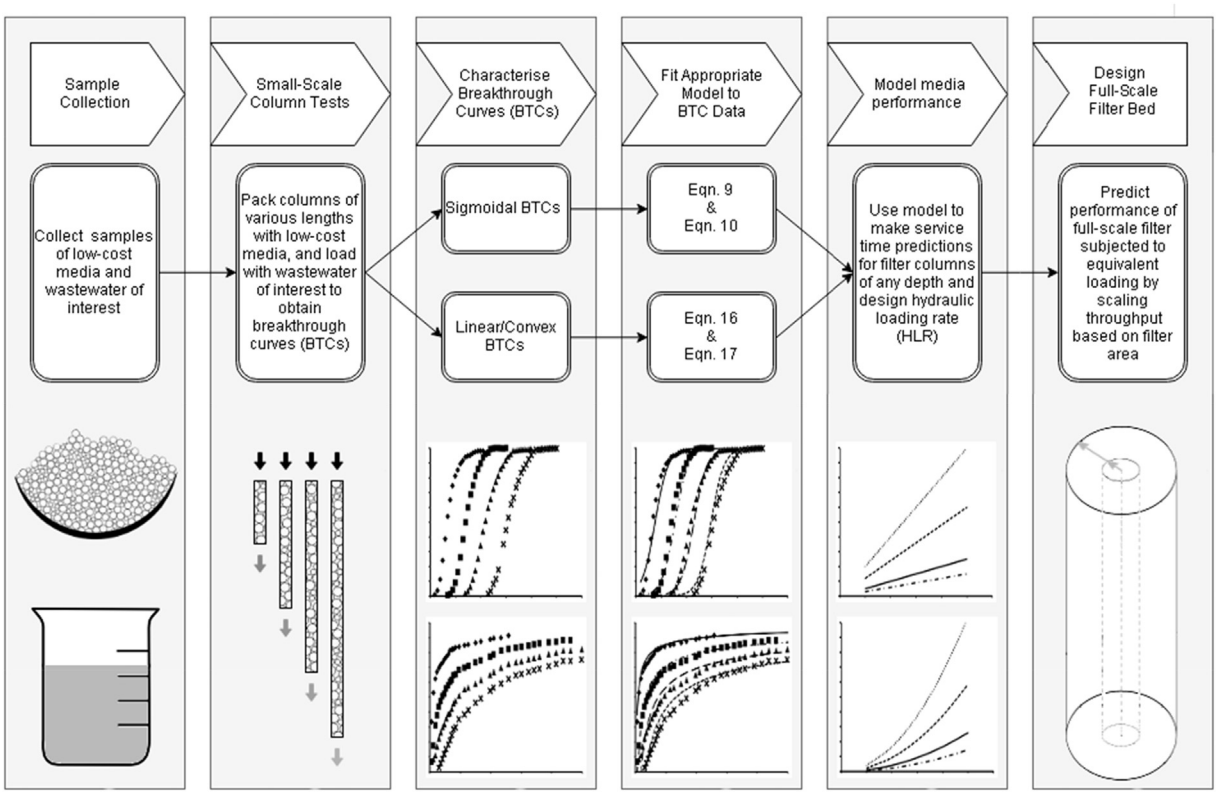

Fig. 1. Step-by-step schematic of the data collection and modelling procedure employed in this study.

constructing Fig. 2, attempts were made to fit the experimental data from the small-scale column tests to each of Eqns. (13)–(15). As can be seen from Table 1, which compares ERRSQ values obtained using each of these equations, Eqn. (15) was found to be optimal for each of the media studied. As it provided the best fit to these initial data (and because Ko et al. (2000, 2002) have already explored the use of Eqns. (13) and (14)), Eqn. (15) was used for the remainder of this study when fitting Eqns. (16) and (17) to experimental data.

3.2. Predicting pore concentrations at multiple depths in large-scale filter columns

Once it was established that Eqn. (15) was capable of describing and predicting the progression of medium saturation in small-scale filter columns of various lengths, it was hypothesized that Eqn. (16) would also be able to predict pore PO_4-P concentrations at any bed depth within the filter bed of a large-scale column. To test this hypothesis, Eqn. (16) (with q_t determined using Eqn. (15)) was fit, using the ERRSQ method, to the data obtained from depth samples taken from various depths within the large-scale filter columns. Fig. 3(a) shows the fit of Eqn. (16) to these experimental data, and the associated ERRSQ values are shown in Table 2. Average ERRSQ values of 0.026, 0.011, and 0.005 were obtained for large-scale filter columns containing Al-WTR, fine concrete, and coarse concrete, respectively. It can be seen that the slight day-to-day variances in influent concentration had a marked influence on the shape of the observed BTCs. While Eqn. (16) was initially proposed to be accurate with the assumption of constant influent concentration, it appeared to display good resilience to these fluctuations, and was nonetheless able to make accurate pore and effluent concentration predictions. With it established that the model could describe the performance of both small- and large-scale filter columns, it was further hypothesized that the coefficients determined from the small-scale columns could also be used to predict the performance of the large-scale filter columns. With these coefficients, the performance of small-scale filters of any depth operated at any HLR could be predicted, and equivalent loadings for large-scale columns subjected to the same HLR were calculated by scaling filter throughput based on the ratio of the small- and large-scale filter areas. Fig. 3(b) shows data from the large-scale column tests fit to models created using data from the small-scale column tests, and the associated ERRSQ values are shown in Table 2. While not fitting quite as closely as when modeled directly on the large-scale column data, the level of precision achieved was still very good, with average ERRSQ values of 0.062, 0.054, and 0.008 obtained for filter columns containing Al-WTR, fine concrete, and coarse concrete, respectively. For practical purposes of preliminary filter design, this level of accuracy was considered more than sufficient, and it allowed for prediction of the adsorptive performance of the large-scale filter columns for the entire duration of their operation. It could reasonably be expected that loading the large-scale filters with a wastewater whose chemical composition was significantly different from that of the wastewater applied to the small-scale filters (in terms of pH, concentration of target contaminant, competing compounds etc.) would invalidate any model predictions of large-scale performance based on the small-scale experiments; a more complex modeling approach would be required to take account of such variations.

3.3. Validation of model using independent data

To further verify the validity and utility of Eqn. (16), it was fit to BTCs published in a number of independent studies. The results of this are shown in Fig. 4, and it can be seen that the model fit these data very well. Poots et al. (1976b) was the first author who

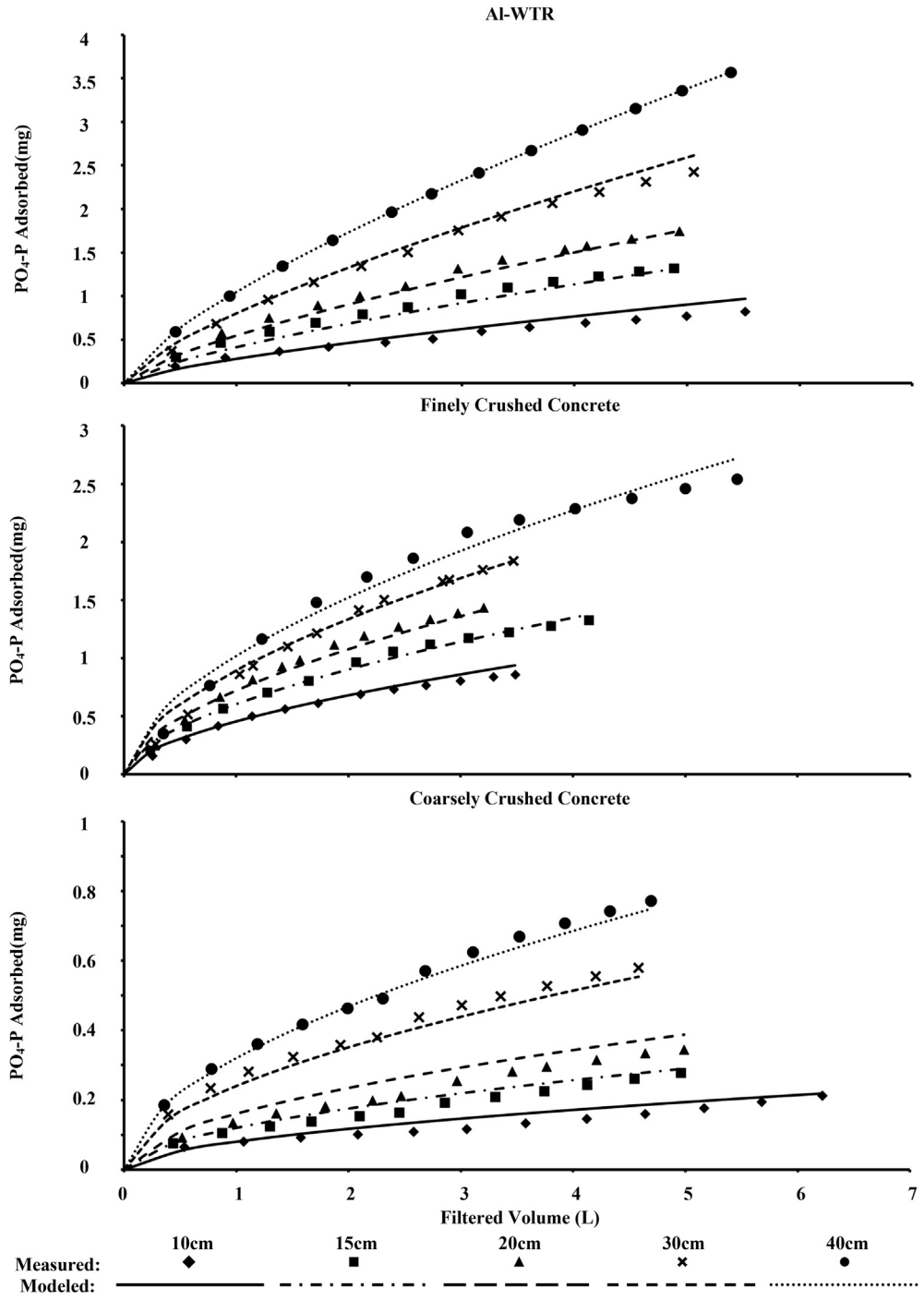

Fig. 2. Phosphorus retained by filter media (y-axis) vs. filter loading (x-axis) for small scale filter columns of various lengths and predictions made by Eqn (15).

Table 1
ERRSQ values obtained using Eqns (13)–(15) to model phosphorus retained by filter media vs. filter loading for small-scale filter columns of various lengths.

Equation	Average model ERRSQ values		
	Al-WTR	Fine Conc.	Coarse Conc.
$q_t = q_e(1 - e^{-at})$	0.0762	0.0687	0.0080
$q_t = q_e(1 - e^{-a^*\sqrt{t}})$	1.0534	0.0873	0.1028
$q_t = q_e\frac{t}{t+a^{**}}$	**0.0737**	**0.0568**	**0.0078**

Bold text denotes lowest observed ERRSQ values for each heading (Al-WTR, Fine Conc., Coarse Conc.).

attempted to apply Hutchins (1973) BDST model to experimental results (according to the Web of Science™ citation index), and found that it was a poorly suited to describing the relationship between bed depth and service time in peat filters designed to remove Telon blue from aqueous solution. However, as can be seen in Fig. 4(a), Eqn. (16) was able to describe the breakthrough behavior of Telon blue at all filter depths, accurately describing the non-linear relationship between bed depth and service time described by the BTCs. A recent study on phosphate adsorption (Nguyen et al., 2015) recorded BTCs from filters packed with a low cost adsorbent (zirconium loaded okara) using phosphate

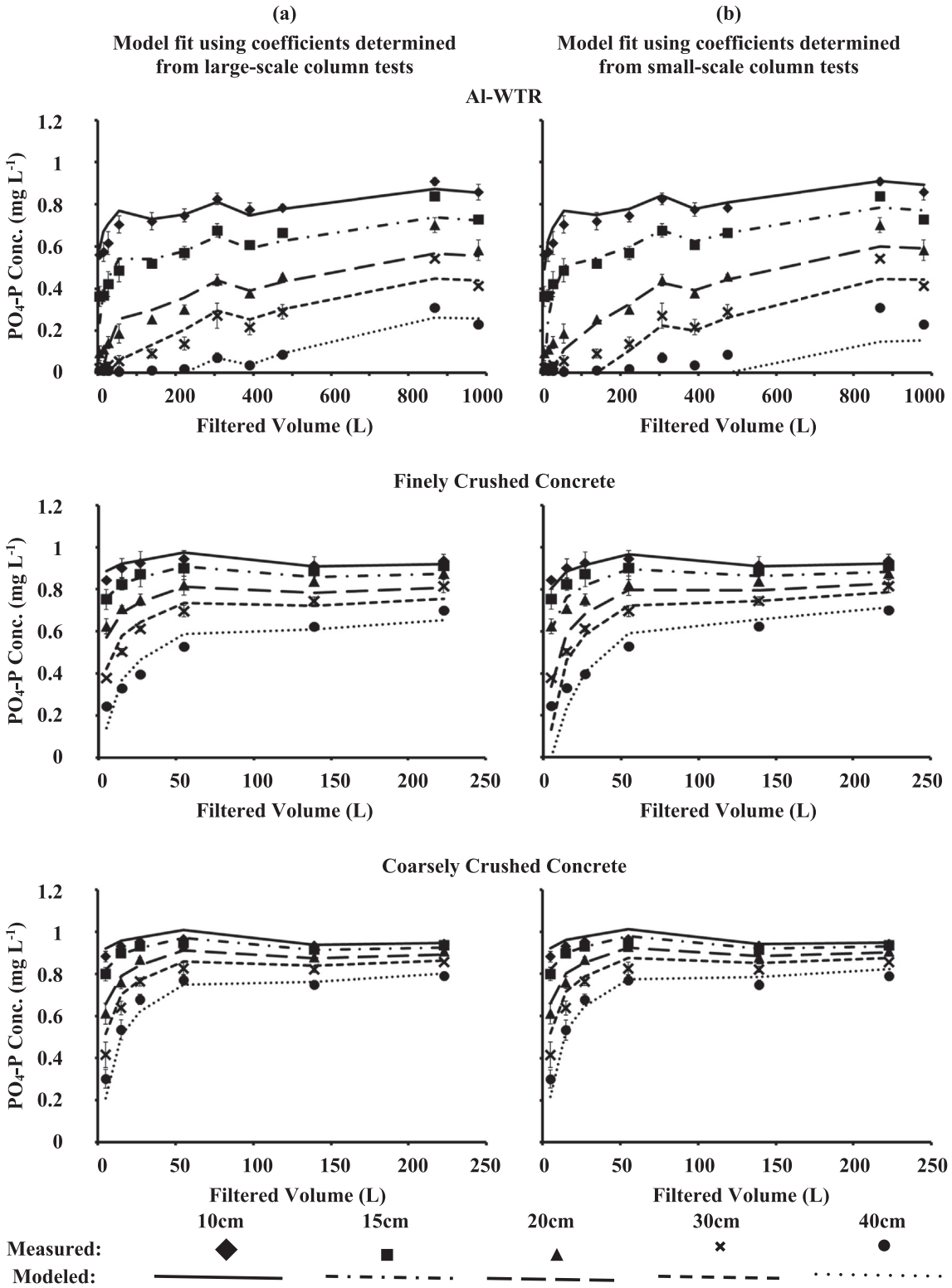

Fig. 3. PO_4-P concentration (y-axis) vs. filter loading (x-axis) for large scale filter columns, showing (a) Eqn (16) fit directly to large scale column data, and (b) predictions made by Eqn (16) with model coefficients determined from small-scale column tests.

Table 2
Comparison of model coefficients and ERRSQ values obtained when (a) fitting Equation (16) directly to concentration data from the large-scale column experiments and (b) when fitting Eqn. (16) to concentration data from the large-scale column experiments using model coefficients determined from small-scale column tests.

		Model parameters determined from Large Column Data			Model parameters determined from Small Column Data		
		Al-WTR	Coarse Concrete	Fine Concrete	Al-WTR	Coarse Concrete	Fine Concrete
Model Parameters	A	0.0105	0.0062	0.0058	0.0163	0.0071	0.0124
	B	1.2370	1.6385	1.3733	1.3692	1.7606	1.7054
	a**	10.6786	9.1300	1.3525	10.1007	9.2322	1.2134
		Model ERRSQ values			Model ERRSQ values		
Filter Depth	5 cm	0.0245	0.0028	0.0038	0.0210	0.0048	0.0026
	10 cm	0.0328	0.0012	0.0027	0.1540	0.0011	0.0282
	18 cm	0.0472	0.0032	0.0105	0.0596	0.0034	0.1034
	25 cm	0.0209	0.0106	0.0144	0.0291	0.0189	0.0641
	40 cm	0.0038	0.0074	0.0228	0.0463	0.0100	0.0735
	μ:	0.0259	0.0050	0.0108	0.0620	0.0076	0.0544

concentrations an order of magnitude higher than those used in the present study; as can be seen from Fig. 4(b), Eqn. (16) was well suited to the description of these curves. Finally, Han et al. (2009) investigated the ability of iron oxide-coated zeolite as an adsorbent for the removal of copper (II) from aqueous solution in filter beds of various depths, and, as shown in Fig. 4(c), the BTCs obtained these can be suitably modeled by Eqn. (16).

3.4. Description of sigmoidal curves

Although Eqn. (15) can describe many of the linear to convex BTCs commonly observed from fixed-bed studies using low-cost adsorbents, it is not suitable for the description of sigmoidal curves. This is perhaps the most commonly observed BTC shape observed in fixed-bed sorption studies (Gupta et al., 2000), and so, an attempt was made to model curves of this shape by modifying the B-A model (Eqn. (2)) to obtain Eqn. (10), as described previously. Using Eqn. (8) (letting t in Eqn. (8) be EBCT) to determine a value for N_t, Eqn. (10) was fit to a number of independent data sets, as shown in Fig. 5. In the B-A model, N_o serves a similar function to q_e in Eqn. (11), as both represent the sorption capacity of the media. The B-A model assumes a rectangular sorption isotherm (highly favorable, irreversible adsorption) and a definite sorption maximum, which is independent of the contact time and the duration for which the filter has operated. However, in reality, it is known that filter-bed adsorption capacity does change depending on contact time (Ko et al., 2002) and duration of operation. Eqn. (11) assumes that there is an exponential distribution of adsorption sites and energies, meaning that adsorption energies become exponentially weaker with increasing duration of filter operation and associated medium saturation; the bed's capacity increases with operating time and, though there is no defined maximum capacity, there are adsorption maxima for any given filter runtime. Making bed capacity dependent on empty bed contact time, i.e. substituting q_t for q_e, proved to be very successful, and similar success was found modifying Eqn. (2) by replacing N_o with N_t. This can be seen in Fig. 5, in which Eqn. (10) (with N_t determined from Eqn. (8)) has been fit to six independent data sets. Ko et al. (2000, 2002) also implemented a similar approach, using Eqn. (6) and Eqn. (7) to modify the BDST model, which is itself derived from the B-A model.

3.5. Prediction of BDST relationship

The relationship between bed depth and service time is not necessarily a linear one; greater bed depths result in longer EBCTs, which in turn allow for increased adsorption due to increased intraparticle diffusion of adsorbate molecules. Fig. S3 of the supplementary file shows some hypothetical BTCs, comparing a linear relationship between bed depth and service time, as proposed by Hutchins' arrangement of the B-A equation (Fig. S3a), and a non-linear relationship between bed depth and service time as predicted by Eqn. (10), the B-A equation modified with Eqn. (8) (Fig. S3b). The non-linear relationship between bed depth and service time as predicted by Eqns. (16) and (17) is also shown in Fig. S3b, illustrating that the BDST plot doesn't necessarily provide any information regarding the shape of the BTC; though the BTCs predicted by Eqn. (10) and Eqn. (16) are very different, both yield the same curved BDST plot.

Ko et al. (2002). modified the BDST model using Eqn. (6) and Eqn. (7), and this made it possible to describe non-linear BDST plots. However, as can be seen in Fig. 6, the BTCs observed in their study were not sigmoidal, and so, the B-A model on which the modified BDST model is based would not be appropriate for the description of entire BTCs. Eqn. (16) was fit to the data from this study, and, as can be seen in Fig. 6, it was capable of describing not only the non-linear BDST relationship, but also the entire BTC for each filter-bed depth investigated. Eqn. (17) can therefore, in this case, be used to predict the BDST relationship at any breakthrough concentration of interest, as well as at any flow rate of interest, as demonstrated in Fig. 6(b).

4. Conclusions

This study described a testing and modelling methodology which uses results from short-term small-scale column tests to predict the long-term performance of large-scale fixed-bed filters.

- The proposed methodology was used to describe the adsorptive performance of small-scale and large-scale filter columns, successfully modelling medium saturation, as well as filter-pore and effluent concentration data.
- Predictions of large-scale filter performance based on small-scale filter performance were highly accurate.
- Two three-parameter models were investigated, and these allowed for the description and prediction of sigmoidal or convex breakthrough curves for multiple filters containing the same media, as well as concentration profiles across multiple depths within single filters.
- The proposed models also allow for the description of non-linear relationships between filter-bed depth and service time, as is commonly observed in fixed-bed systems which take a long time to reach equilibrium.

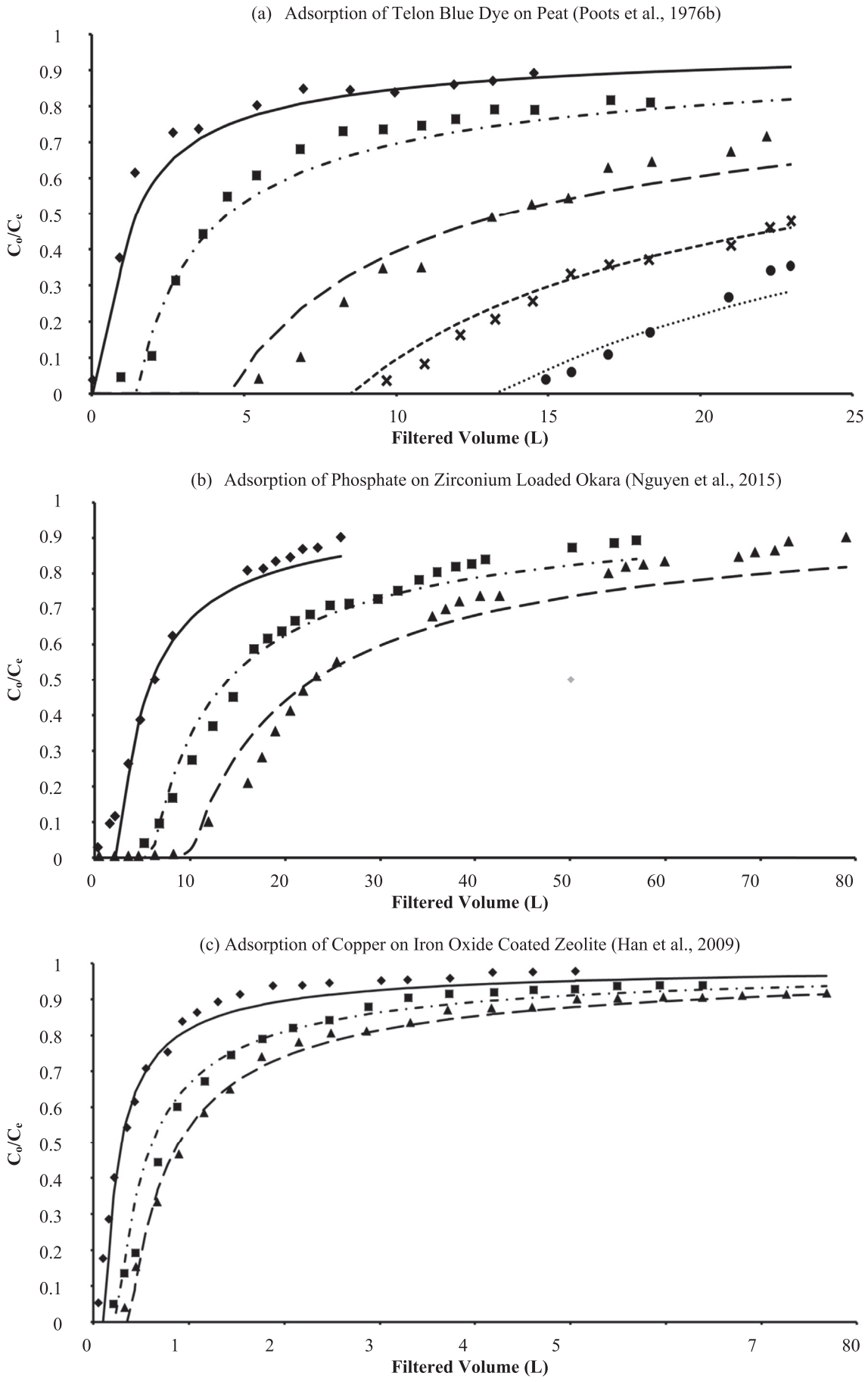

Fig. 4. Eqn (16) fit to independent data sets of normalised pore/effluent contaminant concentration (y-axis) vs. filter loading/operating time (x-axis).

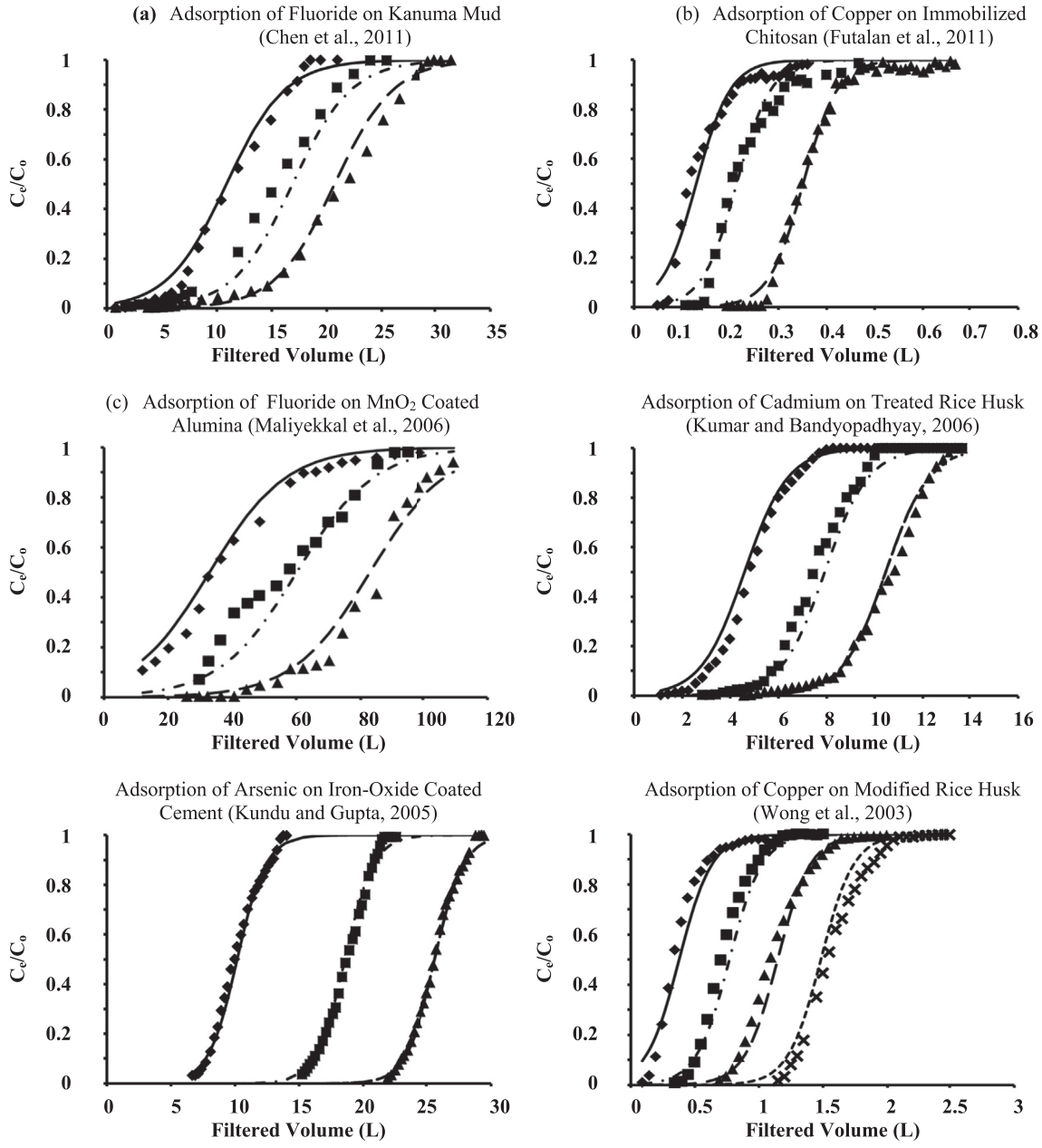

Fig. 5. Eqn (10) fit to independent data sets of normalised pore/effluent contaminant concentration (y-axis) vs. filter loading/operating time (x-axis) (Chen et al., 2011, Futalan et al., 2011, Maliyekkal et al., 2006, Kumar and Bandyopadhyay, 2006, Kundu and Gupta, 2005, Wong et al., 2003)).

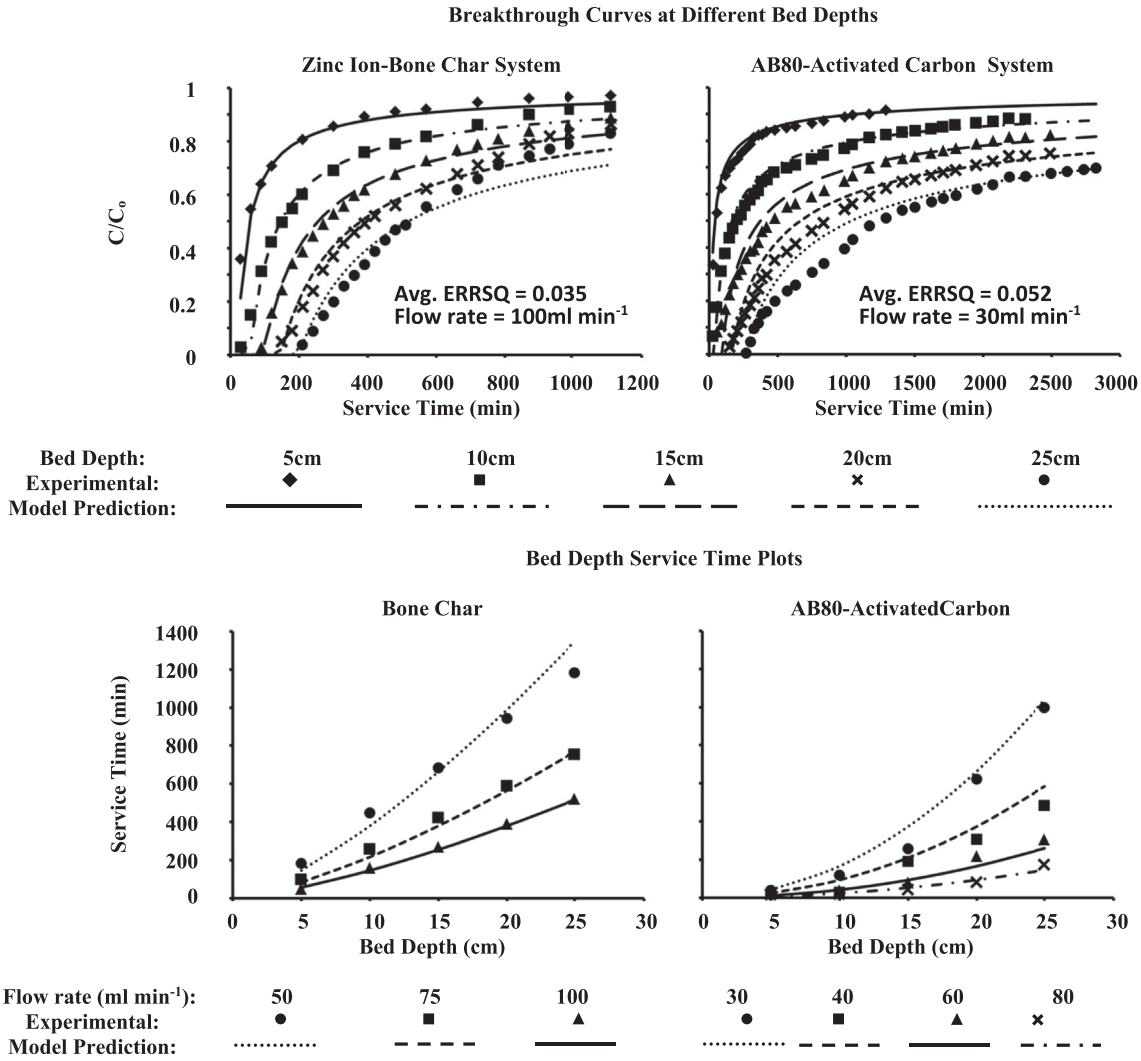

Fig. 6. **(a)** Eqn (16) fit to an independent data set of normalised effluent contaminant concentration (y-axis) vs. filter operating time (x-axis) for various filter-bed depths, and (b) plots of filter service-time (y-axis) vs. filter-bed depth (x-axis) compared to predictions made by Eqn (17) using the same model coefficients.

- The proposed modelling approach was applied to multiple independent data sets and was found to suitably describe the adsorption of various solutes including dyes, phosphate, metals (copper, cadmium, and zinc), fluoride, and arsenic.

Acknowledgement

The first author would like to acknowledge the Irish Research Council (GOIPG/2013/75) for funding.

Appendix A. Supplementary data

Supplementary data related to this article can be found at http://dx.doi.org/10.1016/j.watres.2017.07.010.

References

Al-Degs, Y.S., Khraisheh, M.A.M., Allen, S.J., Ahmad, M.N., 2009. Adsorption characteristics of reactive dyes in columns of activated carbon. J. Hazard. Mater 165, 944–949. http://dx.doi.org/10.1016/j.jhazmat.2008.10.081.

Ayoob, S., Gupta, A.K., 2007. Sorptive response profile of an adsorbent in the defluoridation of drinking water. Chem. Eng. J. 133, 273–281. http://dx.doi.org/10.1016/j.cej.2007.02.013.

Babel, S., Kurniawan, T.A., 2003. Low-cost adsorbents for heavy metals uptake from contaminated water: a review. J. Hazard. Mater. 97, 219–243. http://dx.doi.org/10.1016/S0304-3894(02)00263-7.

Bailey, S.E., Olin, T.J., Bricka, R.M., Adrian, D.D., 1999. A review of potentially low-cost sorbents for heavy metals. Water Res. 33, 2469–2479. http://dx.doi.org/10.1016/S0043-1354(98)00475-8.

Bockris, J.O.M., Conway, B.E., White, R.E., 1995. Modern Aspects of Electrochemistry, vol. 29. Springer.

Bohart, G.S., Adams, E.Q., 1920. Some aspects of the behavior of charcoal with respect to chlorine 1. J. Am. Chem. Soc. 42, 523–544. http://dx.doi.org/10.1021/ja01448a018.

Brown, P., Atly Jefcoat, I., Parrish, D., Gill, S., Graham, E., 2000. Evaluation of the adsorptive capacity of peanut hull pellets for heavy metals in solution. Adv. Environ. Res. 4, 19–29. http://dx.doi.org/10.1016/S1093-0191(00)00004-6.

Callery, O., Healy, M.G., Rognard, F., Barthelemy, L., Brennan, R.B., 2016. Evaluating the long-term performance of low-cost adsorbents using small-scale adsorption column experiments. Water Res. 101, 429–440. http://dx.doi.org/10.1016/j.watres.2016.05.093.

Chen, N., Zhang, Z., Feng, C., Li, M., Chen, R., Sugiura, N., 2011. Investigations on the batch and fixed-bed column performance of fluoride adsorption by Kanuma mud. Desalination 268, 76–82. http://dx.doi.org/10.1016/j.desal.2010.09.053.

Chowdhury, Z.K., Summers, R.S., Westerhoff, G.P., Leto, B.J., Nowack, K.O., Corwin, C.J., 2013. Activated Carbon: Solutions for Improving Water Quality. American Water Works Association, Denver, CO.

Chu, K.H., 2010. Fixed bed sorption: setting the record straight on the Bohart–Adams and Thomas models. J. Hazard. Mater. 177, 1006–1012. http://dx.doi.org/10.1016/j.jhazmat.2010.01.019.

Crini, G., 2006. Non-conventional low-cost adsorbents for dye removal: a review. Bioresour. Technol. 97, 1061–1085.

Crini, G., Badot, P.-M., 2010. Sorption Processes and Pollution: Conventional and Non-conventional Sorbents for Pollutant Removal from Wastewaters. Presses Univ. Franche-Comté.

Crini, G., Badot, P.-M., 2008. Application of chitosan, a natural aminopolysaccharide, for dye removal from aqueous solutions by adsorption processes using batch studies: a review of recent literature. Prog. Polym. Sci. 33, 399–447. http://dx.doi.org/10.1016/j.progpolymsci.2007.11.001.

Crittenden, J.C., Berrigan, J.K., Hand, D.W., 1986. Design of rapid small-scale adsorption tests for a constant diffusivity. J. Water Pollut. Control Fed. 312–319.

Crittenden, J.C., Berrigan, J.K., Hand, D.W., Lykins, B., 1987. Design of rapid fixed-bed adsorption tests for nonconstant diffusivities. J. Environ. Eng. 113, 243–259.

Crittenden, J.C., Reddy, P.S., Arora, H., Trynoski, J., Hand, D.W., Perram, D.L., Summers, R.S., 1991. Predicting GAC performance with rapid small-scale column tests. J. Am. Water Works Assoc. 83, 77–87.

Dąbrowski, A., 2001. Adsorption — from theory to practice. Adv. Colloid Interface Sci. 93, 135–224. http://dx.doi.org/10.1016/S0001-8686(00)00082-8.

Deokar, S.K., Mandavgane, S.A., 2015. Estimation of packed-bed parameters and prediction of breakthrough curves for adsorptive removal of 2,4-dichlorophenoxyacetic acid using rice husk ash. J. Environ. Chem. Eng. 3, 1827–1836. http://dx.doi.org/10.1016/j.jece.2015.06.025.

Eaton, A.D., Clesceri, L.S., Greenberg, A.E., Franson, M.A.H., 1998. American Public Health Association., American Water Works Association., Water Environment Federation. Standard methods for the examination of water and wastewater. American Public Health Association, Washington, DC.

Faust, S.D., Aly, O.M., 1998. Chemistry of Water Treatment, second ed. CRC Press.

Finnegan, J., Regan, J.T., de Eyto, E., Ryder, E., Tiernan, D., Healy, M.G., 2012. Nutrient dynamics in a peatland forest riparian buffer zone and implications for the establishment of planted saplings. Ecol. Eng. 47, 155–164. http://dx.doi.org/10.1016/j.ecoleng.2012.06.023.

Futalan, C.M., Kan, C.-C., Dalida, M.L., Pascua, C., Wan, M.-W., 2011. Fixed-bed column studies on the removal of copper using chitosan immobilized on bentonite. Carbohydr. Polym. 83, 697–704. http://dx.doi.org/10.1016/j.carbpol.2010.08.043.

Goel, J., Kadirvelu, K., Rajagopal, C., Kumar Garg, V., 2005. Removal of lead(II) by adsorption using treated granular activated carbon: batch and column studies. J. Hazard. Mater. 125, 211–220. http://dx.doi.org/10.1016/j.jhazmat.2005.05.032.

Gupta, V.K., Srivastava, S.K., Tyagi, R., 2000. Design parameters for the treatment of phenolic wastes by carbon columns (obtained from fertilizer waste material). Water Res. 34, 1543–1550. http://dx.doi.org/10.1016/S0043-1354(99)00322-X.

Han, R., Zou, L., Zhao, X., Xu, Y., Xu, F., Li, Y., Wang, Y., 2009. Characterization and properties of iron oxide-coated zeolite as adsorbent for removal of copper(II) from solution in fixed bed column. Chem. Eng. J. 149, 123–131. http://dx.doi.org/10.1016/j.cej.2008.10.015.

Ho, Y.S., McKay, G., 1999. Pseudo-second order model for sorption processes. Process Biochem. 34, 451–465. http://dx.doi.org/10.1016/S0032-9592(98)00112-5.

Hutchins, R., 1973. New method simplifies design of activated carbon systems, water bed depth service time analysis. J. Chem. Eng. Lond. 81, 133–138.

Ko, D.C.K., Lee, V.K.C., Porter, J.F., McKay, G., 2002. Improved design and optimization models for the fixed bed adsorption of acid dye and zinc ions from effluents. J. Chem. Technol. Biotechnol. 77, 1289–1295. http://dx.doi.org/10.1002/jctb.707.

Ko, D.C.K., Porter, J.F., McKay, G., 2000. Optimised correlations for the fixed-bed adsorption of metal ions on bone char. Chem. Eng. Sci. 55, 5819–5829. http://dx.doi.org/10.1016/S0009-2509(00)00416-4.

Kumar, U., Bandyopadhyay, M., 2006. Fixed bed column study for Cd(II) removal from wastewater using treated rice husk. J. Hazard. Mater. 129, 253–259. http://dx.doi.org/10.1016/j.jhazmat.2005.08.038.

Kundu, S., Gupta, A.K., 2005. Analysis and modeling of fixed bed column operations on As(V) removal by adsorption onto iron oxide-coated cement (IOCC). J. Colloid Interface Sci. 290, 52–60. http://dx.doi.org/10.1016/j.jcis.2005.04.006.

Lagergren, S., 1898. About the theory of so-called adsorption of soluble substances.

Liu, Y., 2008. New insights into pseudo-second-order kinetic equation for adsorption. Colloids Surf. Physicochem. Eng. Asp. 320, 275–278. http://dx.doi.org/10.1016/j.colsurfa.2008.01.032.

Maliyekkal, S.M., Sharma, A.K., Philip, L., 2006. Manganese-oxide-coated alumina: a promising sorbent for defluoridation of water. Water Res. 40, 3497–3506. http://dx.doi.org/10.1016/j.watres.2006.08.007.

Nguyen, T.A.H., Ngo, H.H., Guo, W.S., Pham, T.Q., Li, F.M., Nguyen, T.V., Bui, X.T., 2015. Adsorption of phosphate from aqueous solutions and sewage using zirconium loaded okara (ZLO): fixed-bed column study. Sci. Total Environ. 523, 40–49. http://dx.doi.org/10.1016/j.scitotenv.2015.03.126.

Poots, V.J.P., McKay, G., Healy, J.J., 1976a. The removal of acid dye from effluent using natural adsorbents—II wood. Water Res. 10, 1067–1070. http://dx.doi.org/10.1016/0043-1354(76)90037-3.

Poots, V.J.P., McKay, G., Healy, J.J., 1976b. The removal of acid dye from effluent using natural adsorbents—I peat. Water Res. 10, 1061–1066. http://dx.doi.org/10.1016/0043-1354(76)90036-1.

Pratt, C., Parsons, S.A., Soares, A., Martin, B.D., 2012. Biologically and chemically mediated adsorption and precipitation of phosphorus from wastewater. Curr. Opin. Biotechnol. Phosphorus Biotechnol. Pharm. Biotechnol. 23, 890–896. http://dx.doi.org/10.1016/j.copbio.2012.07.003.

Qiu, H., Lv, L., Pan, B., Zhang, Qing-jian, Zhang, W., Zhang, Quan-xing, 2009. Critical review in adsorption kinetic models. J. Zhejiang Univ. Sci. A 10, 716–724. http://dx.doi.org/10.1631/jzus.A0820524.

Reddad, Z., Gerente, C., Andres, Y., Le Cloirec, P., 2002. Adsorption of several metal ions onto a low-cost Biosorbent: kinetic and equilibrium studies. Environ. Sci. Technol. 36, 2067–2073. http://dx.doi.org/10.1021/es0102989.

Søvik, A.K., Kløve, B., 2005. Phosphorus retention processes in shell sand filter systems treating municipal wastewater. Ecol. Eng. 25, 168–182. http://dx.doi.org/10.1016/j.ecoleng.2005.04.007.

Spellman, F.R., 2013. Handbook of Water and Wastewater Treatment Plant Operations, third ed. CRC Press.

Thomas, H.C., 1944. Heterogeneous ion exchange in a flowing system. J. Am. Chem. Soc. 66, 1664–1666. http://dx.doi.org/10.1021/ja01238a017.

Wong, K.K., Lee, C.K., Low, K.S., Haron, M.J., 2003. Removal of Cu and Pb from electroplating wastewater using tartaric acid modified rice husk. Process Biochem. 39, 437–445. http://dx.doi.org/10.1016/S0032-9592(03)00094-3.

Xu, Z., Cai, J., Pan, B., 2013. Mathematically modeling fixed-bed adsorption in aqueous systems. J. Zhejiang Univ. Sci. A 14, 155–176.